DTIC FILE COPY

DTIC
S ELECTE
JUN 2 3 1988
D
H

AN ANALYSIS OF LATERAL-DIRECTIONAL
HANDLING QUALITIES AND EIGENSTRUCTURE
OF HIGH PERFORMANCE AIRCRAFT

THESIS

Michael J. Costigan
Major, USAF

AFIT/GAE/AA/88J-1

DEPARTMENT OF THE AIR FORCE

AIR UNIVERSITY

AIR FORCE INSTITUTE OF TECHNOLOGY

Wright-Patterson Air Force Base, Ohio

88 6 23 056

AFIT/GAE/AA/88J-1

AN ANALYSIS OF LATERAL-DIRECTIONAL
HANDLING QUALITIES AND EIGENSTRUCTURE
OF HIGH PERFORMANCE AIRCRAFT

THESIS

Michael J. Costigan
Major, USAF

AFIT/GAE/AA/88J-1

DTIC

JUN 2 3 1988

AFIT/GAE/AA/88J-1

AN ANALYSIS OF LATERAL-DIRECTIONAL HANDLING QUALITIES AND

EIGENSTRUCTURE OF HIGH PERFORMANCE AIRCRAFT

THESIS

Presented to the Faculty of the School of Engineering

of the Air Force Institute of Technology

Air University

in Partial Fulfillment of the

Requirements for the Degree of

Master of Science in Aerospace Engineering

DTIC
S ELECTE D
JUN 2 3 1988
H

Michael J. Costigan, M.S.

Major, USAF

June 1988

Preface

This report presents results of a year long research effort as well as three months of flight testing at Edwards Air Force Base (AFB). It has been a challenge to apply the theoretical basis of the AFIT thesis to the real world of flight testing. Although the flight testing was hindered by technical problems not addressed by the research, the lessons learned in the application of eigenstructure assignment to actual aircraft are enlightening.

Portions of this thesis were included in the Final Report of the HAVE EIGEN flight tests conducted at Edwards AFB (1). However, this report is complete and contains all pertinent results from those tests.

I wish to thank the many faculty members at the Air Force Institute of Technology who assisted in preparing this thesis. I am deeply indebted to Dr Robert Calico and Capt Dan Gleason for advice in some very difficult areas.

I am also deeply indebted to the many people at Edwards Air Force Base, especially the HAVE EIGEN test team, who assisted in the flight testing. In particular, I wish to thank Major Dan McCorry of the Test Pilot School for his guidance in conducting the flight tests, Mr Frank Brink of Honeywell Corporation for his invaluable assistance in programming the control laws in the YA-7D, and Mary Schafer of the National Aeronautics and Space Administration. Finally, I thank my wife, Cindy, for her help and encouragement.

Michael J. Costigan

ii

Table of Contents

Table of Contents (Concluded)

List of Figures

List of Figures (Continued)

List of Figures (Concluded)

List of Tables

List of Abbreviations and Symbols

ITEM	DEFINITION
A	$n \times n$ state matrix
AFCS	Automatic Flight Control System
AFFTC	Air Force Flight Test Center
AMF	Automatic Maneuvering Flaps
B	$n \times m$ control matrix
C	$r \times n$ output matrix
CAS	Control Augmentation System
CG	Center of Gravity
DFCS	Digital Multimode Flight Control System
F	$m \times r$ feedback gain matrix
F_a	Lateral stick force, pounds
F1	First stick state
H_c	pressure altitude
HUD	Head-up Display
Hz	Hertz
I	Identity matrix
IMS	Inertial Measurement System
I_x	moment of inertia, slug-ft^2
I_{xz}	product of inertia, slug-ft^2
I_z	moment of inertia, slug-ft^2
K1...K9	feedback gains
KCAS	Knots Calibrated Airspeed
KIAS	Knots Indicated Airspeed

ITEM	DEFINITION
K_p	pilot gain
K_s	roll CAS command gain
L_p	stability derivative, sec^{-1}
L_r	stability derivative, sec^{-1}
L_β	stability derivative, sec^{-2}
$L_{\delta as}$	stability derivative, $rad^{-1}sec^{-2}$
$L_{\delta r}$	stability derivative, $rad^{-1}sec^{-2}$
LQG	Linear-Quadratic-Gaussian
MAC	Mean Aerodynamic Chord
MIMO	Multiple Input-Multiple Output
N_p	stability derivative, sec^{-1}
N_r	stability derivative, sec^{-1}
N_β	stability derivative, sec^{-2}
$N_{\delta as}$	stability derivative, $rad^{-1}sec^{-2}$
$N_{\delta r}$	stability derivative, $rad^{-1}sec^{-2}$
N_y	lateral acceleration, $feet/sec^2$
SAFTD	Simulator for Aircraft Flight Test and Development
S/N	Serial Number
T	n X n modal matrix of eigenvectors
T_d	damped period of the dutch roll, sec
TM	Telemetry
U_o	reference speed, ft/sec
USAF	United States Air Force

ITEM	DEFINITION
USAFTPS	USAF Test Pilot School
V	matrix of achievable eigenvectors
Yaps	Yaw, Angle of Attack, Pitot-Static System
Y_{cf}	crossfeed parameter
$|Y_{cf}|$	magnitude of the crossfeed parameter
$arg(Y_{cf})$	phase angle of the crossfeed parameter
Y_r	stability derivative, ft/rad-sec
Y_p	stability derivative, ft/rad-sec
Y_p	pilot transfer function
Y_v	stability derivative, sec^{-1}
$Y_{\delta_{as}}$	stability derivative, $ft/rad-sec^2$
Y_{δ_r}	stability derivative, $ft/rad-sec^2$
X_o	distance lateral accelerometer is forward of center of gravity, ft
Z_o	distance lateral accelerometer is below stability x axis, ft
a_f	filtered output of lateral accelerometer
a_y	lateral accelerometer output, ft/sec^2
beta	sideslip angle, rad
dB	decibel
deg	degrees
ft	feet
g	acceleration of gravity, ft/sec^2
i	$(-1)^{1/2}$

ITEM	DEFINITION
lbs	pounds
mils	milliradians, 0.001 rad
msec	milliseconds, 0.001 sec
p	stability axis roll rate, rad/sec
pg	gyro measured roll rate, rad/sec
phi	bank angle, rad
P_{ss}	steady state roll rate, rad/sec
r	stability axis yaw rate, rad/sec
rad	radians
rg	gyro measured yaw rate, rad/sec
r_{wo}	washed out yaw rate, rad/sec
s	Laplace transform
sec	seconds
t	time, sec
$\underline{u}$	m X 1 control vector
$v_1 \ldots v_4$	servo states
$\underline{v}_i$	ith eigenvector
$\underline{v}_{ia}$	achievable eigenvector
$\underline{v}_{dr}$	dutch roll mode eigenvector
$\underline{v}_{nR}$	Real portion of complex eigenvector
$\underline{v}_{nI}$	Imaginary portion of complex eigenvector
$\underline{v}_{rs}$	roll subsidence mode eigenvector
$\underline{v}_{sp}$	spiral mode eigenvector

List of Abbreviations and Symbols (Continued)

ITEM	DEFINITION
$\underline{w}_i$	linear combination of $\underline{v}_i$
$\underline{x}$	n X 1 state vector
$\underline{y}$	r X 1 output vector
Λ	diagonal matrix of eigenvalues
α	angle of attack, rad
β	sideslip angle, rad
β_{max}	maximum sideslip in a turn, rad
δ_{as}	aileron/spoiler deflection, rad
δ_{asc}	aileron/spoiler deflection commanded to servo, rad
δ_r	rudder deflection, rad
δ_{rc}	commanded rudder deflection, rad
λ_i	ith eigenvalue
λ_{dr}	dutch roll mode eigenvalue
λ_{rs}	roll subsidence mode eigenvalue
λ_{sp}	spiral mode eigenvalue
ϕ	bank angle, rad
ϕ_1	phase angle at twice w_{180}, deg
π	3.1415927...
τ_r	effective roll mode time constant, sec
τ_e	effective time delay, sec
w_1	frequency at twice w_{180}, rad/sec
w_{180}	frequency at which phase angle is 180 deg
w_{bw}	bandwidth frequency, rad/sec

ITEM	DEFINITION
w_d	dutch roll natural frequency, rad/sec
w_D	dutch roll damped frequency, rad/sec
w_ϕ	natural frequency of phi to δ_{as} quadratic numerator, rad/sec
w_{co}	crossover frequency, rad/sec
ζ_d	dutch roll damping factor
ζ_ϕ	damping of phi to δ_{as} quadratic numerator
$(p/\phi)_d$	ratio of p and ϕ components of the dutch roll eigenvector
$|p/\phi|_d$	magnitude of $(p/\phi)_d$
$arg(p/\phi)$	phase angle of $(p/\phi)_d$
$(r/\beta)_d$	ratio of r and β components of the dutch roll eigenvector
$|r/\beta|_d$	magnitude of $(r/\beta)_d$
$arg(r/\beta)$	phase angle of $(r/\beta)_d$
$(\phi/\beta)_d$	ratio of ϕ and β components of the dutch roll eigenvector
$|\phi/\beta|_d$	magnitude of $(\phi/\beta)_d$
$arg(\phi/\beta)_d$	phase angle of $(\phi/\beta)_d$

Abstract

This investigation examines the relationship between an aircraft's lateral-directional handling qualities and its eigenstructure. Historical data were used to identify eigenvalues expected to yield satisfactory handling qualities. Intuition and simple mathematical models were used to develop desirable eigenvectors. For conventional aircraft, the dutch roll eigenvector was shown to be a function of the roll to sideslip (phi/beta) ratio. Candidate eigenstructures, developed using the eigenvalues and eigenvectors predicted to yield good flying qualities were developed which varied the phi/beta ratio of the dutch roll eigenvector.

Control laws to produce the candidate eigenstructures were derived using eigenstructure assignment with output feedback. The control laws were based on a 12th order linear model of the lateral-directional dynamics of the YA-7D DIGITAC aircraft at two flight conditions; 0.4 and 0.6 Mach at 15,000 feet pressure altitude.

The handling qualities of the candidate eigenstructures were examined analytically and in flight tests. Analytical examination used simplified pilot models and frequency response characteristics. An A-7D simulator verified the control laws produced the designed open loop response and were safe for flight.

Flight testing was conducted to evaluate the lateral-directional handling qualities of the YA-7D DIGITAC at 15,000 feet and 0.4 and 0.6 Mach. Specific objectives included: confirm the pole and zero locations of the lateral-directional axes, correlate pilot handling

quality ratings with the phi/beta ratio of the dutch roll mode, and
evaluate eigenstructure assignment as a control law synthesis technique.
Two Head-up Display tracking tasks and an air-to-air tracking task were
flown to evaluate the closed loop handling qualities of the various
eigenstructures.

Technical problems prevented flight testing at 0.4 Mach, but
sufficient data were gathered at 0.6 Mach to meet all other test
objectives. The control laws derived from eigenstructure assignment
successfully achieved the designed open loop response.

Cooper-Harper ratings for the closed loop tasks showed no
correlation with the magnitude of the phi/beta ratio. However, pilots
consistently downgraded control laws with a phase angle of 120 degrees.
The lateral stick dynamics of the YA-7D played an important role in the
low pilot ratings given to the control laws.

Eigenstructure assignment was found to be a valid technique for
derivation of control laws. The ease with which new control laws could
be derived was the most positive feature. The major disadvantage was
the the lack of intuitive interpretation of the control laws which made
problem identification and simple changes difficult.

AN ANALYSIS OF LATERAL-DIRECTIONAL HANDLING QUALITIES AND EIGENSTRUCTURE OF HIGH PERFORMANCE AIRCRAFT

I. Introduction

Background

It has long been recognized that classical methods of control system analysis, such as root locus, Bode, and Nyquist techniques, have several drawbacks when applied to aircraft. First, the classical methods rely on analysis in the frequency domain, and therefore must be considered an indirect approach because the time response must be interpreted from the frequency response. Also, the classical methods become cumbersome when applied to Multiple Input-Multiple Output (MIMO) systems. Still, the techniques have been in use a long time and many specifications, including aircraft handling qualities design objectives, are written in terms of the frequency response.

Modern control theory, including linear-quadratic-Gaussian (LQG) and eigenstructure assignment techniques, use state space models which overcome some of the limitations of the classical approaches. MIMO systems are easily handled and analysis is performed directly in the time domain. However, LQG still suffers from its fundamental mathmatical requirement - the scalar performance criteria. When using LQG, the designer must reduce all the performance requirements to a single quadratic criterion, then solve a very complex nonlinear system of equations. While great strides have been made in recent years to characterize aircraft performance criteria in quadratic form, LQG still often turns out to be a trial and error approach with the designer

1

adjusting the quadratic performance criteria until a reasonable solution
is obtained. Thus, LQG may also be considered an indirect approach.
Quadratic performance criteria rather than aircraft response must be
specified.

Eigenstructure assignment overcomes this last limitation. MIMO
systems are easily handled and desired aircraft response is specified
directly in terms of the closed loop eigenvalues and eigenvectors. The
complex mathmatical methods necessary for LQG are also eliminated.
Furthermore, the order of the closed loop system is not increased since
available states are fed back, an important consideration in minimizing
time delays introduced by higher order effects which degrade flying
qualities. However, the price paid for this simplicity is that the
desired closed loop eigenvalues and eigenvectors must be specified. The
desired eigenvalues are equivalent to the closed loop poles of classical
theory, and therefore a great deal of empirical data exists which
relates aircraft flying qualities to eigenvalue placement (or pole
location). Unfortunately, only a few such relationships exist for the
eigenvectors.

This thesis develops approachs to aid in eigenvector selection.
While the emphasis is on high performance aircraft, the techniques apply
to other aircraft as well.

Assumptions and Limitations

A number of assumptions have been made to simplify the complexity
of evaluating several possible designs. As described in detail later,
the mathmatical models have been made as exact as possible. Servo and

2

actuator states, precompensation filters, and sensor dynamics have all been included to make the designs as realistic as possible. However, no other attempt was made to design a practical controller. The feedback gains are based on point designs, using linearized equations of motion and linearized aerodynamics. No evaluation is made of the sensitivity of the controller gains to changes in flight condition. As a result, gain schedules are not developed, nor is the result of deleting feedbacks with small gains analyzed. In addition, the result of failures in the feedback channels on vehicle stability is not discussed. While none of these assumptions restrict the results, they are considerations that would be necessary in the complete design of a practical aircraft controller.

The linearized aerodynamics used were based on wind tunnel data for a clean A-7D aircraft. The YA-7D DIGITAC aircraft used in the flight tests was modified externally with a Yaw, Angle of Attack, Pitot-Static Probe (YAPS) and carried six pylons with two external pods. The inertia effects of these changes were modeled as closely as possible, but corrections to the aerodynamics were not available. Even though the aerodynamics were not precisely modeled, the effects were small compared to other real world effects and did not significantly affect flight test results. A more complete description of the YA-7D DIGITAC aircraft is given in Section IX.

The last assumption applies to the eigenvalues. As explained later, they were picked to provide the best flying qualities. However, there is generally a range of values over which the flying qualities will be the same, all other variables being held constant. Therefore,

3

there is some flexibility in picking the eigenvalues which can be used to improve the "fit" of the associated eigenvector. This procedure is discussed in detail in Reference 2, but here would introduce one additional variable in the attempt to correlate handling qualities and eigenspace selection and therefore has been avoided. But again, in an actual aircraft control system design, this flexibility could be used to improve the system performance.

II. Eigenstructure Assignment

Response of Linear Systems

The principles of eigenstructure assignment and the difficulty of selecting an eigenstructure to yield good flying qualities is best explained reviewing linear system theory. Consider the system defined by

$$\dot{\underline{x}} = A\underline{x} + B\underline{u} \qquad (1)$$

where $\underline{x}$ is a n X 1 state vector

A is a n X n constant matrix

B is a n X m constant matrix

$\underline{u}$ is a m X 1 control vector

The solution to this linear autonomous system is

$$\underline{x}(t) = e^{At}\underline{x}(0) + \int_0^t e^{At}B\underline{u}(t-T)dT \qquad (2)$$

where $\underline{x}(0)$ is the initial condition.

e^{At} is the state transition matrix and can be solved in terms of the system eigenvalues and eigenvectors. Assuming n unrepeated eigenvalues:

$$e^{At} = Te^{\Lambda t}T^{-1} \qquad (3)$$

where Λ is a n X n diagonal matrix of system eigenvalues, λ_i

$e^{\Lambda t}$ is an n X n diagonal matrix

T is the n X n modal matrix of system eigenvectors

Making this substitution, the solution to Eq (1) becomes:

5

$$\underline{x}(t) = Te^{\Lambda t}T^{-1}\underline{x}(0) + T\int_0^t e^{\Lambda t}T^{-1}B\underline{u}(t-\tau)d\tau \qquad (4)$$

Equation (4) illustrates the fundamental ideas of eigenstructure assignment. Close examination reveals the following:

(1) The eigenvalues determine the <u>decay/growth rate</u> of both the free response and the forced response.

(2) The eigenvectors determine the distribution or shape of the response.

(3) The free response depends on the initial condition, $\underline{x}(0)$, which in turn determines the degree to which each mode will participate. The exact modal distribution is complicated by the term $T^{-1}\underline{x}(0)$.

(4) The forced response is of course dependent on the control input $\underline{u}(t)$. However, the control input distribution among the modes is difficult to predict because of the term $T^{-1}B\underline{u}$.

Thus, it is evident that if feedback is to be used to improve aircraft handling qualities, eigenvector selection as well as pole (eigenvalue) placement must be considered. It is also clear that selection of "optimum" eigenvectors to result in good flying qualities will be difficult because of the T^{-1} terms in the response. Pilot control inputs will be distributed among the modes by the term $T^{-1}B$, further clouding efforts to relate flying qualities and eigenvector selection.

Example

As an example consider the lateral-directional dynamics of the A-7D at 0.4 Mach described by:

$$\dot{\underline{x}} = A\underline{x} + B\underline{u} \qquad (1)$$

where $\quad \underline{x} = [\, r \quad \beta \quad p \quad \phi \,]^T$

$\qquad \underline{u} = [\, \delta_{as} \quad \delta_r \,]^T$

$$A = \begin{bmatrix} -.4652 & 3.732 & .1415 & 0 \\ -.9978 & -.1216 & .0014 & .0761 \\ 1.082 & -14.530 & -1.944 & 0 \\ 0 & 0 & 1.000 & 0 \end{bmatrix} \qquad (5a)$$

$$B = \begin{bmatrix} 1.258 & -2.719 \\ .006 & .034 \\ -15.85 & 2.394 \\ 0 & 0 \end{bmatrix} \qquad (5b)$$

One simple measure of lateral-directional flying qualities is the amount of pilot rudder input necessary to coordinate a turn. That is, large sideslip angles resulting from an aileron input will usually degrade pilot opinion. If no rudder is necessary the turn is perfectly coordinated. Clearly then, it is desirable to eliminate the sideslip response as much as possible to improve turn coordination. In addition, without justification at this time, the dutch roll response will be decoupled so it consists of a pure yawing motion. The methods described in the next section can be used to calculate a feedback matrix, F, such that $\underline{u} = F\underline{x}$ will produce the desired eigenstructure. The gains are

$$F = \begin{bmatrix} .1762 & -1.287 & .0488 & -.0055 \\ .7149 & -2.452 & .0804 & -.0628 \end{bmatrix} \qquad (6)$$

After augmentation the system modal characteristics are:

$$T = \begin{bmatrix} 1.000 + 0i & 1.000 - 0i & 1.0 & 1.0 \\ .112 + .313i & .112 - .313i & .0 & -2.49 \\ 0 & 0 & -.329 & -264.95 \\ 0 & 0 & 13.17 & 105.98 \end{bmatrix} \qquad (7)$$

$$\Lambda = \text{diag}(-1.2 + 2.75i, \quad -1.2 - 2.75i, \quad -.025, \quad -2.50)$$

The eigenvalues show a well damped dutch roll and stable roll subsidence and spiral modes. The corresponding eigenvectors show the desired decoupling of roll response in the dutch roll and the elimination of any sideslip response in the spiral modes. For reasons explained later, there is still a small component of sideslip and yaw rate in the roll subsidence eigenvector.

The sideslip response to a unit step aileron input is:

$$\beta(t) = .186 \, e^{-1.2t} \sin(2.75t + 50.833) + .061 \, e^{-2.5t} - .202 \qquad (8)$$

Thus, although nearly all sideslip response was eliminated from the roll subsidence and spiral modes, the turn was not perfectly coordinated. Even though the free response would not show any sideslip response to an initial roll rate, the forced response produces a steady state sideslip. As stated earlier, this is due to the control mixing occurring through the $T^{-1}Bu$ term. Physically, the adverse yaw generated by the step aileron input excites the dutch roll mode. It illustrates that augmenting the three basic aircraft modes alone may not be sufficient to achieve the desired flying qualities. Additional modification of the control inputs may also be necessary.

Eigenstructure Assignment using Output Feedback

The mathematical basis for eigenstructure assignment using output feedback is explained in detail in Reference 3. The purpose here is to explain the fundamentals, without proof, in a clear understandable manner.

Consider the linear time invarient system described by the equations:

$$\dot{\underline{x}}(t) = A\underline{x}(t) + B\underline{u}(t) \tag{1}$$

$$\underline{y}(t) = C\underline{x}(t) \tag{9}$$

where

i) $\underline{x} \in R^n$, $\underline{u} \in R^m$, $\underline{y} \in R^r$ are the state, control, and output, respectively;

ii) A, B, C are real constant matrices;

iii) rank A = n , rank B = m , rank C = r;

iv) the system is fully controllable and fully observable.

The linear control law is of the form:

$$\underline{u}(t) = F\underline{y}(t) \tag{10}$$

It can be shown the number of closed loop eigenvalues that can be assigned, and number of associated eigenvectors that can be partially assigned is equal to the larger of m or r. The number of entries in each vector exactly chosen is the smaller of m or r. Since for typical aircraft control systems r is greater than m, to increase the number of assigned eigenvalues the number of outputs must be increased. Similarly, to increase the number of entries in each eigenvector that are specified (or improve the "fit"), the number of independent control

inputs must be increased. It follows that with a single control input the designer has no control over the eigenvectors. Substituting Eq (10) into Eq (1) yields:

$$\dot{\underline{x}}(t) = (A + BFC)\underline{x}(t) \tag{11}$$

Assume (λ_i) are the r desired closed loop eigenvalues and $\underline{v}_i$ are the corresponding closed loop eigenvectors. Then it follows they must satisfy:

$$(A + BFC)\underline{v}_i = \lambda_i \underline{v}_i \tag{12}$$

or

$$\underline{v}_i = (\lambda_i I - A)^{-1} BFC\underline{v}_i \tag{13}$$

Let $\underline{w}_i = FC\underline{v}_i$. Then after substitution

$$(\lambda_i I - A)^{-1} B\underline{w}_i = \underline{v}_i \tag{14}$$

The implication of Eq (14) is very important. It shows the desired closed loop eigenvector $\underline{v}_i$ must lie in the subspace spanned by the columns of $(\lambda_i I - A)^{-1}B$. $\underline{w}_i$ represents the linear combination of the columns that results in $\underline{v}_i$. The subspace is dimension m which is the rank of B, the number of independent control variables. Therefore, the number of control variables determines how large the subspace is in which achievable closed loop eigenvectors must reside. Thus, as stated earlier, m components of the desired eigenvector can be specified exactly. And it can be concluded that if the eigenvectors $\underline{v}_i$ are chosen to lie precisely in the subspace spanned by the columns of $(\lambda_i I - A)^{-1}B$, they will be achieved exactly.

In general, however, the desired eigenvectors will not lie precisely in the subspace, and therefore cannot be exactly achieved. In other words, more than m components of the eigenvector are specified.

10

An achievable eigenvector is chosen as the projection of $\underline{v}_i$ onto the subspace spanned by the columns of $(\lambda_i I - A)^{-1}B$ to minimize the sum of the squares of the error. This is most easily accomplished as follows:

Let $$L_i = (\lambda_i I - A)^{-1}B \qquad (15)$$

Then the achievable eigenvector is

$$\underline{v}_{ia} = L_i L^+_i \underline{v}_i \qquad (16)$$

where L^+_i is the generalized inverse of L_i. It is best to calculate the generalized inverse using a singular value decomposition to avoid ill-conditioning difficulties (4).

This procedure also allows partial specification of the eigenvector. It would be difficult to specify each component of every eigenvector. Instead, only those components which the designer wishes to specify and their corresponding equations in L_i are used in the least squares solution of $\underline{v}_{ia}$.

With $\underline{v}_{ia}$ calculated it is easy to calculate $\underline{w}_i$ using Eq (14). $\underline{w}_i$ is then used to find the unspecified components in $\underline{v}_{ia}$. It follows directly from the definition of $\underline{w}_i$ that

$$F = W(CV)^{-1} \qquad (17)$$

where V is made up the eigenvectors that lie in the achievable subspace of $(\lambda_i I - A)^{-1}B$. The inverse of CV will exist provided the desired eigenvectors are linearly independent and the multiplicity of each desired eigenvalue is less than or equal to the smaller of Rank C or Rank B. For those instances where the inverse does not exist, there is usually a design flaw such as noncontrollability.

11

While output feedback does not offer the design flexibility of full state feedback, it is more practical to implement, eliminating the need for observers to estimate those states that cannot be measured. Furthermore, notch filters, integral compensation, and high and low pass filters can be included in the closed loop design. Feedforward gain compensation to modify the control inputs can be left for post design.

Eigenstructure assignment using output feedback does suffer from a couple of drawbacks. First, stability is not guaranteed for those eigenvalues not assigned. That is, the free poles can move to unpredictable and sometimes undesirable places. If they do move to an undesirable location, there is no set method to vary the desired eigenstructure to move them to more satisfactory positions. Also, there is no penalty on the control effort required. The desired eigenstructure may be achieved at the cost of saturating control deflections or rates. While these are legitimate design concerns, they did not cause difficulties in this research. Methods exist (5) to overcome these drawbacks, but full state feedback (or estimation) is required.

The procedure described above was programmed in FORTRAN and used in the design of the control laws used throughout this report. A copy of the program and a description of the implementation (including the incorporation of complex eigenvalues and eigenvectors) is included in Appendix A.

Appendix B contains a sample output of the eigenstructure assignment program.

III. YA-7D Linear Model

Twelfth order models were used to describe the system dynamics as accurately as possible. The linear models used in the analysis were carefully developed to match the aircraft dynamics closely so variations in handling qualities due to changes in the eigenstructure would not be confused with modeling errors. Higher order effects with frequencies less than 100 radians/second (rad/sec) were included in the model. This cutoff frequency was arbitrary, but insured the aircraft response in the frequency range of interest was adequately modeled. Thus, instead of a simple fourth order model to simulate the lateral-directional characteristics of the YA-7D, a 12th order model was necessary. In addition to the four basic aircraft rigid body states, actuator and servo states for the aileron and rudder are included, adding a total of six additional states. High pass and noise filters were also added in the precompensation design of the control system for a total of 12 states. The following discussion explains the development of the state space model in detail.

Rigid Body Equations of Motion

The linear perturbation lateral-directional model used in this report was derived from the nonlinear equations of motion (6:259). These linear equations assume:

i) Stability axes are used with the X axis initially aligned with the horizon.

ii) The perturbations from equilibrium are small.

iii) The aircraft is a rigid body of constant mass.

13

iv) The flow is quasisteady and the aerodynamics can be described by linear terms.

The equations of motion of the rigid body in state space form are:

$$\dot{\underline{x}} = A\underline{x} + B\underline{u} \tag{1}$$

where $\underline{x} = [\, r \quad \beta \quad p \quad \phi \,]^T$

$\underline{u} = [\, \delta_{as} \quad \delta_r \,]^T$

$$A = \begin{bmatrix} N_r' & N_\beta' & N_p' & 0 \\ Y_r/U_o-1 & Y_v & Y_p/U_o & g/U_o \\ L_r' & L_\beta' & L_p' & 0 \\ 0 & 0 & 1 & 0 \end{bmatrix} \tag{18a}$$

$$B = \begin{bmatrix} N_{\delta as}' & N_{\delta r}' \\ Y_{\delta as}/U_o & Y_{\delta r}/U_o \\ L_{\delta as}' & L_{\delta r}' \\ 0 & 0 \end{bmatrix} \tag{18b}$$

where: r - yaw rate, rad/sec
β - sideslip angle, rad
p - roll rate, rad/sec
ϕ - bank angle, rad
δ_{as} - aileron/spoiler deflection, rad
δ_r - rudder deflection, rad

The prime on the aerodynamic derivatives refers to a combined stability derivative that includes product of inertia effects (6:257). For a general motion or input quantity designated by the subscript i,

$$L_i' = \frac{L_i + (I_{xz}/I_x)\, N_i}{1 - (I_{xz}^2/I_x I_z)} \tag{19}$$

$$N_i' = \frac{N_i + (I_{xz}/I_z)\, L_i}{1 - (I_{xz}^2/I_x I_z)} \tag{20}$$

In the remainder of the report the prime will be dropped for convenience. Except where noted otherwise, any reference to a stability derivative refers to the primed derivative.

The aerodynamic data were taken from References 7 and 8. Two flight conditions were chosen to investigate: one g level flight at 15,000 feet pressure altitude (Hc) and 0.40 and 0.60 Mach. The YA-7D exhibits relatively poor lateral-directional characteristics at 0.4 Mach with moderate adverse yaw and poor dutch roll characteristics. The second flight condition, 0.6 Mach, represents a more benign condition where the YA-7D has little adverse yaw and slightly improved lateral-directional characteristics.

The aerodynamic data was for a clean A-7D. The aircraft used in the flight tests was the YA-7D DIGITAC described in Section IX. The primary external differences were the addition of a YAPS head, six pylons, a DIGITAC data pod under the right wing, and an inert MK-82 bomb under the left wing. Unfortunately, exact inertia and aerodynamic data for this configuration were not available. Mass properties from Reference 7 were corrected for the pylons, data pod, and MK-82 and were used with the nondimensional aerodynamic coefficients to calculate the dimensional stability derivatives. No corrections were made to the aerodynamic coefficients for the external vehicle differences and reference angle of attack increase (because of the increased weight of the YA-7D DIGITAC).

The dimensional stability derivatives, vehicle mass properties, and flight conditions are listed in Table I and Table II on the following pages.

Table I

YA-7D Aerodynamic and Vehicle Data (0.4 Mach)			
Mach No.	.40	Weight	27,180 lbs
Altitude	15,000 ft	I_x	20,708 slug ft^2
Load Factor	1.0	I_z	83,020 slug ft^2
Configuration	Clean	I_{xz}	-7,412 slug ft^2
C.G. % MAC	28.71	α Trim	9.55 Deg

N_r'	-0.4260	1/sec
N_β'	3.349	1/sec^2
N_p'	0.1592	1/sec
$N_{\delta as}'$	0.9953	1/rad-sec^2
$N_{\delta r}'$	-2.541	1/rad-sec^2
L_r'	0.8392	1/sec
L_β'	-11.25	1/sec2
L_p'	-1.516	1/sec
$L_{\delta as}'$	-12.23	1/rad-sec^2
$L_{\delta r}'$	1.882	1/rad-sec^2
Y_r	0.0021	1/rad
Y_v	-0.1133	1/sec
Y_p	0.0013	1/rad
$Y_{\delta as}$	0.0058	1/rad-sec
$Y_{\delta r}$	0.0316	1/rad-sec
g/Uo	.0761	1/sec

Actuator and Servo States

The aileron and rudder actuators have bandwidths of 20 rad/sec and 33.33 rad/sec, respectively. They are driven by identical 94 rad/sec, $\zeta = 0.7$ servos. In addition, the YA-7D uses an aileron-rudder interconnect to reduce the adverse yaw due to an aileron/spoiler deflection. It is mechanized through the automatic flight control system by feeding back aileron deflection (measured at the roll servo) to the rudder channel. The crossfeed gain is normally a function of horizontal tail deflection and at 0.4 Mach and 15,000 feet has a value of 0.20. Because of the small amount of adverse yaw at 0.6 Mach, the crossfeed gain was set to zero. No attempt was made to further optimize

16

Table II

```
┌─────────────────────────────────────────────────────────────┐
│           YA-7D Aerodynamic and Vehicle Data (0.6 Mach)       │
│                                                               │
│   Mach No.        .60            Weight      27,180 lbs       │
│   Altitude        15,000 ft      Iₓ          19,900 slug ft²  │
│   Load Factor     1.0            Iᵤ          83,828 slug ft²  │
│   Configuration   Clean          Iₓᵤ         -1,978 slug ft²  │
│   C.G. x MAC      28.71          a Trim      4.63 Deg         │
└─────────────────────────────────────────────────────────────┘
```

N_r'	-0.4979	$1/sec$
N_β'	4.243	$1/sec^2$
N_p'	0.0485	$1/sec$
$N_{\delta as}'$	-0.1145	$1/rad\text{-}sec^2$
$N_{\delta r}'$	-4.889	$1/rad\text{-}sec^2$
L_r'	0.7462	$1/sec$
L_β'	-20.30	$1/sec2$
L_p'	-2.323	$1/sec$
$L_{\delta as}'$	-26.54	$1/rad\text{-}sec^2$
$L_{\delta r}'$	4.662	$1/rad\text{-}sec^2$
Y_r	0.0020	$1/rad$
Y_v	-0.1507	$1/sec$
Y_p	0.0008	$1/rad$
$Y_{\delta as}$	0.0105	$1/rad\text{-}sec$
$Y_{\delta r}$	0.0422	$1/rad\text{-}sec$
g/Uo	.05072	$1/sec$

the gains. The crossfeed can be added directly in the servo equations and the state space model of the servos and actuators becomes:

$$\dot{x} = Ax + Bu \qquad (1)$$

where

$$x = [\ \delta_{as}\quad \delta_r \quad v_1 \quad v_2 \quad v_3 \quad v_4\ ]^T$$

$$u = [\ \delta_{asc}\quad \delta_{rc}\ ]^T \quad \text{(the commanded deflections)}$$

$$A = \begin{bmatrix} -20 & 0 & 20 & 0 & 0 & 0 \\ 0 & -33.33 & 0 & 0 & 33.33 & 0 \\ 0 & 0 & 0 & 1 & 0 & 0 \\ 0 & 0 & -8883 & -131.9 & 0 & 0 \\ 0 & 0 & 0 & 0 & 0 & 1 \\ 0 & 0 & 1777 & 0 & -8883 & -131.9 \end{bmatrix} \qquad (21a)$$

$$
B = \begin{bmatrix} 0 & 0 \\ 0 & 0 \\ 0 & 0 \\ 8883 & 0 \\ 0 & 0 \\ 0 & 8883 \end{bmatrix}
\qquad (21b)
$$

where $v_1 \ldots v_4$ - servo states, rad
δ_{asc} - commanded aileron/spoiler deflection, rad
δ_{rc} - commanded rudder deflection, rad

Sensor Dynamics

The YA-7D DIGITAC Digital Multimode Flight Control System (DFCS) had four quantities available for feedback; body roll and yaw rates, roll angle from the Inertial Measurement System (IMS), and lateral acceleration measured by dual accelerometers mounted 4.78 feet forward of the center of gravity (CG). Therefore, four sensors have dynamics which may have to be considered in the state space model; roll rate gyro, yaw rate gyro, roll angle inertial measurement unit, and lateral accelerometer. The roll rate gyro, yaw rate gyro, and lateral accelerometer have second order dynamics with frequencies of 314 rad/sec, 126 rad/sec, and 100 rad/sec, respectively. These are all high enough that any errors induced by ignoring their dynamics are negligible. The IMS sensing roll angle also has second order dynamics, but at a much lower natural frequency, 31.4 rad/sec. However, experience showed these gains to be relatively small, so the dynamics will also be ignored.

While sensor dynamics can be ignored, sensor position corrections cannot. The roll rate and yaw rate gyros measure rates in body fixed axes. But the state space model is in stability axes, which differ from body fixed axes by the equilibrium angle of attack. Therefore, the

18

measured roll rate will consist of components of both roll and yaw rate as measured in stability axes. Similarly, the measured yaw rate will consist of components from both rates. In addition, the yaw rate gyro is tilted down 2.5 degrees. The transformation is:

$$
\begin{bmatrix} pg \\ rg \end{bmatrix} = \begin{bmatrix} \cos \alpha & -\sin \alpha \\ \sin(\alpha - 2.5) & \cos(\alpha - 2.5) \end{bmatrix} \begin{bmatrix} p \\ r \end{bmatrix}
\tag{22}
$$

where: pg - roll rate gyro output, rad/sec
        p - stability axis roll rate, rad/sec
        rg - yaw rate gyro output, rad/sec
        r - stability axis yaw rate, rad/sec

The correction to the measured roll rate is applied directly in the output matrix C using Eq (22). However, since the yaw rate is filtered prior to feedback, the correction is applied differently. This will be explained in more detail in the next section.

The lateral accelerometer incurs significant error because it is not located at the center of gravity, but 4.78 feet forward. The accelerometer is commonly placed forward of the center of gravity so the measured acceleration is more of a true representation of the sideslip. It picks up a significant contribution from the yaw acceleration which will tend to cancel the contribution to lateral acceleration from the rudder, leaving sideslip the dominant contributor (6:483-487). A similar correction because of the use of stability axes must also be made here as in the section above. The equation for the lateral acceleration at a distance X_o forward of the center of gravity and Z_o below it is

$$
ay = U_o \dot{\beta} - U_o r + X_o \dot{r} - Z_o \dot{p} - g\phi
\tag{23}
$$

In body axes the YA-7D lateral accelerometer is 4.78 feet forward of the CG. Therefore:

$$X_O = 4.78 \cos \alpha$$
$$Z_O = -4.78 \sin \alpha$$

(24)

The development of this portion of the state space model is not yet complete, however, since a noise filter must be added to the accelerometer output. This will be explained in more detail in the next section.

Predesign Compensation

A "high pass" filter was added in the yaw rate feedback channel. The transient yaw rate must be isolated from the steady state response so the control system will not fight the steady state yaw rate associated with a turn. This is classically done by adding a "high pass" or washout filter. The transfer function is:

$$\frac{r_{wo}}{rg} = \frac{s}{s + 1}$$

(25)

where r_{wo} is the washed out yaw rate and rg is the yaw gyro output. This filter will have the effect of passing signals with frequencies higher than one rad/sec while suppressing lower frequency signals, thus achieving the desired effect. Its implementation in the state space model is complicated slightly because the rate filtered is the yaw rate sensed by the gyro, not the stability axis yaw rate used in the model. As discussed in the previous section, the gyro yaw rate will consist of a linear combination of the stability axis yaw rate and roll rate. When

20

this is taken into consideration, the resulting differential equation of the washout filter is

$$\dot{r}_{wo} = \cos(a - 2.5)\ \dot{r}\ +\ \sin(a - 2.5)\ \dot{p}\ -\ r_{wo} \qquad (26)$$

When the necessary computations are made, the washout filter in state space form at 0.4 Mach becomes:

$$\dot{\underline{x}} = A\underline{x}$$

$$\underline{x} = [\ r\ \ \beta\ \ p\ \ \phi\ \ \delta_{as}\ \ \delta_r\ \ r_{wo}\ ]^T$$

$$A = \begin{bmatrix} -.3198 & 1.943 & -.0281 & 0 & -.5133 & -2.291 & -1 \end{bmatrix} \qquad (27)$$

At 0.6 Mach, the state space equation becomes:

$$A = \begin{bmatrix} -.4698 & 3.486 & -.0379 & 0 & -1.101 & -4.712 & -1 \end{bmatrix} \qquad (27b)$$

For simplicity, only the entries for the washout filter have been included in the A matrix. The other entries have been discussed elsewhere and are not changed by the addition of the high pass filter.

To eliminate high frequency noise from the lateral acceleration signal, a low pass or "noise filter" was necessary. The break frequency of the filter, 10 rad/sec, was chosen to eliminate most unwanted noise without having a great effect on the low frequency dynamics. The final form of the filter becomes:

$$\frac{a_f}{a_y} = \frac{10}{s + 10} \tag{28}$$

where a_f is the filtered accelerometer signal. The state space representation at 0.4 Mach of the filtered lateral acceleration signal corrected for position becomes:

$$\underline{\dot{x}} = A\underline{x}$$

where $\underline{x} = [\ r \quad \beta \quad p \quad \phi \quad \delta_{as} \quad \delta_r \quad a_f \ ]^T$

$$A = \begin{bmatrix} -17.53 & -245.11 & 22.50 & 0. & 147.34 & -4.62 & -10 \end{bmatrix} \tag{29}$$

At 0.6 Mach, the state space representation becomes:

$$A = \begin{bmatrix} -19.59 & -539.88 & 31.39 & 0. & 332.48 & -20.91 & -10 \end{bmatrix} \tag{29a}$$

All the necessary portions of the YA-7D state space model have now been developed. The resulting 12th order model is given in Table III and Table IV on the following pages for 0.4 and 0.6 Mach, respectively. A spectral decomposition of the models is included in Appendix B.

Table III

YA-7D State Space Model (0.4 Mach)

$$\dot{\underline{x}} = A\underline{x} + B\underline{u} \qquad \underline{y} = C\underline{x}$$

$\underline{x} = [\ r \quad \beta \quad p \quad \phi \quad \delta_{as} \quad \delta_r \quad v_1$

$\qquad \qquad v_2 \quad v_3 \quad v_4 \quad r_{wo} \quad a_f\ ]^T$

$\underline{u} = [\ \delta_{asc} \quad \delta_{rc}\ ]^T$

$\underline{y} = [\ r_{wo} \quad a_f \quad p_g \quad \phi\ ]^T$

$$A = \begin{bmatrix}
-.4260 & 3.349 & 0.1592 & 0 & 0.9953 & -2.541 & 0 & 0 & 0 & 0 & 0 & 0 \\
-.9979 & -.1133 & 0.0013 & 0.076 & 0.0058 & .03159 & 0 & 0 & 0 & 0 & 0 & 0 \\
0.8392 & -11.25 & -1.516 & 0 & -12.23 & 1.882 & 0 & 0 & 0 & 0 & 0 & 0 \\
0 & 0 & 1 & 0 & 0 & 0 & 0 & 0 & 0 & 0 & 0 & 0 \\
0 & 0 & 0 & 0 & -20 & 0 & 20 & 0 & 0 & 0 & 0 & 0 \\
0 & 0 & 0 & 0 & 0 & -33.33 & 0 & 0 & 33.33 & 0 & 0 & 0 \\
0 & 0 & 0 & 0 & 0 & 0 & 0 & 1 & 0 & 0 & 0 & 0 \\
0 & 0 & 0 & 0 & 0 & 0 & -8883 & -131.9 & 0 & 0 & 0 & 0 \\
0 & 0 & 0 & 0 & 0 & 0 & 0 & 0 & 0 & 1 & 0 & 0 \\
0 & 0 & 0 & 0 & 0 & 0 & 1777 & 0 & -8883 & -131.9 & 0 & 0 \\
-.3198 & 1.943 & -.0281 & 0 & -.5133 & -2.291 & 0 & 0 & 0 & 0 & -1 & 0 \\
-17.53 & -245.1 & 22.50 & 0 & 147.34 & -4.623 & 0 & 0 & 0 & 0 & 0 & -10
\end{bmatrix}$$

Table III (Concluded)

YA-7D State Space Model (0.4 Mach)

$$B = \begin{bmatrix} 0 & 0 \\ 0 & 0 \\ 0 & 0 \\ 0 & 0 \\ 0 & 0 \\ 0 & 0 \\ 0 & 0 \\ 8883 & 0 \\ 0 & 0 \\ 0 & 8883 \\ 0 & 0 \\ 0 & 0 \end{bmatrix}$$

$$C = \begin{bmatrix} 0 & 0 & 0 & 0 & 0 & 0 & 0 & 0 & 0 & 0 & 1 & 0 \\ 0 & 0 & 0 & 0 & 0 & 0 & 0 & 0 & 0 & 0 & 0 & 1 \\ -.1659 & 0 & .9861 & 0 & 0 & 0 & 0 & 0 & 0 & 0 & 0 & 0 \\ 0 & 0 & 0 & 1 & 0 & 0 & 0 & 0 & 0 & 0 & 0 & 0 \end{bmatrix}$$

Table IV

YA-7D State Space Model (0.6 Mach)

$$\dot{\underline{x}} = A\underline{x} + B\underline{u} \qquad \underline{y} = C\underline{x}$$

$$\underline{x} = [\; r \quad \beta \quad p \quad \phi \quad \delta_{as} \quad \delta_r \quad v_1$$
$$v_2 \quad v_3 \quad v_4 \quad r_{wo} \quad a_f \;]^T$$

$$\underline{u} = [\; \delta_{asc} \quad \delta_{rc} \;]^T$$

$$\underline{y} = [\; r_{wo} \quad a_f \quad p_g \quad \phi \;]^T$$

$$A =
\begin{bmatrix}
-.4979 & 4.243 & 0.0485 & 0 & -0.1145 & -4.889 & 0 & 0 & 0 & 0 & 0 & 0 \\
-.9980 & -.1507 & 0.0008 & 0.0507 & 0.0105 & .04219 & 0 & 0 & 0 & 0 & 0 & 0 \\
0.7462 & -20.30 & -2.323 & 0 & -26.54 & 4.662 & 0 & 0 & 0 & 0 & 0 & 0 \\
0 & 0 & 1 & 0 & 0 & 0 & 0 & 0 & 0 & 0 & 0 & 0 \\
0 & 0 & 0 & 0 & -20 & 0 & 20 & 0 & 0 & 0 & 0 & 0 \\
0 & 0 & 0 & 0 & 0 & -33.33 & 0 & 0 & 33.33 & 0 & 0 & 0 \\
0 & 0 & 0 & 0 & 0 & 0 & 0 & 1 & 0 & 0 & 0 & 0 \\
0 & 0 & 0 & 0 & 0 & 0 & -8883 & -131.9 & 0 & 0 & 0 & 0 \\
0 & 0 & 0 & 0 & 0 & 0 & 0 & 0 & 0 & 1 & 0 & 0 \\
0 & 0 & 0 & 0 & 0 & 0 & 1777 & 0 & -8883 & -131.9 & 0 & 0 \\
-.4698 & 3.486 & -.0379 & 0 & -1.101 & -4.712 & 0 & 0 & 0 & 0 & -1 & 0 \\
-19.59 & -539.9 & 31.39 & 0 & 332.54 & -20.91 & 0 & 0 & 0 & 0 & 0 & -10
\end{bmatrix}$$

25

Table IV (Concluded)

YA-7D State Space Model (0.6 Mach)

$$B = \begin{bmatrix} 0 & 0 \\ 0 & 0 \\ 0 & 0 \\ 0 & 0 \\ 0 & 0 \\ 0 & 0 \\ 0 & 0 \\ 8883 & 0 \\ 0 & 0 \\ 0 & 8883 \\ 0 & 0 \\ 0 & 0 \end{bmatrix}$$

$$C = \begin{bmatrix} 0 & 0 & 0 & 0 & 0 & 0 & 0 & 0 & 0 & 0 & 1 & 0 \\ 0 & 0 & 0 & 0 & 0 & 0 & 0 & 0 & 0 & 0 & 0 & 1 \\ -.0807 & 0 & .9967 & 0 & 0 & 0 & 0 & 0 & 0 & 0 & 0 & 0 \\ 0 & 0 & 0 & 1 & 0 & 0 & 0 & 0 & 0 & 0 & 0 & 0 \end{bmatrix}$$

IV. Eigenvalue Selection

Fortunately, there is a great deal of empirical data to assist in the selection of the desired closed loop eigenvalues. *Military Specification, Flying Qualities of Piloted Vehicles - MIL-F-8785C* (9) and the background information in Reference 10 have extensive charts relating the eigenvalues of the three basic aircraft lateral-directional modes to pilot opinions. In the following discussion, the eigenvalues are picked to yield Level 1 flying qualities (equivalent to less than 3.5 on the Cooper-Harper scale). They were chosen for Class IV aircraft (fighter- interceptor, attack, etc) and Category A Flight Phase (air-to-air combat, ground attack, etc). These are the most stringent criteria and apply to most of the A-7D missions.

Roll Subsidence Mode

Because of its importance to flying qualities, there is a large empirical data base relating this eigenvalue to pilot opinion. The selection is a little clouded because other factors, such as the stick force shaping, aileron power ($L\delta_{as}$), and adverse yaw ($N\delta_{as}$) all play a role in the optimum value. Prefilters in the YA-7D roll Command Augmentation System (CAS) slow the response and must also be considered. However, it is clear there are upper and lower bounds on this eigenvalue. If it is too large, the roll response will likely be rated too sensitive and abrupt and can lead to "roll ratcheting," a type of pilot induced oscillation. If the value is too small, the response will be "sluggish".

Paragraph 3.3.1.2 of MIL-F-8785C requires a minimum value of 1.0 for the roll mode eigenvalue (9:23). Although a maximum value is not included in current requirements, the supporting data suggests that when the roll mode eigenvalue is greater than 3.0 there is a constant degradation in pilot opinion. Several examples of eigenstructure assignment in the literature (2 and 5) have used 4.0 for the roll subsidence mode eigenvalue, but this is likely too high. A value of 2.5 is near optimum.

Because of the prefilters in the CAS, a faster time constant must be chosen. With this consideration, the optimum value for this eigenvalue is chosen to be:

$$\lambda_{rs} = -4.0 \tag{30}$$

Spiral Mode

The spiral eigenvalue has little direct effect on flying qualities. MIL-F-8785C does not even require stability, specifying a minimum time to double of 12 seconds (9:23). While there are some data that indicates there should be a limit on the degree of positive spiral stability, other data show strong positive spiral stability can be beneficial. However, the degree of positive stability is indirectly limited by the limit on aileron forces in turns and the required roll maneuverability. Thus, from a handling qualities point of view, the selection of this eigenvalue is arbitrary and it could be argued that there is no point in expending the control effort to place it. However, the elimination of sideslip from the spiral modal response is crucial to a coordinated turn. In this case, the eigenvalue is not critical, but

the eigenvector is. Therefore, the spiral eigenvalue is arbitrarily chosen to be:

$$\lambda_{sp} = -.025 \tag{31}$$

This corresponds to a time to half of 28 seconds.

Dutch Roll Mode

Allowable dutch roll oscillations are specified in terms of minimum values of the damping ratio (ζ_d), natural frequency (w_d), and $\zeta_d w_d$; the last of which is a function of the roll angle to sideslip ratio, $|\phi/\beta|$ when that ratio is large. The minimum recommended values from paragraph 3.3.1.1 of MIL-F-8785C (9:22) are:

Min ζ_d	Min $\zeta_d w_d$	Min w_d
0.4	0.4	1.0

When $w_d^2|\phi/\beta|_d$ is greater than 20 (rad/sec)^2, the minimum $\zeta_d w_d$ should be increased by $0.014(w_d^2|\phi/\beta|_d - 20)$. These are minimum values only, however the data base does not support increasing the minimum damping ratio above 0.4 (10:494-502). Also the dutch roll eigenvector, and therefore $|\phi/\beta|_d$, is as yet unspecified. Therefore, the dutch roll eigenvalue must be picked so any anticipated values of $|\phi/\beta|_d$ will still yield Level 1 flying qualities. With this in mind, the value selected for the dutch roll eigenvalue is:

$$\lambda_d = -1.2 \pm 2.75i \quad (\zeta_d = 0.4; w_d = 3.0) \tag{32}$$

This value of λ_d meets Level 1 criteria for $|\phi/\beta|$ less than 8.6.

V. Eigenvector Selection

As discussed in the Section II, the selection of eigenvectors is difficult because of the T^{-1} distribution of control inputs and initial conditions among the modes. However, if the aircraft is to have good handling qualities it must respond with aircraft-like dynamics (10:545), regardless of the complexity of control laws. In other words, the augmented vehicle should have dominant modes corresponding to the dutch roll, roll subsidence, and spiral. The selection of eigenvalues in the last section assured the augmented modes will be near the frequencies of the usual rigid body modes. But, in addition, the augmented mode shapes must be similar to those of the classical modes. For example, an aircraft whose roll subsidence response was primarily in yaw would likely have unacceptable flying qualities. This idea leads to restrictions on the acceptable eigenvectors. Furthermore, because of the fundamental kinematic relationship between roll rate and bank angle, it would make no sense to specify a response in one of these eigenvector components and none in the other. While these intuitional insights provide useful bounds on the eigenvectors, and are particularly useful in choosing the roll subsidence and spiral eigenvectors, they are little help in selecting the dutch roll eigenvector.

In the following discussion, eigenvectors will be selected to yield Level 1 handling qualities. Selection will be based on the intuitional ideas developed earlier as well as the modal characteristics of simplified fourth order lateral-directional models.

The eigenvector components were developed in Section III. and are
repeated here for convenience:

$$\underline{v} = [\ r \quad \beta \quad p \quad \phi \quad \delta_{as} \quad \delta_r \quad v_1 \quad v_2$$

$$v_3 \quad v_4 \quad r_{wo} \quad a_f\ ]^T$$

Only the first four components will be used in the eigenvector design.
Therefore, in the following discussion they are the only ones shown.
The other components are left unspecified.

Roll Subsidence Eigenvector

This eigenvector has the most effect on the sideslip which develops
while rolling and is very important in attaining good turn coordination.
Sideslip may develop in a turn either from yaw-roll coupling or through
adverse yaw from the aileron input. The roll subsidence eigenvector
will determine the magnitude and sign of the yaw-roll coupling.
Ideally, the response should be in roll rate and bank angle with no
sideslip or yaw response. That is, a roll rate should not produce
yawing moments or sideforce. The roll subsidence eigenvector becomes:

$$\underline{v}_{rs} = [\ 0 \quad 0 \quad 1 \quad x\ ]^T \tag{33}$$

where the x indicates the value is not specified and is arbitrary. It
is not necessary to specify the bank angle mode content because of the
kinematic relationship between p and phi. Since there are three
components specified, they will not be achieved precisely. As explained
in Section II, only m components of each eigenvector can be exactly
achieved. Since there are only two independent lateral-directional
control inputs and three desired components of the eigenvector to be

31

placed, they will be projected into the achievable eigenspace in a least squares manner. Therefore, this mode will still make a very small contribution to the sideslip and yaw rate.

An example illustrates the effects of this eigenvector. It is possible to use this eigenvector to control the sideslip and improve turn coordination, even with adverse yaw present. For the classical fourth order lateral-directional system, yaw-roll coupling will be minimized when $Np = g/U_o$. However, for aircraft with large $N\delta_{as}$ the aileron will still introduce significant yaw, producing an uncoordinated roll. The roll subsidence eigenvector can be selected to balance the moment produced by the adverse yaw with moments from the roll itself through the augmented Np. Consider again the simple example for the A-7D used in section II. In that example, the roll subsidence eigenvector given by Eq (33) was used in the eigenstructure assignment. If the roll subsidence eigenvector is instead specified by

$$\underline{v}_{rs} = [1 \quad 0 \quad -12.6 \quad x]^T \qquad (34)$$

the sideslip response to a step aileron input becomes

$$\beta(t) = .14 \, e^{-1.2t} \sin(2.75t + 108.6) - .116 \, e^{-2.5t} - .039 \qquad (35)$$

Figures 1 and 2 show the beta time response for a step aileron input for the two cases. Clearly, the second eigenstructure produces much less sideslip and would likely receive a higher pilot rating. The roll rate response is unaffected by the change in the roll subsidence eigenvector and is shown in Figure 3 for both cases.

BETA VS TIME FOR STEP AILERON

F(T) RESPONSE 010⁻¹

TIME (SECONDS)
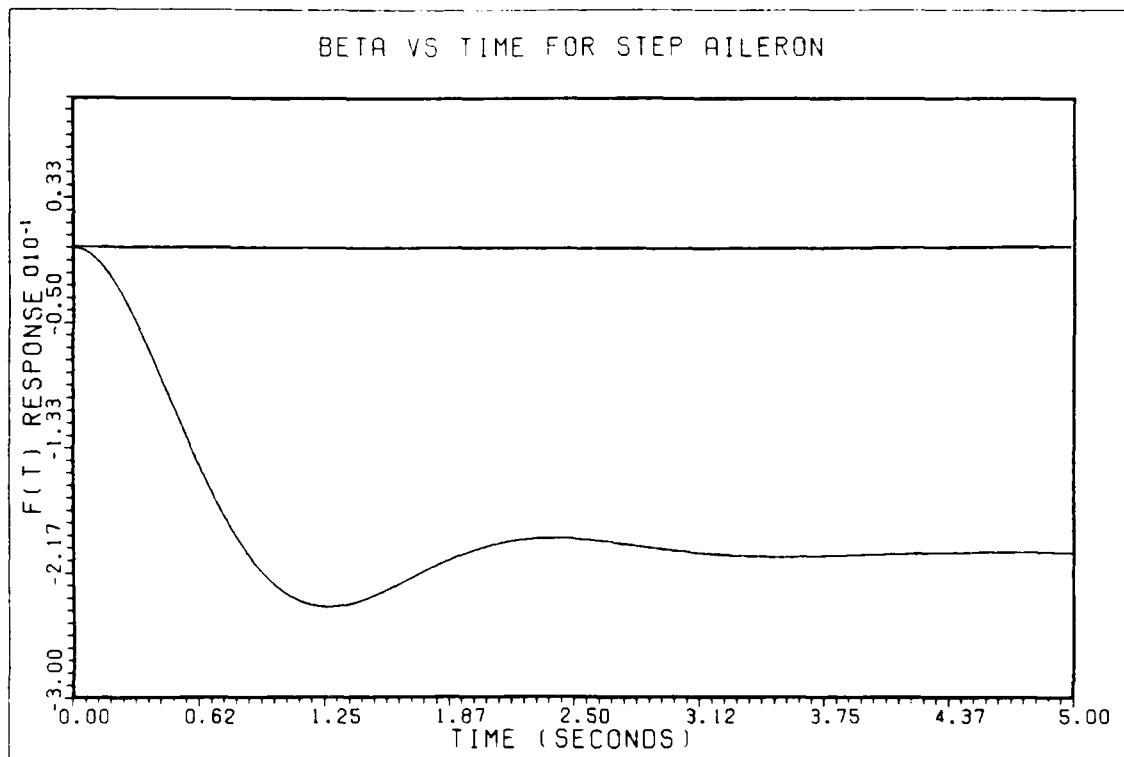
Figure 1. Beta vs Time for $\underline{v}_{rs}$ = [0   0   1   x]

BETA VS TIME FOR STEP AILERON

F(T) RESPONSE 010⁻¹

TIME (SECONDS)
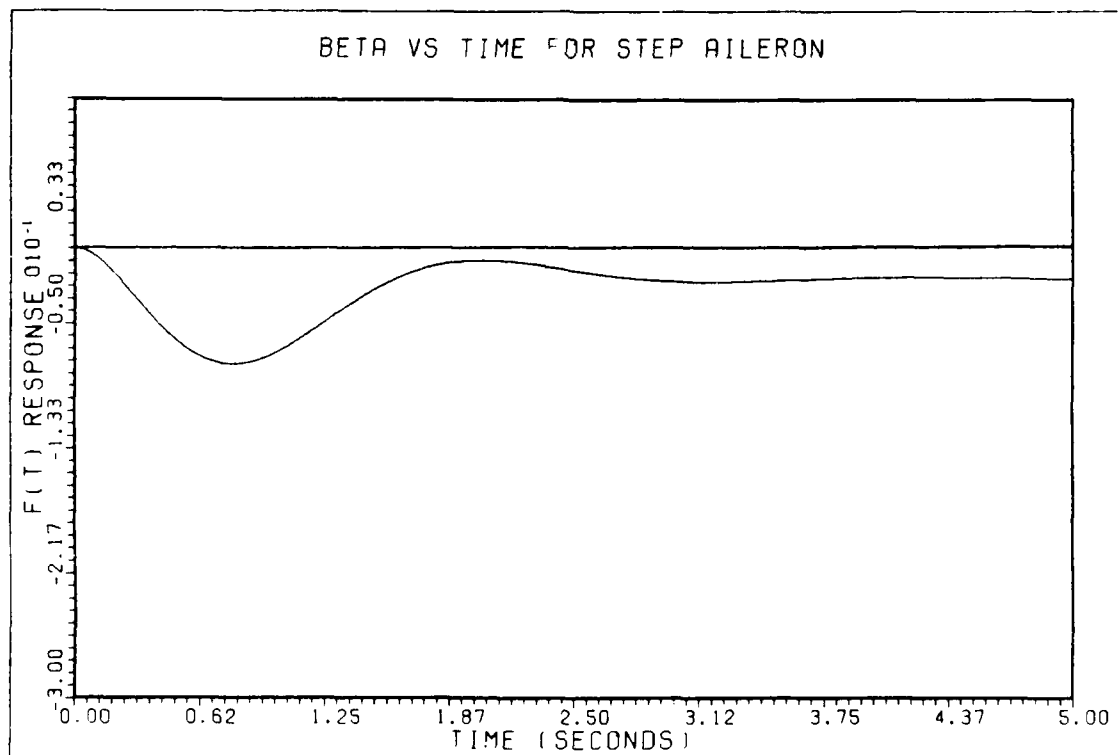
Figure 2. Beta vs Time for $\underline{v}_{rs}$ = [1   0   -12.6   x]
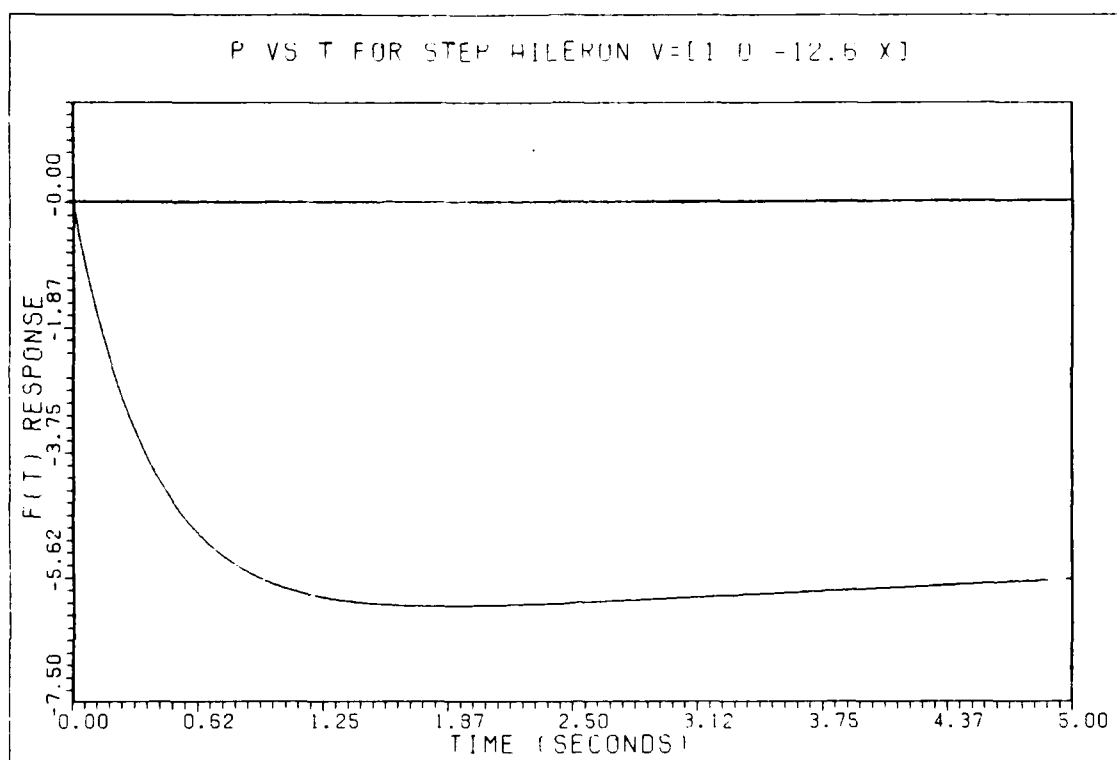
Figure 3. Roll Rate vs Time for Step Aileron Input

While it is theoretically possible to improve turn coordination with this method, it is not practical. An aileron-rudder crossfeed as used in the A-7D design and many other modern aircraft is a better method to reduce the adverse yaw. Although the sideslip buildup for a forced response is reduced using the eigenvector in Eq (34), the free response to a roll rate disturbance would be unconventional, with sideslip content. This is undesirable and would violate the notion that an aircraft should behave like a conventional aircraft to have good flying qualities. Therefore, Eq (33) will be used to specify the eigenstructure.

Spiral Mode Eigenvector

As in the case of the roll subsidence eigenvector, an understanding of the dynamics makes specification of this eigenvector relatively easy. Since a stable spiral mode was specified, there will be small mode contents in yaw rate, but the primary response should be in roll rate and bank angle. Sideslip content must be zero to prevent a continuous buildup over this long acting mode and is necessary for a coordinated turn. The desired spiral eigenvector is:

$$\underline{v}_sp = [\begin{array}{cccc} x & 0 & x & 1 \end{array}]^T \quad (36)$$

Since there are only two components specified, they will be achieved exactly in the eigenstructure assignment.

Dutch Roll Eigenvector

The dutch roll eigenvector is the most difficult to specify. Because the eigenvalue is a complex quantity, the corresponding eigenvector must also be complex. Therefore, the designer must specify at least some of the real and imaginary quantities. Or in other words, the relative magnitude and phase relationship (or portions of each) of the eigenvector components must be designated.

Physical intuition, which was helpful in the design of the real eigenvectors, gives less guidance in this case. So the fourth order rigid body lateral-directional equations of motions discussed in Section III will be used to develop modal response ratios. By examining the modal response ratios for this simplified model, it will be possible to gain insight into the makeup of the dutch roll eigenvector. Since one of the eigenvector components is arbitrary, there are three modal

35

response ratios to be analyzed. The ones chosen are $(p/\phi)_d$, $(r/\beta)_d$, and $(\phi/\beta)_d$.

The examination of the modal response ratios of the simplified equations of motion will begin with $(p/\phi)_d$. This is a simple kinematic relationship which can be determined exactly (6:82). The magnitude of the response ratio is determined by the natural frequency:

$$|p/\phi|_d = w_d \qquad (37)$$

Similarly, the phase angle is given by:

$$\arg(p/\phi) = \pi/2 + \sin^{-1} \zeta_d \quad \text{rad} \qquad (38)$$

Thus, with positive damping, the roll rate will always lead the bank angle by at least 90 degrees. It is important to note that the ratio of these eigenvector components is determined entirely by the dutch roll eigenvalue. Once a desired damping ratio and natural frequency are chosen, $(p/\phi)_d$ is uniquely specified. Also, since this is a kinematic relationship, it will hold for higher order linear systems as well.

The ratio of the yaw rate and beta eigenvector components, $(r/\beta)_d$, is also determined by a relatively simple relationship (6:418):

$$(r/\beta)_d = - \lambda_d + Y_v + g/U_o \, (\phi/\beta)_d \qquad (39)$$

The designer has little more flexibility here than for $(p/\phi)_d$. This is because without direct sideforce control, the effective Y_v can only be slightly modified by the closed loop controls. Thus, once $(\phi/\beta)_d$ and the dutch roll eigenvalue are chosen, $(r/\beta)_d$ is determined.

36

For conventional aircraft with moderate $(\phi/\beta)_d$, the following approximations give good results even with higher order dynamics:

$$|\dot{r}/\beta|_d \doteq w_d \tag{40}$$

and

$$\arg(\dot{r}/\beta) \doteq \cos^{-1}(\zeta_d) - \pi \quad \text{rad} \tag{41}$$

Intuitively, this makes sense. If sideforces are ignored and the dutch roll is "snakey" with small $(\phi/\beta)_d$, sideslip rate is equal to yaw rate.

It is clear that for conventional aircraft $(p/\beta)_d$ and $(r/\beta)_d$ are largely determined by the dutch roll eigenvalue. Thus, the last modal response ratio, $(\phi/\beta)_d$, will be most critical in determining the desired structure of the dutch roll eigenvector. For a fourth order lateral-directional system (6:416-417):

$$(\phi/\beta)_d \doteq \frac{-L_r(s - [Y_v + (L_\beta/L_r)])}{s^2 - L_p s - (g/U_o)L_r} \tag{42}$$

where s is evaluated at the complex dutch roll root. The approximate magnitude response is

$$|\dot{\phi}/\beta|_d \doteq$$
$$\left[\frac{(L_\beta + Y_v L_r)^2 + 2\zeta_d w_D L_r(L_\beta + Y_v L_r) + (w_D L_r)^2}{w_D^2(L_p^2 + 2\zeta_d w_D L_p + w_D^2)} \right]^{1/2} \tag{43}$$

and the corresponding phase angle is approximately

37

$$\arg(\phi/\beta)_d =$$

$$\tan^{-1} \frac{(1-\zeta_d^2)^{1/2}(L_pL_\beta + 2\zeta_d w_D L_\beta + w_D^2 L_r)}{w_D(2\zeta_d^2-1)L_\beta + \zeta_d w_D^2 L_r + \zeta_d w_D L_p L_\beta + w_D L_r L_p} \tag{44}$$

where w_D is the damped frequency of the dutch roll.

Thus, the problem of selecting the dutch roll eigenvector has been reduced to selecting an "optimum" value of $(\phi/\beta)_d$, which is typically a complex function of L_β, L_r, and the system eigenvalues, λ_d and λ_{rs}. $(\phi/\beta)_d$ is addressed in MIL-F-8785C only indirectly. First, as $|\phi/\beta|_d$ increases, the minimum acceptable dutch roll damping and frequency are increased as discussed in Section IV. As long as the dutch roll has reasonable frequency and damping the magnitude of $(\phi/\beta)_d$ can be quite large. For the eigenvalue selected in this report, $|\phi/\beta|_d$ as large as 8.6 still meets Level 1 criteria. Presently no lower limits on $|\phi/\beta|_d$ exist because of conflicting data. Some data (10:417) indicate pilots like dihedral to damp the dutch roll by ailerons alone. This is typically done by KC-135 pilots in the power approach configuration. On the other hand, pilots evaluating the YC-15 with zero effective dihedral liked it, commenting on the uncoupled yaw response to rudder (10:417). With the dutch roll well controlled, pilot damping should not be necessary, so zero dihedral should not be a problem. Thus, $|\phi/\beta|_d$ from zero to approximately eight meet Level 1 criteria.

Paragraph 3.3.6.3 of MIL-F-8785C (9:33) restricts the phase angle, $\arg(\phi/\beta)$. Pilots have been trained to expect the aircraft to roll left when left rudder is applied. This requirement specifies that for an increase in right sideslip, the pilot must add zero or right bank to

38

maintain equilibrium. This is equivalent to specifying the effective dihedral be positive. Dihedral in flying qualities work normally refers to the phasing of the roll and sideslip motion in the dutch roll, $\arg(p/\beta)_d$. With positive dihedral, left rolling accompanies right sideslipping and vice versa in the dutch roll oscillation. This definition is still somewhat ambiguous. A more precise definition which makes intuitive sense from a pilots point of view is to define positive dihedral as p leading β by 90 deg to 270 degrees. At 90 and 270 degrees a pilots rudder input will cause no rolling motion from the dutch roll, while at 180 degrees the rolling moment will be greatest. This definition also appears to comply with paragraph 3.3.6.3 of MIL-F-8785C since a left rudder will produce a left rolling moment from the dutch roll. However, it may not always produce an overall aircraft left rolling moment due to rolling moment contribution from the rudder deflection itself which opposes the dutch roll.

The phase angle between p and phi, 113.6 degrees, can be calculated directly from Eq (38) using the design damping ratio. Using this relationship, it is easy to show the range of $\arg(\phi/\beta)_d$ for positive dihedral as defined above is from 336.4 to 156.4 degrees. Because of the rudder contribution to the rolling moment, compliance with paragraph 3.3.6.3 requires this range of phase angles to be decreased. For this study, $\arg(\phi/\beta)_d$ from 0 to 120 degrees was arbitrarily chosen.

The last requirement of MIL-F-8785C puts implicit limits on $(\phi/\beta)_d$ by restricting the oscillations in the roll response to a step aileron input (9:24). When the dutch roll content in the roll response becomes excessive, precise roll response becomes difficult and pilot opinion

39

will be downgraded. Paragraph 3.3.2.2 restricts the amount of
oscillation in the roll response. This indirectly limits the position
of the zeros of the quadratic numerator of the phi to δ_{as} transfer
function, which in turn determines the degree of dutch roll excitation
due to aileron deflection. The indirect effects of $(\phi/\beta)_d$ can be seen
in the following equations (6:463):

$$(w_\phi/w_d)^2 = 1 - (L_\beta/N_\beta) \ (N_{\delta_{as}}/L_{\delta_{as}}) \qquad (45)$$

$$2(\zeta_\phi w_\phi - \zeta_d w_d) = L_\beta/N_\beta(N_p - g/U_o) \qquad (46)$$

For nonzero $N_{\delta_{as}}$, the position of the zero relative to the pole
changes as L_β and L_r vary. Changes in L_β and L_r will, of course affect
$(\phi/\beta)_d$. For $N_{\delta_{as}}$ equal to zero, the dutch roll pole and zero will
exactly cancel and $(\phi/\beta)_d$ will have no effect on the phi to δ_s transfer
function. Intuitively, if there is no adverse or proverse yaw, the
dutch roll mode will not be excited by aileron inputs and there will be
no oscillations in the roll response regardless of $(\phi/\beta)_d$. When the
numerators do not cancel, the dutch roll content occurs primarily in yaw
and sideslip if $|\phi/\beta|_d$ is low (less than 1.5) or primarily in the roll
axis when $|\phi/\beta|_d$ is large.

This requirement of MIL-F-8785C generally applies for aircraft with
dutch roll frequency and damping close to the Level 1 boundary. In this
case, the dutch roll frequency and damping were chosen to be well within
Level 1 criteria, even for large $|\phi/\beta|_d$. Thus, the dutch roll effects
on the roll response will be small because of the high damping. Also,
adverse yaw in the YA-7D is effectively controlled using aileron-rudder

40

feedback. Thus, this specification adds no direct restrictions on $(\phi/\beta)_d$.

Another effect for nonzero $N\delta_{as}$ is the reduction of steady state roll performance with increasing $L\beta/N\beta$. This follows from Eq (45) and (6:376)

$$P_{ss} = L\dot{\delta}_{as}/L_p \ (w\phi/w_d)^2 \ \delta_{as} \qquad (47)$$

For adverse yaw ($N\delta_{as} < 0$) and negative $L\beta$, significant degradation in roll performance can occur. The effect of $(\phi/\beta)_d$ is not obvious because of the phase angle, but the reduction in roll performance should be greatest when p leads β by 180 degrees.

MIL-F-8785C puts no other restrictions on $(\phi/\beta)_d$. So, compliance requires $|\phi/\beta|_d$ less than 8.6 and $\arg(\phi/\beta)_d$ from 0 to 120 degrees. Another consideration is response in gusty wind conditions. For increasing $(\phi/\beta)_d$, more of the dutch roll response will occur in roll. Therefore, in gusty wind conditions the pilot will have to work harder to maintain a desired bank angle. Exact limits on pilot acceptance of this condition are difficult to identify, more so in this case since the dutch roll is very well damped which reduces the gust perturbations. Thus, there is no easy way to include these considerations.

One other criteria for selecting the dutch roll eigenvector has no direct bearing on the handling qualities. It has been shown that the eigenstructure will be most tolerant to errors in modeling when the eigenvectors are orthogonal in the state space (11). Selecting $(\phi/\beta)_d$ of zero will meet this criteria.

VI. Flight Control System Design

YA-7D Digital Multimode Flight Control System

The Digital Multimode Flight Control System (DFCS) was designed to duplicate the operation and functions of the standard Automatic Flight Control System (AFCS) and to provide pilot selectable "multimodes" which implemented specified control laws. For this test, the standard DIGITAC multimodes were replaced with the controls derived in the this report. The new control laws were individually selectable from the cockpit using the Multimode Control Panel shown in Figure 4. The control laws were selected using switches P2, P3, and P4. The P7 switch was used to make the roll CAS prefilter time constant cockpit selectable from 0.300, 0.125, or 0.025 seconds. The remaining switches were not used. The standard control modes provided by the DFCS are described in the Flight Manual, USAF Series A-7D Aircraft (12) and included the standard CAS modes of:

1. Yaw Stability Augmentation
2. Pitch and Roll Control Augmentation
3. Attitude Hold
4. Heading Hold
5. Heading Select
6. Altitude Hold

During the test, the pitch CAS, and roll CAS described in the following paragraph were on. The other CAS modes were used between test points, but were off during testing.
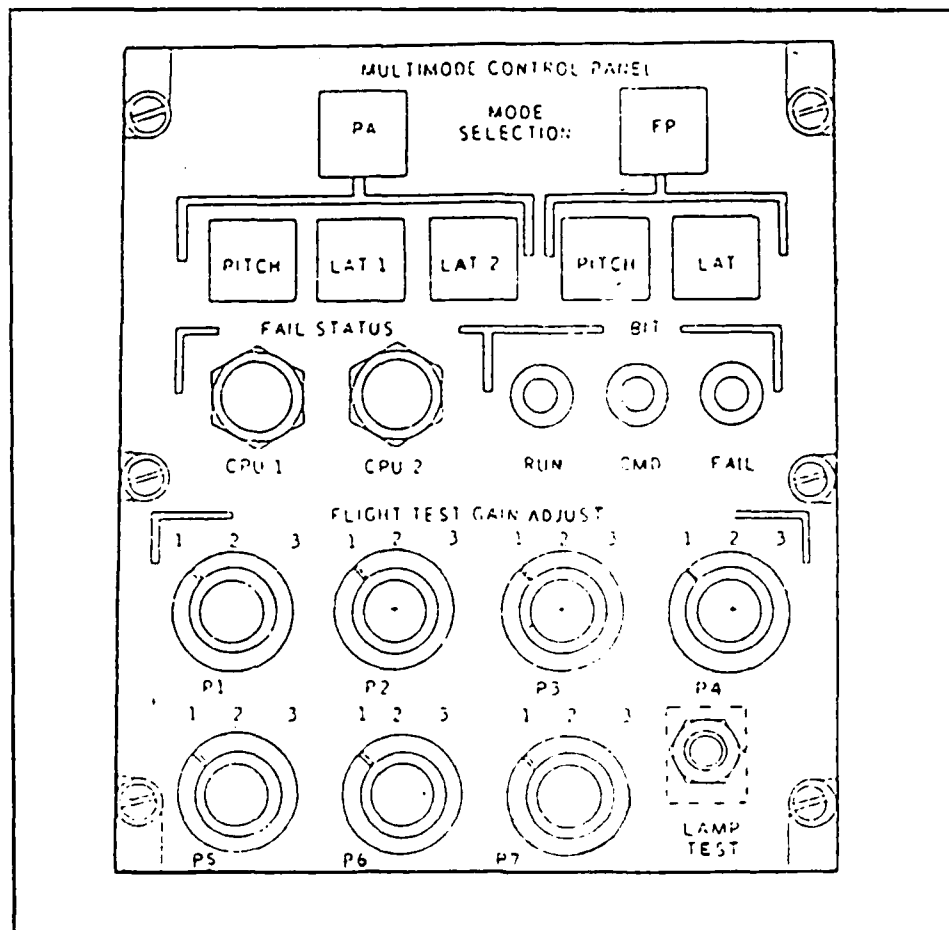
42

Figure 4. Multimode Control Panel

YA-7D Roll Command Augmentation System Design

The roll and yaw control systems are shown in Figures 5 and 6, respectively. The YA-7D used a combination of electrical and mechanical systems to feed pilot lateral inputs to the ailerons. The mechanical system was a conventional direct link to the aileron actuator, and was limited to 15 degrees of commanded deflection. The electrical CAS, limited to 10 degrees, provided a more uniform roll response. The CAS used lateral stick force as the input. Because the emphasis of this investigation was on eigenstructure assignment and not on control
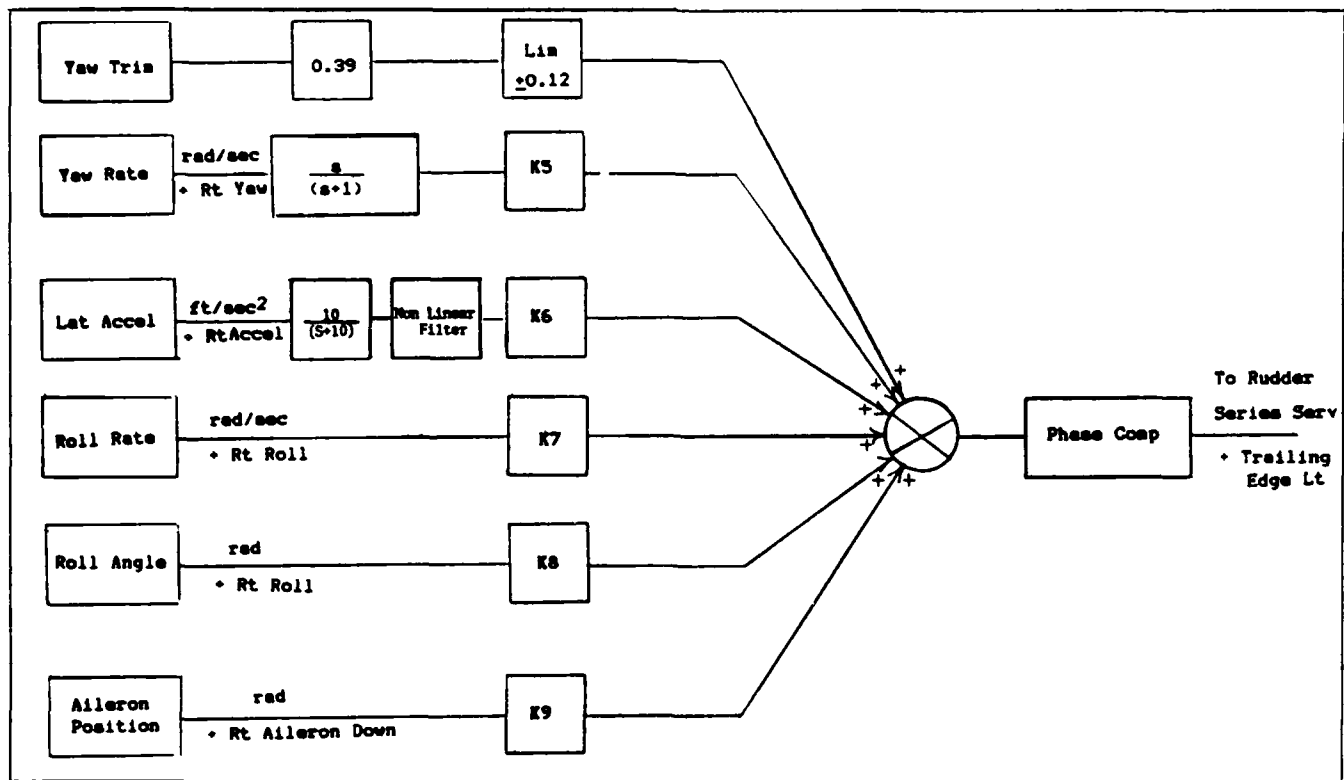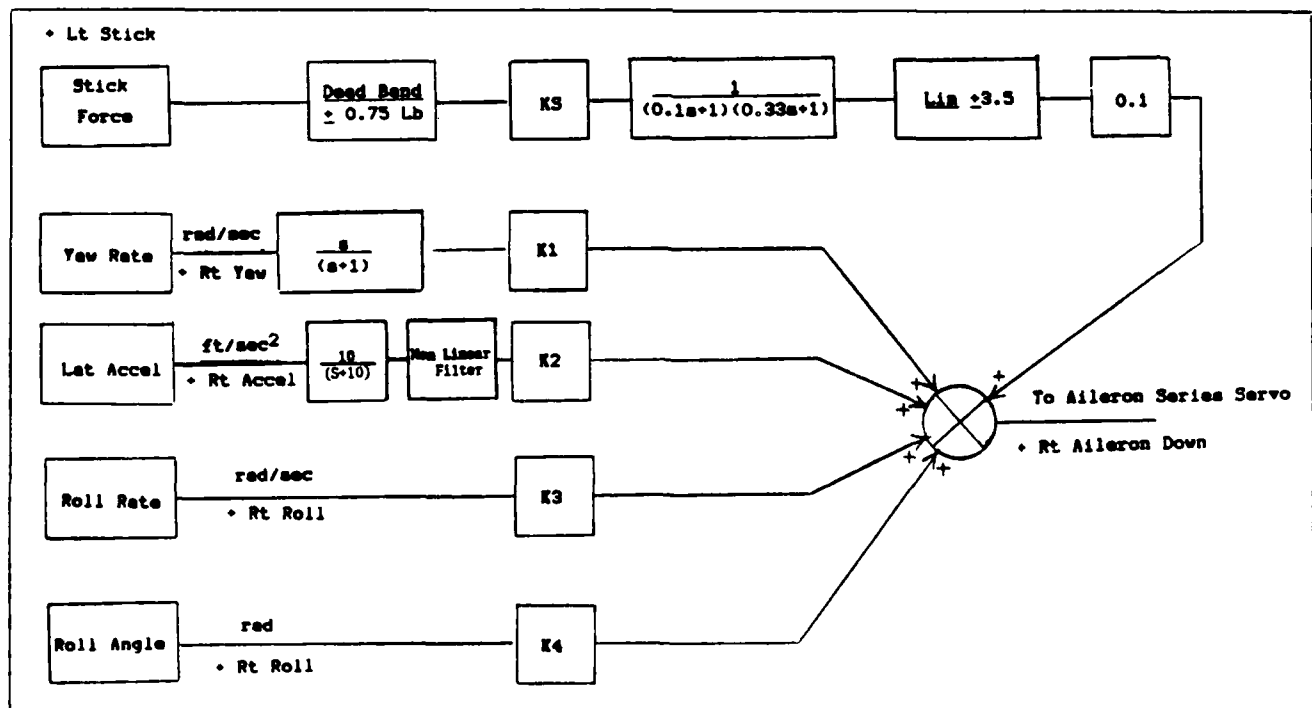
Figure 5.   Yaw Axis Control System

Figure 6.   Roll Axis Control System

44

system design, the mechanical system was unchanged. The electrical CAS command gain, Ks, was left variable to allow the roll response per stick force, p_{ss}/F_s, to be adjusted if necessary. In addition, the two linear prefilters in the CAS command path were left unmodified.

The resulting roll CAS is unconventional. Typically, an error signal is calculated from the stick force and roll rate, multiplied by the command gain, and fed to the aileron series servo as shown in Figure 7. However, with eigenstructure assignment, roll rate alone does not augment the roll subsidence mode, which is the response controlled by the lateral stick. Therefore, all four quantities that are being fed back are compared to the stick force to calculate the error signal.
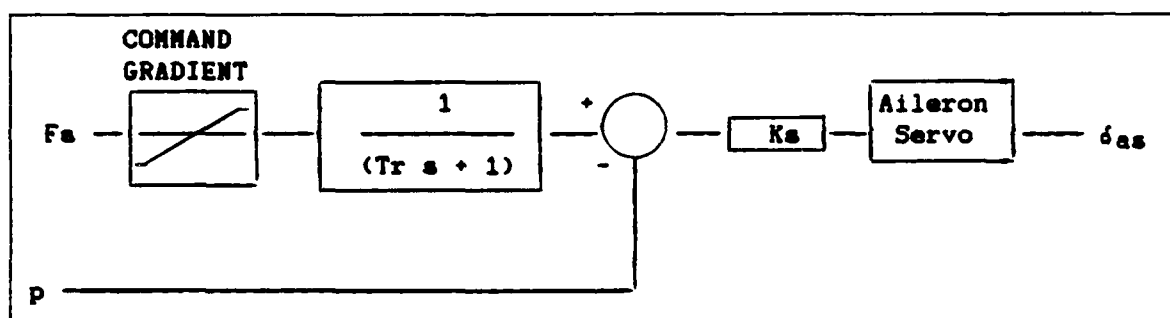
Figure 7. Block Diagram of Typical Roll CAS

Feedback Gain Calculation

The inputs necessary to calculate the feedback gain matrix, F, were developed in the previous sections. A unique set of eigenvalues were derived which yield modes equivalent to the dutch roll, roll subsidence, and spiral. A unique set of eigenvectors for the roll subsidence and spiral modes were also developed, but insufficient historical data were available to uniquely identify the optimum dutch roll eigenvector. Sufficient data did exist, however, to bound it. Therefore, gains were

45

calculated to yield eigenstructures for a range of $(\phi/\beta)_d$ which met
requirements of MIL-F-8785C (9). Flight testing was then conducted on
all candidate eigenstructures. The test matrix is shown in Table V.
Gain matrices were calculated using the computer program in Appendix A
and the linear models for the two flight conditions, 0.4 and 0.6 Mach at
15,000 feet Hc. The control law gains are shown in Tables VI and VII
for 0.4 and 0.6 Mach, respectively.

Table V

Phi To Beta Test Matrix			
Phi/Beta Magnitude Ratio	Phi/Beta Phase Angle		
	0	60	120
0	x		
1.5	x	x	x
3.0	x	x	x

Table VI

Control Law Gains (0.4 MACH)

PHI/BETA RATIO		FEEDBACK GAINS				
MAGNITUDE	PHASE ANGLE	K1 K6	K2 K7	K3 K8	K4 K9	K5
0	0	.4596 .0798	.0401 -.0835	.1088 -.0063	.1049 .2000	1.172
1.5	0	.4115 .0708	.0122 -.0868	.1094 -.0072	.0124 .2000	1.178
1.5	60	-.0567 .0650	.0002 -.0581	.1841 -.0070	.0133 .2000	.9958
1.5	120	-.0734 .0725	.0245 -.0514	.1932 -.0061	.0157 .2000	.9670
3.0	0	.3381 .0621	-.0144 -.0882	.1146 -.0080	.0102 .2000	1.172
3.0	60	-.5030 .0520	-.0353 -.0365	.2489 -.0076	.0119 .2000	.8448
3.0	120	-.6117 .0642	.0054 -.0193	.2786 -.0060	.0163 .2000	.7609

Note: Ka equal 0.02 for all control laws.

Table VII

Control Law Gains (0.6 MACH)					
PHI/BETA RATIO		FEEDBACK GAINS			
MAGNITUDE	PHASE ANGLE	K1 K6	K2 K7	K3 K8	K4 K9	K5

MAGNITUDE	PHASE ANGLE	K1	K2	K3	K4	K5
		K6	K7	K8	K9	
0	0	.3091	.0155	.0485	.0057	.5725
		.0180	-.0033	-.0032	.0000	
1.5	0	.2897	.0086	.0428	.0049	.6098
		.0184	-.0048	-.0031	.0000	
1.5	60	.0301	.0045	.0516	.0046	.5593
		.0167	-.0040	-.0033	.0000	
1.5	120	.0336	.0109	.0575	.0052	.5238
		.0164	-.0026	-.0033	.0000	
3.0	0	.2511	.0018	.0381	.0042	.6472
		.0187	-.0063	-.0031	.0000	
3.0	60	-.2293	-.0051	.0549	.0036	.5492
		.0155	-.0046	-.0034	.0000	
3.0	120	-.2325	.0066	.0664	.0048	.4814
		.0148	-.0019	-.0035	.0000	

Note: Ks equal 0.02 for all control laws.

VII. Analytical Estimation of Handling Qualities

Handling qualities are those qualities or characteristics of an aircraft that govern the ease and precision with which a pilot is able to perform tasks required in support of an aircraft role (13). This definition has several implications which are important to understand. It requires the pilot in the control loop, therefore evaluation of the open loop response alone is insufficient to insure acceptable handling qualities. (A good example of the importance of analysis with pilot in the loop is the dramatic effect time delays in the forward loop can have on pilot opinion.) Therefore, the eigenstructure of the lateral-directional axes, which determine stability, is only one portion of the total control system which affects the handling qualities. It is also important to realize the handling qualities must be evaluated in a task required in the aircraft role. For fighter aircraft such as the YA-7D, precision in air-to-air or air-to-ground tracking is a valid criteria.

Two criteria will be used to evaluate the handling qualities analytically, bank angle tracking and turn coordination. These are typically the parameters of most interest in lateral-directional motion. Precision in bank angle control is necessary for the pilot to be able to precisely orient the lift vector and turn the aircraft. In addition to good bank angle control, satisfactory turn coordination is necessary for precision in nose pointing. Bank angle tracking can be thought of as an inner loop closure with heading control as the outer loop. If the inner loop bank angle characteristics and turn coordination are good, the

49

pilot will be able to precisely control both lift vector and nose
position.

In the following analysis, the augmented eigenstructures at 0.4 and
0.6 Mach will be used. The resulting 12th order eigenstructures are
still insufficient to completely analyze the handling qualities. The
two linear prefilters in the CAS are of low enough frequency that they
must be considered. The mechanical system, which commands the aileron
power actuator directly, has a gain of .01453 rad/lb. In state space
form, the dynamics of the two prefilters and mechanical system may be
described as:

$$\dot{x} = A x + B u$$

$$x = [\begin{array}{cccc} F1 & \delta_{asc} & \delta_{as} & v_2 \end{array}]^T \qquad u = [\begin{array}{cc} Fs & \delta_{rc} \end{array}]^T$$

$$A = \begin{bmatrix} -3 & 0 & 0 \\ -.2 & -10 & 0 \\ 0 & 0 & 0 \\ 0 & 8883 & 0 \end{bmatrix} \qquad B = \begin{bmatrix} 3 & 0 \\ 0 & 0 \\ .291 & 0 \\ 0 & 0 \end{bmatrix} \qquad (48)$$

where F1 is the first stick state and Fs is the stick force. The other
states and inputs are as previously defined, and only the changed
portion of the δ_{as} and v_2 states has been shown. The 14th order
eigenstructures will be the basis for analysis.

Estimation Techniques

Handling qualities estimation is still a very inexact procedure as
evidenced by the amount of data in MIL-F-8785C (9) which does not
correlate well with the specifications and the amount of research being
conducted on handling qualities of highly augmented aircraft.

Nevertheless, most aircraft which meet the specifications will have good
flying qualities. This points to the difficulty in analyzing the flying
qualities of the eigenstructures developed in the previous sections.
Even after eliminating the eigenstructures which do not meet the
criteria of MIL-F-8785C, there are many left that do. Differences in
the handling qualities between them can be expected to be small.

Many techniques have been developed for analyzing pitch dynamics of
higher order systems, including pilot models such as the Neal-Smith
criteria (10:226), and several criteria on the time response (10:233).
The time response techniques do not have direct application to
lateral-directional dynamics, and pilot models are somewhat dependent on
the criteria assumed for the pilot. Hoh's bandwidth criteria (14 and
10:215) is a technique that is intuitively attractive and can be adapted
to a wide variety of problems.

One measure of the handling qualities of an aircraft is its
stability margin when operated in a closed loop tracking task. In
classical control theory, the maximum frequency at which such closed
loop tracking can occur without threatening stability is the bandwidth,
w_{bw}. The pilot can be thought of as a pure gain controller with unity
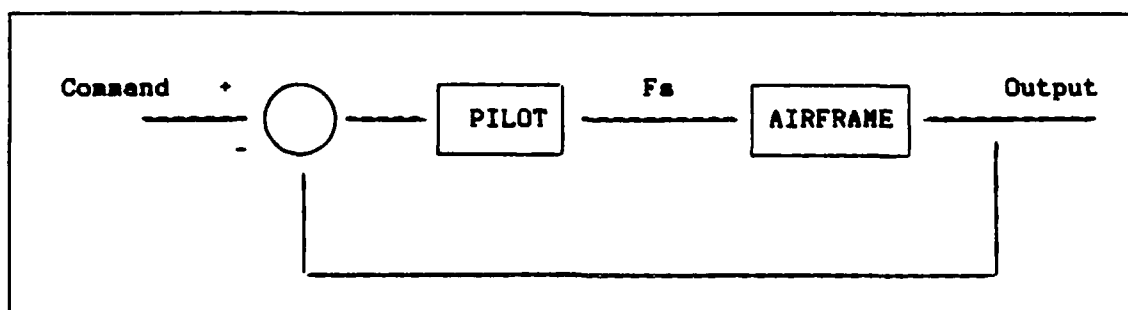feedback as in Figure 8. Although a simple assumption, an

Figure 8. Pilot Model

aircraft with good handling qualities will require minimal pilot
compensation. It is further assumed the pilot will close the loop and
add gain to achieve 45 degrees of phase margin or 6 decibels (dB) of
gain margin, whichever produces the lower bandwidth. The higher the
bandwidth, the more precise the pilot will be able to control the system
output without going unstable. Bandwidth will be determined from the
Bode plot using the criteria in Figure 9. This method makes the system
bandwidth independent of the actual pilot gain.

Another aspect of handling qualities is the ability of the pilot to
increase the bandwidth by increasing gain while adding compensation.
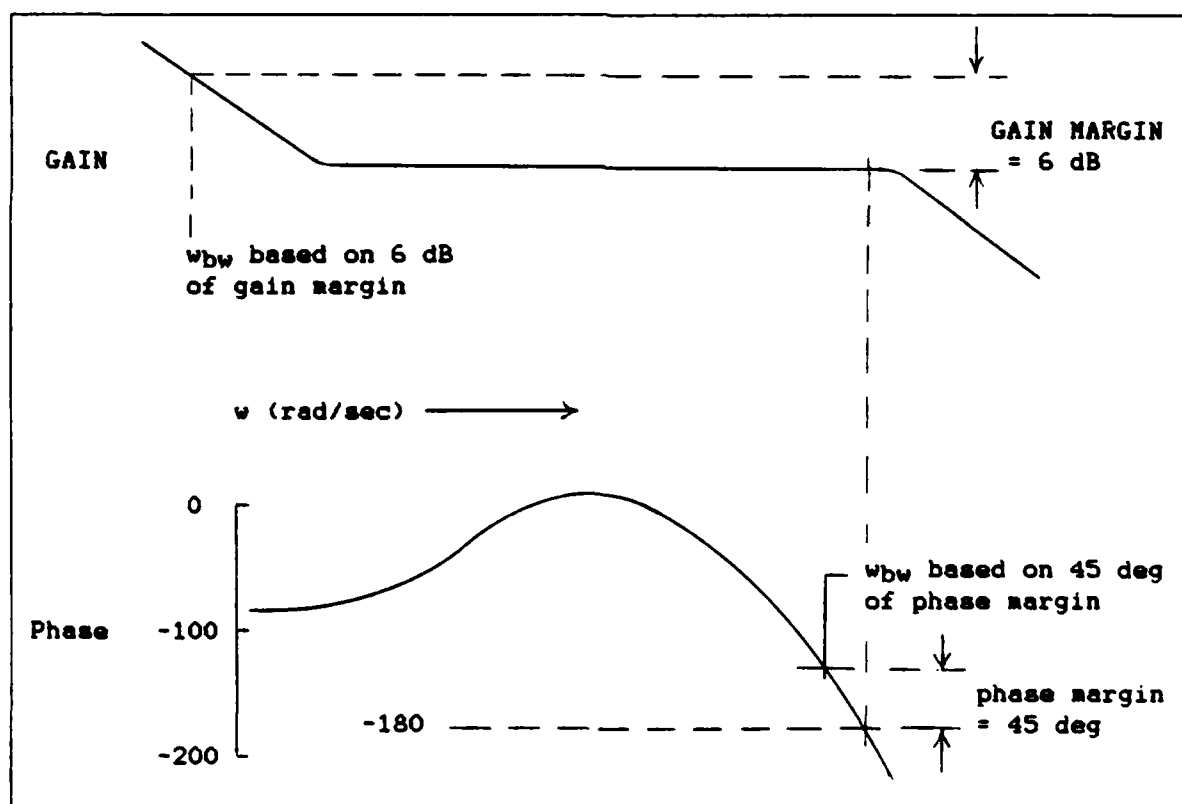
Figure 9. Bandwidth Defined by Gain and Phase Margins

The capability to do this is tied to the phase characteristics above the bandwidth frequency. Systems which have a rapid falloff in phase can tolerate only small gain increases and require large pilot compensation. The high frequency phase characteristics, which are a function of the higher order dynamics, can be represented by an equivalent amount of pure time delay, τ_e. The equivalent time delay can be accurately estimated from the frequency response using the equation:

$$\tau_e = \frac{- \phi_1 - 180}{57.3 \, w_1} \tag{49}$$

where ϕ_1 and w_1 are the phase angle and frequency at twice the frequency where the phase angle is 180 degrees, w_{180} (10:218).

The third criteria for satisfactory handling qualities is for the magnitude response to have a K/s slope in the region of the bandwidth where the pilot is operating at maximum gain. A "shelf" in the magnitude response in this region is highly undesirable, indicating a rapid decrease in phase margin as gain is increased.

Hence, the flying qualities in a particular closed loop task are dependent on three parameters:

1) The bandwidth, w_{bw}

2) The shape of the phase curve at frequencies above w_{bw}, as measured by the effective time delay, τ_e.

3) The shape of the magnitude curve near w_{bw}.

The bandwidth required to achieve satisfactory (Level 1) handling qualities is dependent on the task. In a bank angle tracking task, the pilot is closing the phi to stick force loop, therefore the transfer

function of interest is ϕ/F_s. Exact categorization of the
eigenstructures into Level 1, Level 2, etc. is difficult. By analogy to
a pure first roll order response, in which the bandwidth is equal to the
roll subsidence eigenvector, it would be reasonable to assume bandwidths
between one and three radians/second will produce Level 1 handling
qualities. Bandwidths less than one radian/second will be too sluggish,
and greater than three radians/second too abrupt. Also, Reference 10
(10:407) indicates a degradation in handling qualities when τ_e exceeds
100 msec. This will be explained in more detail later.

Techniques to analyse turn coordination are not as well developed.
The pilot loop closures are not as clear and the motion involves two
axes. One measure of turn coordination is the pilot rudder input
necessary to maintain sideslip at zero. Large or complex rudder inputs
are indicative of complex nose motion which will increase pilot workload
during tracking maneuvers. Reference 10 (10:542) presents guidelines
for allowable rudder shaping, however, they are based on historical data
for coordination in the landing configuration. Rather than evaluate
compliance with these guidelines, a slightly different approach will be
taken based on similar principles. While specific categorization of
flying qualities will not be possible, a better understanding of the
effects of the various eigenstructures is possible.

The rudder crossfeed, Y_{cf}, necessary to maintain zero sideslip in a
turn can be defined as:

$$\delta_{rp} = Y_{cf} F_s \qquad (50)$$

For a particular aircraft, Y_{cf} may be evaluated as:

$$Y_{cf} = \frac{\text{Numerator of } \beta \text{ to Fs transfer function}}{\text{Numerator of } \beta \text{ to } \delta_{rp} \text{ transfer function}} \qquad (51)$$

Y_{cf} can be calculated from the the 14th order eigenstructures, and the frequency response plotted. An understanding of the dynamics aids in interpretation. Sideslip in a turn can arise from two sources, adverse/proverse yaw due to aileron deflection, and yaw coupling due to roll. Pilots typically can tolerate more adverse yaw than proverse, since the rudder deflection is in the same sense as the stick input and is more natural. The eigenstructure will only effect the adverse/proverse yaw indirectly. The aileron to rudder feedback is designed to minimize the adverse yaw, and the higher dutch roll frequency resulting from augmentation will help minimize the magnitude of any resulting sideslip. Low values of $(\phi/\beta)_d$ will result in more sideslip, since more of the dutch roll response, excited by adverse/proverse yaw, is in beta. The second contribution to sideslip is from roll-yaw coupling, which was minimized through the design of the roll subsidence eigenvector.

From a handling qualities viewpoint, large magnitudes of the crossfeed parameter, $|Y_{cf}|$, in the 5 to 10 rad/sec frequency range indicates the pilot must initially apply a large rudder input to keep sideslip at zero. Phase angles of the crossfeed parameter, $\arg(Y_{cf})$, greater than 180 degrees in this frequency range indicates proverse yaw, which may be objectionable with large $|Y_{cf}|$. If $\arg(Y_{cf})$ goes through 180 degrees (in either direction) in the frequency range one to five rad/sec, the pilot will have to reverse pedal deflection during the roll which may also be objectionable. Frequency ranges are approximate, and

55

merely indicate the ranges in which pilots most often operate in high gain tasks.

The techniques chosen here are not unique. Other techniques are available which provide similar estimation of handling qualities. The main advantage of working in the frequency domain is the effects of higher order dynamics can be seen. It must be remembered the gains only control the modal response of the four basic rigid body modes. Other modes, such as the rudder and aileron dynamics may move into a frequency range noticeable to the pilot. The roll CAS dynamics will certainly have a significant effect on the aircraft roll response. Also, only very simple assumptions about pilot behavior are required.

Evaluation of Bank Angle Tracking

An example of bank angle tracking using classical dynamics will illustrate the technique. For classical airplanes, roll bandwidth is only a function of λ_{rs}, w_ϕ, and w_d. When there is no roll-yaw coupling ($w_\phi = w_d$), the bandwidth will be phase margin limited and will be exactly equal to λ_{rs} as shown in Figure 10. As is well known, when w_ϕ is greater than w_d, closing the loop reduces system stability. This is also reflected in the lower bandwidth shown in Figure 11.

It has already been shown how w_ϕ/w_d is influenced by the dutch roll eigenvector, thus it is expected variations in $(\phi/\beta)_d$ will influence roll stability. Of course the damping and frequency of the dutch roll will also influence this loop closure, however the augmentation should have increased these to satisfactory values.
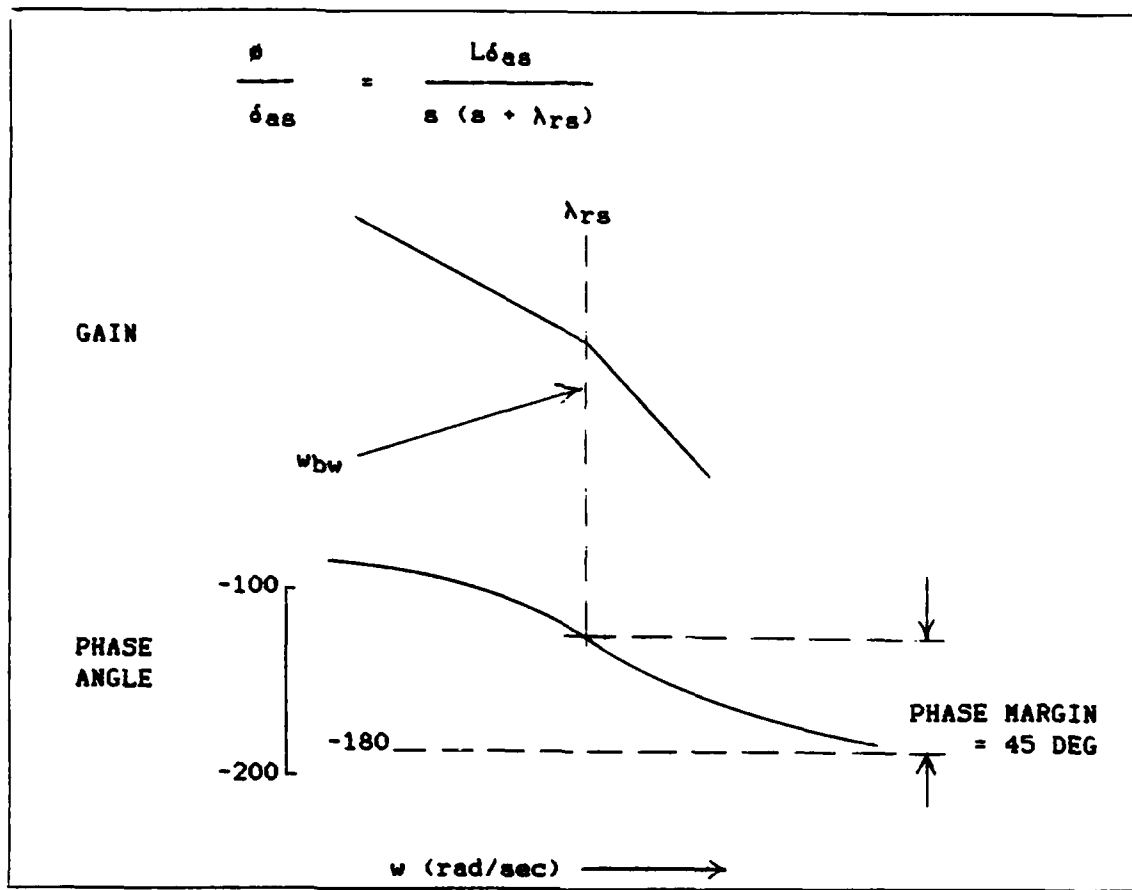
$$\frac{\phi}{\delta_{as}} = \frac{L\delta_{as}}{s\,(s + \lambda_{rs})}$$

Figure 10. Classical Roll Dynamics with $w_\phi = w_d$

Frequency response plots for the unaugmented YA-7D are shown in Appendix C for the unaugmented YA-7D and the seven lateral-directional eigenstructures described in the previous section. Results are summarized in Table VIII.

At 0.4 Mach the unaugmented YA-7D has acceptable bandwidth and time delay characteristics, but has a reversal in the gain and phase curves near the bandwidth frequency due to a poorly damped dutch roll with moderate adverse yaw (Figure C1). The pilot may have difficulty in high gain tasks because of the rapid decrease in phase margin as gain is

57

$$\frac{\phi}{\delta_{as}} = \frac{L\delta_{as}\ (s^2 + 2\zeta_\phi\ w_\phi\ s + w_\phi{}^2)}{(s + \lambda_{sp})\ (s + \lambda_{rs})\ (s^2 + 2\zeta_d\ w_d\ s + w_d{}^2)}$$
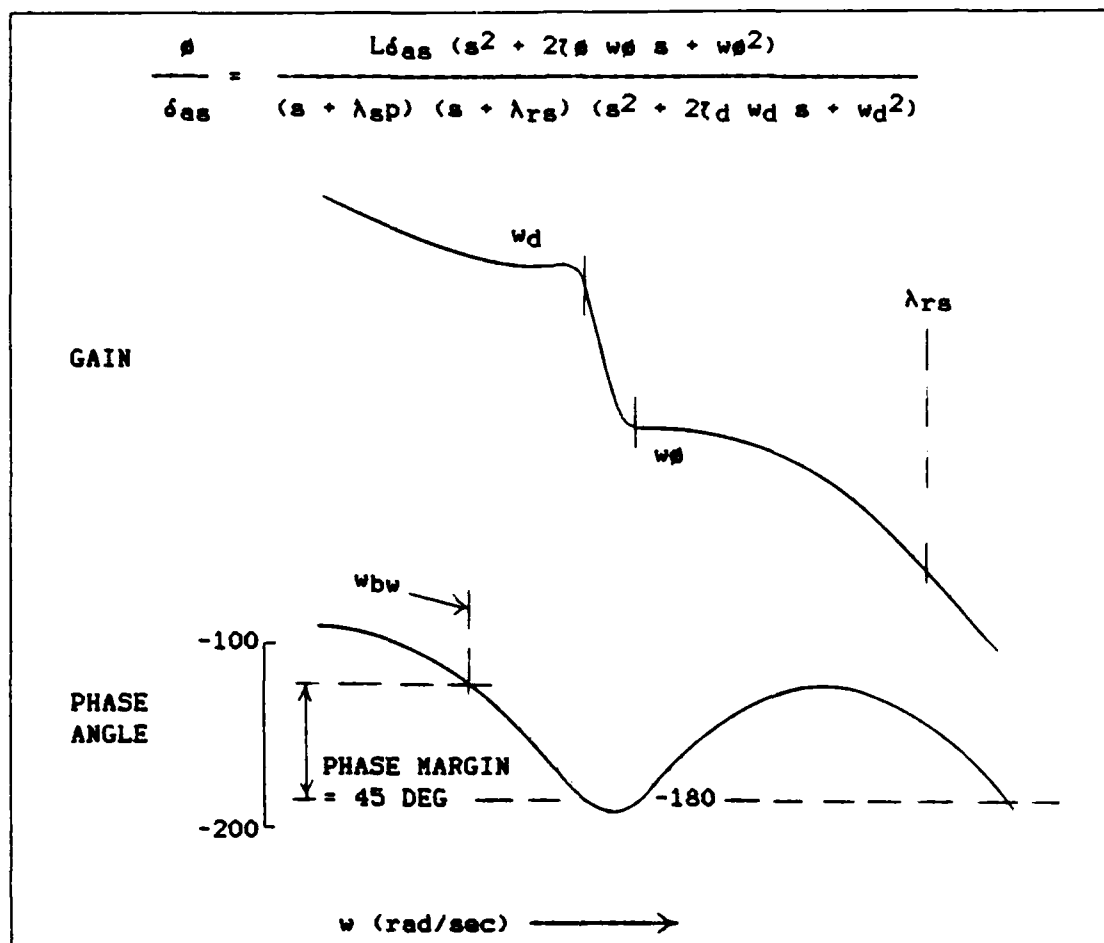
Figure 11. Effect of Roll-Yaw Coupling on Roll Dynamics

increased in this frequency range. Figures C2 to C8 show the response

is much improved with augmentation. There is no longer a shelf in the

magnitude response, and the effective time delay is acceptable. Even

though the roll mode was designed to give a bandwidth of four radians

per second, the prefilters in the stick and other higher order effects

have slowed the response considerably. With the aileron to rudder

feedback, adverse yaw is well controlled, although not perfectly.

Little variation in the response is noted with $|\phi/\beta|_d$ of 1.5. With

$|\phi/.|_d$ of three, $\arg(\phi/\beta)_d$ now has a noticeable effect on both bandwidth

58

Table VIII.

	Bandwidth and Time Delay of Eigenstructures		
Mach	$(\phi/\beta)_d$	Bandwidth	Time Delay
0.4	unaugmented	2.17	0.066
	0	1.43	0.077
	1.5 arg(0)	1.51	0.093
	1.5 arg(60)	1.50	0.081
	1.5 arg(120)	1.43	0.067
	3.0 arg(0)	2.10	0.105
	3.0 arg(60)	2.93	0.082
	3.0 arg(120)	1.43	0.066
0.6	unaugmented	1.83	0.062
	0	1.57	0.074
	1.5 arg(0)	1.64	0.081
	1.5 arg(60)	1.61	0.083
	1.5 arg(120)	1.54	0.074
	3.0 arg(0)	1.72	0.091
	3.0 arg(60)	1.65	0.096
	3.0 arg(120)	1.51	0.077

and time delay. The shape of response has a noticeable shelf at

$arg(\phi/\beta)_d$ of 120 degrees. It is expected that handling qualities will

be satisfactory with all eigenstructures with the possible exception of

$(\phi/\beta)_d$ equal to 3 arg(120).

As shown in Figure C9 in Appendix C, the roll characteristics of

the YA-7D at 0.6 Mach are already satisfactory. There is only a slight

amount of proverse yaw, so variations in $(\phi/\beta)_d$ has almost no effect. The magnitude responses shown in Figures C10 to C16, have the desired K/s shape, and bandwidth and time delay are satisfactory. All the feedback gains should produce satisfactory handling qualities.

Evaluation of Turn Coordination

Figures C17 to C32 show frequency response plots for the rudder crossfeed parameter at 0.4 and 0.6 Mach. The magnitude and phase responses show only slight variations with the different eigenstructures.

At 0.4 Mach, the unaugmented YA-7D shows an initial rudder deflection needed to counter the adverse yaw, followed by a slight decrease, then steadily increasing rudder as the turn develops. Although the response shows typical high frequency characteristics, the low frequency response shows a poorly coordinated turn. All augmented eigenstructures show similar responses, with deflection needed to counter the adverse yaw, followed by decreasing deflection as the turn develops.

At 0.6 Mach, the unaugmented YA-7D needs only slight rudder initially, but again has poor low frequency characteristics. With augmentation the low frequency characteristics are much improved.

In summary, variations in $(\phi/\beta)_d$ have only slight effects on turn coordination. When adverse/proverse yaw is small, variations in $(\phi/\beta)_d$ also have small effects on the roll response. When adverse yaw is present, increasing $|\phi/\beta|_d$ can have an adverse impact on the shape of the magnitude response, particularly for phase angles near 120 degrees.

60

VIII. Simulator Results

The simulator for aircraft Flight Test and Development (SAFTD) was a low fidelity simulator consisting of a fixed generic fighter cockpit with a cathode ray tube display. Programmable software enabled simulation of a variety of aircraft. The YA-7D simulation used a five degree of freedom linear aerodynamic model with a digital emulation of the DIGITAC control system. Open loop tasks described in Appendix F were flown by project pilots and results recorded on two eight channel stripchart recorders. These data were used to verify the control laws produced the desired response. Closed loop tasks were not evaluated in the simulator due to excessive time delay in the visual display and poor fidelity of the simulation.

Initial SAFTD results indicated the control laws performed as predicted. The closed loop eigenstructure as measured by the roll mode time constant (τ_r), dutch roll frequency (w_d) and damping ratio (ζ_d), and ($\phi/\beta)_d$, agreed well with design parameters. Dutch roll damping tended to be slightly low, but was still within 15 percent of the minimum requirement and design condition (0.4) listed in MIL-F-8785C (9). The stick force command gain produced acceptable roll rate per pound gradients (p_{ss}/Fs). Tables VIII and IX summarize the results at 0.4 and 0.6 Mach. The lateral-directional characteristics of the unaugmented YA-7D and standard aircraft with augmentation are included for comparison.

Qualitatively, control system designs at both 0.4 and 0.6 Mach flew well with no adverse characteristics. The roll CAS command gain, Ka,

61

was evaluated, and a constant value of 0.02 rad/sec per pound selected for all control laws.

Representative time response plots for a step lateral stick input and release from wings level sideslip, generated in the SAFTD, are included in Appendix C.

Table IX

Simulator Lateral-Directional Characteristics - 0.4 Mach					
Design $(\phi/\beta)_d$[1] (mag/phase ang)	w_d	ζ_d	τ_r	P_{ss}/F_s	$(\phi/\beta)_d$
Unaugmented	1.8	0.16	0.40	5.6	3.4 arg(46)
DFCS on[2]	2.9	0.70	0.30	6.7	1.9 arg(72)
0 / 0	3.2	0.35	0.33	6.0	0 arg(0)
1.5 / 0	3.2	0.35	0.30	6.4	1.7 arg(17)
1.5 / 60	3.2	0.37	0.28	5.2	1.8 arg(43)
1.5 / 120	3.1	0.38	0.25	5.2	1.4 arg(106)
3.0 / 0	3.6	0.40	0.28	5.6	3.0 arg(0)
3.0 / 60	2.9	0.40	0.25	4.7	3.2 arg(46)
3.0 / 120	2.9	0.37	0.25	4.4	3.6 arg(105)

[1] Note: Design conditions were $\tau_r = 0.25$, $w_d = 3.0$, and $\zeta_d = 0.40$.

[2] Note: Includes effects of prefilters in CAS.

Table X

Simulator Lateral-Directional Characteristics - 0.6 Mach					
Design $(\phi/\beta)_d$[1] (mag/phase ang)	w_d	ζ_d	τ_r	Pas/Fa	$(\phi/\beta)_d$
Unaugmented	1.9	0.18	0.40	6.3	3.3 arg(38)
DFCS on[2]	2.9	0.70	0.40	7.5	1.0 arg(120)
0 / 0	3.2	0.33	0.30	10.3	0 arg(0)
1.5 / 0	3.0	0.40	0.30	10.0	1.7 arg(24)
1.5 / 60	3.1	0.38	0.25	10.0	2.0 arg(57)
1.5 / 120	3.1	0.42	0.30	10.3	2.2 arg(112)
3.0 / 0	3.2	0.38	0.30	10.0	3.1 arg(9)
3.0 / 60	3.3	0.43	0.33	10.0	3.3 arg(51)
3.0 / 120	3.2	0.45	0.25	10.0	3.1 arg(114)

[1] Note: Design conditions were $\tau_r = 0.25$, $w_d = 3.0$, and $\zeta_d = 0.40$.

[2] Note: Includes effects of prefilters in CAS.

IX. Flight Test Results

General

A limited flight test program based on the control laws developed in this report was conducted at the Air Force Flight Test Center (AFFTC), Edwards Air Force Base (AFB), California, between 8 October and 17 November 1987. Seventeen sorties (28.3 flight hours) were flown in the YA-7D DIGITAC aircraft. Seventeen additional chase sorties (29.7 flight hours) were flown in A-7D aircraft. All tests were flown within limitations contained in the Flight Manual, USAF Series A-7D Aircraft (12) and the Partial Flight Manual, YA-7D Serial Number 67-14583 (15). A more detailed description of the test limitations and complete description of test procedures is given in the HAVE EIGEN Test Plan (16).

Objectives

The overall objective of the HAVE EIGEN test program was to evaluate the lateral-directional handling qualities of the YA-7D at 15,000 feet pressure altitude (Hc), 0.4 and 0.6 Mach, with the control laws designed from eigenstructure assignment. Specific objectives were to:

1. Confirm the closed loop eigenstructure of the lateral-directional axes agreed with the design eigenstructure.

2. Correlate pilot handling quality ratings to $(\phi/\beta)_c$.

3. Evaluate the use of eigenstructure assignment as a control law synthesis technique.

Aircraft Description and Instrumentation

The YA-7D test aircraft, USAF serial number (S/N) 67-14583, was a prototype for the A-7D single seat, light attack aircraft and was powered by a single Allison TF-41-A-1 engine. A complete description of A-7D is given in the Flight Manual (12). The test aircraft was modified for the DIGITAC test program as described in the Partial Flight Manual (15). An instrumentation pod on the aircraft's right inboard wing station provided data acquisition and telemetry (TM) capability. An inert Mk-82 bomb was installed opposite the DIGITAC instrumentation pod for symmetry. The two outboard stations on each wing had pylons, but carried no stores.

The test aircraft had a control augmentation, stick steering flight control system. For the DIGITAC program, the analog computer of the AFCS was replaced with a programmable DFCS. The mechanical flight control system was unchanged by the installation of the DFCS. For this test, the longitudinal control laws and lateral CAS prefilters for the standard YA-7D were used. The lateral-directional control laws derived from eigenstructure assignment were added to the DFCS.

The weapon sight system of the YA-7D DIGITAC aircraft consisted of a gunsight computer electronic unit, an inertial sensor unit, a control panel, a signal generator, and a standard A-7D Head-up Display (HUD) (AN/AVQ-7(V)). All controls on the HUD control panel functioned as described in the Flight Manual (12) with the exception of the TEST, SCALES, and BARO/RDR ALT switches, which were deactivated.

The HUD was equipped with a camera that recorded HUD video onto 16mm color film. The camera was armed by a switch on the the pilot's

65

right rear console. The film camera was activated by depressing the trigger switch to the first detent, or by activating the camera run switch on the left canopy bow.

The test aircraft was also equipped with a Yaw, Angle-of-attack, Pitot-Static (YAPS) nose boom, Ampex AR-700 magnetic tape recorder, TM transmitter, Millikan DBM-2 Head-Up Display camera, and sensitive cockpit instruments. A complete description of the data acquisition system was in the Partial Flight Manual (15). Specific parameter measurement device descriptions and resolutions were in the Instrumentation Handbook (17). Additional information on test instrumentation is included in Appendix E.

The weight of the aircraft varied from approximately 31,000 pounds at takeoff to 24,000 pounds at landing with 2,000 pounds of fuel remaining. The center of gravity (CG) moved aft from 27.1 percent mean aerodynamic chord (MAC) to 27.6 percent MAC as fuel was burned. The center of gravity also dropped from 2 inches above the waterline at engine start, to the waterline at the end of the mission. The weight changes and center of gravity movement, as well as longitudinal control system characteristics, had negligible effects on the lateral-directional flying qualities of the aircraft.

Test Methods and Conditions

Testing was conducted in three phases. Ground testing of the aircraft was conducted at twice the normal loop gain to check for limit cycle and structural resonance oscillations. Simultaneously, the open loop simulator testing described in the previous section was performed

66

to evaluate how closely the control laws achieved the desired response. And finally, open and closed loop airborne testing was flown.

Open and closed loop testing was performed with each control law. Stripchart data were used to estimate the roll mode time constant, dutch roll frequency and damping, and $(\phi/\beta)_d$. Further information on open loop testing is given in Appendix F.

Three closed loop tests were performed; two HUD tracking tasks and an air-to-air tracing task with another A-7D as a cooperative target. The project pilots rated each control law in each task at least twice. The test engineer assigned the points, and to prevent biasing, the pilots did not know which phi/beta ratio was being tested. The specific criteria and description of the tasks is given in more detail in Appendix F.

Test and Evaluation

Ground Testing. Initial ground testing of the control systems revealed small amplitude, high frequency oscillations in the ailerons with several of the control laws. Smaller oscillations were also present in the rudder. Investigation revealed high gains in the lateral accelerometer to aileron channel were amplifying structural vibrations producing a structural resonance in the flight control system centered at 10.5 Hertz (Hz). Frequency analysis showed actual modes of the resonance to have frequency content at 10.5, 13 and 15 Hz. The first lateral bending mode of the YA-7D was at 10.5 Hz and the natural frequency of the lateral accelerometers was at 13 Hz. It was felt these were the causes of the structural resonance. Unfortunately, the rather

67

broad frequency band prevented using a notch filter in the accelerometer channel.

The 10 rad/sec first order noise filter, described in Section III, was not initially included as part of the design. When the noise filter was added to the ground testing, it eliminated the feedback at normal gain levels. Standard AFFTC procedure was to ground test at twice normal gain to provide at least six decibels (Db) of gain margin from the resonance. At these increased gain levels a small amount of structural resonance was still present. Finally, a non-linear digital filter already used in the standard DIGITAC yaw channel was added to the first order lag filter. The non-linear filter had very little phase or gain loss below five Hz and therefore had little effect on the dynamic modes of interest. Above 5 Hz, the gain dropped off rapidly, providing 11 Db of gain margin above 10 Hz. This was sufficient to eliminate all structural resonances. The gains of the control laws were recomputed with the 10 rad/sec lag filter added in the accelerometer channel, and the configuration reflown in the simulator with both lag filter and non-linear digital filter in place. Simulator results showed the non-linear filter had no noticeable effect on the lateral-directional modes of interest. Open loop data with the newly computed gains and noise filters were within measurement accuracy of previous simulator results. No further structural resonance problems were encountered on the ground or in flight.

Flight Test Results - 0.4 Mach. The control laws derived from eigenstructure assignment produced unflyable characteristics at 0.4 Mach. Although some of the control laws were better than others, all

68

suffered from very poor dutch roll characteristics, in some cases divergent. This was particularly puzzling because initial flight test results at 0.6 Mach agreed with simulator results.

The problem was finally traced to inaccurate assumptions in the YA-7D linear model used in the derivation of the control laws. In the linear model, it was assumed the lateral accelerometer was 4.78 feet forward of the center of gravity. Corrections to the lateral accelerometer output were made in the model to account for the yaw acceleration which would be sensed by the accelerometers. However, not modeled in the linear model or SAFTD was the vertical position of the accelerometers, approximately 17 inches below the center of gravity. Thus, in addition to sensing yaw acceleration, the accelerometers also sensed roll acceleration. Although the moment arm was relatively small, roll acceleration can be quite high, more than 100 degrees/sec^2. The SAFTD was used to evaluate affects on the dutch roll of having the accelerometers 17 inches below the CG. Results are shown in Table XI. While the dutch roll period and phi/beta ratio were not changed significantly, damping was greatly reduced. The effects at 0.4 Mach were much greater than at 0.6 Mach. This was to be expected since the lateral acceleration gains were more than five times greater. More importantly, the control laws at 0.4 Mach were now found to be very sensitive to changes in airspeed. A 20 knot increase was enough to drive the dutch roll divergent in some cases. The dutch roll response was also no longer a second order function, but became non-linear. These effects corresponded closely to flight test results at 0.4 Mach.

Table XI

Simulator Results Showing Effects of Lateral Accelerometer Position 17 Inches Below CG				
Mach	Design $(\phi/\beta)_d$ mag / phase	w_d	ζ_d	$(\phi/\beta)_d$
0.4	0 / 0	3.0	0.32	0 arg(0)
	1.5 / 0	2.5	0.28	2.2 arg(14)
	1.5 / 60	2.7	0.25	1.8 arg(60)
	1.5 / 120	2.9	0.10	1.5 arg(114)
	3.0 / 0	2.3	0.28	3.3 arg(0)
	3.0 / 60	2.4	0.22	2.6 arg(53)
	3.0 / 120	2.9	0.01	2.3 arg(98)
0.6	0 / 0	3.2	0.35	0 arg(0)
	1.5 / 0	2.8	0.27	1.8 arg(23)
	1.5 / 60	3.0	0.29	1.9 arg(57)
	1.5 / 120	3.1	0.27	1.5 arg(86)
	3.0 / 0	2.7	0.32	3.9 arg(22)
	3.0 / 60	2.9	0.29	3.4 arg(55)
	3.0 / 120	3.2	0.26	2.9 arg(88)

Those control laws found divergent in flight were also found divergent in the simulator.

The limited scope of the flight test investigation did not permit correcting the gains for the actual lateral accelerometer position and retesting. However, the close correlation between simulations with the correct accelerometer position and flight test results at 0.4 Mach indicate the problem was correctly identified.

The rather dramatic effects of the lateral accelerometer vertical position error in the model can be analyzed by examination of the equations for the YA-7D lateral acceleration (Ny). The lateral acceleration at the CG modeled in Section III for the YA-7D at 0.4 Mach and 15,000 feet is:

$$Ny = 0.88r - 48.0\beta + 0.55p + 2.47\delta_{as} + 13.37\delta_r \qquad (52)$$

Ny is primarily a function of sideslip and rudder deflection. At the accelerometer, 4.8 feet forward of the CG, a component of yaw acceleration is sensed. The accelerometer output becomes:

$$Ny = -0.47r - 41.0\beta + 0.098p - 2.55\delta_{as} + 2.84\delta_r \qquad (53)$$

The accelerometer output is now primarily a function of sideslip, and the signal may be used in place of sideslip with good results. This was the relationship used in the linear model. At 0.6 Mach the relationship is similar.

If the accelerometer is now moved 4.8 feet forward of the CG and 17 inches down, it will now sense a component of roll acceleration also. The accelerometer output becomes:

$$Ny = -1.75r - 24.5\beta + 2.25p + 14.73\delta_{as} - 0.46\delta_r \qquad (54)$$

The output is now primarily a function of sideslip and aileron deflection. If this is not modeled, the feedback gains will not produce the desired results as was evident in both simulator and flight test results. Although the gains were small enough so significant errors

71

were not introduced at 0.6 Mach, instabilities were introduced at 0.4 Mach.

Flight Test Results - 0.6 Mach. Although the problem with the lateral accelerometer position was also present at 0.6 Mach, it had much less effect because the control system gains were much smaller. The open and closed loop testing described in Appendix F were accomplished.

Open Loop Test Results. Open loop tests were performed to verify the flight control laws produced the desired aircraft response. The closed loop lateral-directional eigenstructure (as measured by the roll mode time constant, dutch roll frequency and damping, and $(\phi/\beta)_d$) were measured as described in Appendix F. Results are shown in Table XII. Flight test results generally agreed within 15 percent of design conditions and simulator results. This was an excellent correlation considering wind tunnel aerodynamic data used to derive the control laws was in error as shown in Table XIII. Flight test results indicated the aircraft had a much larger N_β than estimated by the aerodynamic data. It was also noted by the project test pilots that the aircraft had noticeable adverse yaw not predicted by the aerodynamic data. Nevertheless, the control laws derived in the previous sections were successful in attaining the desired open loop response in both ground simulations and flight testing.

An unusual characteristic of the control laws was discovered during open loop testing. The control laws with $|\phi/\beta|_d$ of 0 and $(\phi/\beta)_d$ of 1.5 arg(0) required unnatural aileron control during sideslips. Although unusual and in violation of paragraph 3.3.6.3 of MIL-F-8785C (9), this

72

Table XII

Design $(\phi/\beta)_d$[1] (mag/phase ang)	w_d	ζ_d	τ_r[2]	P_{ss}/F_s	$(\phi/\beta)_d$ (mag/phase ang)
Flight Test Lateral-Directional Characteristics - 0.6 Mach					
Unaugmented	2.8	0.16	0.50	N/A	2.6 / 58
DFCS on	2.9	0.45	0.36	8.3	2.7 / 63
0 / 0	3.4	0.40	0.44	9.7	0 / 0
1.5 / 0	3.4	0.40	0.42	8.3	1.5 / 14
1.5 / 60	3.4	0.32	0.36	8.0	1.3 / 60
1.5 / 120	3.6	0.35	0.35	7.9	1.2 / 113
3.0 / 0	3.2	0.36	0.44	7.9	2.8 / 0
3.0 / 60	3.2	0.35	0.44	8.9	2.8 / 52
3.0 / 120	3.4	0.32	0.44	8.7	2.6 / 100

[1] Note: Design conditions were $\tau_r = 0.25$, $w_d = 3.0$, and $\zeta_d = 0.40$.

[2] Note: Includes effects of prefilters in CAS.

Table XIII

	τ_r	w_d	ζ_d	$(\phi/\beta)_d$
Comparison of Math Model with Flight Test Results at 0.6 Mach				
Math Model	0.43	2.1	0.15	3.4 arg(40)
Flight Test	0.50	2.8	0.16	2.6 arg(58)

did not produce any objectionable characteristics during the closed loop tasks.

Based on open loop data, all flight control laws would be expected to produce satisfactory flying qualities. The dutch roll frequency was higher than expected and the damping ratio slightly lower, but were still near minimum requirements of MIL-F-8785C (9). The effective roll mode time constants, which included effects of lag prefilters in the CAS, and stick force command gradient, were satisfactory.

Closed Loop Test Results. The three project pilots evaluated each control law using three closed loop tasks a minimum of two times. The exact procedures are described in detail in Appendix F. Evaluations of the unaugmented aircraft and standard DIGITAC DFCS were also performed for comparison. The raw data are given in Tables E1 through E3.

Figures E1 through E3 present data comparing pilot repeatability and pilot-to-pilot repeatability. In general, each pilot was consistent in his ratings within plus or minus one Cooper-Harper rating. Also, the inter pilot ratings generally agreed within the same tolerance.

The following narrative will discuss each closed loop task and pilot ratings in detail, as well as give an overall summary.

All pilots found HUD Task 1 the most demanding and difficult to perform. As the pilot increased the gain and excited the dutch roll, capturing the target became extremely difficult. All pilots also agreed they had to reduce their gain just to accomplish the task. Most complaints centered on mechanization of the task. The target was not inertially stabilized and moved toward the pipper as the aircraft was

banked without regard to aircraft nose position. The illogical target movement caused the task to be ineffective, except for small movements of less than five milliradians (mils) around the pipper. In principle, the task was perhaps the best for evaluating lateral and directional characteristics, but all pilots ranked it lowest of the three closed loop tasks for its ability to discriminate flying qualities. Due to software development delays, the task was not available until late in the flight test period, and only limited evaluations were performed. Insufficient time remained to correct the software problems and refly the tests.

Despite technical problems with the task, pilots were able to identify differences in the control system designs. Figure 12 on the following page shows pilot rating as a function of phi/beta magnitude and phase angle. Pilots were very consistent in ranking zero degree phase angle as the best, with 120 degrees as the worst. Results show no consistent variation of pilot rating with magnitude, although none of the pilots liked a phi/beta magnitude of zero.

Many pilot comments centered on residual yaw oscillations. Although adverse yaw was not a complaint, there was a sufficient amount to excite the dutch roll. The pilots felt the damping ratio was too low, and that increased damping would have improved the Cooper-Harper ratings.

HUD Task 2 was not expected to show much variation in the pilot ratings since it primarily was a roll task and all control laws produced similar roll mode time constants and roll response to stick force
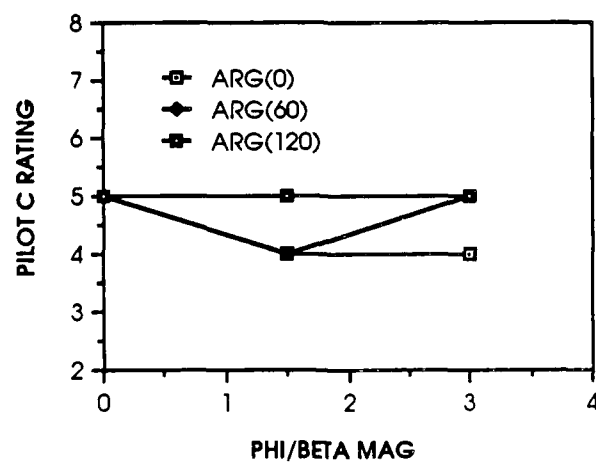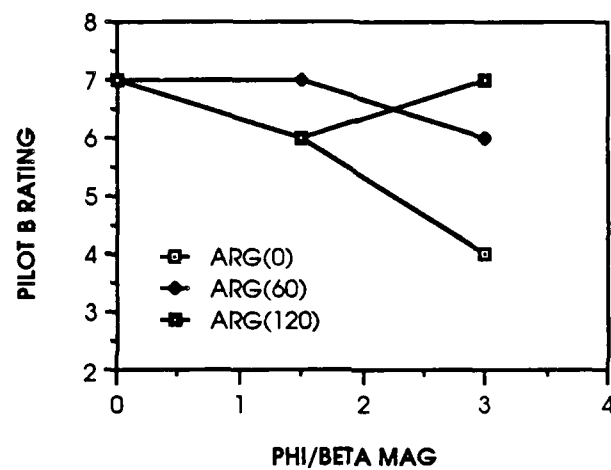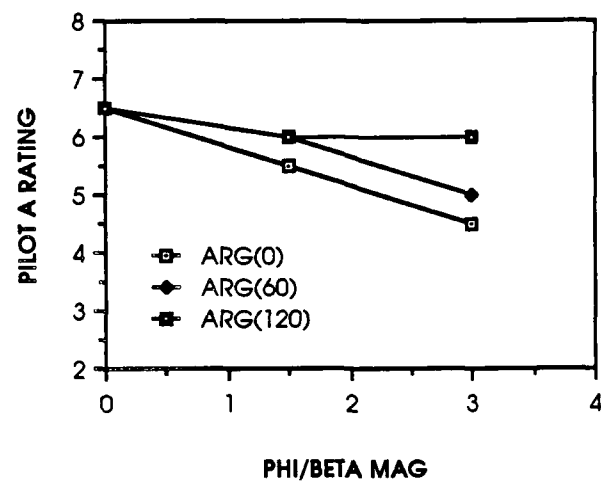
Figure 12. HUD Task 1 - Cooper-Harper Ratings

gradients. It was expected all control laws would produce satisfactory flying qualities. Results are shown in Figure 13 on the following page. The pilots were unanimous in objecting to the roll response. Aircraft response was abrupt, causing poor predictability. As pilot gain increased, cockpit roll and yaw accelerations became very high which made tracking difficult. Again, project pilots felt increased dutch roll damping would have helped. This conclusion was surprising because the dutch roll damping ratio was near the MIL-F-8785C requirement, yet all pilots felt the damping ratio was too low.

None of the control laws produced satisfactory flying qualities in HUD Task 2, including the standard DIGITAC DFCS, even though the stick gradients and roll mode time constant were good. Pilots A and C even preferred the unaugmented aircraft most because of its good predictability, although stick forces were high. Two possible explanations were explored.

Excessive time delay was first suspected as causing the degradations in pilot ratings. All control laws had an effective time delay of approximately 110 milliseconds (msec). Approximately 60 msecs was due to hydraulic actuators, the digital FCS, and higher order effects. Most of the delay was due to the three rad/sec linear prefilter in the CAS. The time constant for the CAS prefilter was reprogrammed to be cockpit selectable to 0.300, 0.125, and 0.025 seconds. While reducing the prefilter time constant reduced the effective time delay, it also reduced the effective roll mode time
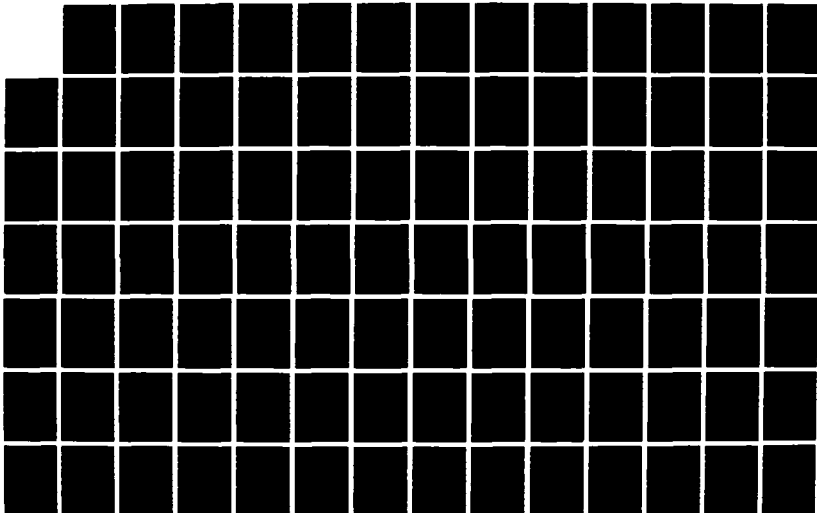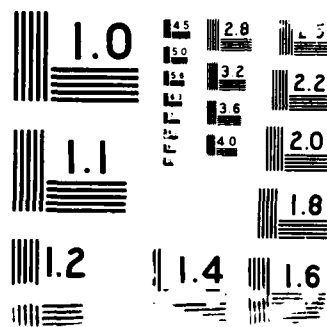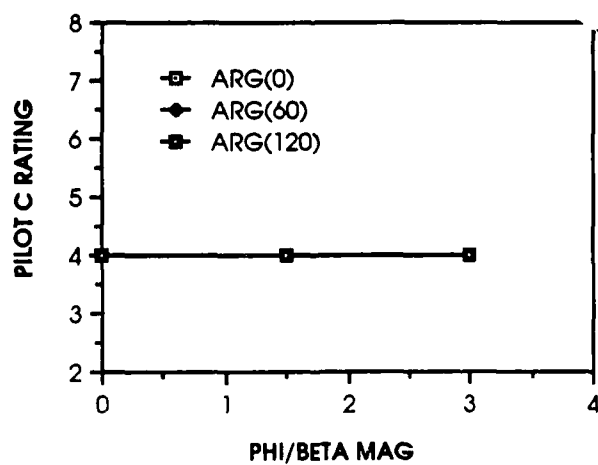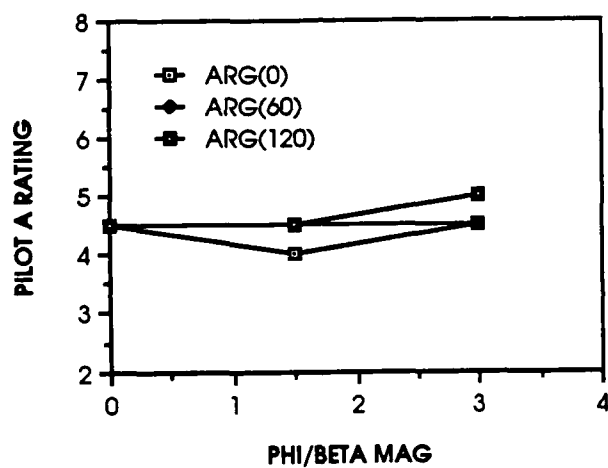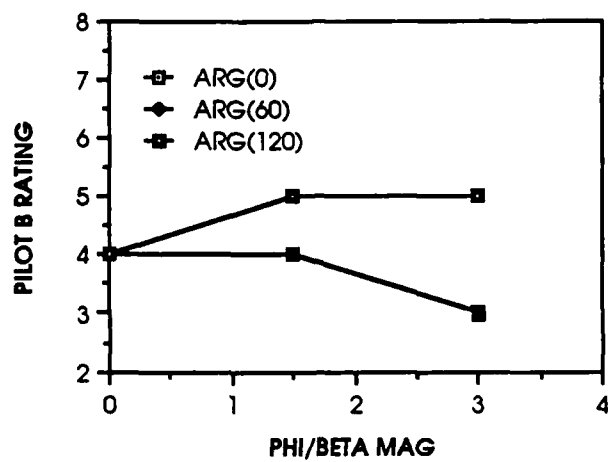
Figure 13. HUD Task 2 - Cooper-Harper Ratings

constant. This increased the roll response, but the effective roll mode time constant was still greater than 0.25 seconds. HUD Task 2 was then reflown to evaluate the different prefilters. Reducing the time constants of the prefilter reduced the time delay below 80 msec, but degraded pilot ratings also. With the 0.025 second prefilter the aircraft became very prone to lateral pilot induced oscillations leading to Cooper-Harper ratings as high as eight. Cockpit accelerations were worse and roll response even more abrupt.

Investigation then focused on stick dynamics. The YA-7D stick was a force command stick with little lateral movement because of the small cockpit. Stripchart data showed significant variation in stick force even when the pilot was attempting to hold the stick steady during rolling maneuvers. It is believed the combination of a sensitive stick with high cockpit accelerations produced the poor pilot ratings. For example, if the pilot put in a five pound force, the aircraft would produce lateral accelerations in the cockpit on the order of three ft/sec^2. Assuming the stick and pilot's arm weighed 10 pounds, this produced a force variation of one pound, or 20 percent. When pilots specifically looked for variations in stick force, all commented on the large effect of the cockpit accelerations. Pilot B reflew several of the control laws with both hands on the stick to minimize the effects of stick-arm dynamics. Even though he was using the most sensitive stick (with a CAS prefilter time constant of 0.025 seconds) he noted a marked improvement. The Cooper-Harper rating for HUD Task 2 dropped from an eight to a three. Thus, it is felt the stick dynamics, rather than a problem in the control laws produced the low pilot ratings in the roll

response. In fact, the pilots felt stick dynamics were the most
important factor in the DIGITAC's lateral handling qualities.

Results in Figure 13 show little variation of pilot rating with
phi/beta magnitude or phase angle. With a phi/beta magnitude ratio of
three, slight roll oscillations were excited by adverse yaw, but they
were well damped and did not significantly degrade pilot ratings.

Pilot opinions of the air-to-air tracking task differed. Pilot A
disliked it and felt he was not able to increase his gain sufficiently
because of pendulum effects inherent in the sight. However, pilot C
liked it the best of all closed loop tasks and felt it most illustrated
the differences in the control systems. This is reflected in the
results shown in Figure 14 on the following page. Pilot C was able to
use the task to break out differences in the control laws very
consistently. All pilots were consistent in disliking the phi/beta
phase angle of 120 degrees, which agreed with test results from HUD Task
1. Again, there was no strong breakout of pilot rating with phi/beta
magnitude ratio. Dutch roll damping ratio was sufficient in this task.
Many of the pilot's complaints centered on the abrupt roll response,
which has already been discussed.

Figure 15 on page 82 shows Cooper-Harper ratings for the three
closed loop tasks using the average of all three pilots' ratings.
Results are similar to those previously discussed. The phi/beta
magnitude ratio did not have a noticible effect on the flying qualities,
but the pilot ratings consistently degraded for a phi/beta phase angle
of 120 degrees. HUD Task 1 showed a phase angle of zero degrees to be
the best, while the other tasks did not show a breakout between zero and

80
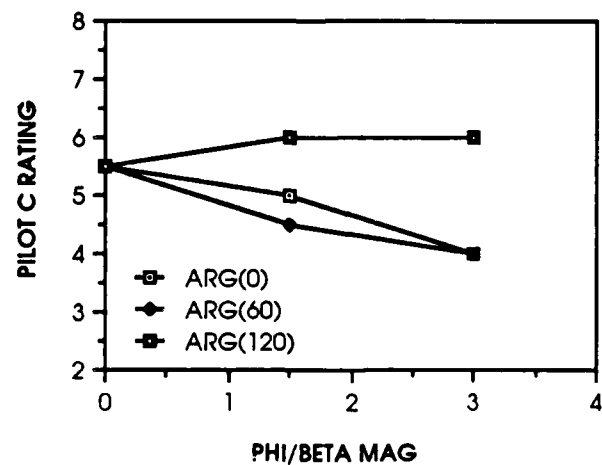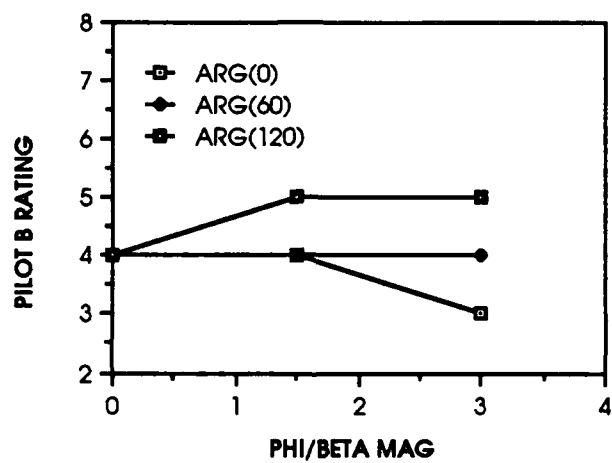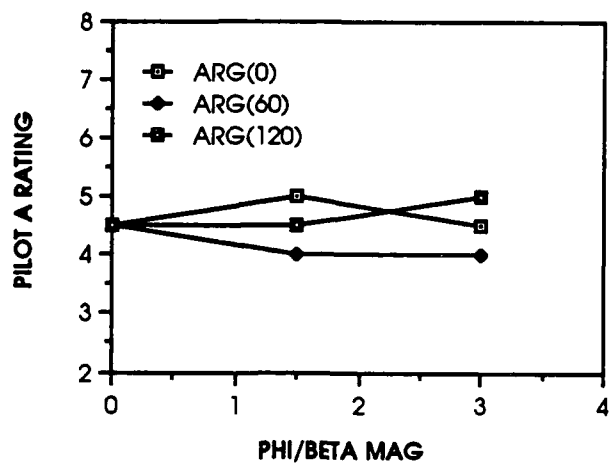
Figure 14. Air-to-Air Tracking - Cooper-Harper Ratings
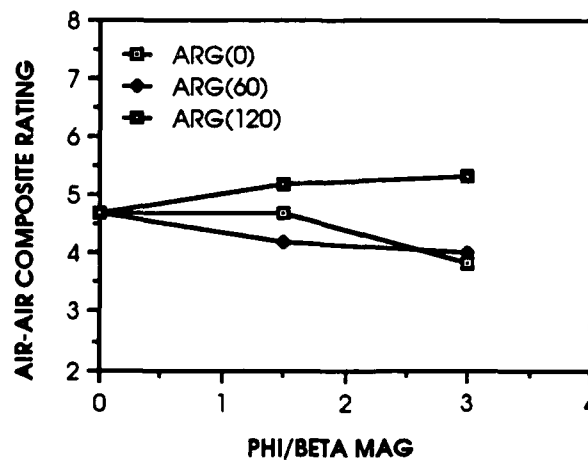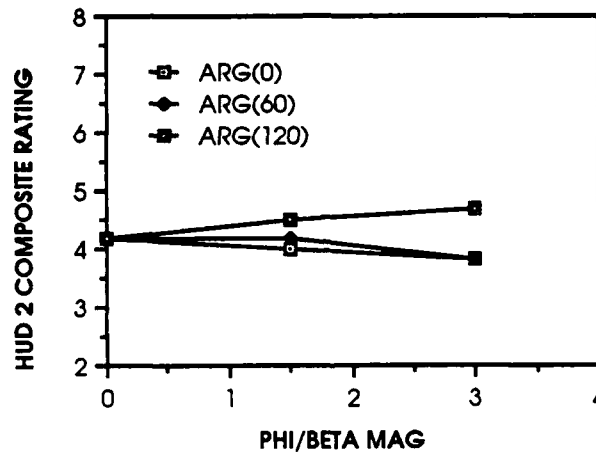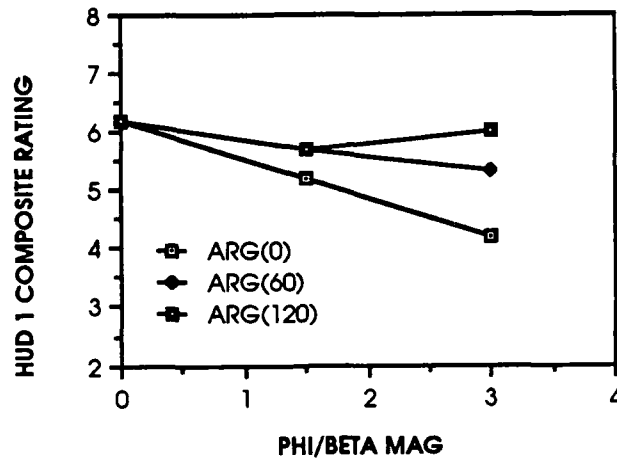
Figure 15. Composite Pilot Ratings

60 degrees. The pilots felt with a phase angle of 120 degrees the dutch roll tended to get out of phase with the pilot's inputs.

The dramatic effects of lateral stick dynamics influenced pilot ratings in all tasks. It was felt that breakout of pilot rating with phi/beta magnitude and phase angle may have actually been greater than reported, but poor stick dynamics overshadowed the moderate differences in aircraft response created by the control system designs. For example, the pilots felt the aircraft response with phi/beta of zero was the most abrupt, and overly sensitive. It was difficult to identify how much of this was due to the natural response of the aircraft and how much due to stick dynamics.

The effects of lateral stick dynamics also illustrated that achieving good flying qualities is much more than compliance with open loop requirements. Guidance given in MIL-F-8785C is insufficient to insure satisfactory handling qualities. All components between the pilot's input and the aircraft response must be considered in detail.

Evaluation of Eigenstructure Assignment

The results of the flight tests verified eigenstructure assignment as a valid technique to derive flight control laws. Despite gross uncertainties in the aerodynamic data and errors introduced by a digital flight control system, the control laws produced the desired open loop responses. The ease with which new control laws could be derived when changes had to be incorporated proved to be the most positive feature of eigenstructure assignment. Using the interactive computer software in Appendix A, derivation of 14 new control laws due to the addition of the

noise filters took less than one hour. Changes in mass properties, aerodynamic data, etc., could be incorporated as easily.

Several practical problems arose which illustrated serious deficiencies with eigenstructure assignment. Lateral acceleration feedback was very noisy and sensitive to center of gravity position. Although the structural resonance and position problems with the lateral acceleration signal were not unique to eigenstructure assignment, they did show inaccurate modeling coupled with high gains can lead to unexpected results.

The major disadvantage of eigenstructure assignment was the lack of intuitive interpretation of the control laws, making specific solutions to problems very difficult. Many hours of analysis and simulation were required to identify the vertical displacement of the lateral accelerometer as the cause for the poor performance at 0.4 Mach. Furthermore, it was recognized early that dutch roll damping was insufficient, but increased damping could not be accomplished with an increase of a single gain, as might be done in a conventional control system. The interaction of all feedback loops must be considered to produce the desired response. Results from adjustment of a single gain were unpredictable making fine tuning of the control laws based on pilot comments impossible.

VIII. Conclusions and Recommendations

This research provided much practical experience with eigenstructure assignment. The most attractive aspect of the method is the ease with which gains can be derived. Once a desired eigenstructure is selected, and a state space model developed, gain calculation is quick and easy. Development of even complicated state space models is relatively easy, since a building block approach can be used to expand the model. Changes to the model or desired eigenstructure can be incorporated quickly, and new gains calculated.

Eigenstructure assignment was successful in achieving the desired lateral-directional eigenstructures. Despite a poor aerodynamic model, and errors in modeling the lateral accelerometer output, the desired eigenvalues and eigenvectors were achieved. The gains produced the desired $(\phi/\beta)_d$ over a wide range of magnitudes and phase angles.

Both mathmatical analysis and flight test data showed the handling qualities of the YA-7D to be relatively insensitive to changes in $(\phi/\beta)_d$. This gives the designer leeway in selecting eigenstructures which can yield different gains and yaw-roll coupling. However, the complexity of the feedback laws pose serious practical difficulties. The control laws lack intuitive interpretation, making isolation of handling qualities problems difficult. Failure analysis, which was never addressed in this limited study, would also be complicated. The YA-7D lateral-directional flying qualities showed no improvement over those of the standard DFCS, which used conventional control laws. These

85

problems, although certainly not insurmountable, would seem to make eigenstructure impractical for conventional aircraft.

Eigenstructure assignment may offer significant advantages for unconventional aircraft. With an additional control, such as direct side force, derivation of control laws with conventional methods no longer offers a clear advantage. Analysis with conventional techniques would be very complex, while derivation of control laws with eigenstructure assignment would be hardly more complicated than for the two control case.

Most of the analysis in this report is valid and directly applicable with the addition of direct side force. Not only does this additional control allow one more of the eigenvector components to be exactly placed, but it allows modification of components which could not be effected by the two conventional controls. The clearest example of this is the dutch roll eigenvector. It was shown in Section V that the dutch roll eigenvector was almost totally determined by the ratio of only two components, $(\phi/\beta)_d$. However, in that analysis it was assumed Y_v and consequently $(r/\beta)_d$ could not be greatly changed by the closed loop controls. With direct sideforce control this assumption is no longer true. The designer can now control both $(\phi/\beta)_d$ and $(r/\beta)_d$, which allows the handling qualities to be modified in a manner not possible with conventional aircraft. Sideslip angle can be controlled directly, and turn coordination can be improved. It also allows control of the lateral acceleration, which may improve handling qualities by reducing pilot station acceleration. In fact, the aircraft can now be made to roll about any desired axis. It is not clear how to select $(r/\beta)_d$ to

achieve the best combination of sideslip angle and lateral acceleration control. And direct sideforce control makes selection of $(\phi/\beta)_d$ even more confusing. This area deserves future study to determine if handling qualities can be usefully improved with direct side force control, and the relationship of $(r/\beta)_d$ to such improvements.

The final conclusions from this study are certainly not new to experienced aircraft designers and not unique to eigenstructure assignment, but are important to emphasize nonetheless. Satisfactory handling qualities can only be achieved by considering the aircraft as a whole. Everything that affects the pilot must be considered. In the case of the YA-7D, cockpit acceleration coupled with the stick design to produce unusual lateral dynamics. The study also pointed out the importance of flight testing. Regardless of the care used in the math model and control law design, satisfactory handling qualities can only be guaranteed through carefully planned and conducted flight tests.

Eigenstructure assignment is a valid technique for derivation of control laws. Although of questionable value for conventional airplanes, it promises more usefulness in unconventional aircraft.

APPENDIX A. FORTRAN Program for Eigenstructure

Assignment Using Output Feedback

This FORTRAN implementation of eigenstructure assignment follows the description in Section II. International Mathematics and Statistics Library (IMSL) subroutines were used to calculate $(\lambda_i I - A)^{-1}$ and the generalized inverse, L^+_i as well as matrix products and additions. The only difficulty is in incorporating complex eigenvalues and eigenvectors into the algorithm. This can be done by converting certain complex operations to real ones and using available library routines to perform complex operations as described below.

Accuracy is usually best if $(\lambda_i I - A)^{-1}$ is calculated directly using complex arithmetic. It is then fairly easy to multiply by B to produce the complex matrix $L_i = (\lambda_i - A)^{-1}B$. Up to this point the operations have been the same for complex and real eigenvalues, although the routines used will of course differ. For real eigenvalues the generalized inverse, L^+ is found next using a singular value decomposition. However, for complex matrices library subroutines do not exist to find the generalized inverse. Even if available it would still not be desirable because it would then not be possible to specify only the real portion or only the imaginary portion of a given eigenvector component. To get around this problem a _real_ matrix, L_i' is defined

$$L_i' = \left[\begin{array}{c|c} \mathrm{Re}(L_i) & -\mathrm{Im}(L_i) \\ \hline \mathrm{Im}(L_i) & \mathrm{Re}(L_i) \end{array} \right] \qquad (55)$$

where $Re(L_i)$ and $Im(L_i)$ are the real and imaginary portions of L_i, respectively. L_i is an n X m complex matrix so L_i' is a 2n X 2m real matrix. The corresponding complex eigenvector, $\underline{v}_i$, becomes

$$\underline{v}_i' = [\ \underline{v}_{1R} \quad \underline{v}_{2R} \quad \cdots \quad \underline{v}_{nR} \quad \underline{v}_{1I} \quad \underline{v}_{2I} \quad \cdots \quad \underline{v}_{nI} \ ] \qquad (56)$$

where $\underline{v}_{nR}$ and $\underline{v}_{nI}$ are the nth real and imaginary components of the eigenvector, $\underline{v}_i$. Thus, $\underline{v}_i'$ is of length 2n. The rows in L_i' corresponding to the rows in $\underline{v}_i'$ which are to specified are then used to find the generalized inverse. The achievable eigenvector and $\underline{w}_i$ are found exactly as for real eigenvalues, except of course they are both of length 2n. They can then be divided into real and imaginary portions again so each complex eigenvalue will take up two rows of $\underline{w}_i$ and V instead of one. Therefore the calculation of F is not affected.

The FORTRAN program listed below uses eigenstructure assignment to calculate F assuming there are two controls and four output quantities which are linear combinations of the state.

```
C**********************************************************
C
C     PROGRAM NAME: EIGEN4
C     AUTHOR: MICHAEL COSTIGAN
C     DATE: 16 JUL 86
C     PURPOSE: TO CALCULATE A FEEDBACK MATRIX F
C              THAT WILL ASSIGN CLOSED LOOP EIGENVALUES
C              AND EIGENVECTORS USING OUTPUT FEEDBACK.
C     INPUTS:
C       TITLE - 30 CHARACTER TITLE PRINTED IN OUTPUT
C       N - ORDER OF THE SYSTEM
C       A - AN N X N STATE MATRIX
C       B - AN N X 2 CONTROL MATRIX
C       C - AN N X 4 OUTPUT MATRIX
C     THE ABOVE MATRICES ARE READ FROM FILE STATE
C       LABEL - 30 CHARACTER LABEL PRINTED IN OUTPUT
C       LAMDR - DESIRED COMPLEX DUTCH ROLL E-VALUE
C       LAMSP - DESIRED SPIRAL MODE E-VALUE
C       LAMRS - DESIRED ROLL MODE E-VALUE
C       VDDRR - REAL PORTION OF DESIRED DUTCH ROLL E-VECTOR
C       VDDRI - IMAG PORTION OF DESIRED DUTCH ROLL E-VECTOR
C       VDSP -  DESIRED COMPONENTS OF SPIRAL E-VECTOR
C       VDRS -  DESIRED COMPONENTS OF ROLL E-VECTOR
C       IDRR -  N X 1 VECTOR IDENTIFYING ROWS OF REAL DUTCH
C               ROLL E-VECTOR TO BE SPECIFIED
C       IDRI -  N x 1 VECTOR IDENTIFYING ROWS OF IMAG DUTCH
C               ROLL E-VECTOR TO BE SPECIFIED
C       IDSP -  N X 1 VECTOR IDENTIFYING ROWS OF SPIRAL
C               E-VECTOR TO BE SPECIFIED
C       IDRS -  N X 1 VECTOR IDENTIFYING ROWS OF ROLL
C               E-VECTOR TO BE SPECIFIED
C     THE ABOVE VARIABLES IDENTIFY THE DESIRED EIGENVALUES
C      AND EIGENVECTORS AND ARE READ FROM FILE EIGENV
C
C**********************************************************
C
      REAL A(20,20),B(20,2),C(5,20),LAMSP,LAMRS,VDDRR(20),
     *VDDRI(20),VDSP(20),VDRS(20),VDRR(20),VDRI(20),VSP(20),
     *VRS(20),V(20,5),AAUG(20,20),BAUG(20,20),WK(350),F(2,5)
     *,W(2,5)
      INTEGER N,ISUM(5),IDRR(20),IDRI(20),IDSP(20),IDRS(20)
      COMPLEX LAMDR,EVEC(20,20),EVAL(20),ZN,EVECA(20,20),
     *EVALA(20),ZNA
      CHARACTER TITLE*30,LABEL*30
C
C     READ INPUT DATA FROM FILES
C
      OPEN(4,FILE='STATE',STATUS='OLD')
      REWIND(4)
      READ(4,*)TITLE
```

```fortran
          READ(4,*)N
          READ(4,*) ((A(I,J) , J=1,N) , I=1,N),((B(I,J),J=1,2 ),
         *I=1,N),((C(I,J) , J=1,N) , I=1,4)
          CLOSE(4)
          OPEN(4,FILE='EIGENV',STATUS='OLD')
          REWIND(4)
          READ(4,*)LABEL
          READ(4,*)LAMDR,LAMSP,LAMRS,(IDRR(I),I=1,N),
         *(IDRI(I),I=1,N),(IDSP(I),I=1,N),(IDRS(I),I=1,N)
          DO 10 I=1,N
            ISUM(1)=ISUM(1)+IDRR(I)
            ISUM(2)=ISUM(2)+IDRI(I)
            ISUM(3)=ISUM(3)+IDSP(I)
    10      ISUM(4)=ISUM(4)+IDRS(I)
          READ(4,*)(VDDRR(I),I=1,ISUM(1)),(VDDRI(I),I=1,ISUM(2))
         *,(VDSP(I),I=1,ISUM(3)),(VDRS(I),I=1,ISUM(4))
          CLOSE(4)
    C
    C     CALCULATE SPIRAL MODE E-VECTOR
    C
          CALL REVEC(A,B,N,W,IDSP,VDSP,LAMSP,VSP,ISUM(3),3)
    C
    C     CALCULATE ROLL MODE E-VECTOR
    C
          CALL REVEC(A,B,N,W,IDRS,VDRS,LAMRS,VRS,ISUM(4),4)
    C
    C     CALCULATE DUTCH ROLL MODE E-VECTOR
    C
          CALL DRVEC(A,B,N,W,IDRR,IDRI,VDDRR,VDDRI,LAMDR,VDRR,
         *VDRI,ISUM(1),ISUM(2))
    C
    C     FORM MATRIX OF EIGENVECTORS
    C
          DO 20 I=1,N
            V(I,1)=VDRR(I)
            V(I,2)=VDRI(I)
            V(I,3)=VSP(I)
    20      V(I,4)=VRS(I)
    C
    C     CALCULATE FEEDBACK MATRIX, F
    C
          CALL FCALC(C,W,N,V,F)
    C
    C     CALCULATE AUGMENTED A MATRIX
    C
          CALL VMULFF(F,C,2,4,N,2,5,AAUG,20,IER)
          CALL VMULFF(B,AAUG,N,2,N,20,20,BAUG,20,IER)
          DO 30 I=1,N
            DO 30 J=1,N
    30 AAUG(I,J)=A(I,J)+BAUG(I,J)
    C
    C     CALCULATE E-VALUES AND E-VECTORS OF AUGMENTED SYSTEM
```

91

```
C
      CALL EIGRF(AAUG,N,20,2,EVAL,EVEC,20,WK,IER)
      IF(WK(1) .GT. 1.)PRINT*,'WARNING - EIGENVECTORS'
     *,' OF AUGMENTED A MATRIX MAY NOT BE ACCURATE'
C
C     CALCULATE E-VALUES AND E-VECTORS OF UNAUGMENTED SYSTEM
C
      CALL EIGRF(A,N,20,2,EVALA,EVECA,20,WK,IER)
      IF(WK(1) .GT. 1.)PRINT*,'WARNING - EIGENVECTORS'
     *'OF UNAUGMENTED SYSTEM MAY NOT BE ACCURATE'
C
C     NORMALIZE E-VECTORS
C
      DO 40 J=1,N
        K=1
        M=1
35      ZN=EVEC(K,J)
        IF(CABS(ZN) .LT. 1.E-4 .AND. K.LE.N) THEN
          K=K+1
          GO TO 35
        ELSEIF(K .GT. N) THEN
          PRINT*,'WARNING - THERE IS A ZER  E-VECTOR'
          CALL EXIT
        ENDIF
45      ZNA=EVECA(M,J)
        IF(CABS(ZNA) .LT. 1.E-4 .AND. M.LE.N) THEN
          M=M+1
          GO TO 45
        ELSEIF(M .GT. N)THEN
          PRINT*,'WARNING - THERE IS A ZERO E-VECTOR'
          CALL EXIT
        ENDIF
        DO 40 I=1,N
          EVEC(I,J)=EVEC(I,J)/ZN
40        EVECA(I,J)=EVECA(I,J)/ZNA
C
C     PRINT CALCULATED VALUES
C
      WRITE(6,50)TITLE
      WRITE(6,50)LABEL
      WRITE(6,55)((F(I,J) , J=1,4) , I=1,2)
50 FORMAT(/17X,A)
55 FORMAT(//20X,'FEEDBACK GAIN MATRIX F '
     *//2(10X,4(F8.4,2X)/)///)
      WRITE(6,60)
      DO 65 I=1,N
65 WRITE(6,70)(AAUG(I,J),J=1,N)
60 FORMAT(//20X,'AUGMENTED A MATRIX'//)
70 FORMAT(2(6(1X,F10.3)/)///)
      WRITE(6,75)
75 FORMAT(//20X,'DUTCH ROLL MODE - REAL'
     *  /2X,'EIGENVALUE',
```

```
      *3X,'DESIRED EIGENVECTOR',5X,'ACHIEVED EIGENVECTOR'//)
       K=1
       IF(IDRR(1).EQ.1)THEN
           WRITE(6,85)REAL(LAMDR),VDDRR(K),VDRR(1)
           K=K+1
        ELSE
           WRITE(6,90)REAL(LAMDR),VDRR(1)
        ENDIF
       DO 80 I=2,N
         IF(IDRR(I).EQ.1)THEN
           WRITE(6,95)VDDRR(K),VDRR(I)
           K=K+1
         ELSE
           WRITE(6,100)VDRR(I)
         ENDIF
   80 CONTINUE
   85 FORMAT(4X,F7.3,10X,F10.3,11X,F10.3)
   90 FORMAT(4X,F7.3,15X,'X',15X,F10.3)
   95 FORMAT(21X,F10.3,11X,F10.3)
  100 FORMAT(26X,'X',15X,F10.3)
      WRITE(6,110)
  110 FORMAT(///20X,'DUTCH ROLL MODE - IMAG'
     *//2X,'EIGENVALUE',
     *3X,'DESIRED EIGENVECTOR'5X,'ACHIEVED EIGENVECTOR'//)
       K=1
       IF(IDRI(1) .EQ. 1)THEN
         WRITE(6,85)AIMAG(LAMDR),VDDRI(K),VDRI(1)
         K=K+1
       ELSE
         WRITE(6,90)AIMAG(LAMDR),VDRI(1)
       ENDIF
       DO 120 I=2,N
         IF(IDRI(I).EQ.1)THEN
           WRITE(6,95)VDDRI(K),VDRI(I)
           K=K+1
         ELSE
           WRITE(6,100)VDRI(I)
         ENDIF
  120 CONTINUE
      WRITE(6,130)
  130 FORMAT(///24X,'SPIRAL MODE'//2X,'EIGENVALUE',3X,
     *'DESIRED EIGENVECTOR',5X,'ACHIEVED EIGENVECTOR'//)
       K=1
       IF(IDSP(1) .EQ. 1)THEN
         WRITE(6,85)LAMSP,VDSP(K),VSP(1)
         K=K+1
       ELSE
         WRITE(6,90)LAMSP,VSP(1)
       ENDIF
       DO 140 I=2,N
         IF(IDSP(I).EQ.1)THEN
           WRITE(6,95)VDSP(K),VSP(I)
```

```
                K=K+1
              ELSE
                WRITE(6,100)VSP(I)
              ENDIF
    140   CONTINUE
          WRITE(6,150)
    150   FORMAT(///24X,'ROLL MODE'//2X,'EIGENVALUE',3X,
         *'DESIRED EIGENVECTOR',5X,'ACHIEVED EIGENVECTOR'//)
          K=1
          IF(IDRS(1) .EQ. 1)THEN
            WRITE(6,85)LAMRS,VDRS(K),VRS(1)
            K=K+1
          ELSE
            WRITE(6,90)LAMRS,VRS(1)
          ENDIF
          DO 160 I=2,N
            IF(IDRS(I).EQ.1)THEN
              WRITE(6,95)VDRS(K),VRS(I)
              K=K+1
            ELSE
              WRITE(6,100)VRS(I)
            ENDIF
    160   CONTINUE
          WRITE(6,170)
          DO 180 K=1,N
            WRITE(6,190)EVALA(K),EVECA(1,K)
            DO 180 M=2,N
    180       WRITE(6,200)EVECA(M,K)
          WRITE(6,210)
          DO 220 K=1,N
            WRITE(6,190)EVAL(K),EVEC(1,K)
            DO 220 M=2,N
    220       WRITE(6,200)EVEC(M,K)
    170   FORMAT(//15X,'OPEN LOOP SPECTRAL DECOMPOSITION'//
         *10X,'EIGENVALUES',15X,'EIGENVECTORS'/)
    210   FORMAT(//15X,'CLOSED LOOP SPECTRAL DECOMPOSITION'//
         *10X,'EIGENVALUES',15X,'EIGENVECTORS'/)
    190   FORMAT(//2X,F10.3,3X,F10.3,'i',5X,F10.3,3X,F10.3,'i')
    200   FORMAT(31X,F10.3,3X,F10.3,'i')
          STOP
          END
    C
    C***********************************************************  **
    C
          SUBROUTINE REVEC
         *(A,B,N,W,IDRE,VDRE,LAMRE,VRE,INUM,IRUN)
    C
    C     THIS SUBROUTINE CALCULATES THE LEAST SQUARES
    C     PROJECTION OF THE DESIRED EIGENVECTOR COMPONENTS
    C     INTO THE ALLOWABLE SUBSPACE.  AT LEAST TWO
    C     COMPONENTS MUST BE SPECIFIED.
    C
```

94

```
          REAL WK(550),
     *A(20,20),B(20,2),VDRE(20),LAMRE,VRE(20),LAMDAI(20,20),
     *LAMINV(20,20),L(20,2),LTILDA(20,2),L2TILDA(20,2),
     *S(20),LTILIV(2,20),LPROJ(20,20),VPROJ(20),Z(20),W(2,5)
          INTEGER N,IDGT,IDRE(20),IER,INUM,IROW(20),MROW,IRUN
          IDGT=0
C
C     CALCULATE  (LAMDA*I - A) INVERSE
C
          DO 10 I=1,N
            DO 10 J=1,N
              IF(I.EQ.J) THEN
                LAMDAI(I,I)=LAMRE-A(I,I)
              ELSE
                LAMDAI(I,J)=-A(I,J)
              ENDIF
   10 CONTINUE
          CALL LINV2F(LAMDAI,N,20,LAMINV,IDGT,WK,IER)
          IF(IER.EQ.129.AND.IRUN.EQ.3)PRINT*,'WARNING - THE '
     *,'SPIRAL LAMDA*I-A MATRIX IS SINGULAR'
          IF(IER.EQ.129.AND.IRUN.EQ.4) PRINT*,'WARNING - THE '
     *,'ROLL MODE LAMDA*I-A MATRIX IS SINGULAR'
C
C     CALCULATE LAMDA*I-A INVERSE X B
C
          CALL VMULFF(LAMINV,B,N,N,2,20,20,L,20,IER)
C
C     CALCULATE ROWS OF LAMDA*I-A INVERSE X B TO BE USED
C     IN CALCULATING LEAST SQUARES PROJECTION
C
          MROW=1
          DO 20 I=1,N
            IF(IDRE(I) .EQ. 1) THEN
               IROW(MROW)=I
               MROW=MROW+1
            ENDIF
   20   CONTINUE
          DO 30 I=1,INUM
            DO 30 J=1,2
              LTILDA(I,J)=L(IROW(I),J)
   30       L2TILDA(I,J)=LTILDA(I,J)
C
C     CALCULATE GENERALIZED INVERSE
C
          CALL LGINF(LTILDA,20,INUM,2,0,LTILIV,2,S,WK,IER)
          IF(IER.EQ.33)PRINT*,'WARNING - GENERALIZED INVERSE IS '
     *,'ILL CONDITIONED'
          IF(IER.EQ.29)PRINT*,'WARNING - GENERALIZED INVERSE'
     *,' NOT OBTAINED - COMPUTATION TERMINATED'
C
C     FIND PROJECTION OF DESIRED VECTOR
C
```

```
            CALL VMULFF(L2TILDA,LTILIV,INUM,2,INUM,20,2,LPROJ,
       *20,IER)
            CALL VMULFF(LPROJ,VDRE,INUM,INUM,1,20,20,VPROJ,20,IER)
C
C       CALCULATE LINEAR COMBINATION OF SUBSPACE AND
C       REMAINING COMPONENTS OF VECTOR
C
            CALL VMULFF(LTILIV,VPROJ,2,INUM,1,2,20,Z,20,IER)
            CALL VMULFF(L,Z,N,2,1,20,20,VRE,20,IER)
            DO 40 I=1,INUM
       40 VRE(IROW(I))=VPROJ(I)
            DO 50 I=1,2
       50 W(I,IRUN)=Z(I)
            RETURN
            END
C
C****************************************************** **
C
            SUBROUTINE DRVEC(A,B,N,W,IDRR,IDRI,VDDRR,VDDRI,LAMDR,
       *VDRR,VDRI,IRNUM,IINUM)
C
C       THIS SUBROUTINE COMPUTES THE LEAST SQUARES PROJECTION
C       OF THE COMPLEX DUTCH ROLL EIGENVECTOR.  AT LEAST TWO
C       COMPONENTS OF EACH OF THE REAL AND IMAG PARTS MUST BE
C       SPECIFIED.
C
            REAL A(20,20),B(20,2),VDRR(20),VDRI(20),VDDRR(20),
       *VDDRI(20),WK(150),LTILDA(40,4),L2TILDA(40,4),
       *VDPRIM(40),S(8,0),LPRIM(40,40),
       *LTILIV(4,40),LPROJ(40,40),VPROJ(40),Z(40),
       *VDPRIM(40),W(2,5)
            INTEGER N,
       *IDRR(20),IDRI(20),INUM,IRNUM,IINUM,MROW,IROW(20)
            COMPLEX LAMDR,LAMDAI(20,20),LAMINV(20,20),WA(550),
       *L(20,20)
C
C       CALCULATE LAMDA*I-A INVERSE
C
            DO 10 I=1,N
              DO 10 J=1,N
                IF(I.EQ.J) THEN
                  LAMDAI(I,I)=LAMDR-A(I,I)
                  LAMINV(I,I)=(1.0,0.)
                ELSE
                  LAMDAI(I,J)=-A(I,J)
                  LAMINV(I,J)=(0.,0.)
                ENDIF
       10 CONTINUE
            CALL LEQ2C(LAMDAI,N,20,LAMINV,N,20,0,WA,WK,IER)
            IF(IER.EQ.129)PRINT*,'WARNING - LAMDA*I-A FOR THE'
       *,' DUTCH ROLL MODE IS SINGULAR'
            IF(IER.EQ.130)PRINT*,'WARNING - LAMDA*I-A FOR THE'
```

```
     *,' DUTCH ROLL MODE IS ILL CONDITIONED'
C
C     CALCULATE LAMDA*I-A INVERSE X B
C
      DO 20 I=1,N
         DO 20 J=1,2
         L(I,J)=(0.,0.)
          DO 20 M=1,N
20         L(I,J)=L(I,J)+LAMINV(I,M)*B(M,J)
C
C     CALCULATE ROWS TO BE USED IN FINDING LEAST SQUARES FIT
C
      NROW=1
      DO 30 I=1,N
        IF(IDRR(I). EQ. 1) THEN
          IROW(NROW)=I
          NROW=NROW+1
        ENDIF
30 CONTINUE
      DO 40 I=1,N
        IF(IDRI(I) .EQ. 1) THEN
          IROW(NROW)=I+N
          NROW=NROW+1
        ENDIF
40 CONTINUE
      INUM=IRNUM+IINUM
C
C     FORM REAL MATRIX REPRESENTATION TO FIND GENERALIZED
C     INVERSE
C
      DO 50 I=1,N
        DO 50 J=1,2
           LPRIM(I,J)=REAL(L(I,J))
           LPRIM(I,J+2)=-AIMAG(L(I,J))
           LPRIM(I+N,J)=AIMAG(L(I,J))
50         LPRIM(I+N,J+2)=LPRIM(I,J)
      DO 55 I=1,INUM
        DO 55 J=1,4
           LTILDA(I,J)=LPRIM(IROW(I),J)
55         L2TILDA(I,J)=LTILDA(I,J)
      DO 60 I=1,IRNUM
60 VDPRIM(I)=VDDRR(I)
      DO 70 I=1,IINUM
70 VDPRIM(I+IRNUM)=VDDRI(I)
C
C     CALCULATE GENERALIZED INVERSE OF AUGMENTED MATRIX
C
      CALL LGINF(LTILDA,40,INUM,4,0,LTILIV,4,S,WK,IER)
      IF(IER.EQ.33)PRINT*,'WARNING - GENERALIZED INVERSE OF'
     *,'DUTCH ROLL AUGMENTED MATRIX IS ILL CONDITIONED'
      IF(IER.EQ.29)PRINT*,'WARNING - GENERALIZED INVERSE OF'
     *,'DUTCH ROLL AUGMENTED MATRIX NOT OBTAINED -
```

97

```fortran
     *,' COMPUTATION TERMINATED'
C
C     CALCULATE PROJECTION OF DESIRED VECTOR
C
      CALL VMULFF(L2TILDA,LTILIV,INUM,4,INUM,40,4,LPROJ,
     *40,IER)
      CALL VMULFF
     *(LPROJ,VDPRIM,INUM,INUM,1,40,40,VPROJ,40,IER)
C
C     FIND LINEAR COMBINATION OF THE SUBSPACE AND CALCULATE
C     THE UNSPECIFIED E-VECTOR COMPONENTS
C
      CALL VMULFF(LTILIV,VPROJ,4,INUM,1,4,40,Z,40,IER)
      CALL VMULFF(LPRIM,Z,2*N,4,1,40,40,VDPRIM,40,IER)
      DO 75 I=1,INUM
   75 VDPRIM(IROW(I))=VPROJ(I)
      DO 80 I=1,N
        VDRR(I)=VDPRIM(I)
   80   VDRI(I)=VDPRIM(N+I)
      DO 90 I=1,2
      W(I,1)=Z(I)
   90 W(I,2)=Z(I+2)
      RETURN
      END
C
C*********************************************************
C
      SUBROUTINE FCALC(C,W,N,V,F)
C
C     THIS SUBROUTINE CALCULATES THE FEEDBACK MATRIX, F
C     TO PLACE THE EIGENVALUES AND EIGENVECTORS
C
      REAL C(5,20),W(2,5),V(20,5),F(2,5),WK(350),
     *CV(5,20),CVINV(20,20)
      INTEGER N,IDGT
C
C     CALCULATE FEEDBACK MATRIX F
C
      CALL VMULFF(C,V,4,N,4,5,20,CV,5,IER)
      IDGT=0
      CALL LINV2F(CV,4,5,CVINV,IDGT,WK,IER)
      IF(IER.EQ.129 .OR. IER.EQ.131)PRINT*,'WARNING - ',
     *'THE CV MATRIX IS EITHER SINGULAR OR VERY'
     *' ILL-CONDITIONED'
      CALL VMULFF(W,CVINV,2,4,4,2,5,F,2,IER)
      RETURN
      END
```

APPENDIX B.   Sample Output and Spectral

Decomposition of YA-7D System

   Listed below are sample outputs of the eigenstructure assignment
program. These examples are from the 12th order models of the YA-7D
described in the text. The desired eigenstructures are also derived in
the text with, $(\phi/\beta)_d$ of zero in these cases. Also included as part of
the output are spectral decompositions of the open loop and closed loop
systems. It is easily verified that the desired eigenvalues and
eigenvectors were exactly achieved.

YA-7D at 0.4 Mach

phi/beta = 0

FEEDBACK GAIN MATRIX F

0.4596	0.0401	0.1088	0.0149
1.1719	0.0798	-0.0835	-0.0063

DUTCH ROLL MODE - REAL

EIGENVALUE	DESIRED EIGENVECTOR	ACHIEVED EIGENVECTOR
-1.200	X	3.851
	1.000	1.000
	X	-0.000
	0.	0.000
	X	-0.610
	X	0.299
	X	-0.344
	X	4.953
	X	0.622
	X	9.928
	X	4.570

99

		X	-57.349

DUTCH ROLL MODE - IMAG

EIGENVALUE	DESIRED EIGENVECTOR	ACHIEVED EIGENVECTOR
2.750	X	-1.805
	1.000	1.000
	X	0.000
	0.	0.000
	X	-1.667
	X	-4.052
	X	-1.651
	X	1.036
	X	-3.882
	X	6.370
	X	-0.456
	X	-36.299

SPIRAL MODE

EIGENVALUE	DESIRED EIGENVECTOR	ACHIEVED EIGENVECTOR
-0.025	X	0.076
	0.	-0.000
	X	-0.025
	1.000	1.000
	X	0.007
	X	-0.011
	X	0.007
	X	-0.000
	X	-0.011
	X	0.000
	X	-0.002
	X	-0.086

ROLL MODE

EIGENVALUE	DESIRED EIGENVECTOR	ACHIEVED EIGENVECTOR
-4.000	0.	-0.001
	0.	0.003
	1.000	1.000

X	-0.250
X	0.224
X	0.153
X	0.179
X	-0.717
X	0.135
X	-0.539
X	0.163
X	-0.236

OPEN LOOP SPECTRAL DECOMPOSITION

EIGENVALUES			EIGENVECTORS		
-1.000	0.	i	0.	0.	i
			0.	0.	i
			0.	0.	i
			0.	0.	i
			0.	0.	i
			0.	0.	i
			0.	0.	i
			0.	0.	i
			0.	0.	i
			0.	0.	i
			1.000	0.	i
			0.	0.	i
-10.000	0.	i	0.	0.	i
			0.	0.	i
			0.	0.	i
			0.	0.	i
			0.	0.	i
			0.	0.	i
			0.	0.	i
			0.	0.	i
			0.	0.	i
			0.	0.	i
			0.	0.	i
			1.000	0.	i
-1.311	0.	i	1.000	0.	i
			0.286	0.	i
			-11.566	0.	i
			8.824	0.	i
			-0.000	0.	i
			-0.000	0.	i
			0.	0.	i

101

			0.	0.	i
			0.	0.	i
			0.	0.	i
			-1.802	0.	i
			-15.372	0.	i
-0.037	0.	i	1.000	0.	i
			0.140	0.	i
			-0.494	0.	i
			13.273	0.	i
			-0.000	0.	i
			-0.000	0.	i
			0.	0.	i
			0.	0.	i
			0.	0.	i
			0.	0.	i
			-0.036	0.	i
			-6.275	0.	i
-0.354	1.721i		1.000	0.	i
			0.157	0.580i	
			-2.853	-1.387i	
			-0.446	1.750i	
			0.000	-0.000i	
			0.000	-0.000i	
			0.	0.	i
			0.	0.	i
			0.	0.	i
			0.	0.	i
			0.606	0.189i	
			-11.541	-22.787i	
-0.354	-1.721i		1.000	0.	i
			0.157	-0.580i	
			-2.853	1.387i	
			-0.446	-1.750i	
			0.000	0.000i	
			0.000	0.000i	
			0.	0.	i
			0.	0.	i
			0.	0.	i
			0.	0.	i
			0.606	-0.189i	
			-11.541	22.787i	
-33.330	0.	i	1.000	0.	i
			0.018	0.	i
			-0.785	0.	i

		0.024	0. i
		-0.000	0. i
		12.923	0. i
		0.	0. i
		0.	0. i
		0.	0. i
		0.	0. i
		0.924	0. i
		-15.419	0. i
-20.000	0. i	1.000	0. i
		0.054	0. i
		-11.887	0. i
		0.594	0. i
		-17.947	0. i
		-0.000	0. i
		0.	0. i
		0.	0.' i
		0.	0. i
		0.	0. i
		-0.491	0. i
		-41.611	0. i
-65.950	67.332i	1.000	0. i
		-0.005	0.008i
		-0.753	-0.012i
		0.006	0.005i
		-0.000	0.000i
		25.733	-26.489i
		0.	0. i
		0.	0. i
		28.328	77.909i
		-7114.024	-3230.746i
		0.907	0.005i
		-12.124	-0.890i
-65.950	-67.332i	1.000	0. i
		-0.005	-0.008i
		-0.753	0.012i
		0.006	-0.005i
		-0.000	-0.000i
		25.733	26.489i
		0.	0. i
		0.	0. i
		28.328	-77.909i
		-7114.024	3230.746i
		0.907	-0.005i
		-12.124	0.890i

-65.950	67.332i	1.000	0. i
		-0.005	0.008i
		-0.753	-0.012i
		0.006	0.005i
		0.000	-0.000i
		25.733	-26.489i
		0.001	0.002i
		-0.173	-0.078i
		28.328	77.910i
		-7114.066	-3230.758i
		0.907	0.005i
		-12.124	-0.890i
-65.950	-67.332i	1.000	0. i
		-0.005	-0.008i
		-0.753	0.012i
		0.006	-0.005i
		0.000	0.000i
		25.733	26.489i
		0.001	-0.002i
		-0.173	0.078i
		28.328	-77.910i
		-7114.066	3230.758i
		0.907	-0.005i
		-12.124	0.890i

CLOSED LOOP SPECTRAL DECOMPOSITION

EIGENVALUES		EIGENVECTORS	
-67.371	67.963i	1.000	0. i
		-0.005	0.008i
		-0.900	-0.235i
		0.005	0.008i
		-2.160	-0.413i
		25.437	-26.912i
		6.522	-6.362i
		-6.964	871.880i
		28.897	79.355i
		-7339.977	-3382.228i
		0.889	-0.022i
		-12.291	-1.164i
-67.371	-67.963i	1.000	0. i
		-0.005	-0.008i
		-0.900	0.235i
		0.005	-0.008i

		-2.160	0.413i
		25.437	26.912i
		6.522	6.362i
		-6.964	-871.880i
		28.897	-79.355i
		-7339.977	3382.228i
		0.889	0.022i
		-12.291	1.164i
-65.050	66.612i	1.000	0. i
		-0.005	0.007i
		-0.595	0.171i
		0.006	0.003i
		1.938	0.097i
		26.148	-26.156i
		-4.689	6.237i
		-110.424	-718.068i
		27.390	77.150i
		-6920.886	-3194.049i
		0.926	0.028i
		-11.942	-0.660i
-65.050	-66.612i	1.000	0. i
		-0.005	-0.007i
		-0.595	-0.171i
		0.006	-0.003i
		1.938	-0.097i
		26.148	26.156i
		-4.689	-6.237i
		-110.424	718.068i
		27.390	-77.150i
		-6920.886	3194.049i
		0.926	-0.028i
		-11.942	0.660i
-33.747	0. i	1.000	0. i
		0.017	0. i
		-0.580	0. i
		0.017	0. i
		0.574	0. i
		13.324	0. i
		-0.395	0. i
		13.324	0. i
		-0.167	0. i
		5.627	0. i
		0.949	0. i
		-15.043	0. i

-14.597	0. i	1.000	0. i
		0.019	0. i
		28.103	0. i
		-1.925	0. i
		33.247	0. i
		20.385	0. i
		8.981	0. i
		-131.105	0. i
		11.457	0. i
		-167.253	0. i
		4.769	0. i
		52.053	0. i
-9.248	0. i	1.000	0. i
		0.091	0. i
		5.993	0. i
		-0.648	0. i
		4.666	0. i
		5.794	0. i
		2.508	0. i
		-23.197	0. i
		4.187	0. i
		-38.722	0. i
		1.938	0. i
		16.990	0. i
-1.200	2.750i	1.000	0. i
		0.113	0.313i
		-0.000	-0.000i
		-0.000	0.000i
		0.037	-0.416i
		0.468	-0.833i
		0.092	-0.386i
		0.951	0.715i
		0.520	-0.764i
		1.476	2.346i
		1.019	0.359i
		-8.588	-13.452i
-1.200	-2.750i	1.000	0. i
		0.113	-0.313i
		-0.000	0.000i
		-0.000	-0.000i
		0.037	0.416i
		0.468	0.833i
		0.092	0.386i
		0.951	-0.715i
		0.520	0.764
		1.476	-2.346.

106

			1.019	-0.359i	
			-8.588	13.452i	
-4.000	0.	i	1.000	0.	i
			-4.126	0.	i
			-1473.740	0.	i
			368.431	0.	i
			-330.197	0.	i
			-225.710	0.	i
			-264.158	0.	i
			1056.710	0.	i
			-198.623	0.	i
			794.923	0.	i
			-239.873	0.	i
			347.673	0.	i
-1.328	0.	i	1.000	0.	i
			0.655	0.	i
			-3.160	0.	i
			2.379	0.	i
			-0.349	0.	i
			0.883	0.	i
			-0.326	0.	i
			0.432	0.	i
			0.848	0.	i
			-1.129	0.	i
			2.448	0.	i
			-27.970	0.	i
-0.025	0.	i	1.000	0.	i
			-0.000	0.	i
			-0.330	0.	i
			13.184	0.	i
			0.087	0.	i
			-0.145	0.	i
			0.086	0.	i
			-0.002	0.	i
			-0.144	0.	i
			0.004	0.	i
			-0.024	0.	i
			-1.136	0.	i

YA-7D at 0.6 Mach

phi/beta = 0

FEEDBACK GAIN MATRIX F

| 0.3091 | 0.0155 | 0.0485 | 0.0057 |
| 0.5725 | 0.0180 | -0.0033 | -0.0032 |

DUTCH ROLL MODE - REAL

EIGENVALUE	DESIRED EIGENVECTOR	ACHIEVED EIGENVECTOR
-1.200	X	3.819
	1.000	1.000
	X	-0.000
	0.	-0.000
	X	-0.582
	X	0.429
	X	-0.399
	X	3.491
	X	0.538
	X	3.261
	X	4.560
	X	-112.282

DUTCH ROLL MODE - IMAG

EIGENVALUE	DESIRED EIGENVECTOR	ACHIEVED EIGENVECTOR
2.750	X	-1.779
	1.000	1.000
	X	-0.000
	0.	0.000
	X	-1.080
	X	-1.510
	X	-1.095
	X	0.218
	X	-1.421
	X	3.185
	X	-0.445
	X	-61.930

SPIRAL MODE

EIGENVALUE	DESIRED EIGENVECTOR	ACHIEVED EIGENVECTOR
-0.025	X	0.051
	0.	-0.000
	X	-0.025
	1.000	1.000
	X	0.003
	X	-0.005
	X	0.003
	X	-0.000
	X	-0.005
	X	0.000
	X	-0.001
	X	-0.077

ROLL MODE

EIGENVALUE	DESIRED EIGENVECTOR	ACHIEVED EIGENVECTOR
-4.000	0.	-0.001
	0.	0.003
	1.000	1.000
	X	-0.250
	X	0.063
	X	0.010
	X	0.050
	X	-0.201
	X	0.009
	X	-0.036
	X	0.049
	X	-0.935

OPEN LOOP SPECTRAL DECOMPOSITION

EIGENVALUES			EIGENVECTORS		
-1.000	0.	i	0.	0.	i
			0.	0.	i
			0.	0.	i
			0.	0.	i
			0.	0.	i
			0.	0.	i
			0.	0.	i

		0.	0. i
		0.	0. i
		0.	0. i
		1.000	0. i
		0.	0. i
-10.000	0. i	0.	0. i
		0.	0. i
		0.	0. i
		0.	0. i
		0.	0. i
		0.	0. i
		0.	0. i
		0.	0. i
		0.	0. i
		0.	0. i
		0.	0. i
		1.000	0. i
-2.316	0. i	1.000	0. i
		0.052	0. i
		-42.036	0. i
		18.153	0. i
		0.000	0. i
		-0.000	0. i
		0.000	0. i
		-0.000	0. i
		0.000	0. i
		0.000	0. i
		-0.991	0. i
		0.916	0. i
-0.036	0. i	1.000	0. i
		0.117	0. i
		-0.713	0. i
		19.970	0. i
		0.000	0. i
		-0.000	0. i
		0.000	0. i
		-0.000	0. i
		0.000	0. i
		0.000	0. i
		-0.036	0. i
		-10.514	0. i
-0.310	2.039i	1.000	0. i
		0.076	0.507i
		-2.752	-2.328i

		-0.915	1.488i
		0.000	0.000i
		-0.000	-0.000i
		0.000	0.000i
		-0.000	-0.000i
		0.000	0.000i
		0.000	0.000i
		0.802	0.321i
		-15.386	-40.025i
-0.310	-2.039i	1.000	0. i
		0.076	-0.507i
		-2.752	2.328i
		-0.915	-1.488i
		0.000	-0.000i
		-0.000	0.000i
		0.000	-0.000i
		-0.000	0.000i
		0.000	-0.000i
		0.000	-0.000i
		0.802	-0.321i
		-15.386	40.025i
-20.000	0. i	1.000	0. i
		-0.132	0. i
		682.003	0. i
		-34.095	0. i
		454.378	0. i
		-0.000	0. i
		0.000	0. i
		-0.000	0. i
		0.000	0. i
		0.000	0. i
		27.738	0. i
		1946.593	0. i
-33.330	0. i	1.000	0. i
		0.022	0. i
		-1.021	0. i
		0.031	0. i
		0.000	0. i
		6.724	0. i
		0.000	0. i
		-0.000	0. i
		0.000	0. i
		0.000	0. i
		0.991	0. i
		-14.186	0. i

-65.950	67.332i	-0.113	0.088i
		-0.001	-0.001i
		1.000	0. i
		-0.007	-0.008i
		2.334	-2.043i
		-0.346	2.793i
		1.516	12.552i
		-945.130	-725.759i
		-5.304	-3.432i
		580.882	-130.777i
		-0.077	0.088i
		2.864	-0.692i
-65.950	-67.332i	-0.113	-0.088i
		-0.001	0.001i
		1.000	0. i
		-0.007	0.008i
		2.334	2.043i
		-0.346	-2.793i
		1.516	-12.552i
		-945.130	725.759i
		-5.304	3.432i
		580.882	130.777i
		-0.077	-0.088i
		2.864	0.692i
-65.950	67.332i	1.000	0. i
		-0.001	0.009i
		-0.483	-2.999i
		-0.019	0.026i
		-6.362	-8.360i
		13.531	-13.599i
		42.760	-2.212i
		-2671.058	3024.966i
		14.229	40.643i
		-3674.957	-1722.330i
		0.989	-0.105i
		-10.419	-5.748i
-65.950	-67.332i	1.000	0. i
		-0.001	-0.009i
		-0.483	2.999i
		-0.019	-0.026i
		-6.362	8.360i
		13.531	13.599i
		42.760	2.212i
		-2671.058	-3024.966i
		14.229	-40.643i
		-3674.957	1722.330i

0.989	0.105i
-10.419	5.748i

CLOSED LOOP SPECTRAL DECOMPOSITION

EIGENVALUES		EIGENVECTORS	
-66.236	67.251i	1.000	0. i
		-0.000	0.008i
		-4.135	0.087i
		0.031	0.031i
		-7.325	8.232i
		13.577	-13.940i
		-10.747	-43.659i
		3647.965	2169.080i
		14.723	41.157i
		-3743.072	-1735.940i
		0.852	0.010i
		-16.894	-0.979i
-66.236	-67.251i	1.000	0. i
		-0.000	-0.008i
		-4.135	-0.087i
		0.031	-0.031i
		-7.325	-8.232i
		13.577	13.940i
		-10.747	43.659i
		3647.965	-2169.080i
		14.723	-41.157i
		-3743.072	1735.940i
		0.852	-0.010i
		-16.894	0.979i
-66.564	67.167i	1.000	0. i
		-0.002	0.008i
		0.328	-0.420i
		-0.006	0.001i
		2.126	-4.250i
		13.465	-13.637i
		9.324	17.034i
		-1764.760	-507.601i
		14.055	40.732i
		-3671.422	-1767.285i
		1.019	-0.008i
		-9.350	-1.325i

-66.564	-67.167i	1.000	0. i
		-0.002	-0.008i
		0.328	0.420i
		-0.006	-0.001i
		2.126	4.250i
		13.465	13.637i
		9.324	-17.034i
		-1764.760	507.601i
		14.055	-40.732i
		-3671.422	1767.285i
		1.019	0.008i
		-9.350	1.325i
-30.793	0. i	1.000	0. i
		0.024	0. i
		-1.087	0. i
		0.035	0. i
		-0.066	0. i
		6.208	0. i
		0.035	0. i
		-1.089	0. i
		0.473	0. i
		-14.553	0. i
		0.991	0. i
		-14.638	0. i
-13.450	2.365i	1.000	0. i
		0.063	0.014i
		9.826	-3.207i
		-0.749	0.107i
		4.288	-2.310i
		2.701	-0.449i
		1.678	-0.249i
		-21.972	7.321i
		1.643	-0.076i
		-21.913	4.909i
		1.472	-0.108i
		29.704	1.953i
-13.450	-2.365i	1.000	0. i
		0.063	-0.014i
		9.826	3.207i
		-0.749	-0.107i
		4.288	2.310i
		2.701	0.449i
		1.678	0.249i
		-21.972	-7.321i
		1.643	0.076i
		-21.913	-4.909i

		1.472	0.108i
		29.704	-1.953i
-1.200	2.750i	1.000	0. i
		0.115	0.315i
		-0.000	-0.000i
		-0.000	0.000i
		-0.017	-0.291i
		0.244	-0.282i
		0.024	-0.276i
		0.729	0.397i
		0.258	-0.252i
		0.381	1.012i
		1.026	0.361i
		-17.948	-24.580i
-1.200	-2.750i	1.000	0. i
		0.115	-0.315i
		-0.000	0.000i
		-0.000	-0.000i
		-0.017	0.291i
		0.244	0.282i
		0.024	0.276i
		0.729	-0.397i
		0.258	0.252i
		0.381	-1.012i
		1.026	-0.361i
		-17.948	24.580i
-4.000	0. i	-0.249	0. i
		1.000	0. i
		381.376	0. i
		-95.344	0. i
		24.013	0. i
		3.910	0. i
		19.210	0. i
		-76.842	0. i
		3.441	0. i
		-13.766	0. i
		18.567	0. i
		-356.685	0. i
-1.384	0. i	1.000	0. i
		0.659	0. i
		-4.401	0. i
		3.180	0. i
		-0.195	0. i
		0.714	0. i

			-0.181	0.	i
			0.251	0.	i
			0.684	0.	i
			-0.950	0.	i
			3.010	0.	i
			-58.599	0.	i
-0.025	0.	i	1.000	0.	i
			-0.000	0.	i
			-0.494	0.	i
			19.775	0.	i
			0.053	0.	i
			-0.103	0.	i
			0.053	0.	i
			-0.001	0.	i
			-0.103	0.	i
			0.003	0.	i
			-0.025	0.	i
			-1.520	0.	i

APPENDIX C. <u>Frequency Response Plots for Selected</u>

<u>Eigenstructures</u>

This appendix contains frequency response plots of ϕ/Fs and Y_{cf} for
the unaugmented and augmented YA-7D at 0.4 and 0.6 Mach. The responses
were generated from the 14th order eigenstructures described in the
text. The unaugmented YA-7D includes only the mechanical flight control
system, while the augmented eigenstructures contain effects from both
the mechanical system and roll CAS. The only difference in the
augmented eigenstructures is the design $(\phi/\beta)_d$.
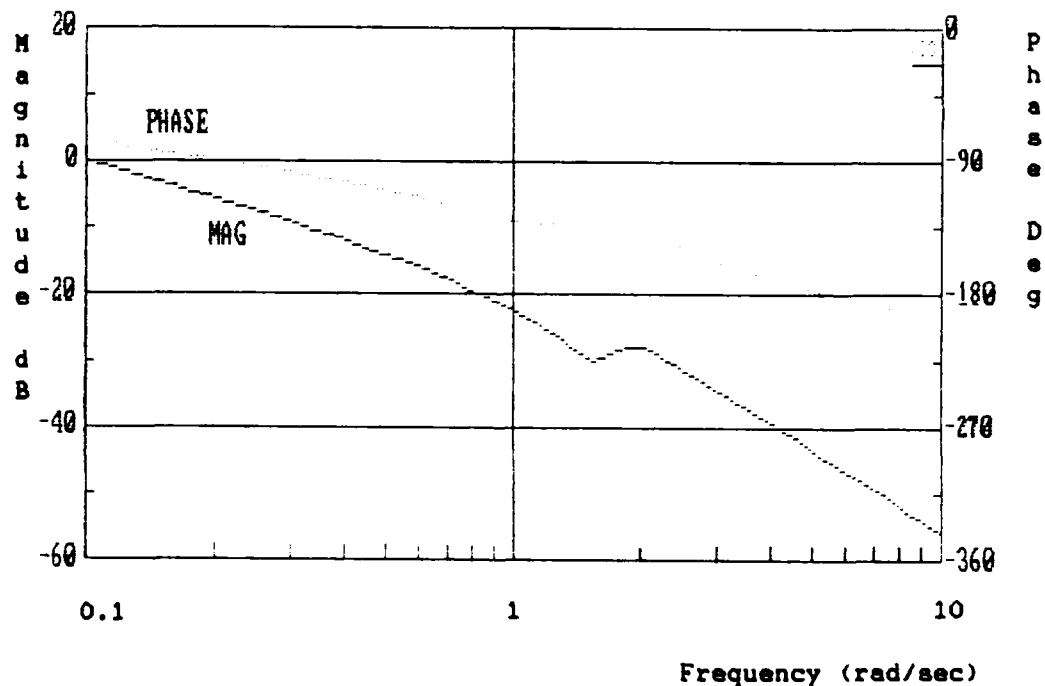
Figure C1. ϕ/Fs Frequency Response for Unaugmented YA-7D - 0.4M

Figure C2. ∅/Fa Frequency Response for (∅/β)$_d$ = 0 - 0.4M
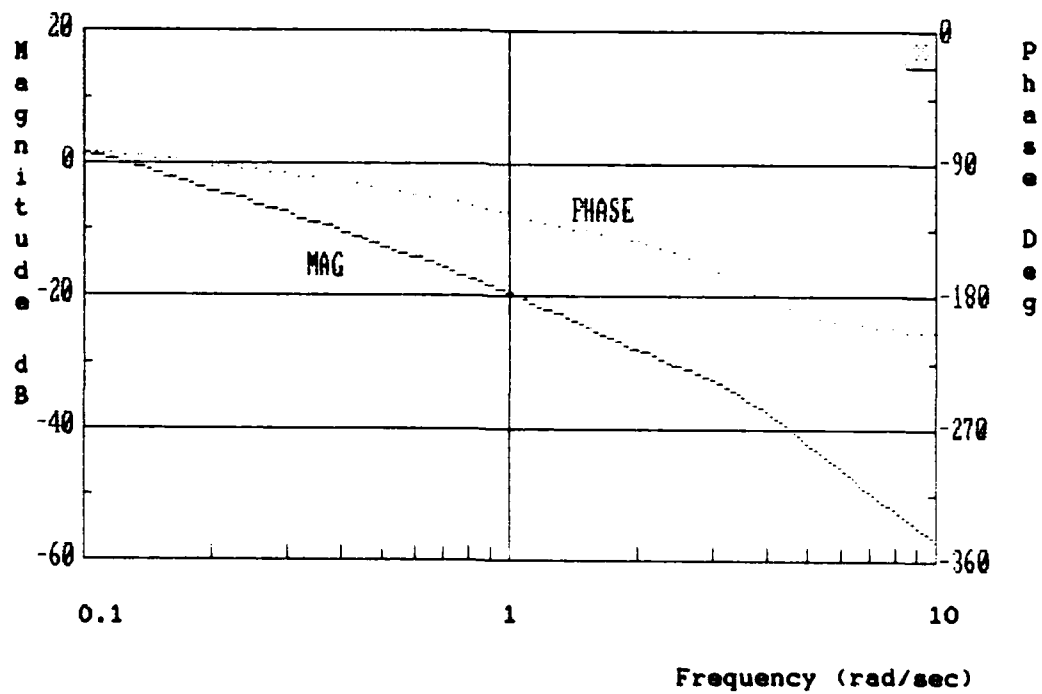
Figure C3. ∅/Fa Frequency Response for (∅/β)$_d$ = 1.5 arg(0) - 0.4M

Figure C4. ø/Fs Frequency Response for (ø/β)$_d$ = 1.5 arg(60) - 0.4M

Figure C5. ø/Fs Frequency Response for (ø/β)$_d$ = 1.5 arg(120) - 0.4M

Figure C6. ø/Fs Frequency Response for (ø/β)$_d$ = 3.0 arg(0) - 0.4N

Figure C7. ø/Fs Frequency Response for (ø/β)$_d$ = 3.0 arg(60) - 0.4N

Figure C8. ∮/Fs Frequency Response for (∮/β)$_d$ = 3.0 arg(120) - 0.4M
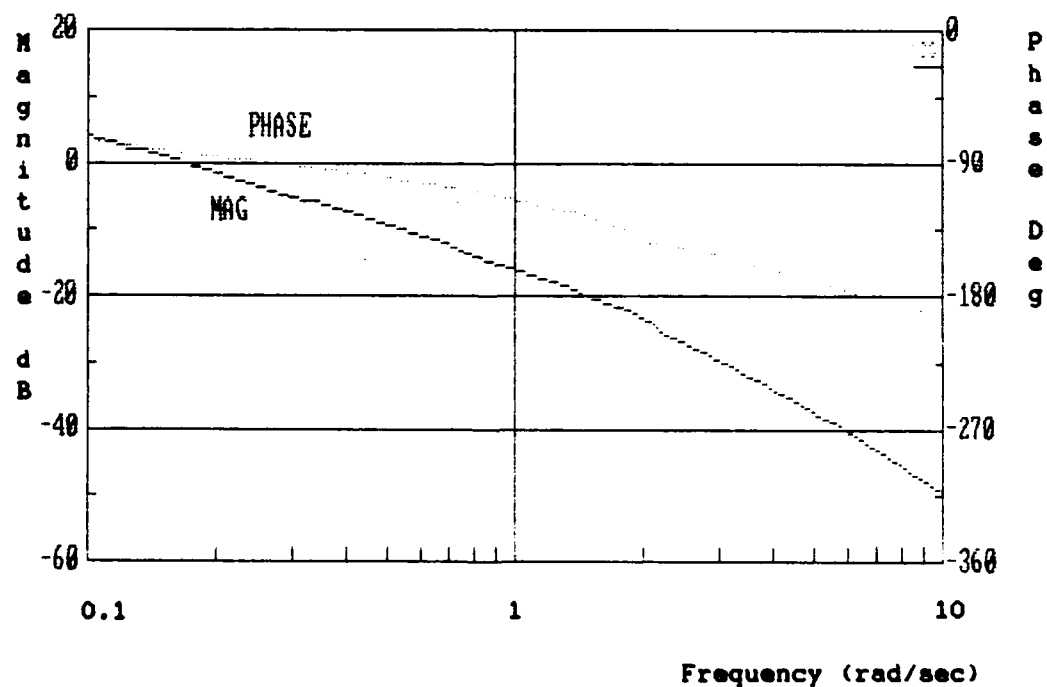
Figure C9. ∮/Fs Frequency Response for Unaugmented YA-7D - 0.6M
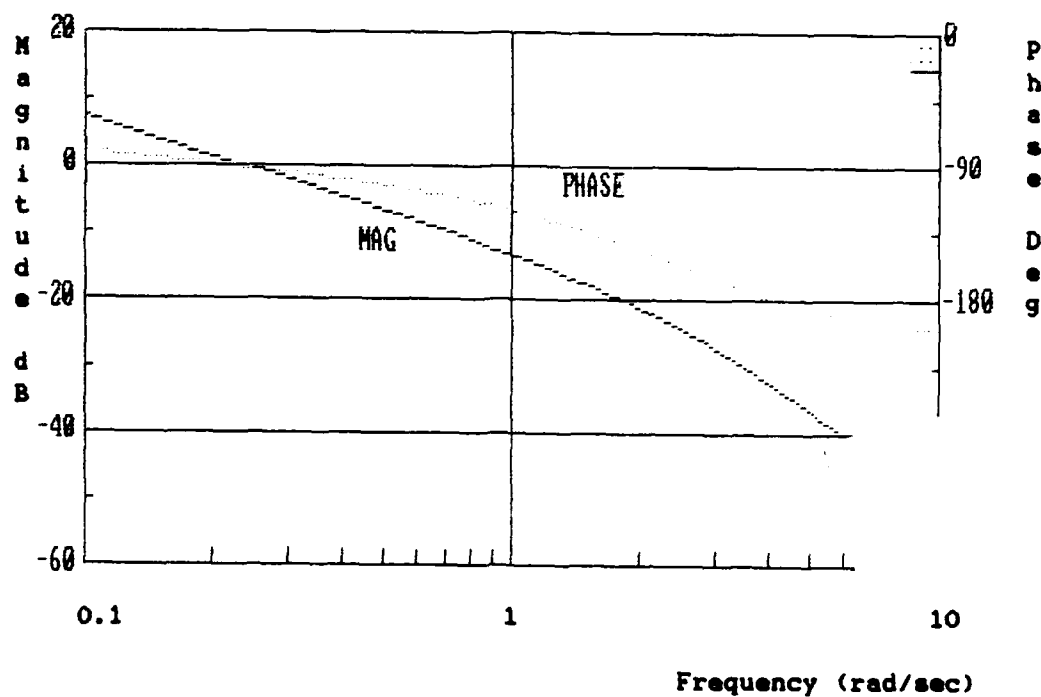
Figure C10. ∅/Fa Frequency Response for (∅/β)_d = 0 - 0.6M
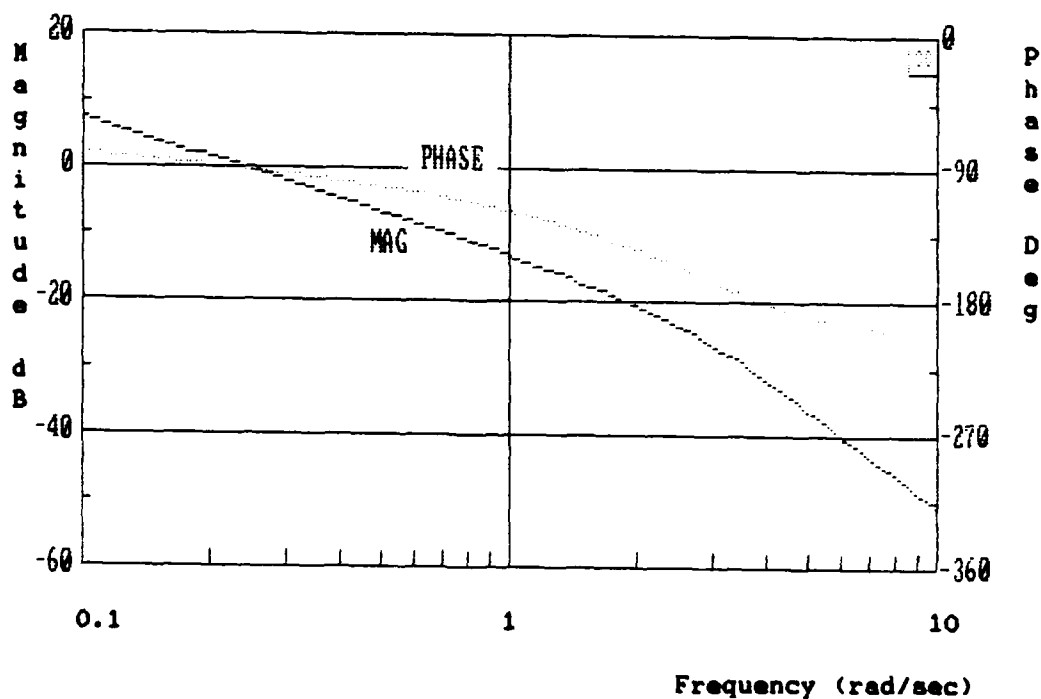
Figure C11. ∅/Fa Frequency Response for (∅/β)_d = 1.5 arg(0) - 0.6M

122

Figure C12. ø/Fs Frequency Response for (ø/β)_d = 1.5 arg(60) - 0.6M

Figure C13. ø/Fs Frequency Response for (ø/β)_d = 1.5 arg(120) - 0.6M

123

Figure C14. ø/Fs Frequency Response for $(ø/β)_d$ ≈ 3.0 arg(0) - 0.6M

Figure C15. ø/Fs Frequency Response for $(ø/β)_d$ ≈ 3.0 arg(60) - 0.6M

124
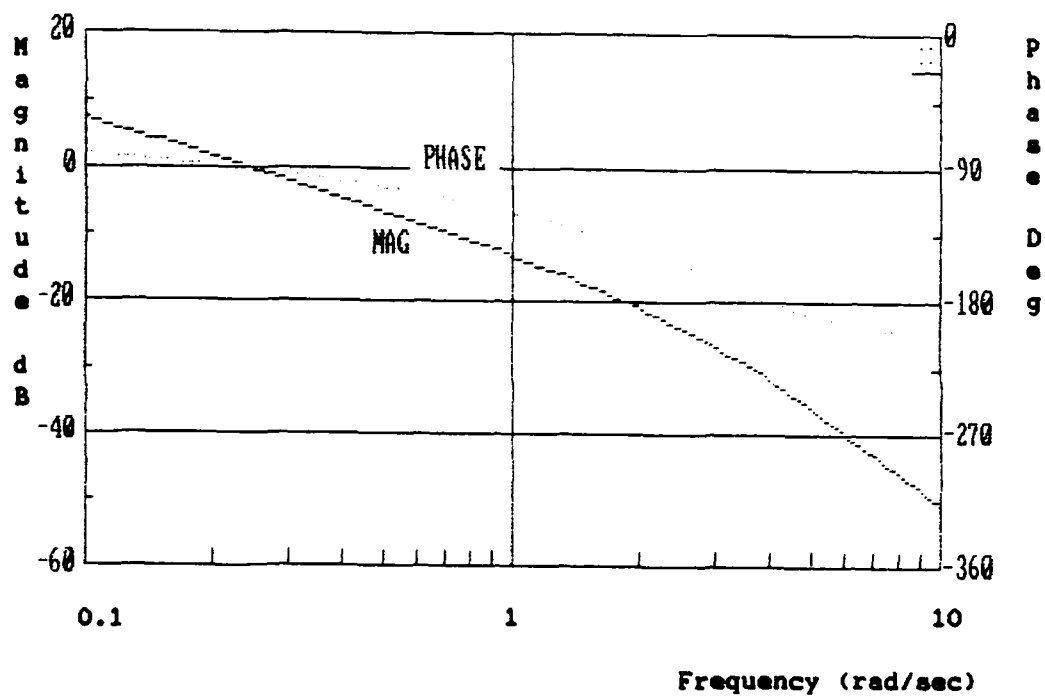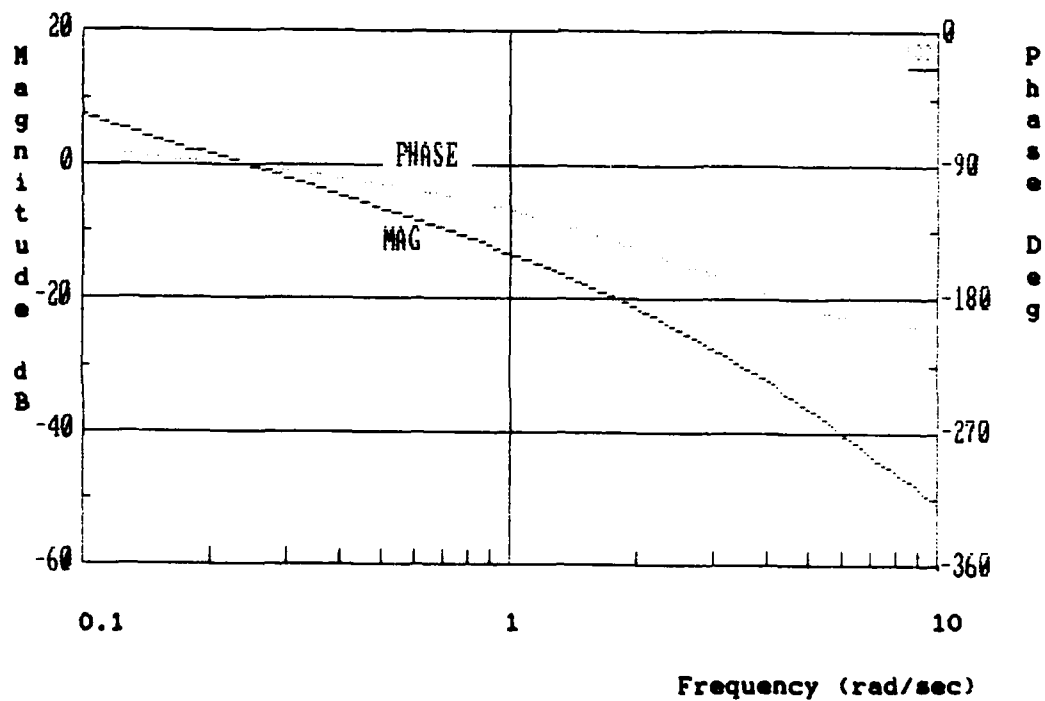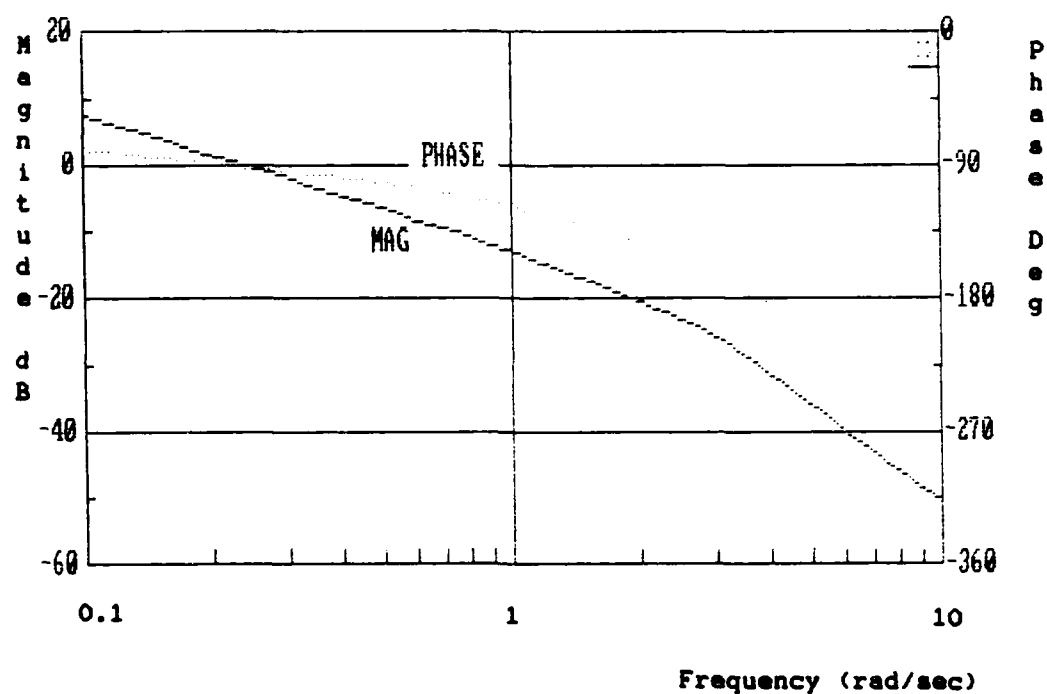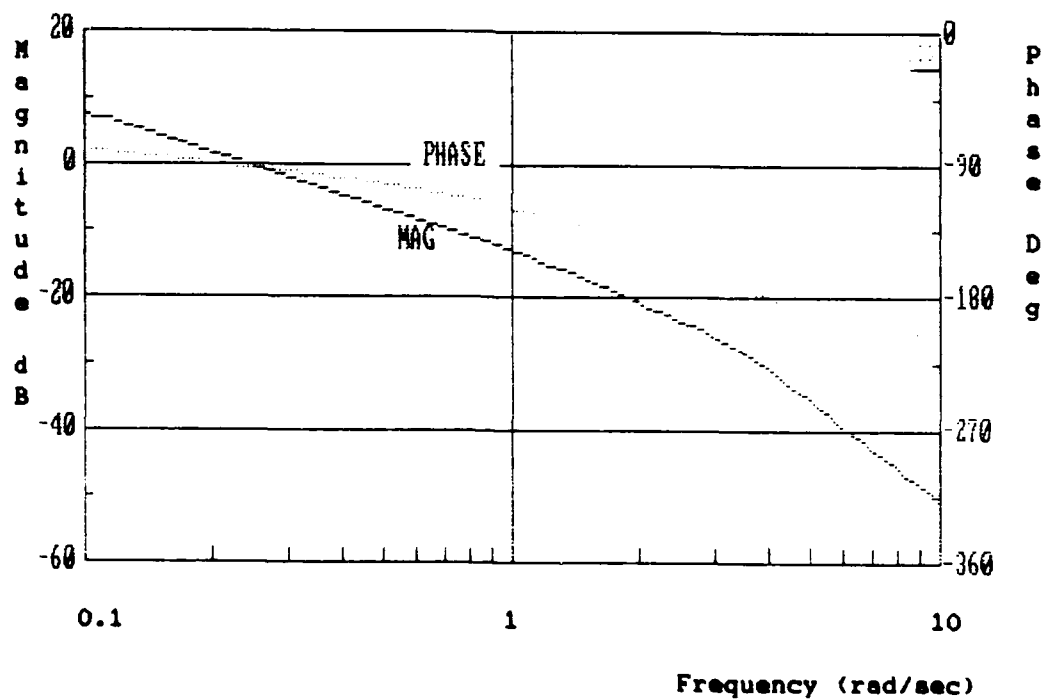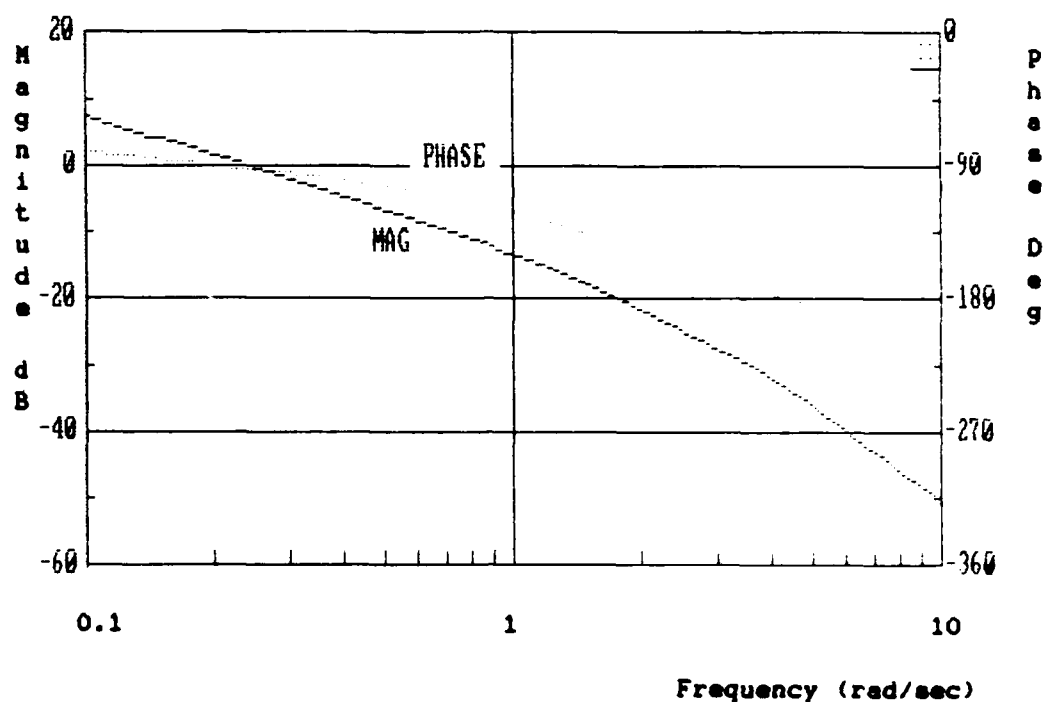
Figure C16. ø/Fa Frequency Response for (ø/ß)d = 3.0 arg(120) - 0.6M

Figure C17. Ycf Frequency Response for Unaugmented YA-7D - 0.4M

125
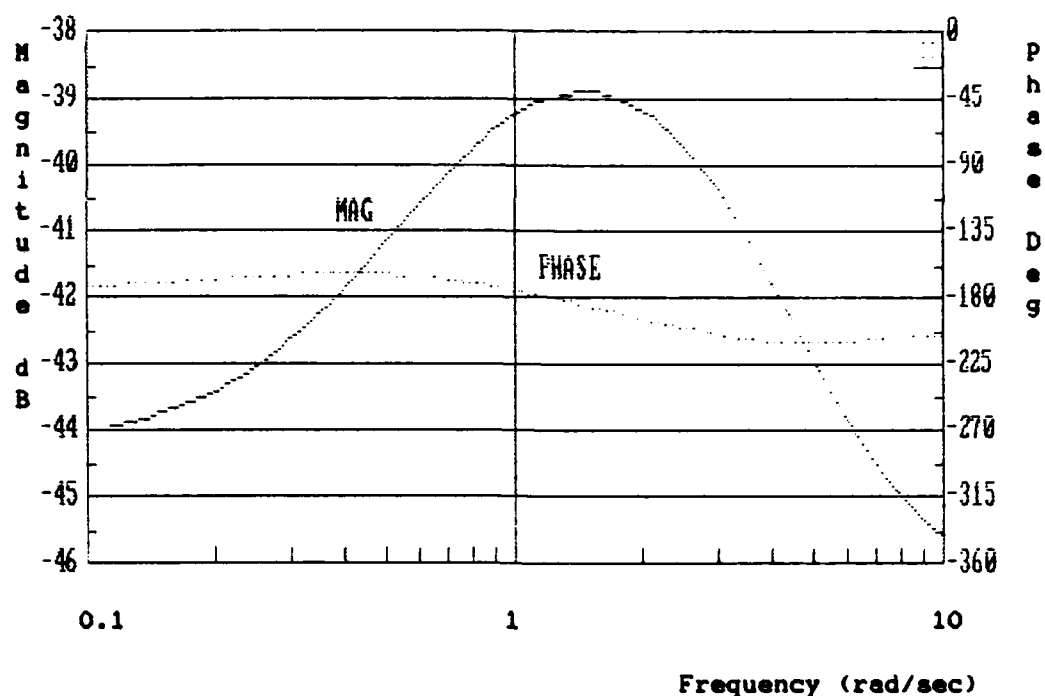
Figure C18. Y_{cf} Frequency Response for $(\phi/\beta)_d = 0 - 0.4M$
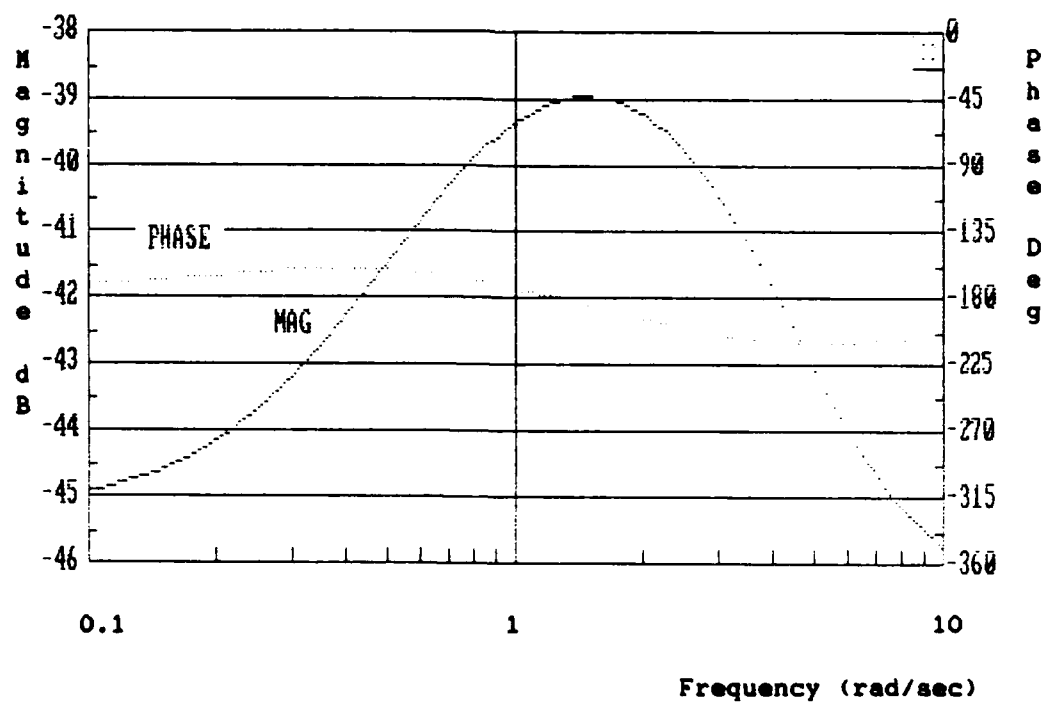
Figure C19. Y_{cf} Frequency Response for $(\phi/\beta)_d = 1.5 \ arg(0) - 0.4M$
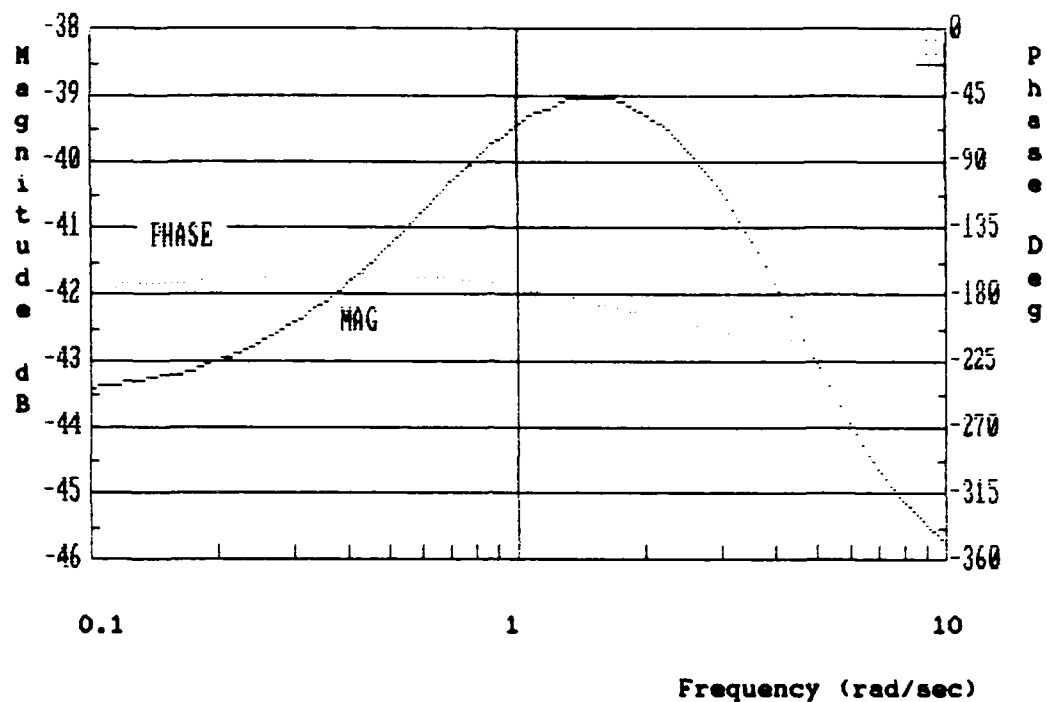
Figure C20. Y_{cf} Frequency Response for $(\phi/\beta)_d = 1.5$ arg(60) - 0.4M
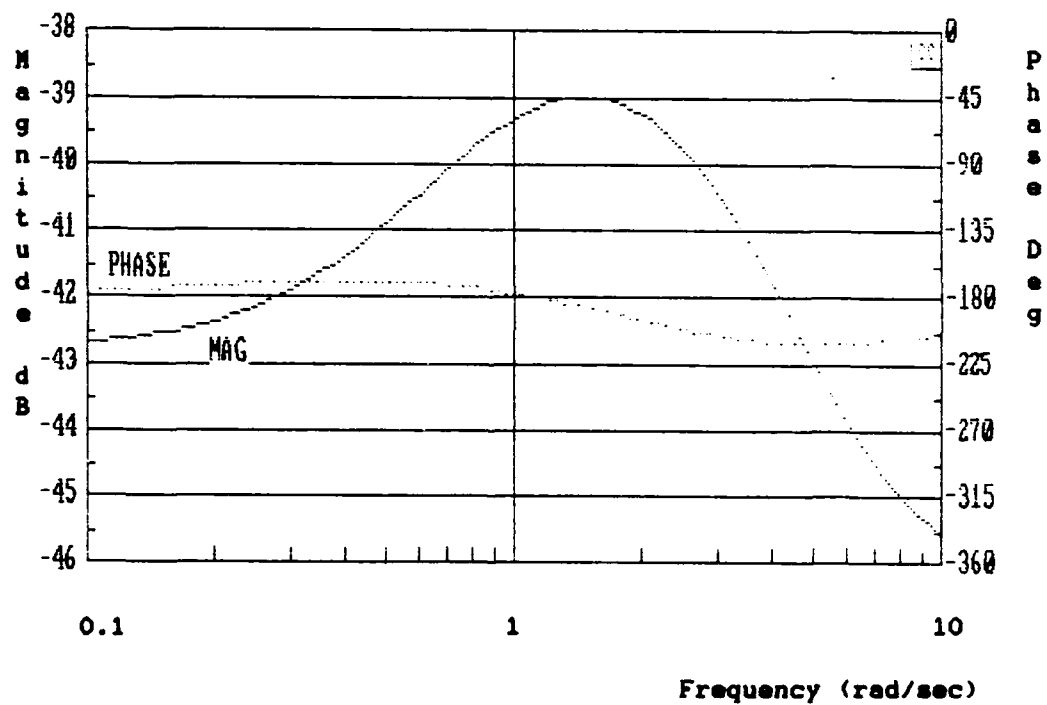
Figure C21. Y_{cf} Frequency Response for $(\phi/\beta)_d = 1.5$ arg(120) - 0.4M
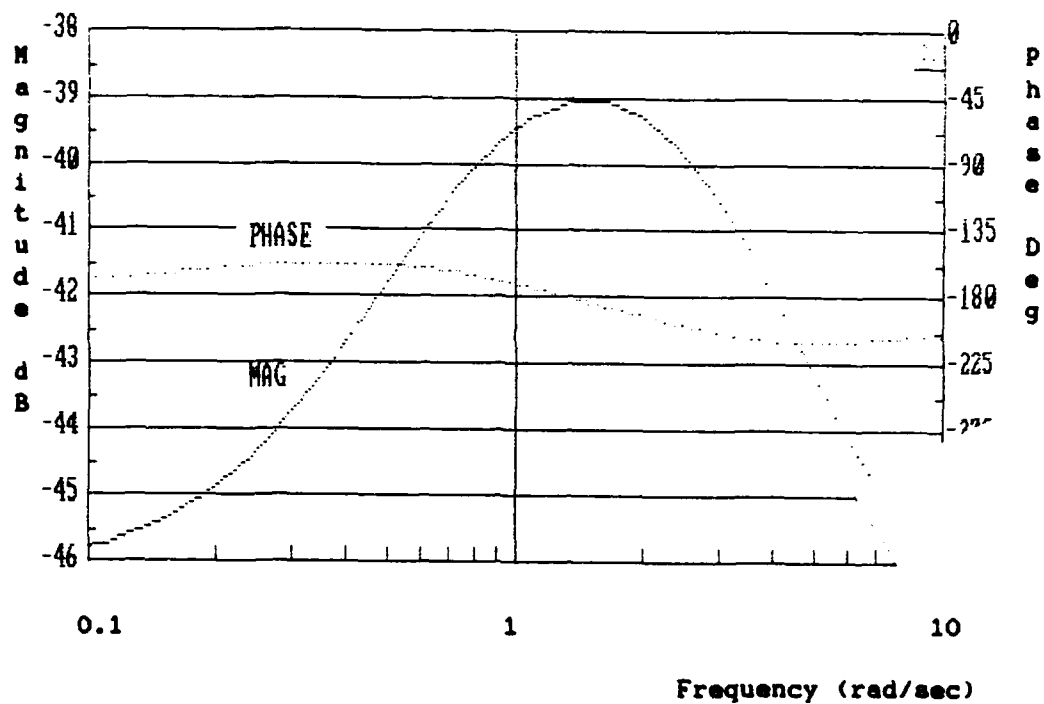
Figure C22. Y_{cf} Frequency Response for $(\phi/\beta)_d = 3.0$ arg(0) - 0.4M
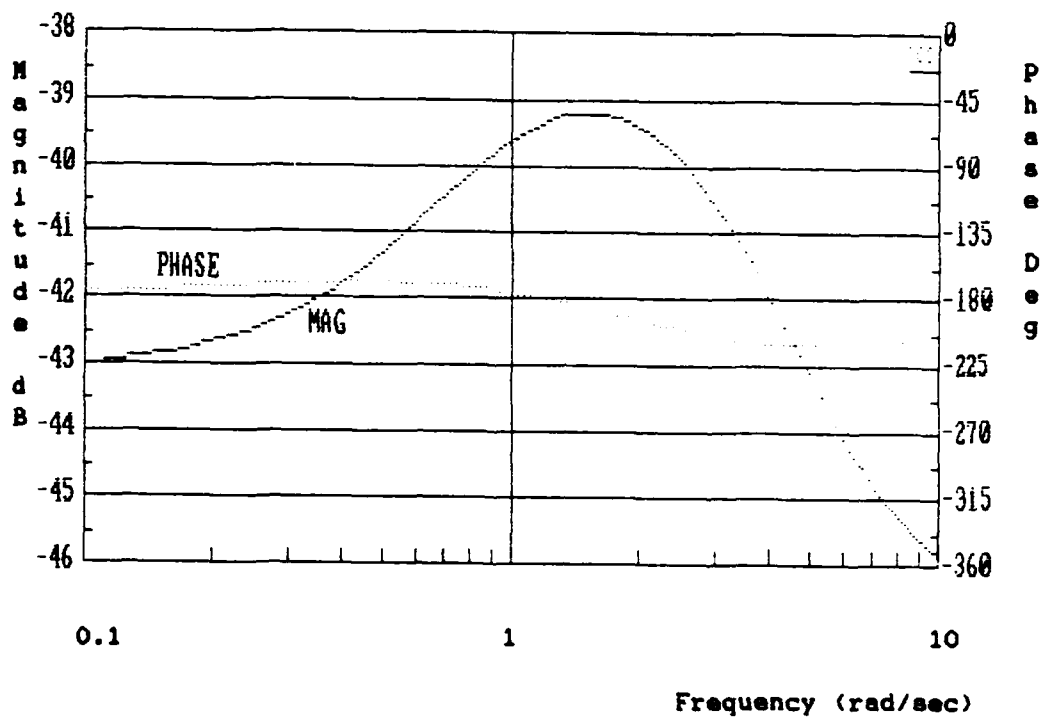
Figure C23. Y_{cf} Frequency Response for $(\phi/\beta)_d = 3.0$ arg(60) - 0.4M
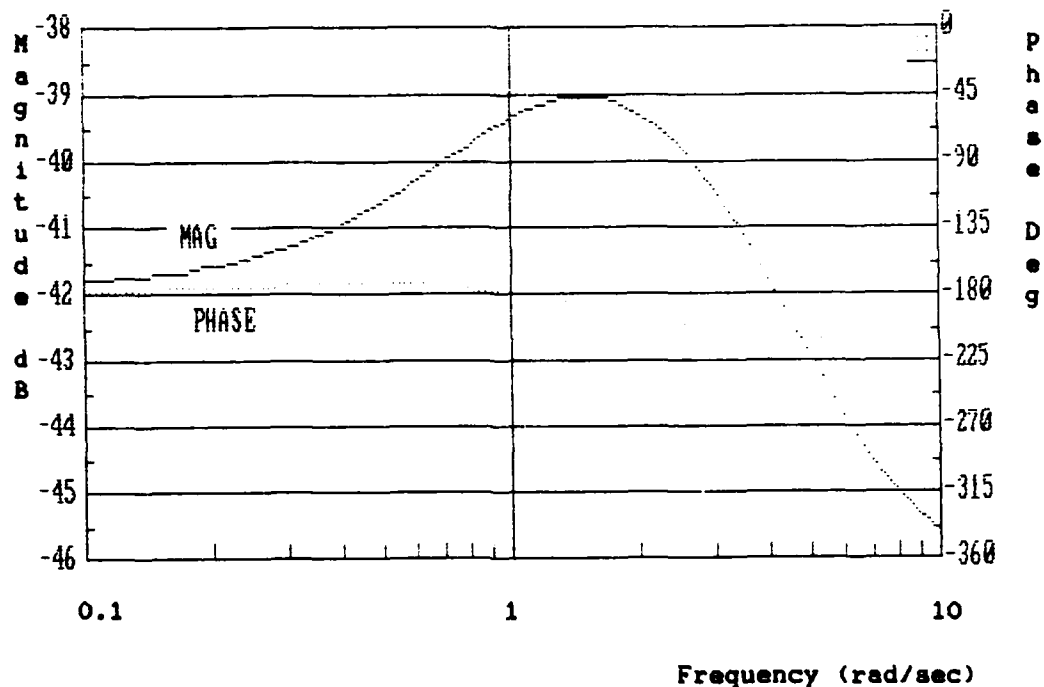
Figure C24. Y_{cf} Frequency Response for $(\phi/\beta)_d$ = 3.0 arg(120) - 0.4M
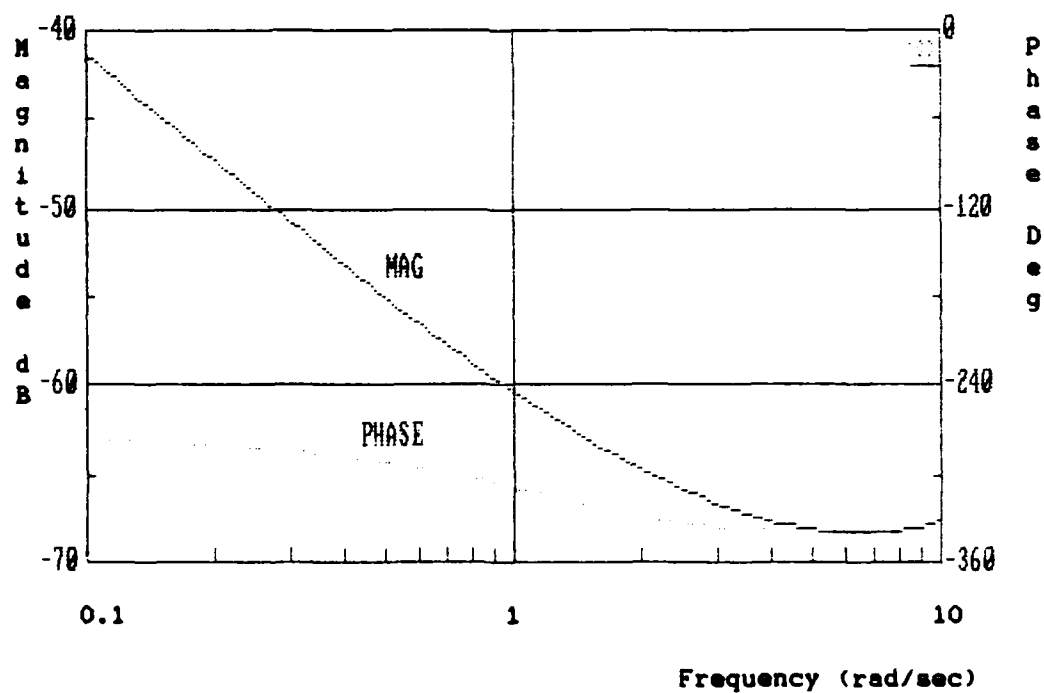
Figure C25. Y_{cf} Frequency Response for Unaugmented YA-7D - 0.6M
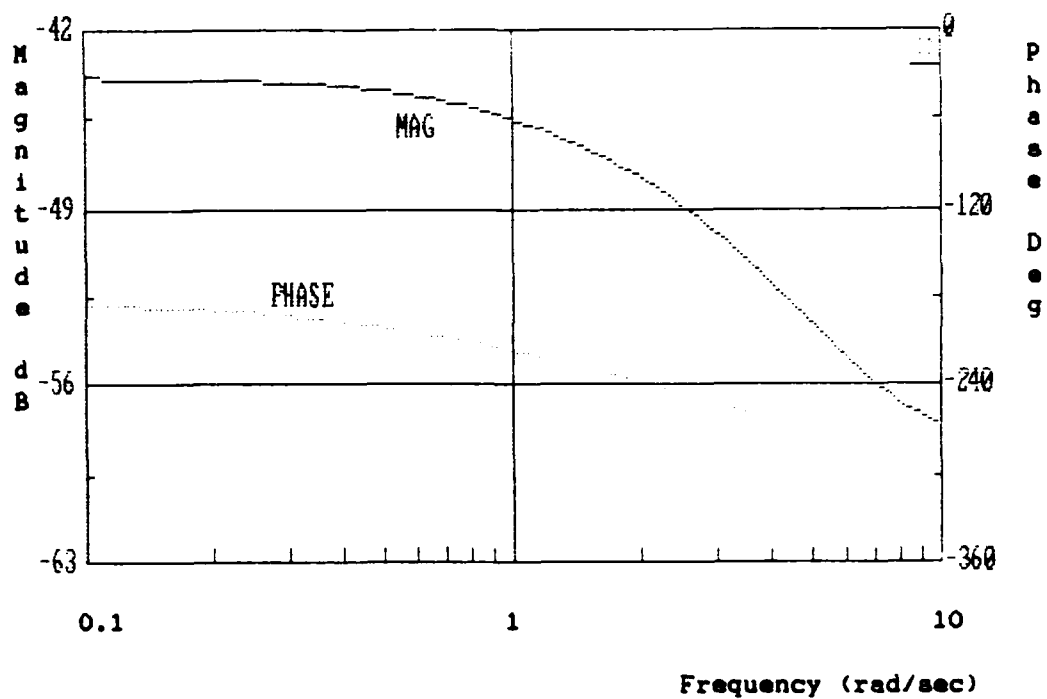
Figure C26. Y_{cf} Frequency Response for $(\phi/\beta)_d = 0 - 0.6M$
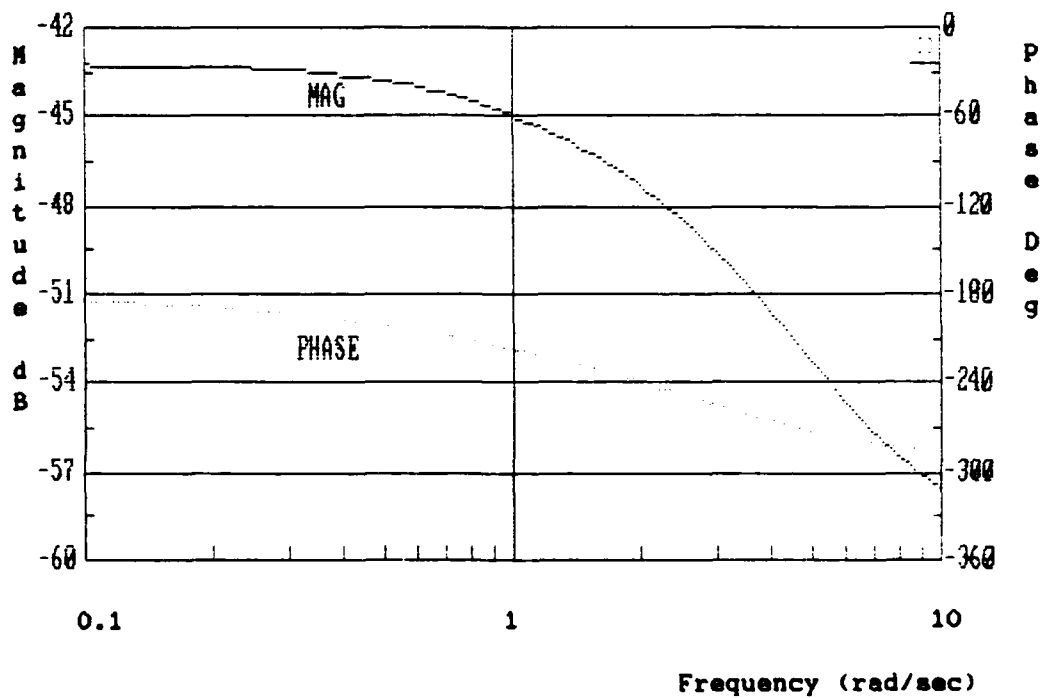
Figure C27. Y_{cf} Frequency Response for $(\phi/\beta)_d = 1.5 \arg(0) - 0.6M$
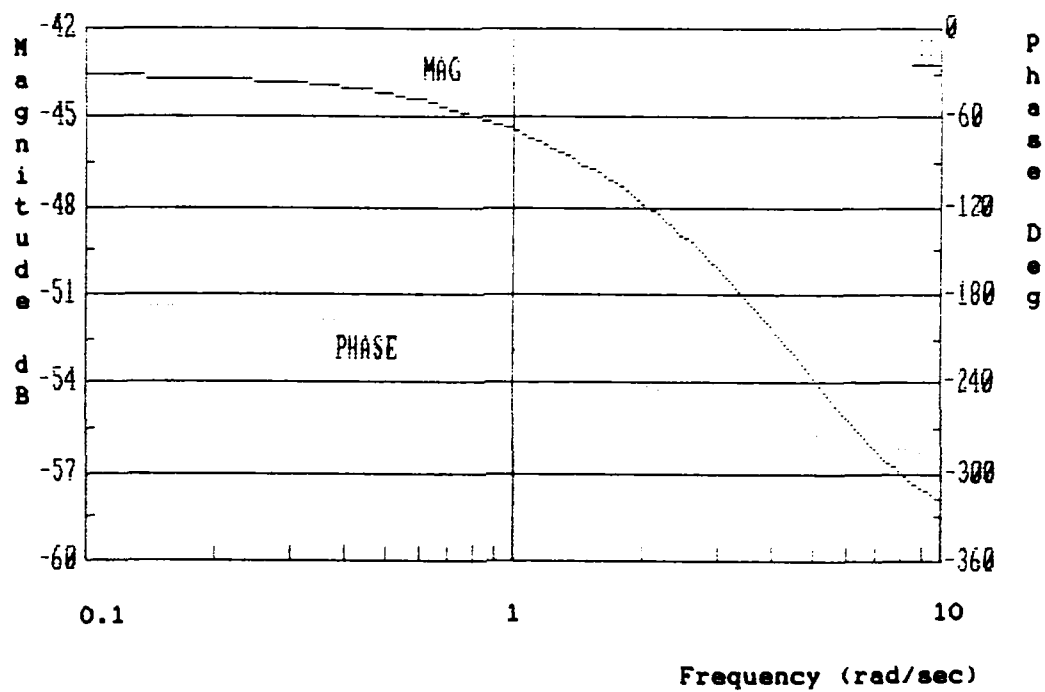
Figure C28. Y_{cf} Frequency Response for $(\phi/\beta)_d = 1.5$ arg(60) - 0.6M
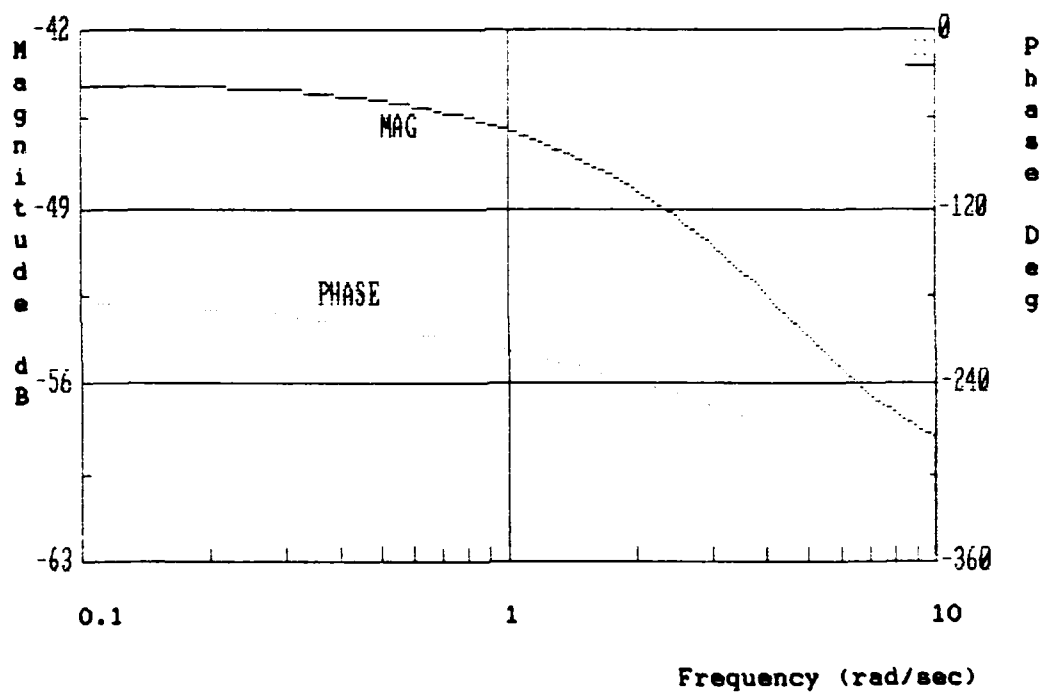
Figure C29. Y_{cf} Frequency Response for $(\phi/\beta)_d = 1.5$ arg(120) - 0.6M
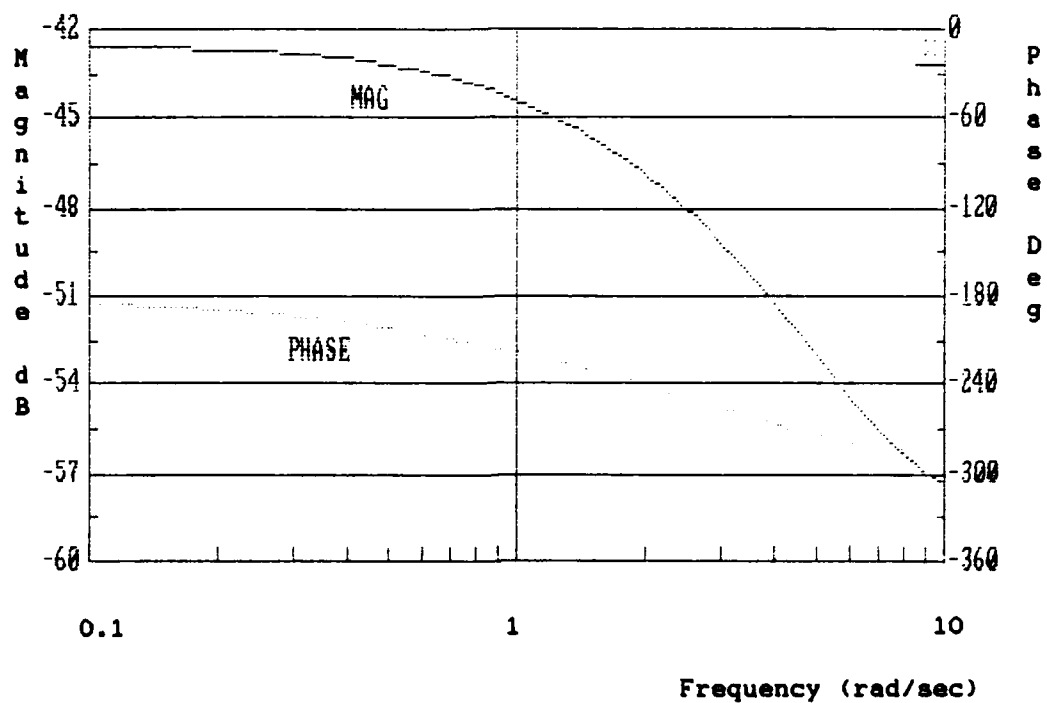
Figure C30. Y_{cf} Frequency Response for $(\phi/\beta)_d = 3.0$ arg(0) - 0.4M
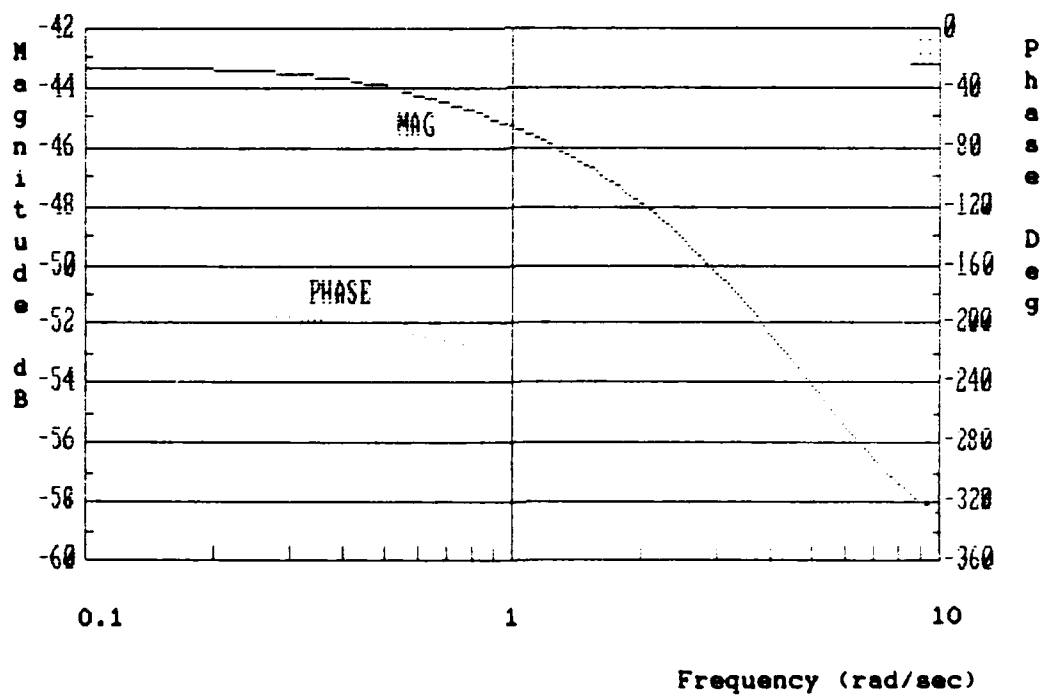
Figure C31. Y_{cf} Frequency Response for $(\phi/\beta)_d = 3.0$ arg(60) - 0.6M
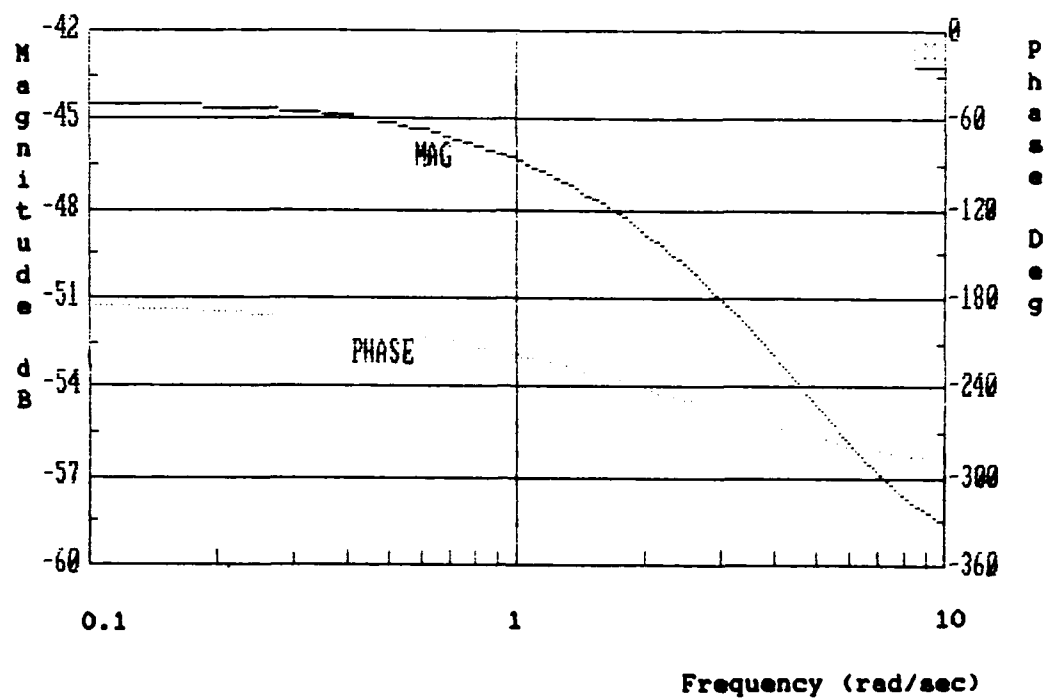
Figure C32. Y_{cf} Frequency Response for $(\phi/\beta)_d = 3.0 \ arg(120) - 0.6M$

APPENDIX D. Simulator <u>Time</u> <u>Response</u> <u>Plots</u>

<u>for</u> <u>Selected</u> <u>Eigenstructures</u>

Time response plots were generated using the Simulator for Aircraft
Flight Test and Development (SAFTD). Both free and forced responses at
the most severe flight condition, 0.4 Mach, are included for the
unaugmented YA-7D, $(\phi/\beta)_d$ of zero, and $|\phi/\beta|_d$ of 1.5, and 3.0, at phase
angles of 0, 60, and 120 degrees. At 0.6 Mach, only the free and forced
response of the unaugmented YA-7D and $(\phi/\beta)_d$ of zero are shown. The
variables are in body axes, and include effects of sensor dynamics and
the digital flight control system.

Inputs were applied by test team pilots. The free response was a
release from a wings level sideslip of approximately three degrees. The
forced response was a step lateral stick input.
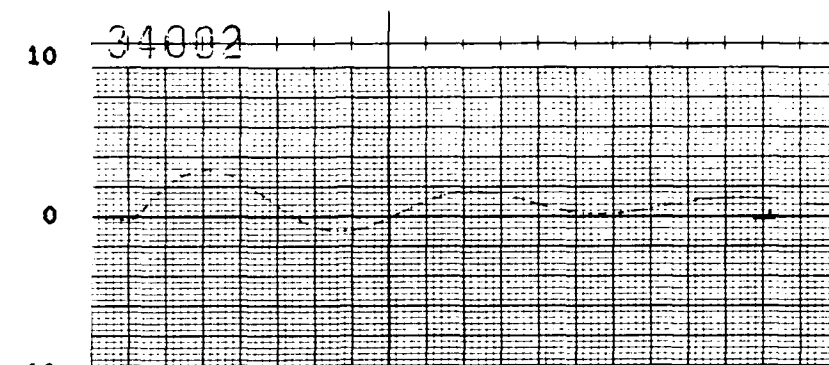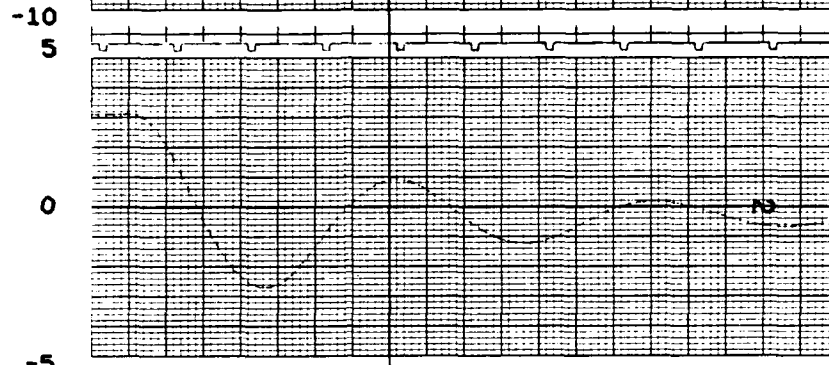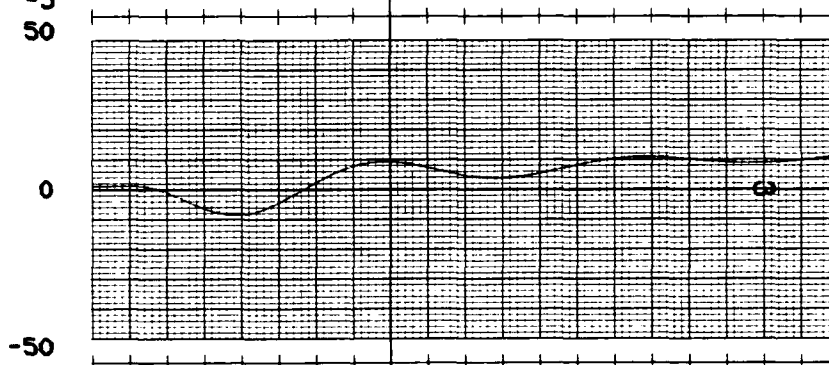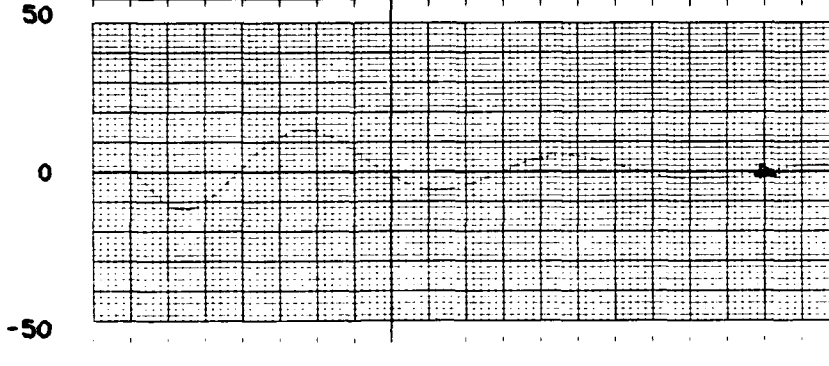
Figure D1. Unaugmented YA-7D Free Response - 0.4M
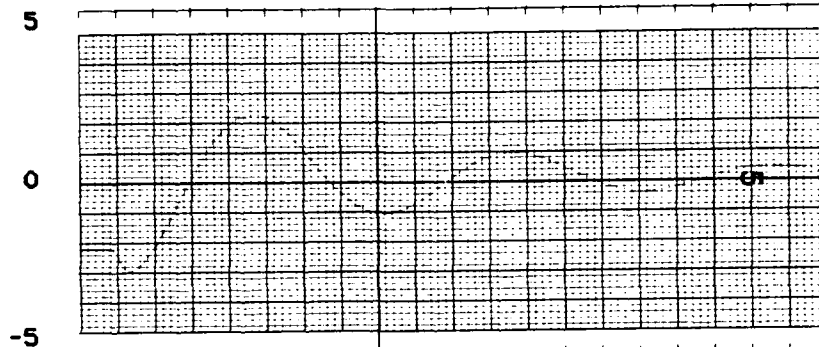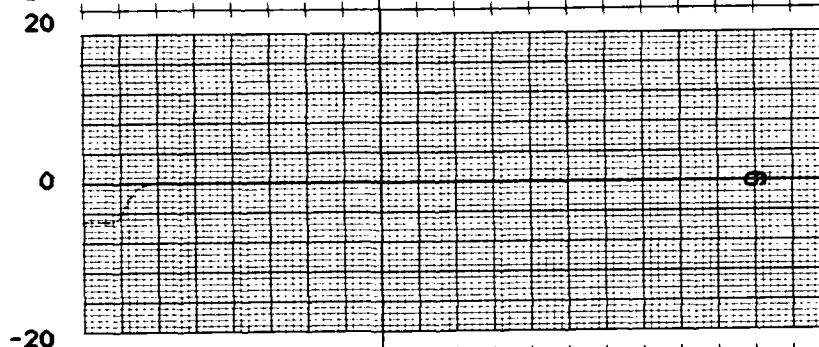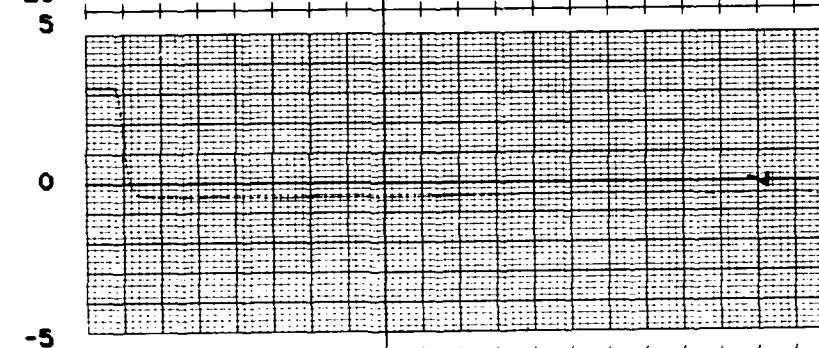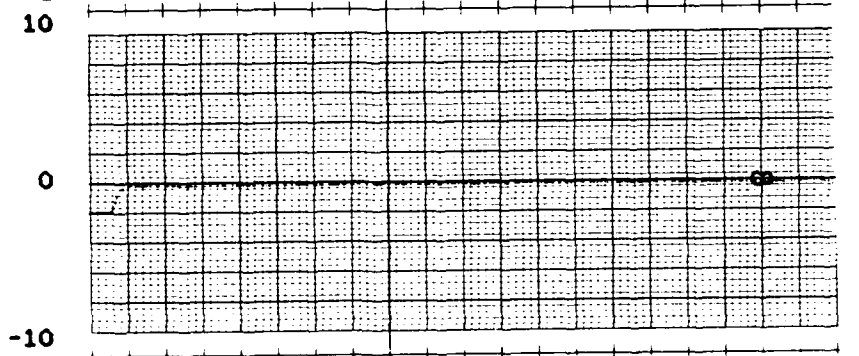
Figure D1 (CONTINUED). Unaugmented YA-7D Free Response - 0.4M

136
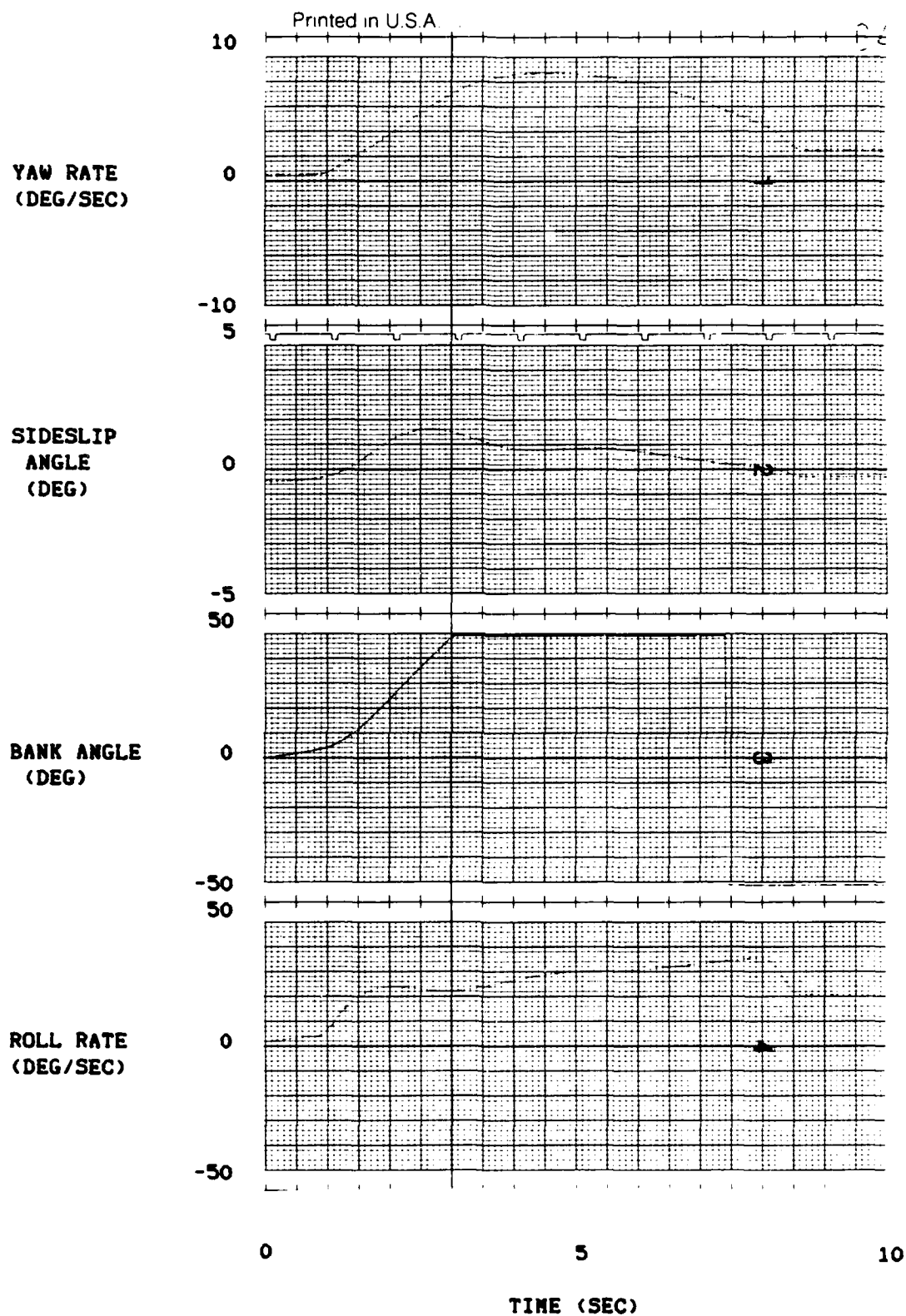
Figure D2.   Unaugmented YA-7D Forced Response - 0.4M
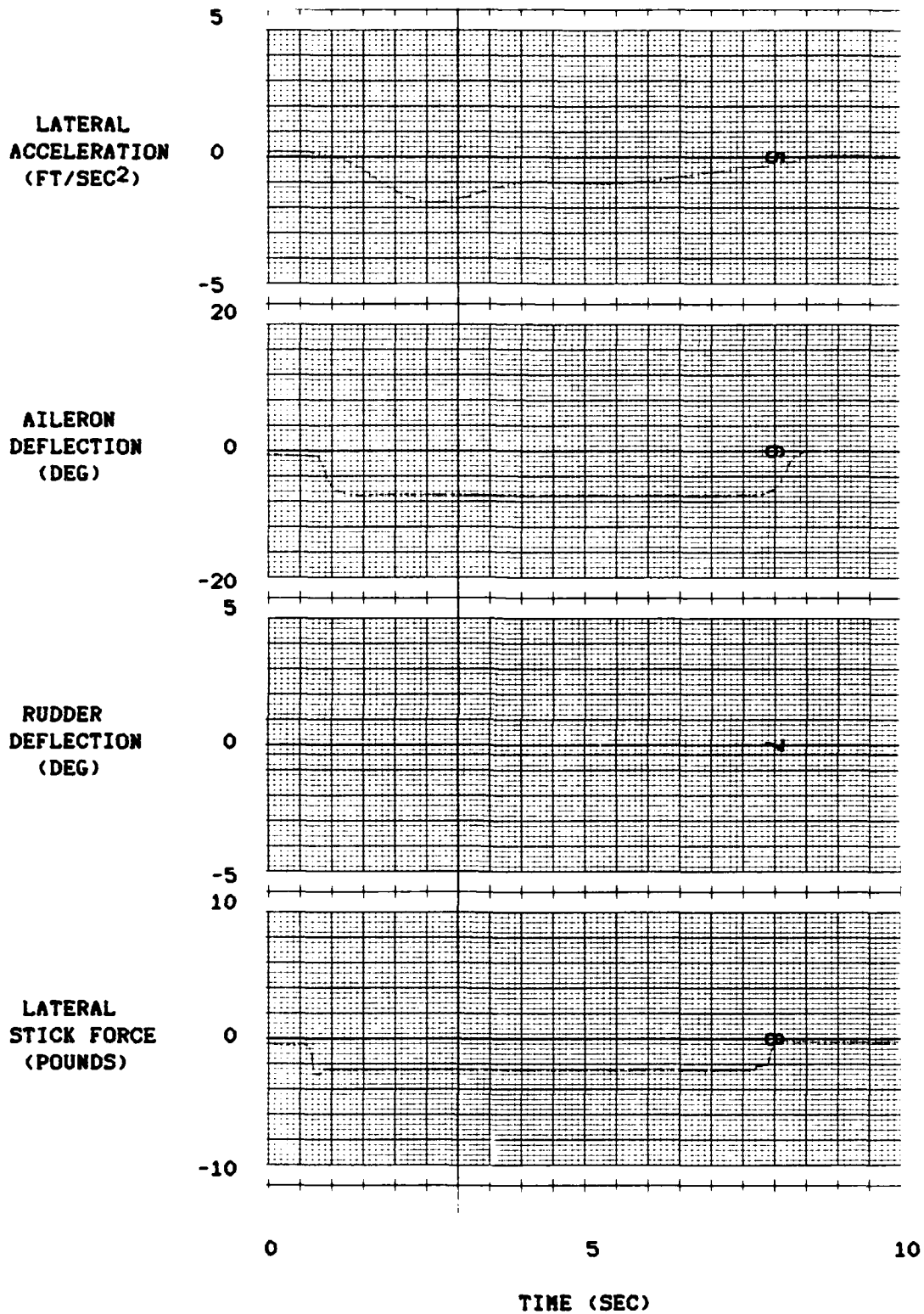
Figure D2 (CONTINUED). Unaugmented YA-7D Forced Response - 0.4M
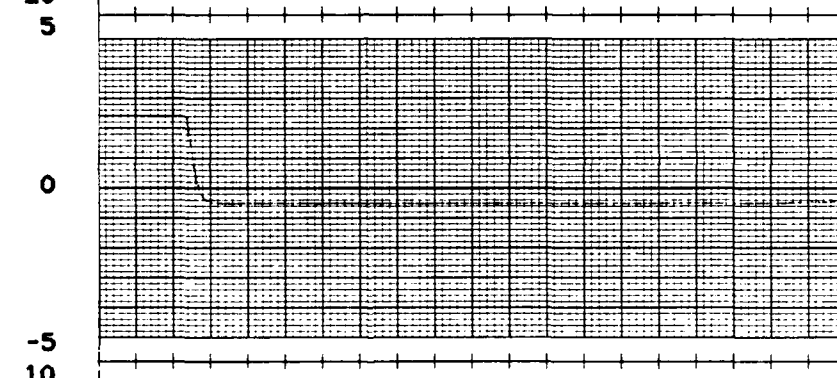
Figure D3. Free Response $(\phi/\beta)_d = 0 - 0.4M$

LATERAL
ACCELERATION
(FT/SEC^2)
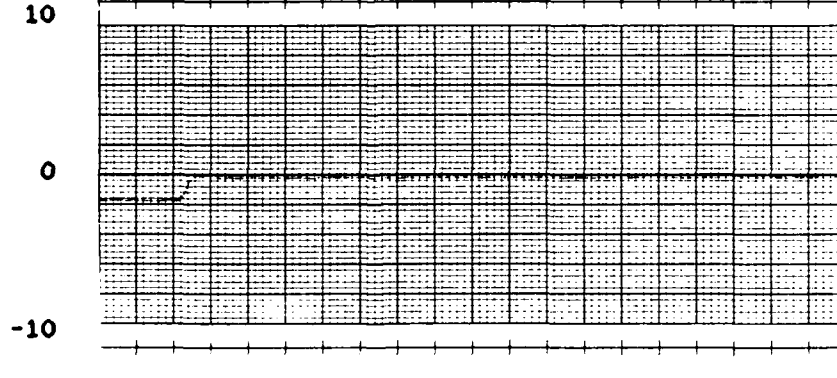
AILERON
DEFLECTION
(DEG)

RUDDER
DEFLECTION
(DEG)

LATERAL
STICK FORCE
(POUNDS)

TIME (SEC)
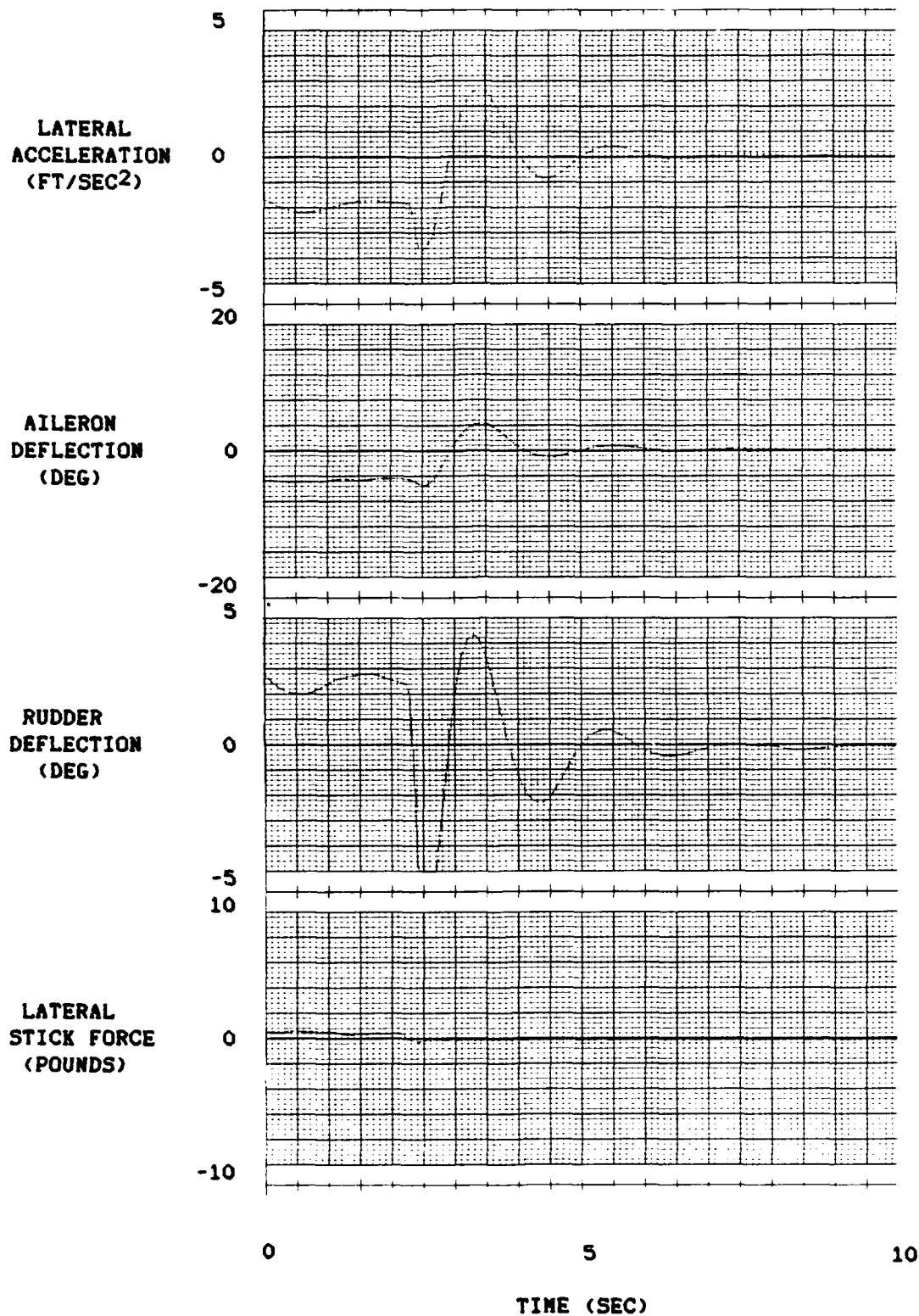
Figure D3 (CONTINUED). Free Response $(\phi/\beta)_d$ = 0 - 0.4M
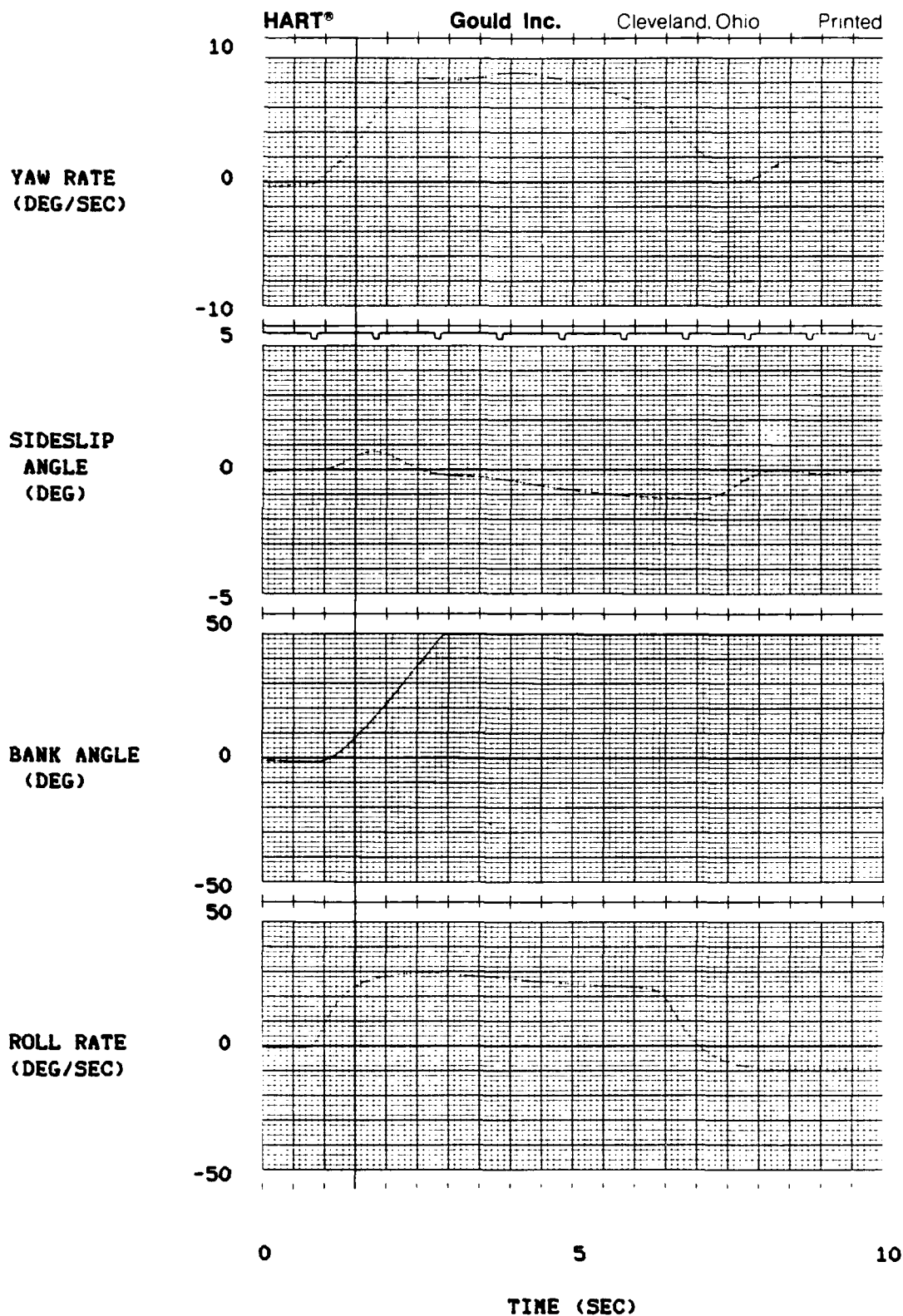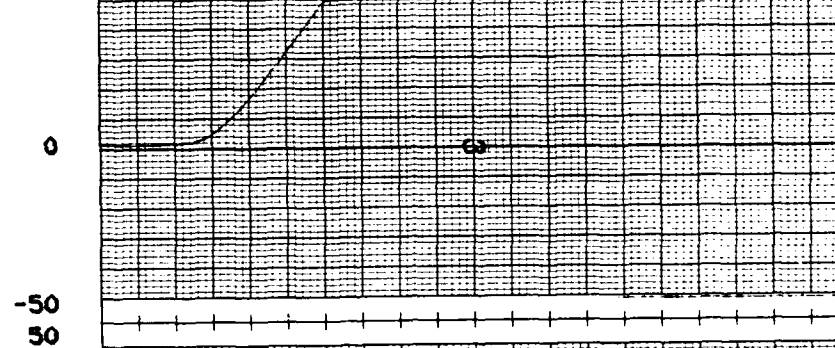
Figure D4. Forced Response $(\phi/\beta)_d = 0 - 0.4N$
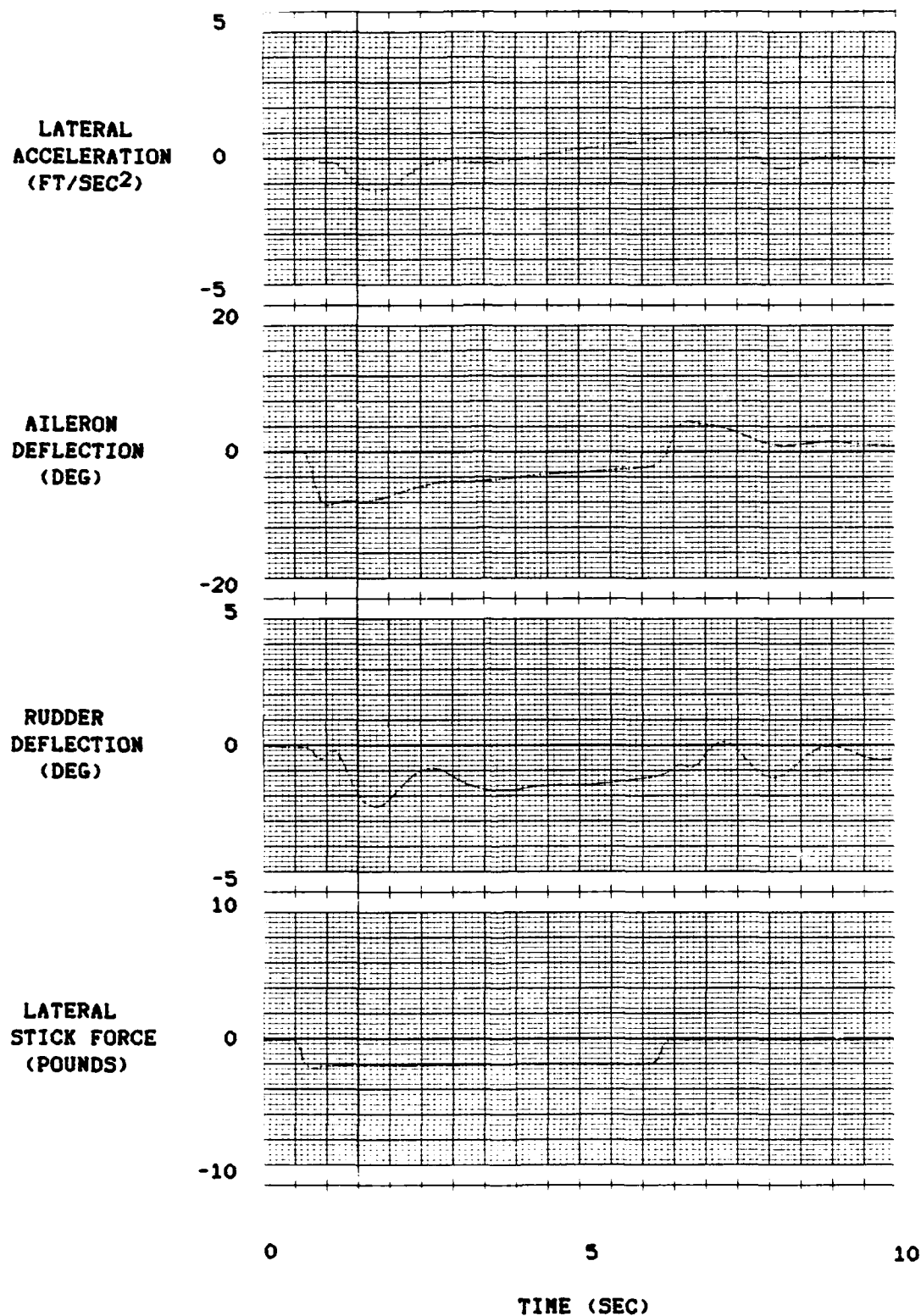
Figure D4 (CONTINUED). Forced Response $(\phi/\beta)_d = 0 - 0.4N$
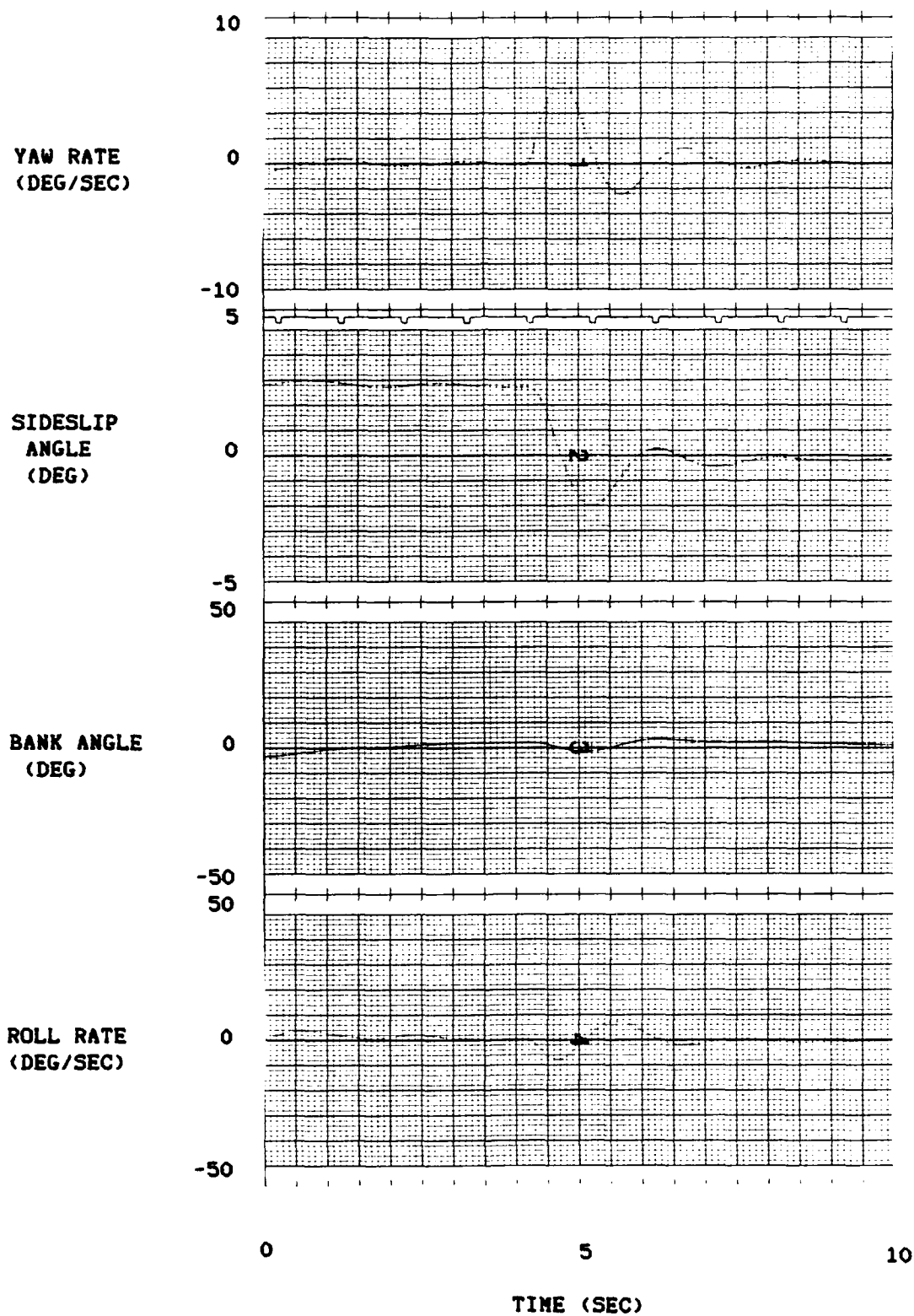
Figure D5. Free Response $(\phi/\beta)_d = 1.5$ arg(0) - 0.4M
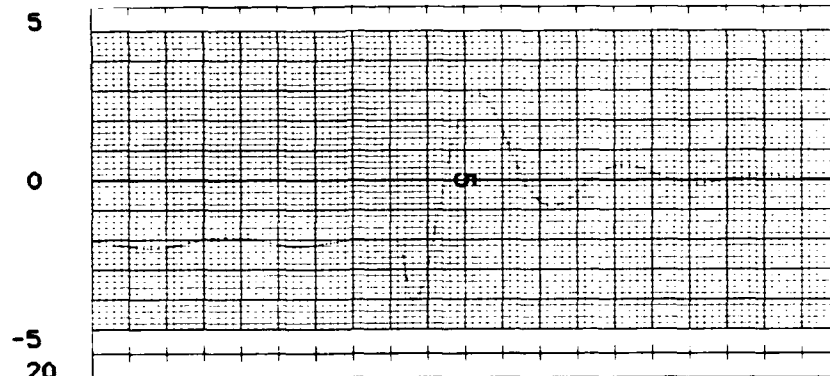
143
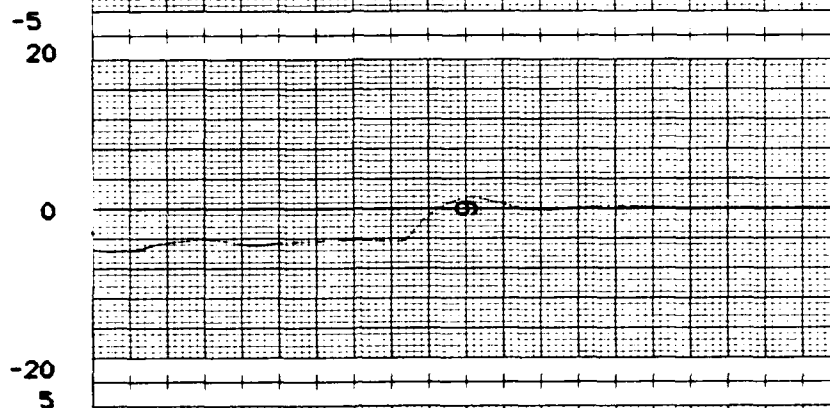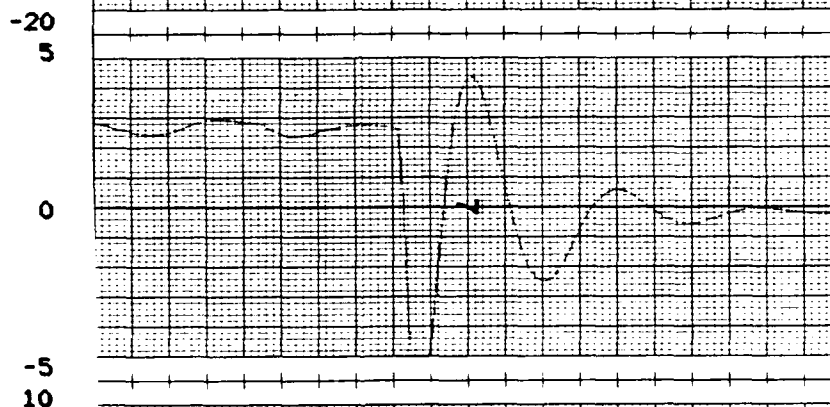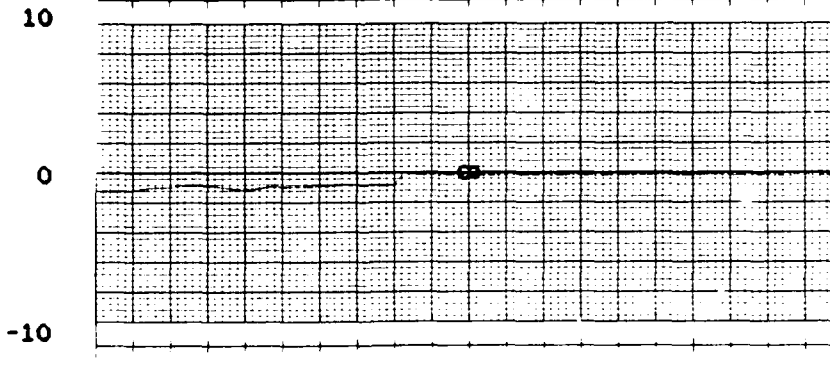
Figure D5 (CONTINUED). Free Response $(\phi/\beta)_d = 1.5$ arg(0) - 0.4N

144
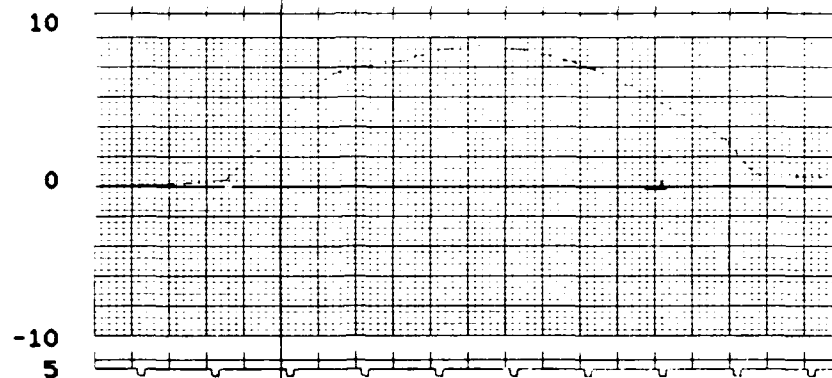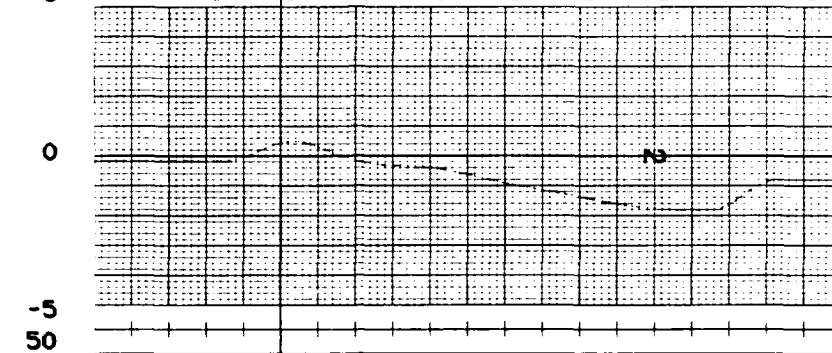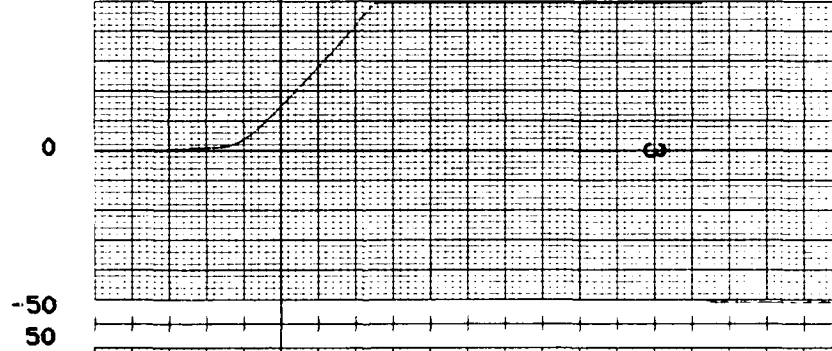
Figure D6. Forced Response $(\phi/\beta)_d = 1.5 \arg(0) - 0.4M$
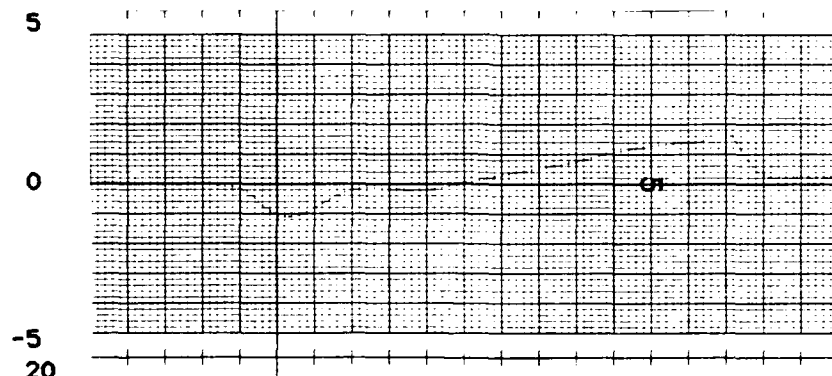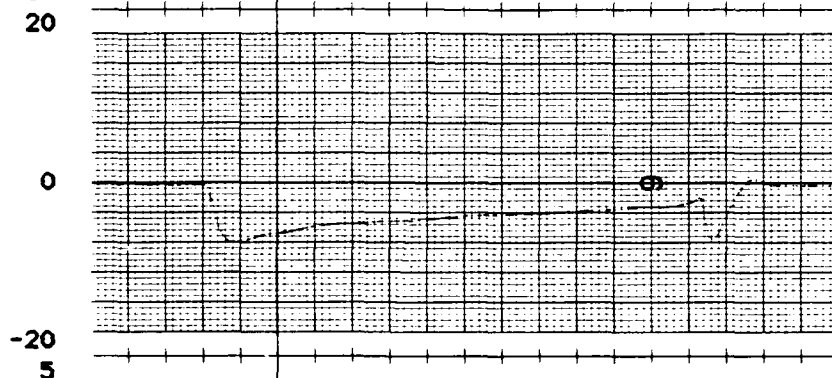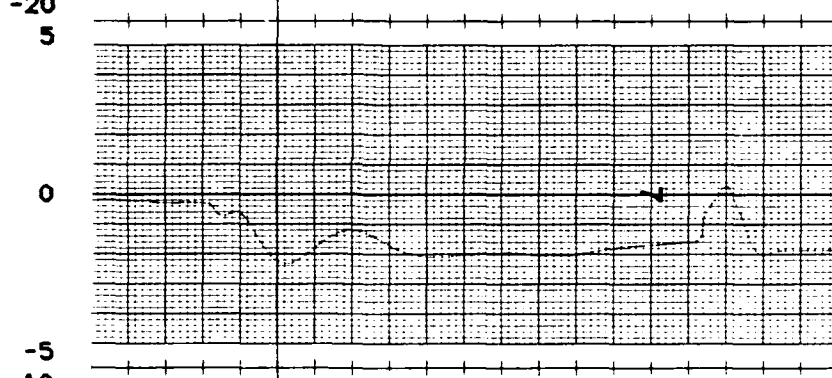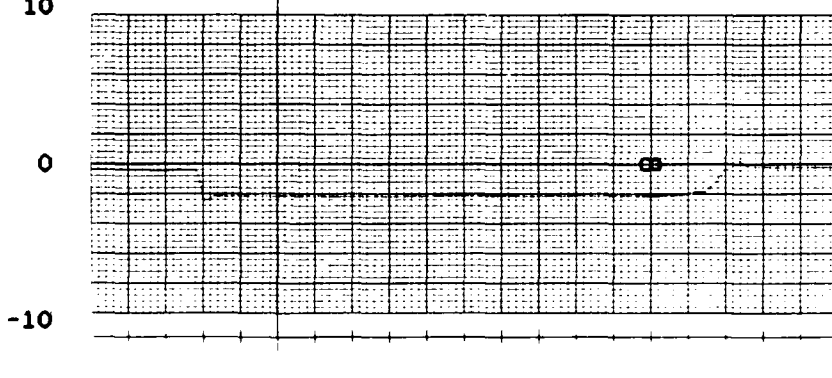
Figure D6 (CONTINUED). Forced Response $(\emptyset/\beta)_d$ = 1.5 arg(O) - 0.4H
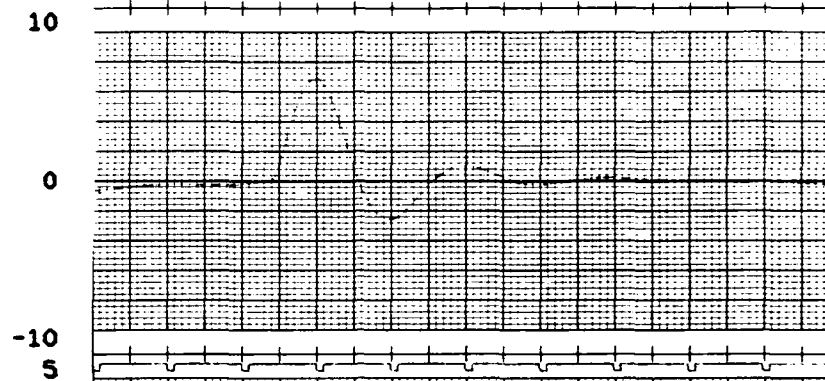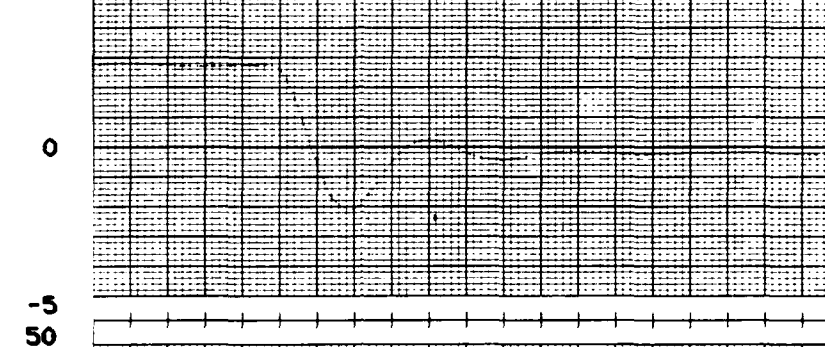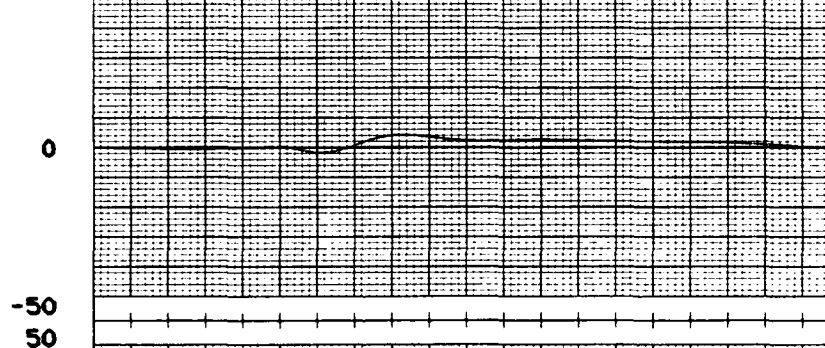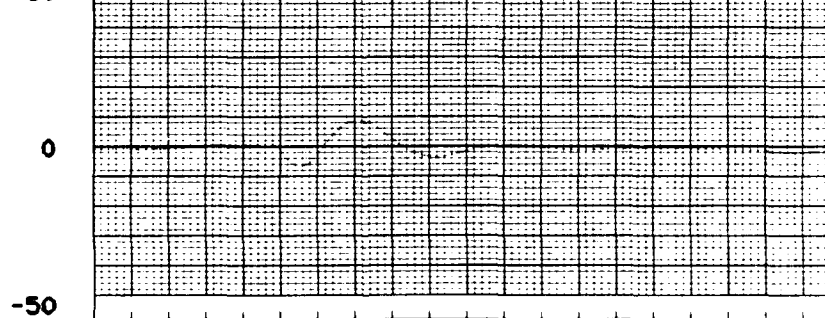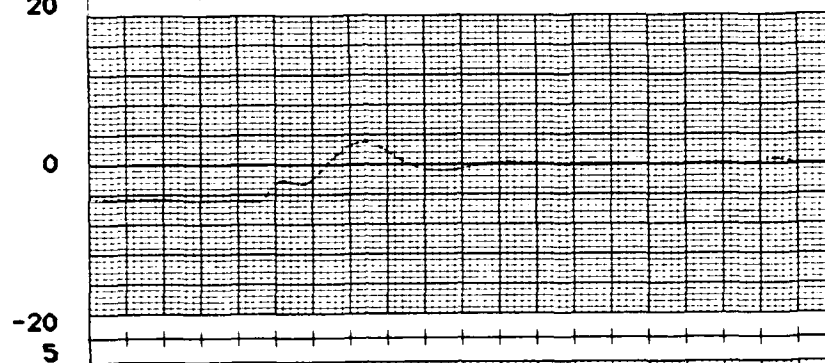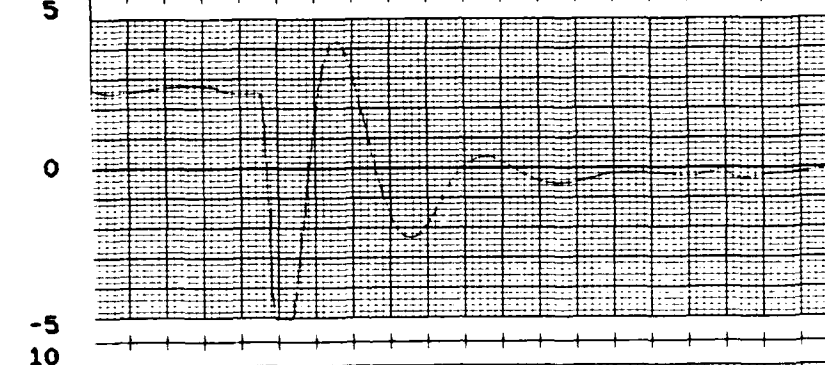
Figure D7. Free Response $(\phi/\beta)_d$ = 1.5 arg(60) - 0.4M
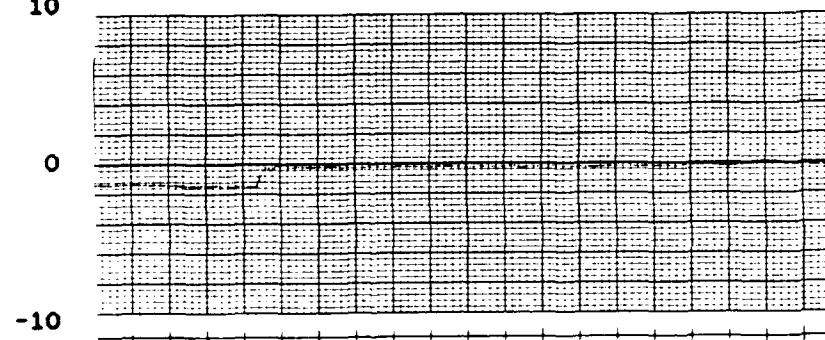
Figure D7 (CONTINUED). Free Response $(\phi/\beta)_d = 1.5$ arg(60) - 0.4N
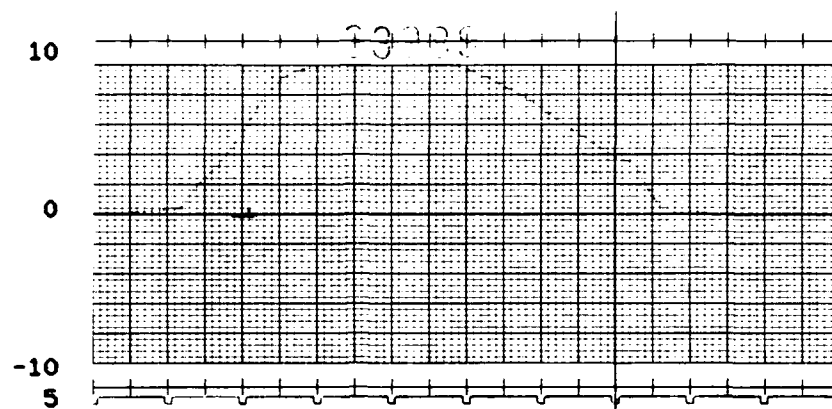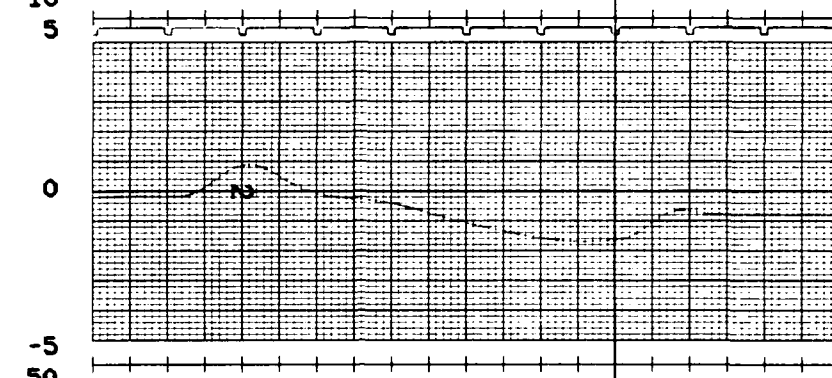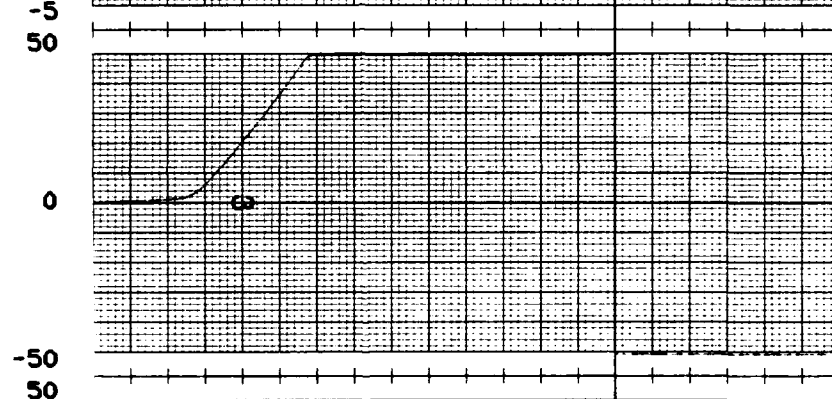
Figure D8. Forced Response $(\phi/\beta)_d = 1.5$ arg(60) - 0.4N
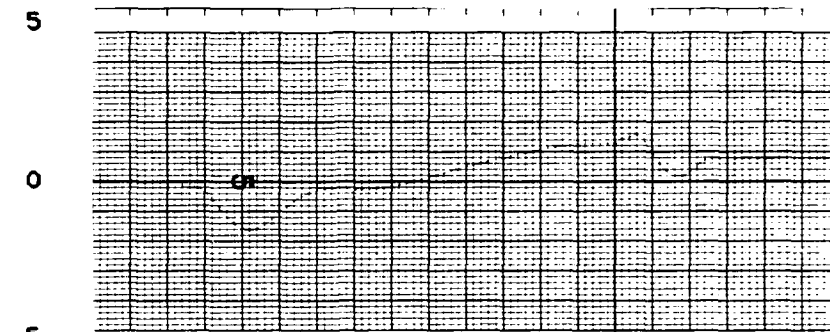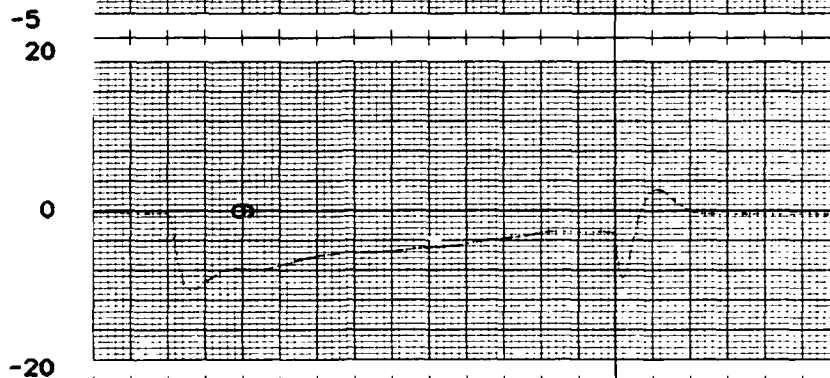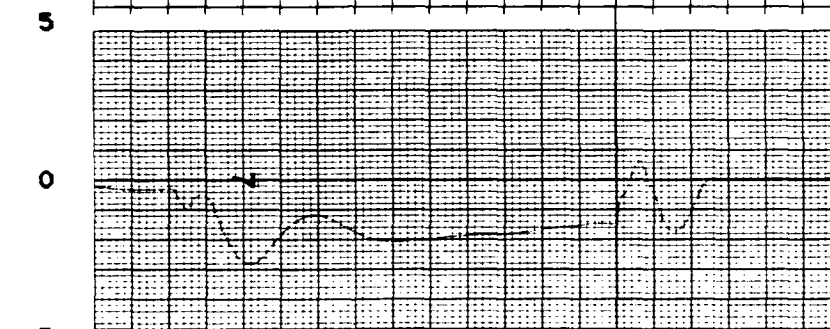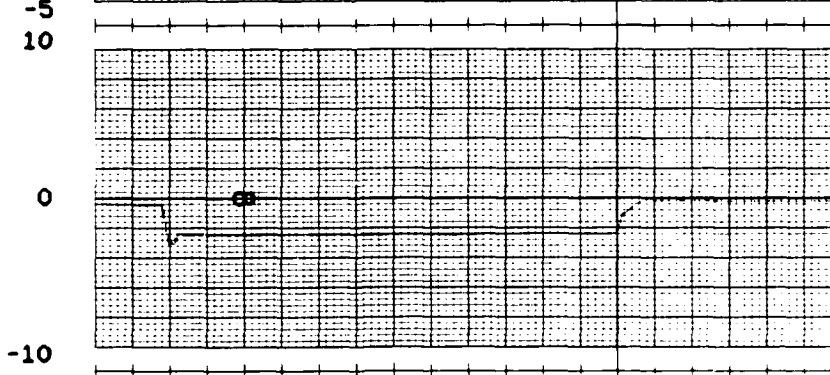
Figure D8 (CONTINUED). Forced Response $(\phi/\beta)_d$ = 1.5 arg(60) - 0.4H
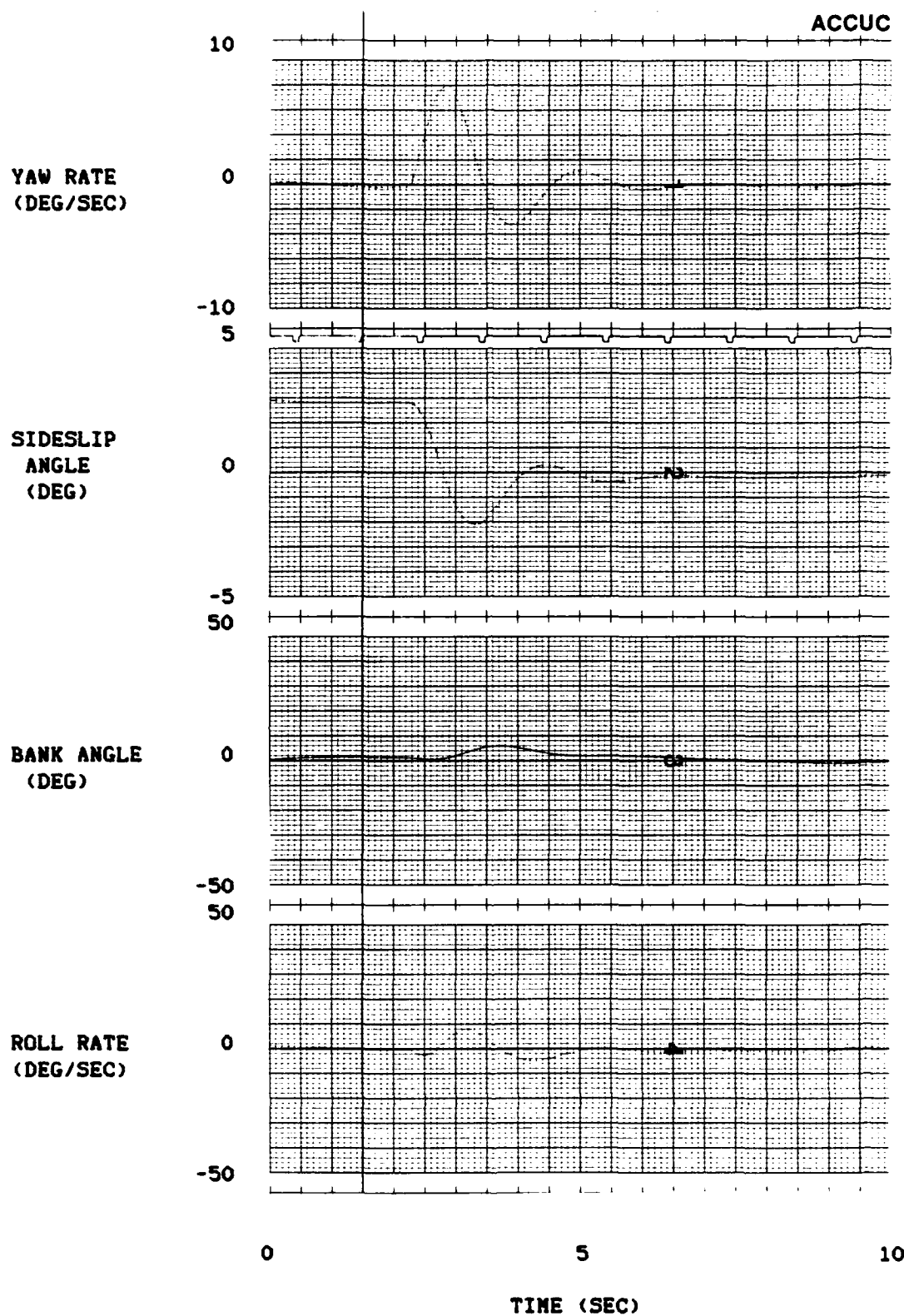
Figure D9. Free Response $(\phi/\beta)_d$ = 1.5 arg(120) - 0.4N

151

Figure D9 (CONTINUED). Free Response $(\phi/\beta)_d = 1.5$ arg(120) ~ 0.4N
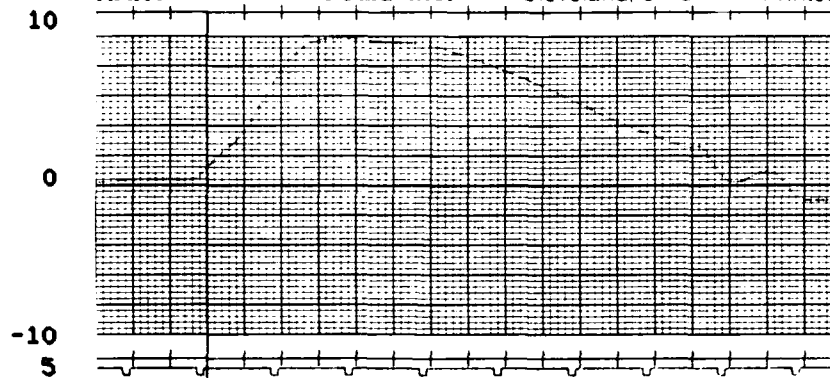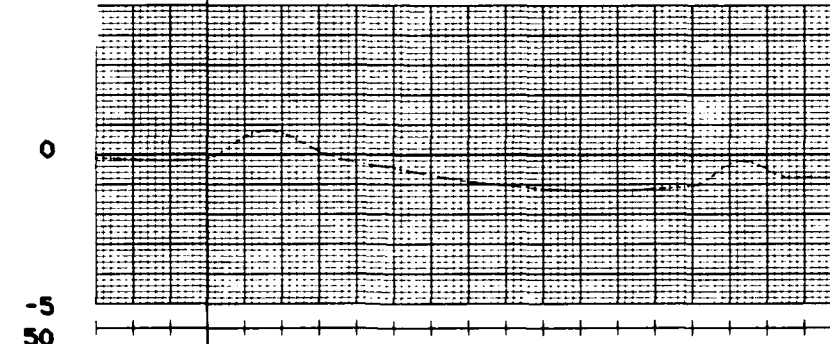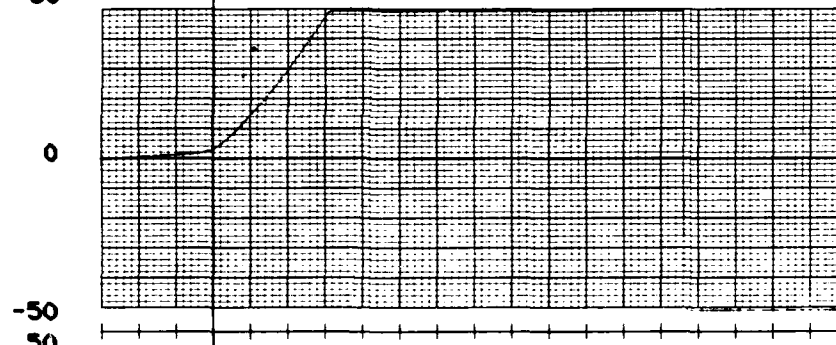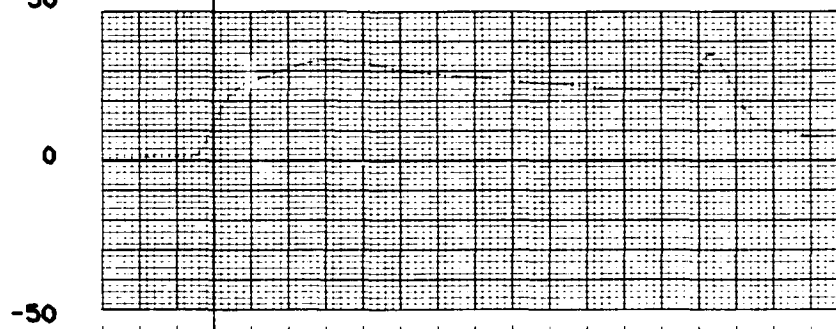
Figure D10. Forced Response $(\phi/\beta)_d$ = 1.5 arg(120) - 0.4M

LATERAL
ACCELERATION
(FT/SEC^2)

AILERON
DEFLECTION
(DEG)

RUDDER
DEFLECTION
(DEG)

LATERAL
STICK FORCE
(POUNDS)
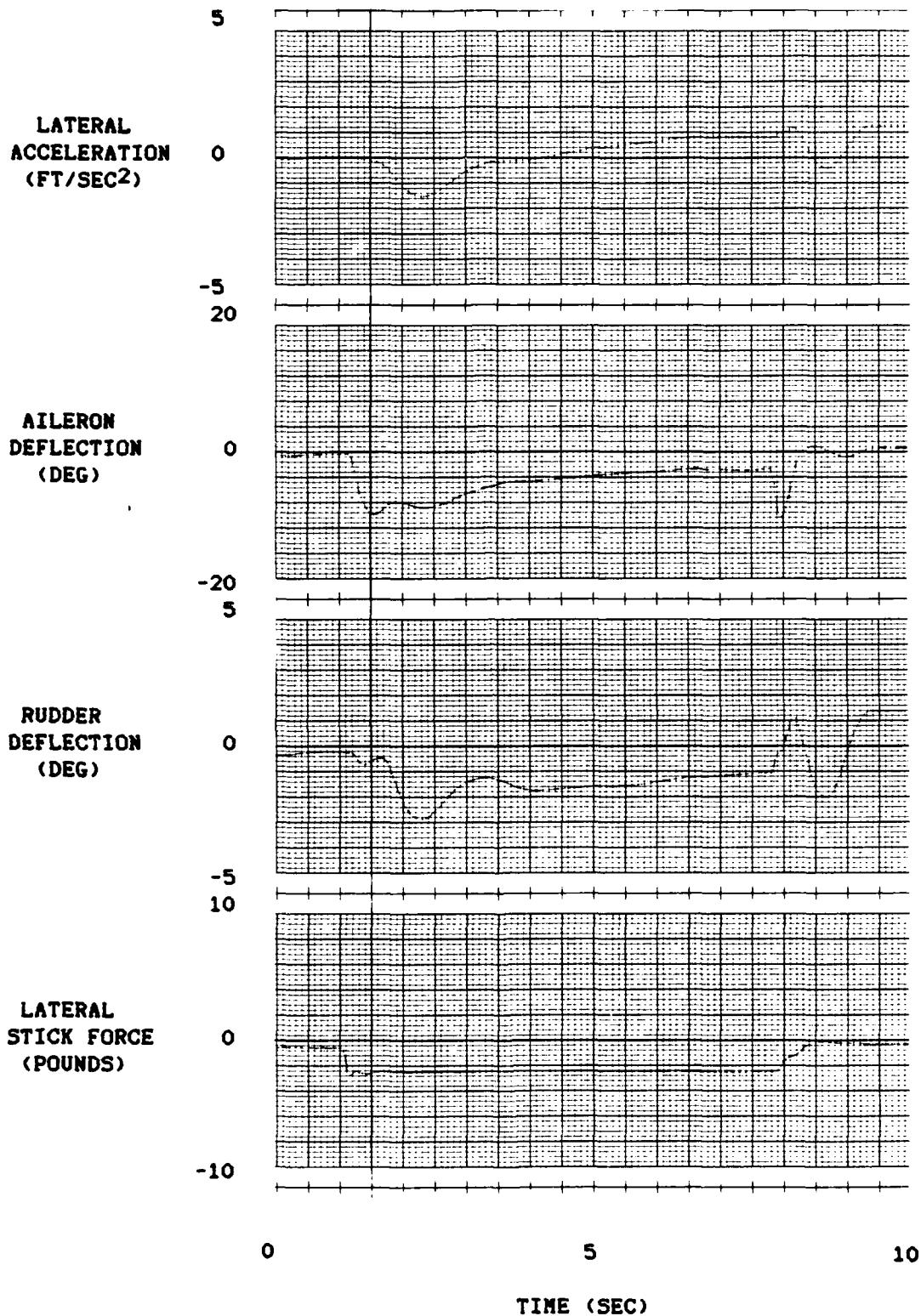
TIME (SEC)

Figure D10 (CONTINUED). Forced Response $(\phi/\beta)_d$ = 1.5 arg(120) - 0.4M
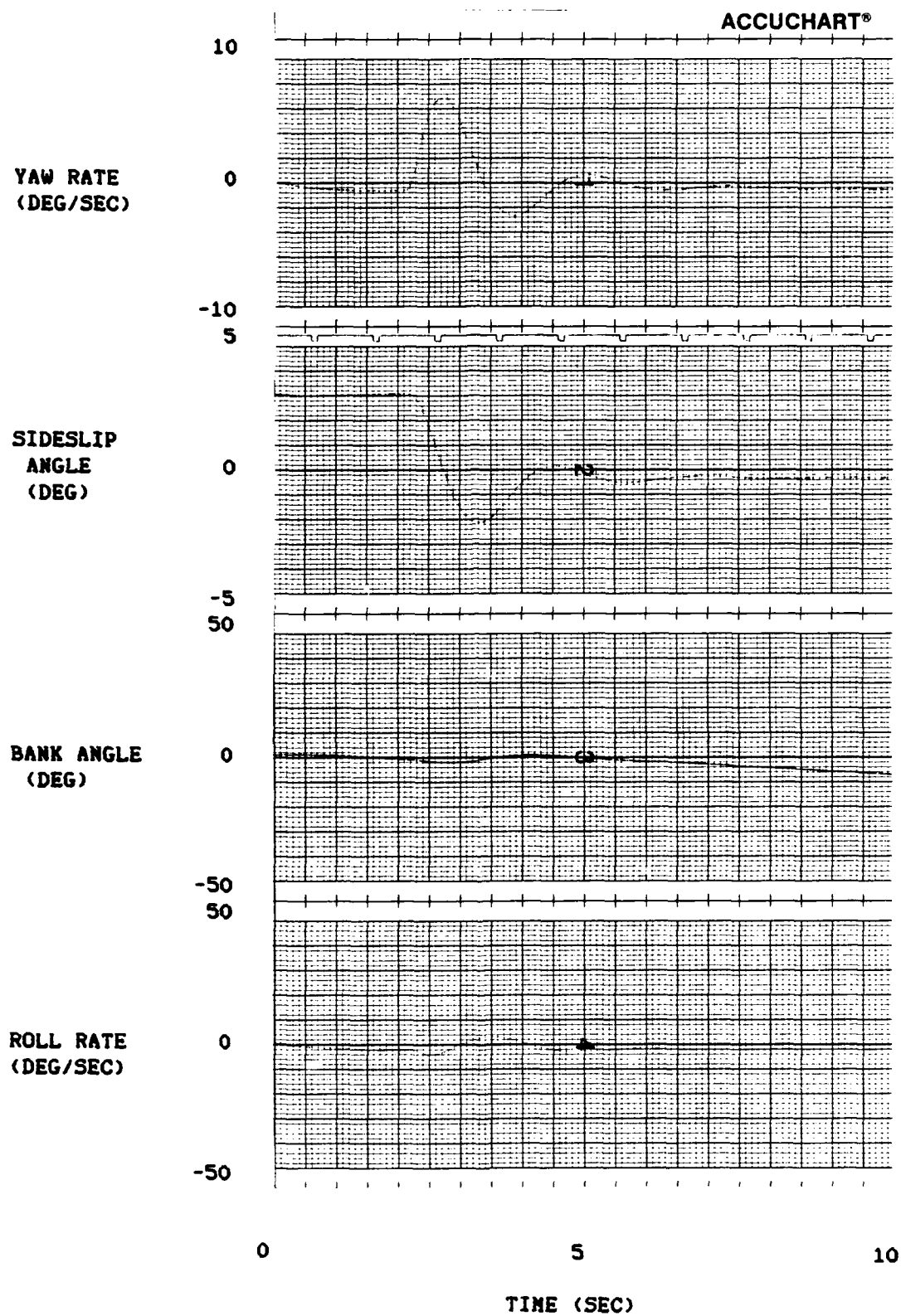
154

ACCUCHART®

YAW RATE (DEG/SEC)

SIDESLIP ANGLE (DEG)

BANK ANGLE (DEG)

ROLL RATE (DEG/SEC)
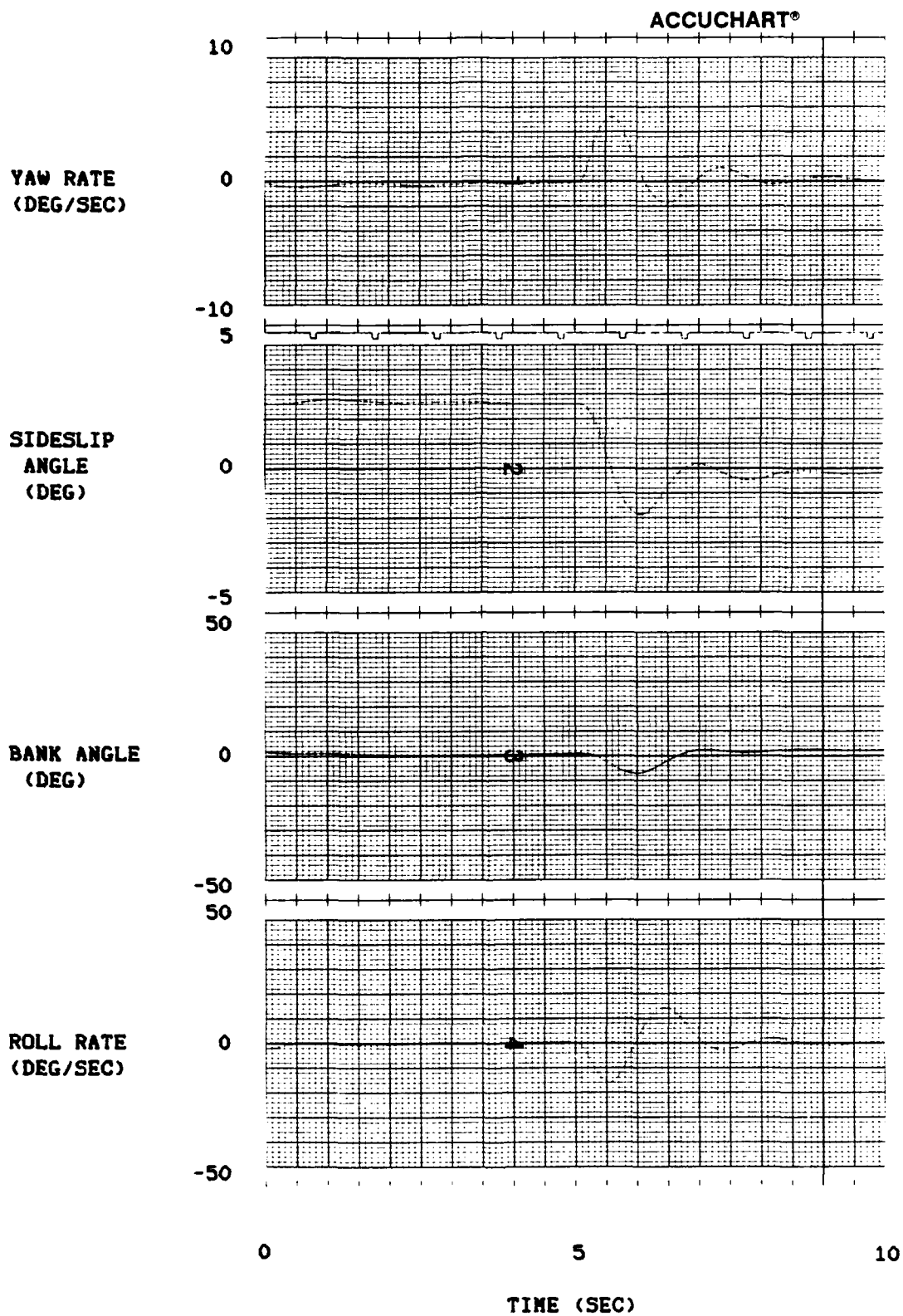
TIME (SEC)

Figure D11.   Free Response $(\phi/\beta)_d$ = 3.0 arg(0) - 0.4N
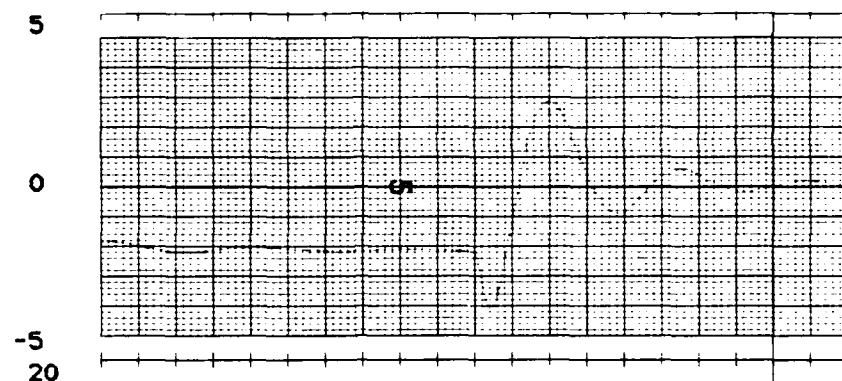
155
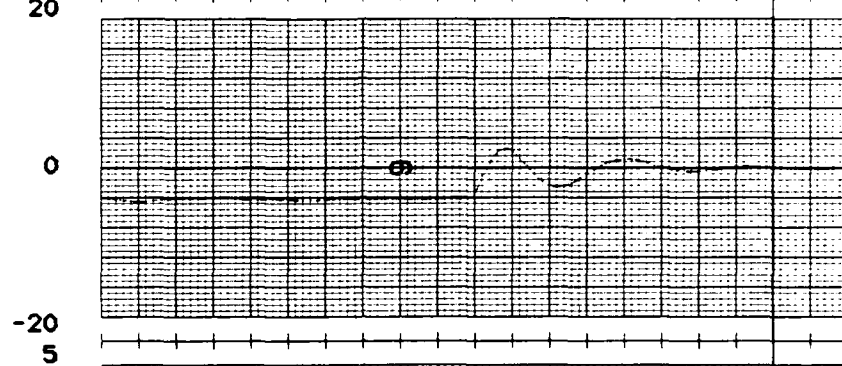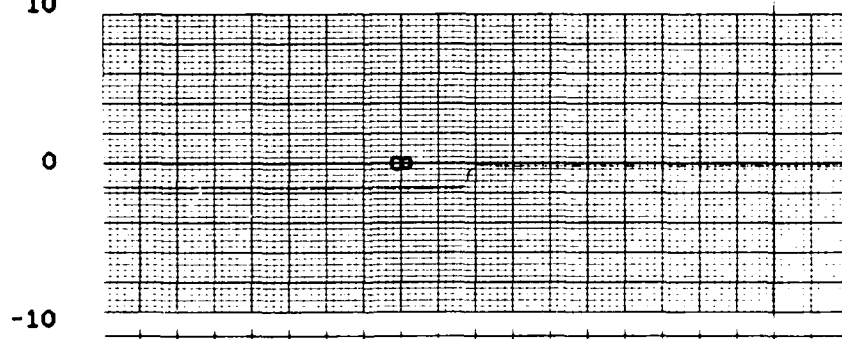
Figure D11 (CONTINUED). Free Response $(\phi/\beta)_d$ = 3.0 arg(0) - 0.4M

156
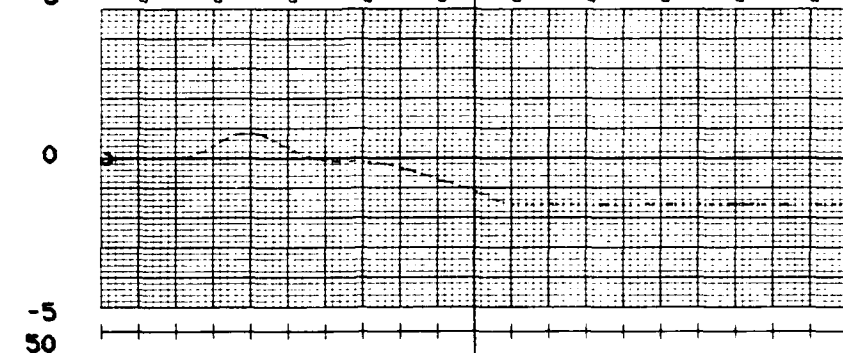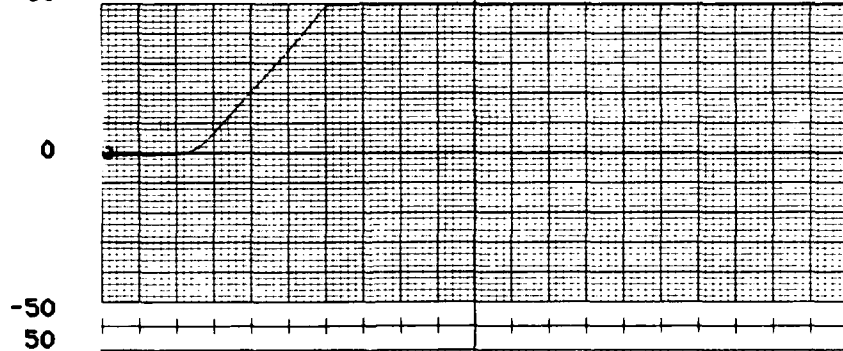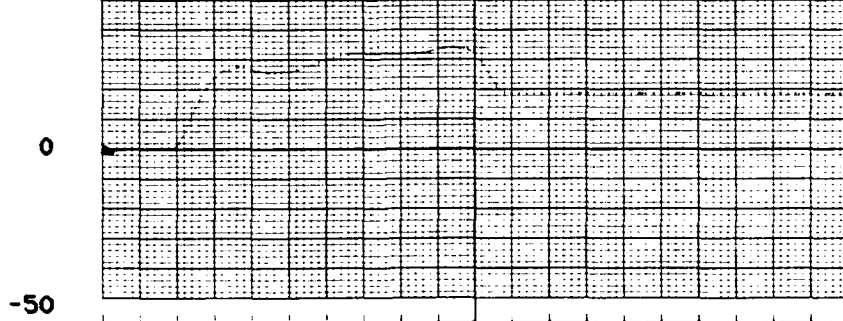
Figure D12. Forced Response $(\phi/\beta)_d = 3.0$ arg(0) - 0.4N
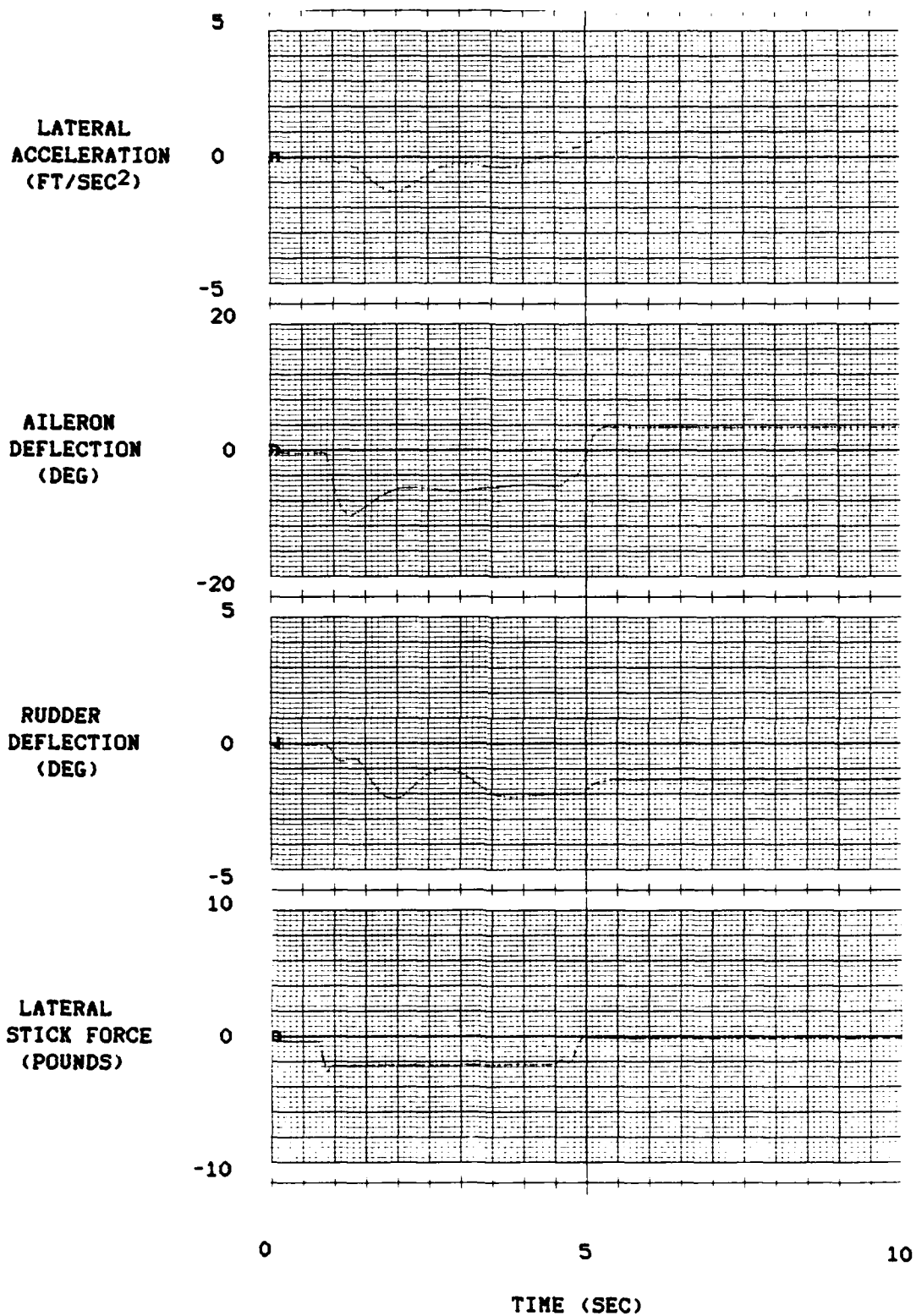
Figure D12 (CONTINUED). Forced Response $(\phi/\beta)_d = 3.0 \text{ arg}(0) - 0.4N$
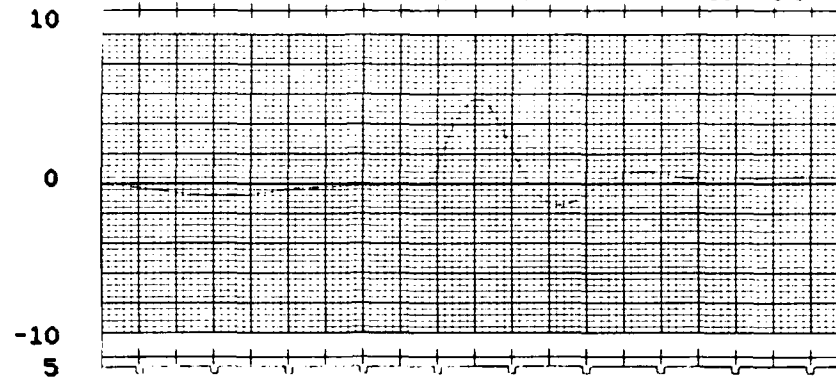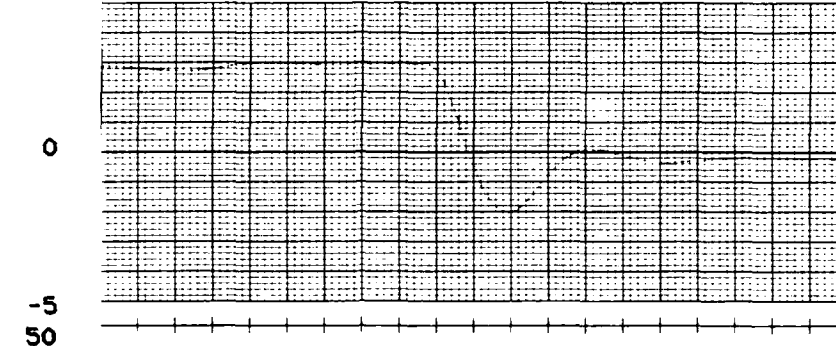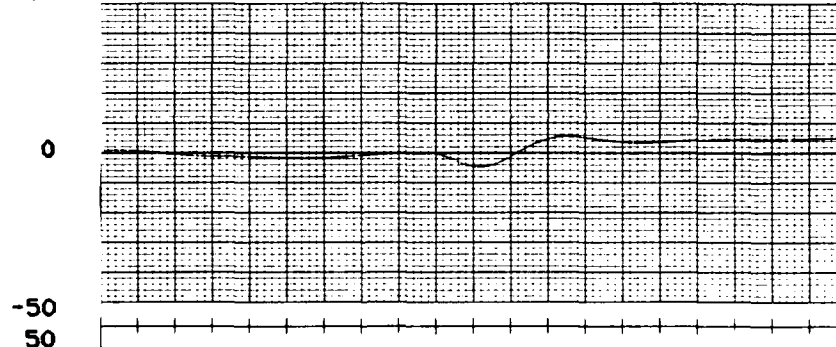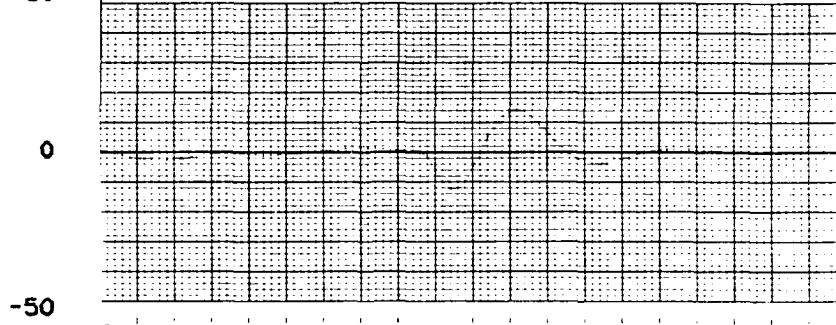
Figure D13. Free Response $(\phi/\beta)_d$ = 3.0 arg(60) - 0.4N
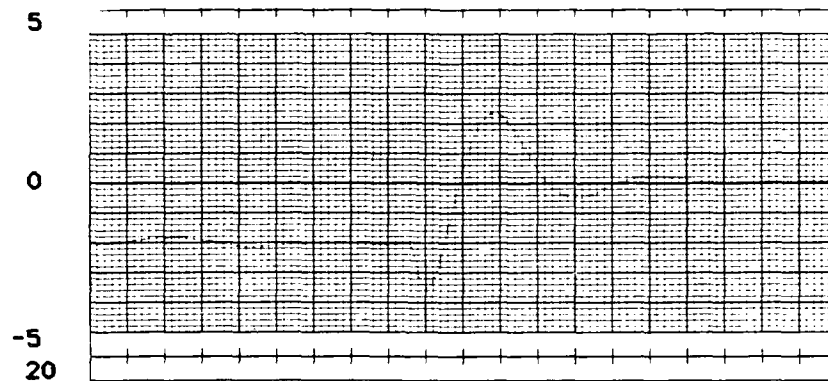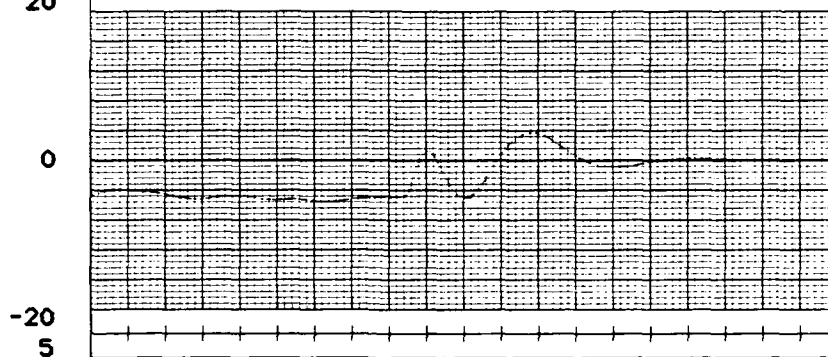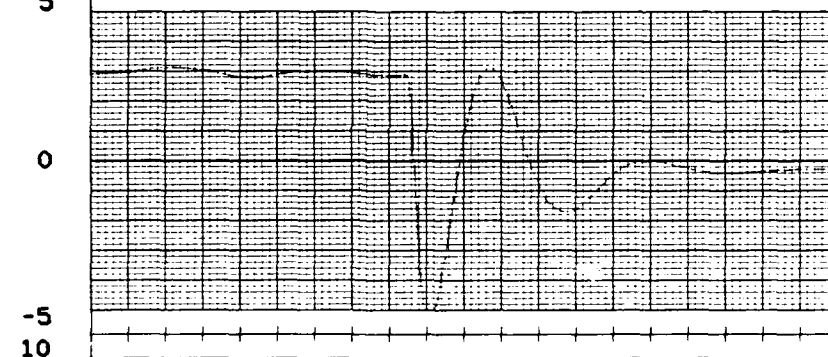
Figure D13 (CONTINUED). Free Response $(\phi/\beta)_d = 3.0$ arg(6u) - 0.4M
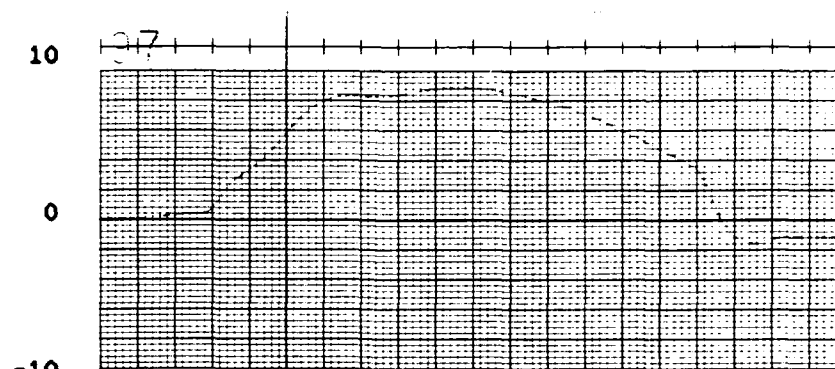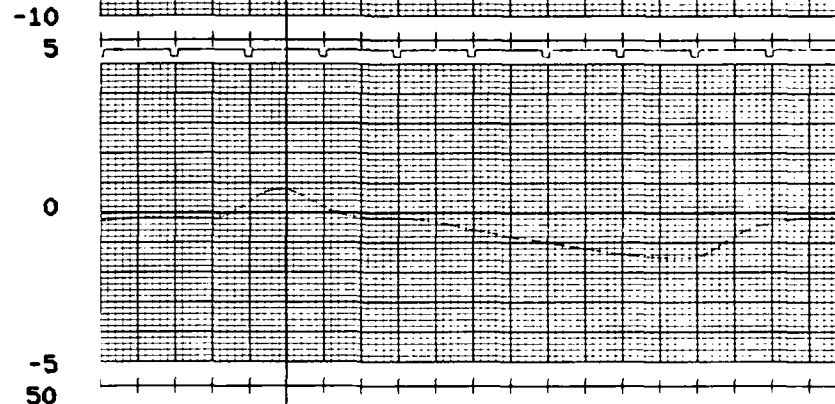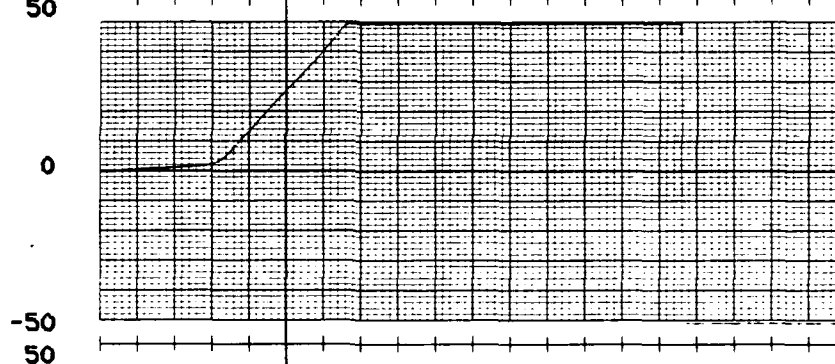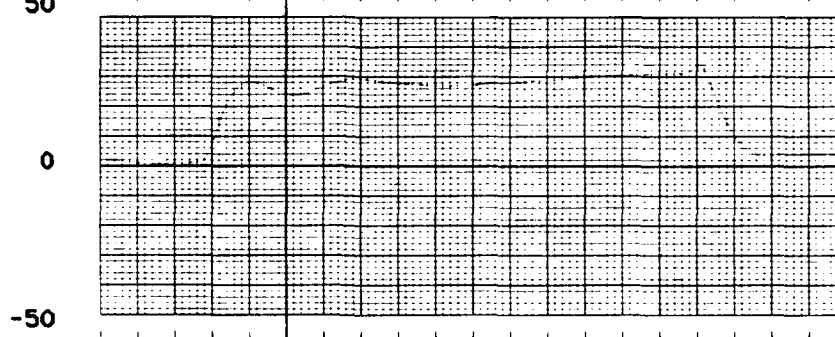
Figure D14. Forced Response $(\phi/\beta)_d = 3.0$ arg(60) - 0.4M
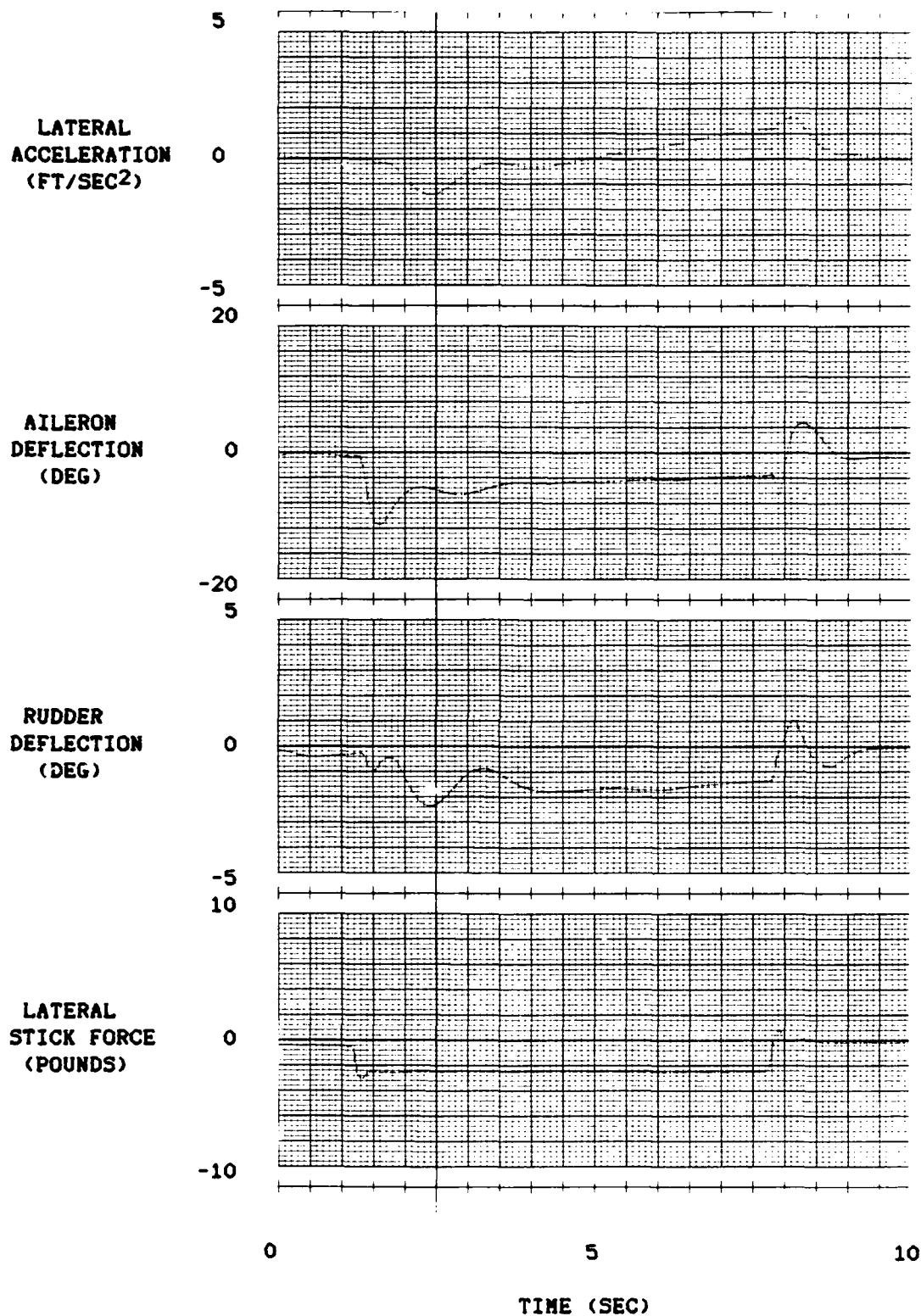
Figure D14 (CONTINUED). Forced Response $(\phi/\beta)_d = 3.0 \text{ arg}(60) - 0.4N$

ACCUC
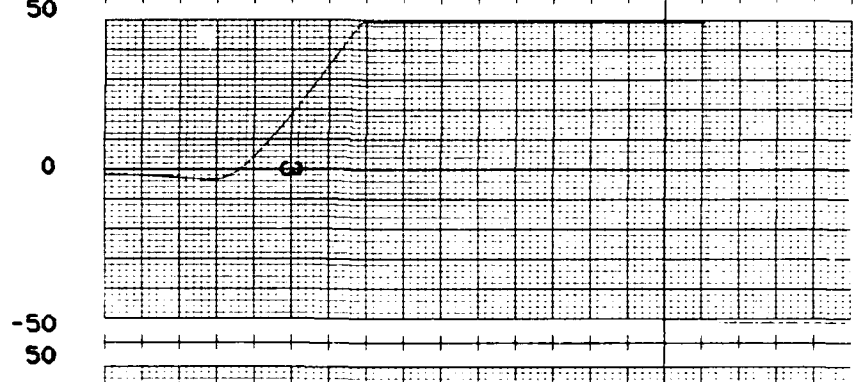
YAW RATE (DEG/SEC)

SIDESLIP ANGLE (DEG)

BANK ANGLE (DEG)

ROLL RATE (DEG/SEC)
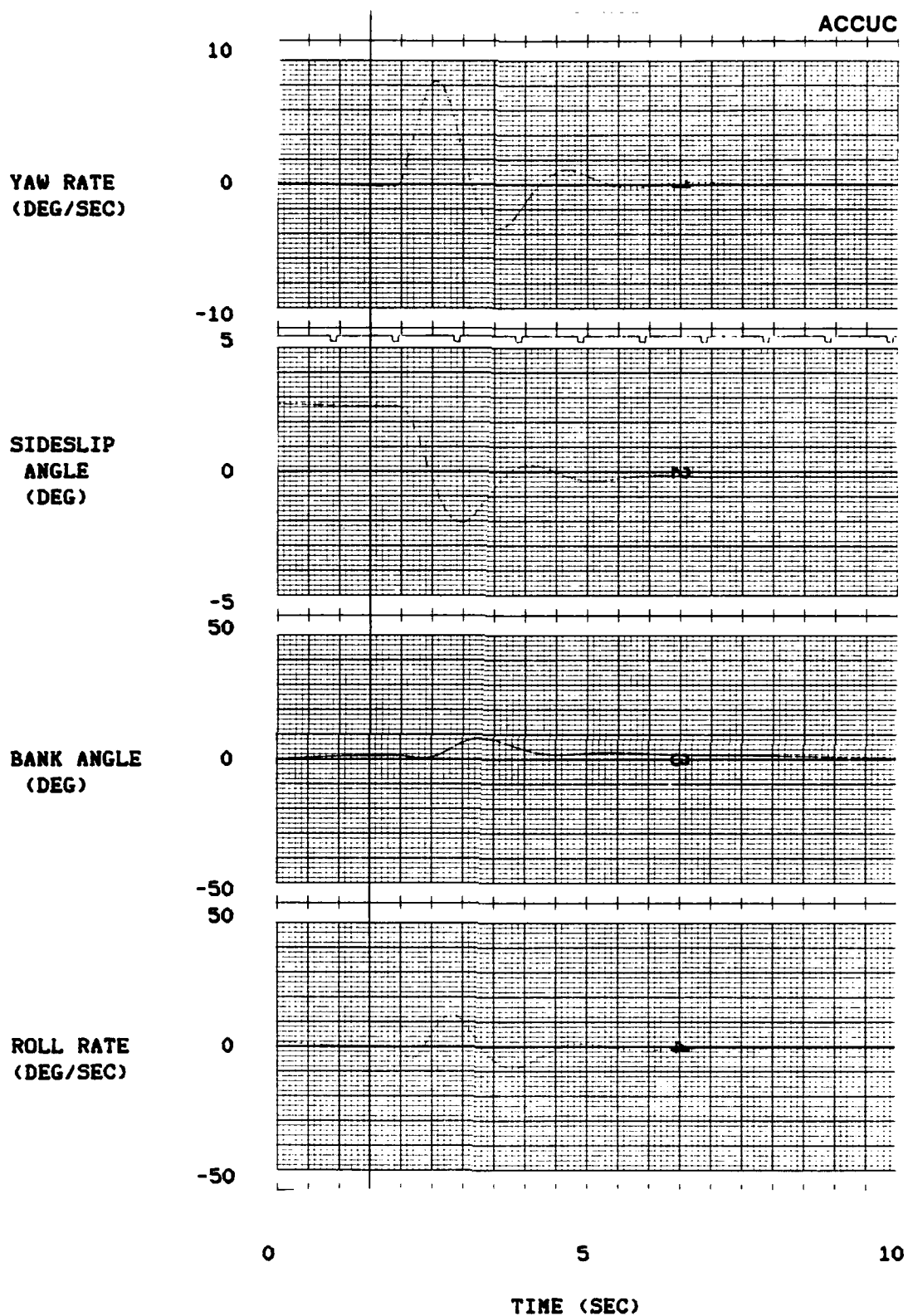
TIME (SEC)

Figure D15. Free Response $(\phi/\beta)_d = 3.0 \ arg(120) - 0.4N$
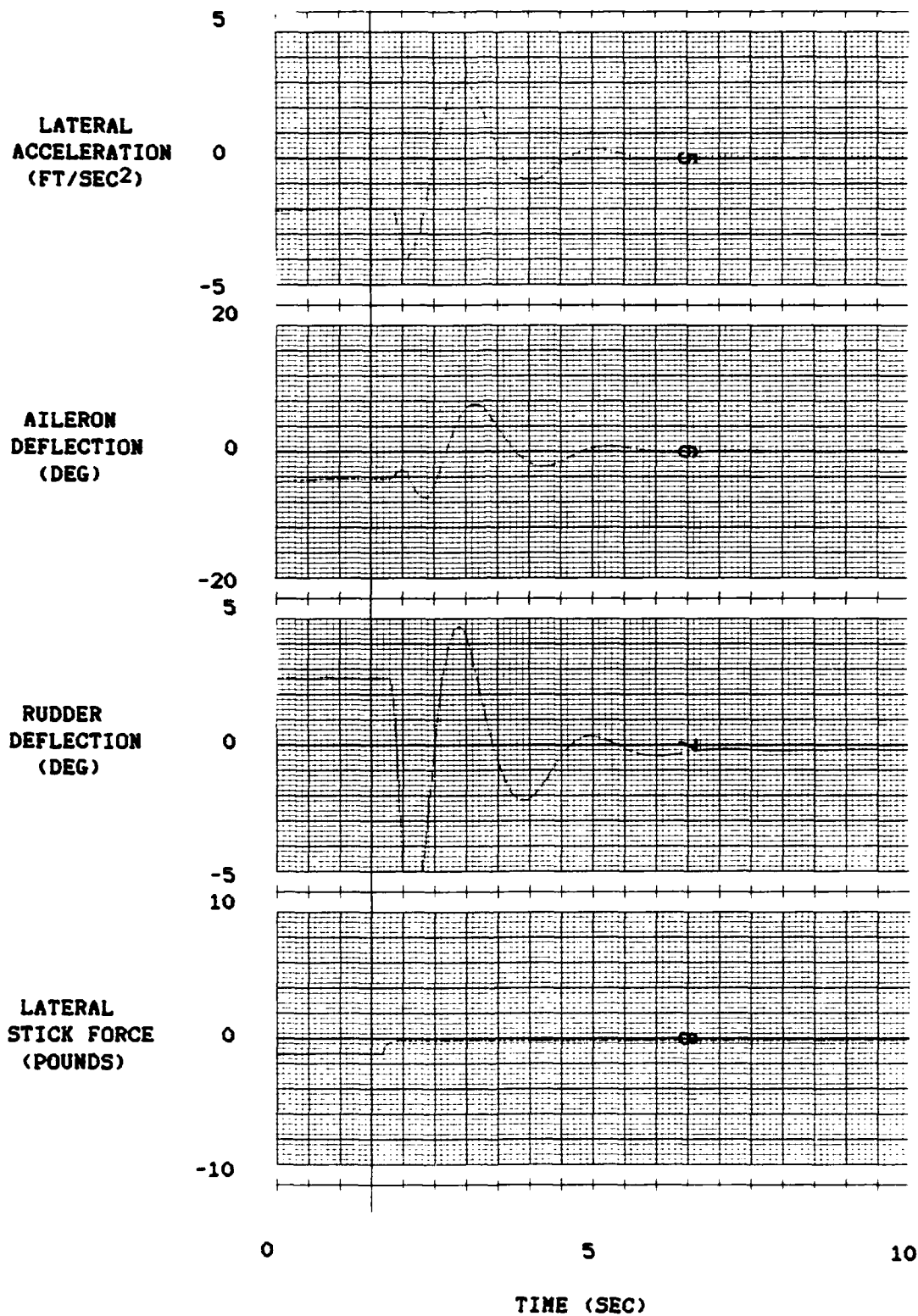
Figure D15 (CONTINUED). Free Response $(\phi/\beta)_d = 3.0$ arg(120) - 0.4N
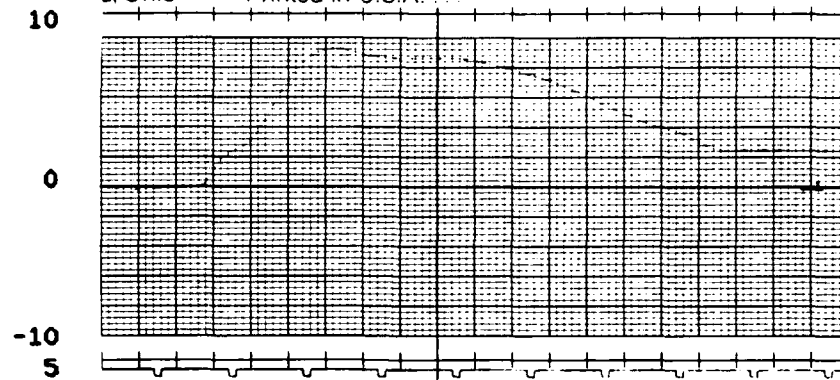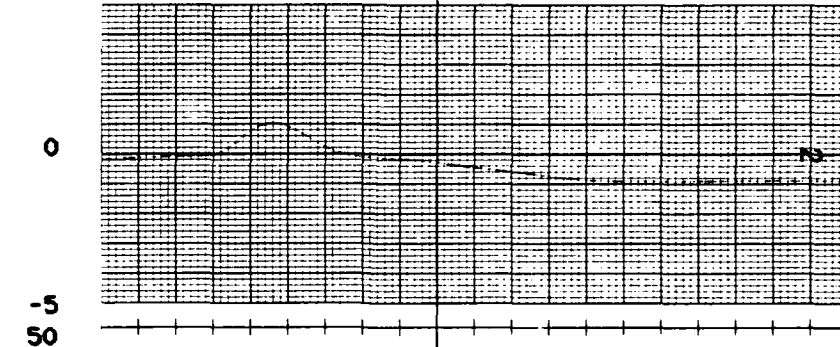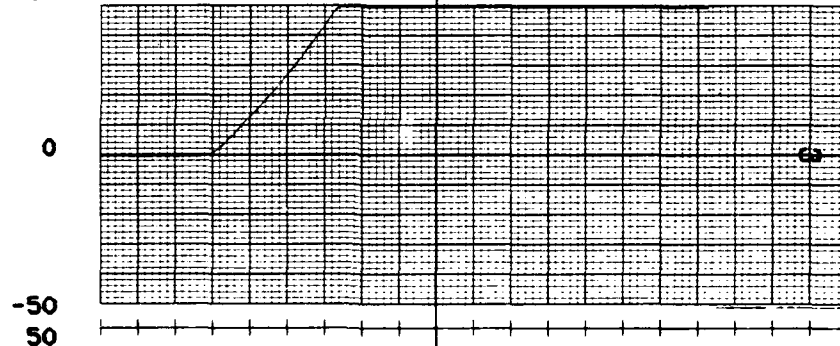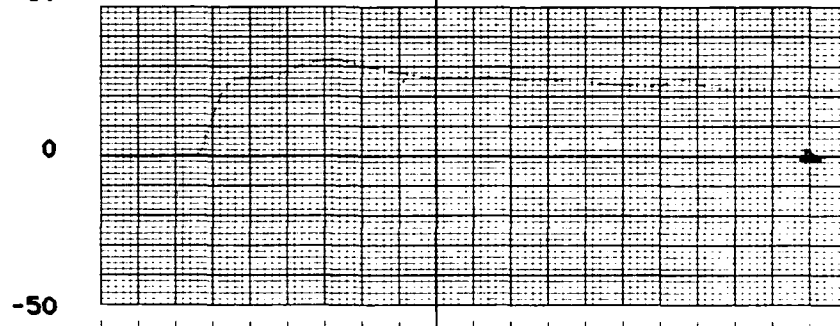
Figure D16. Forced Response $(\phi/\beta)_d = 3.0$ arg(120) - 0.4N

165
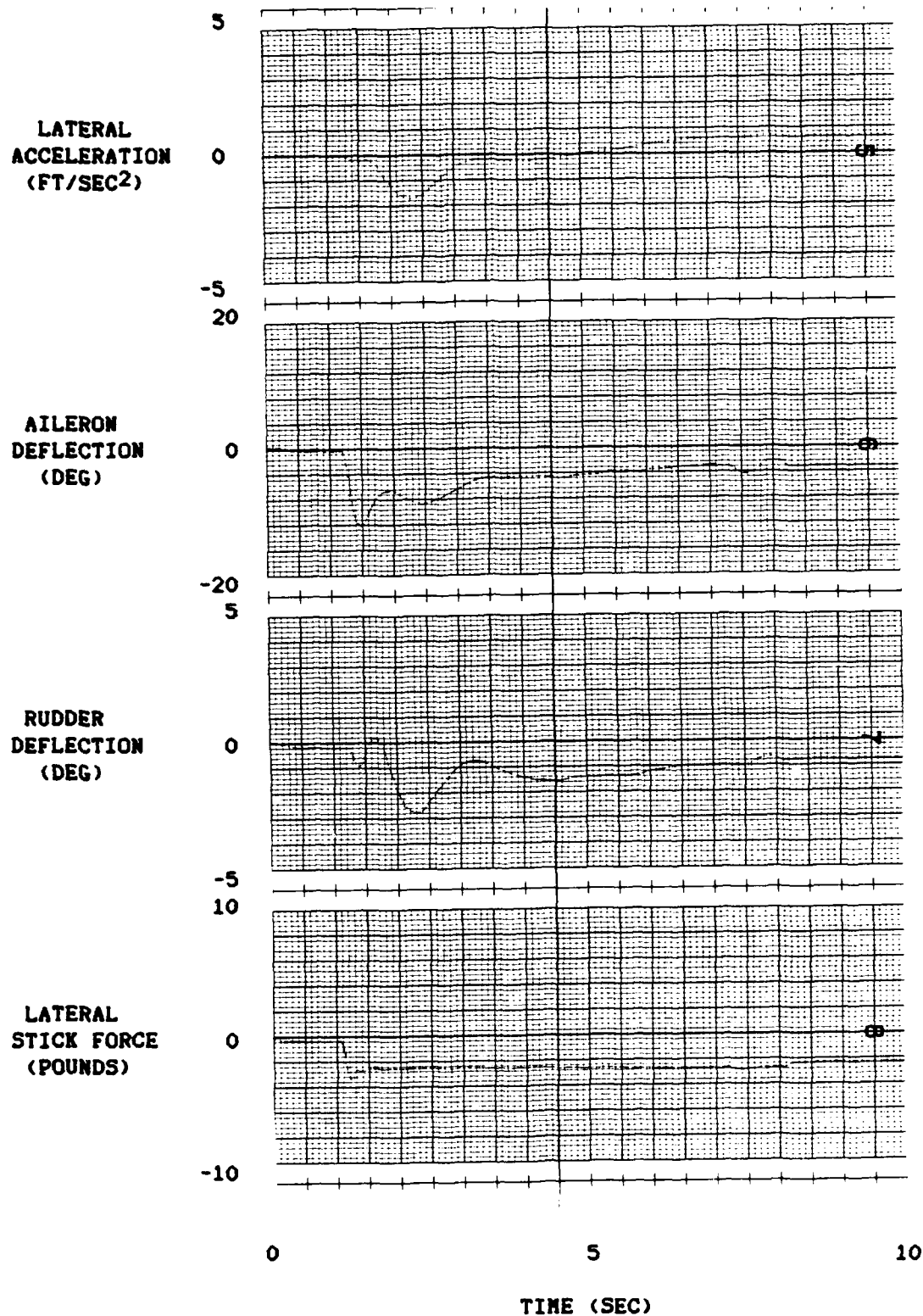
Figure D16 (CONTINUED). Forced Response $(\phi/\beta)_d = 3.0$ arg(120) - 0.4H

Figure D17. Unaugmented YA-7D Free Response - 0.6M
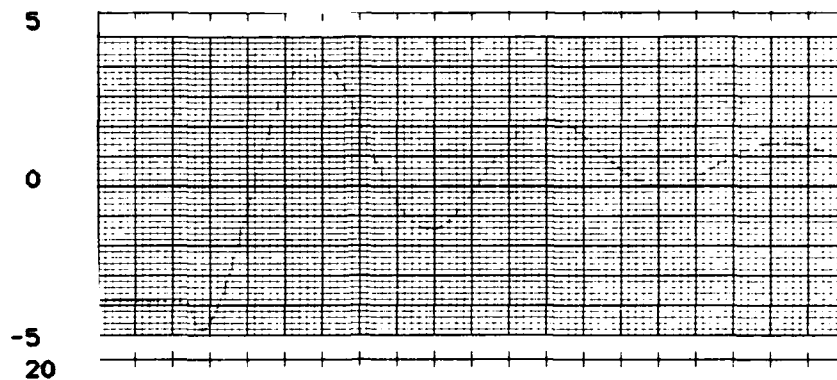
167
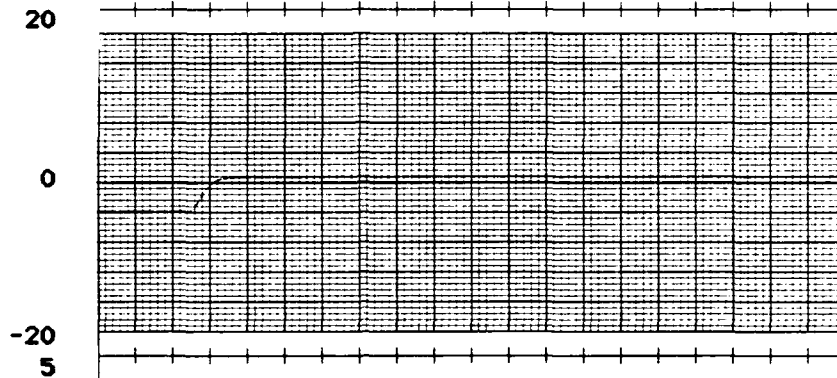
Figure D17 (CONTINUED). Unaugmented YA-7D Free Response - 0.6M
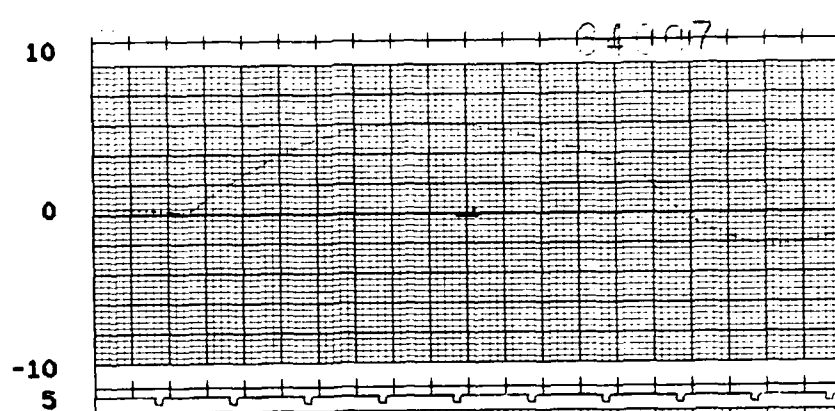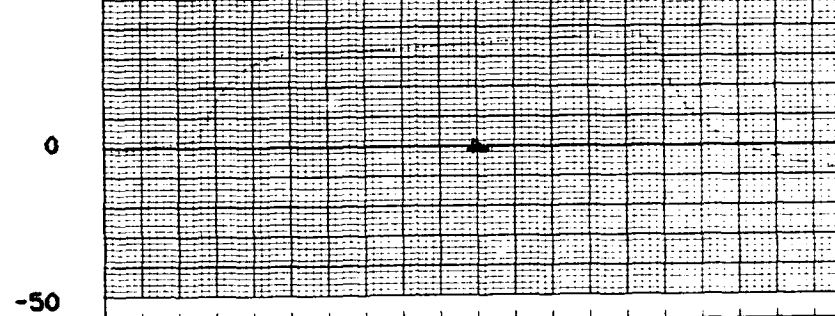
Figure D18. Unaugmented YA-7D Forced Response - 0.6M
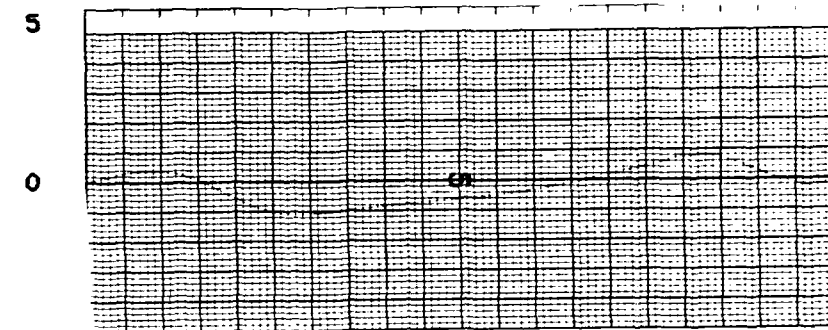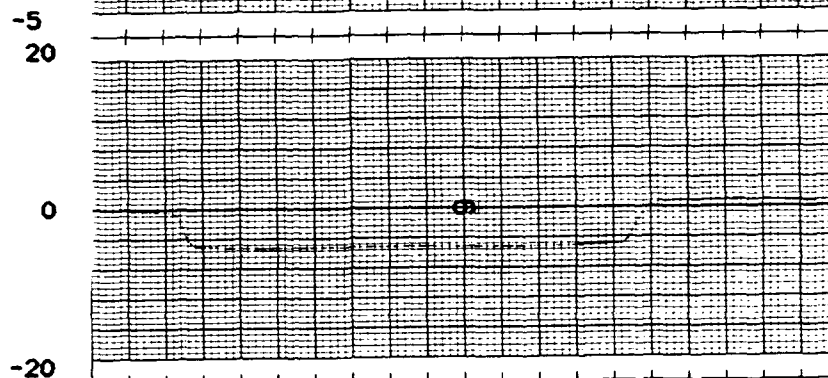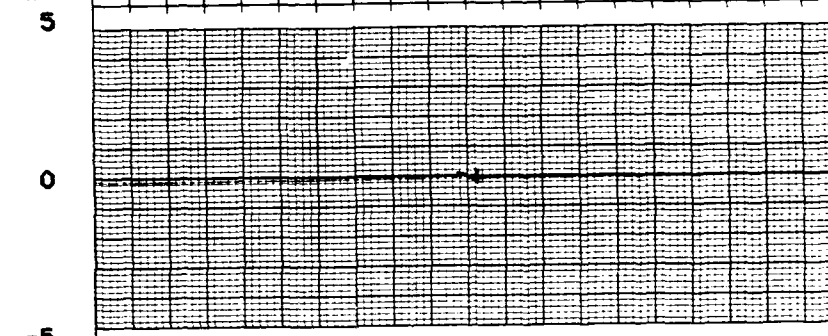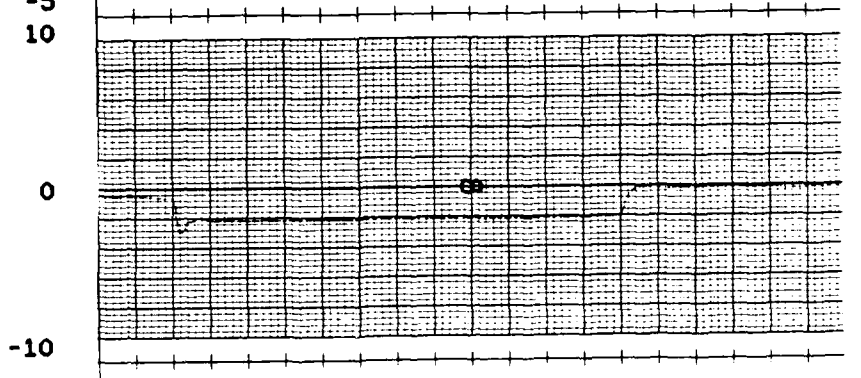
Figure D18 (CONTINUED). Unaugmented YA-7D Forced Response - 0.6M

Figure 19. Free Response $(\phi/\beta)_d = 0 - 0.6M$

171
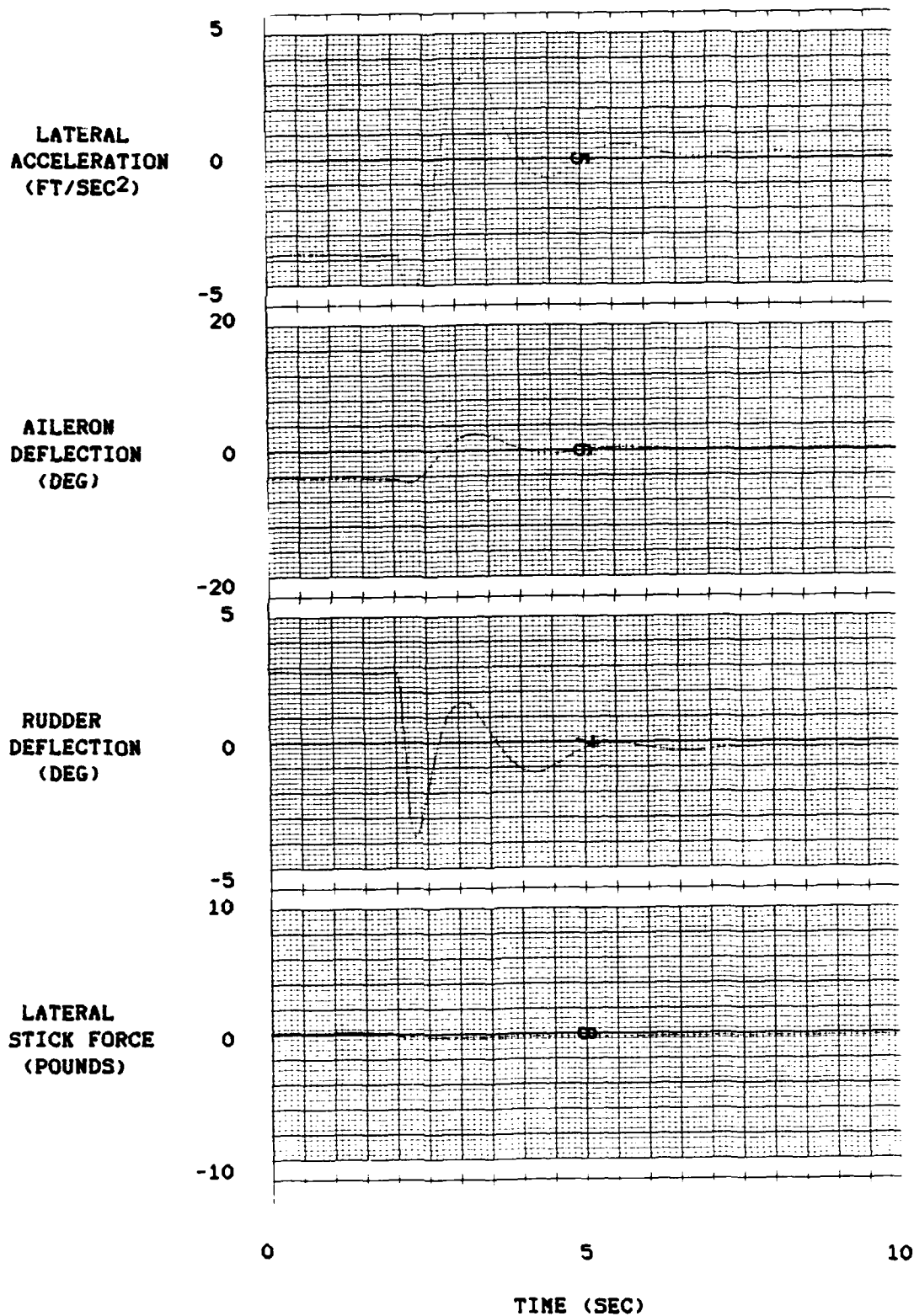
Figure D19 (CONTINUED). Free Response $(\phi/\beta)_d = 0 - 0.6M$

172
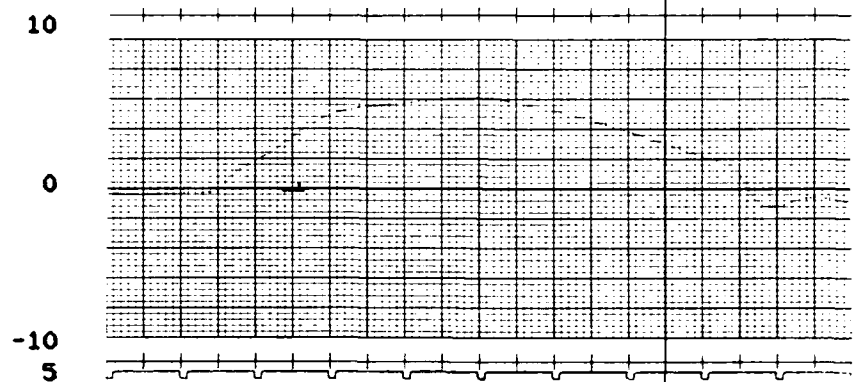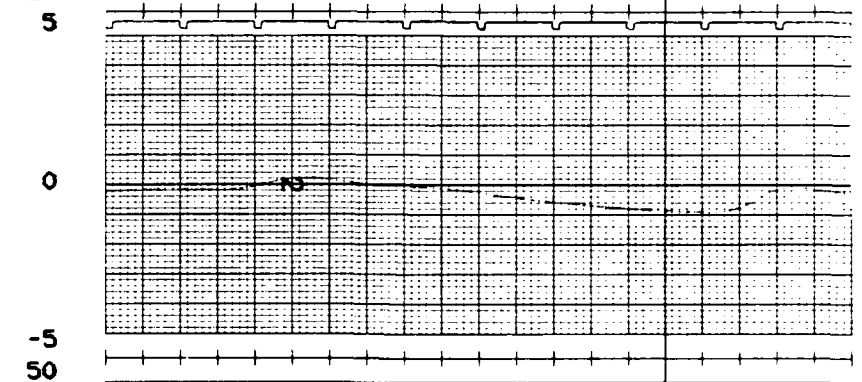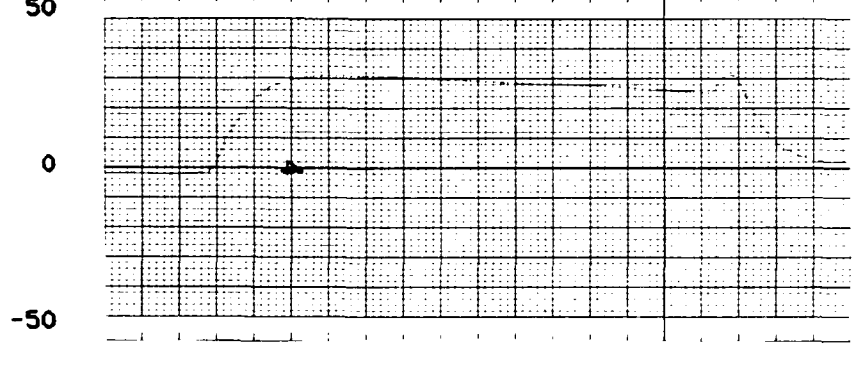
Figure D20.   Forced Response $(\phi/\beta)_d$ = 0 - 0.6M
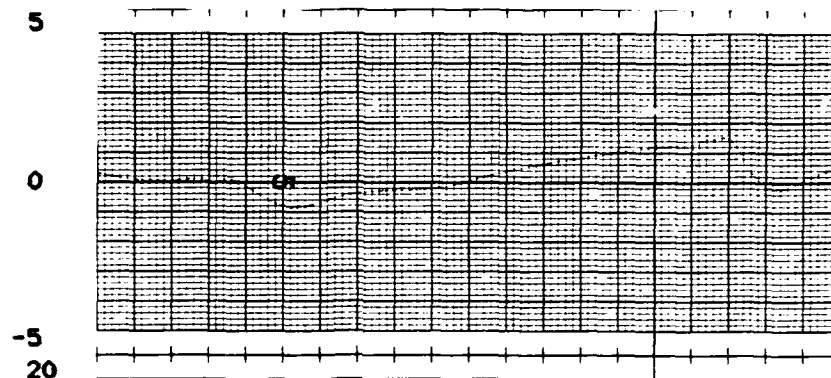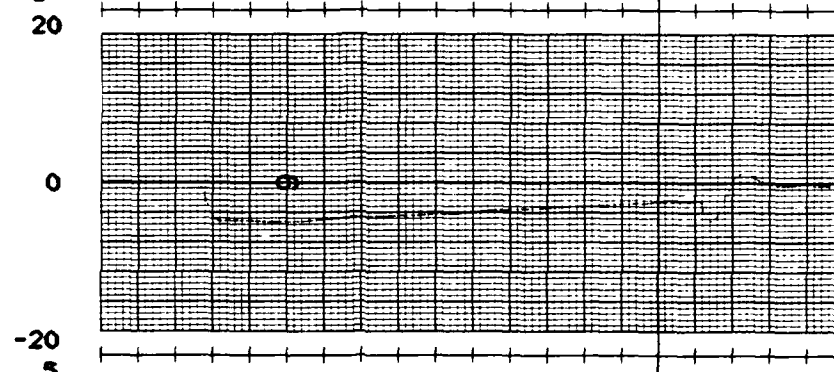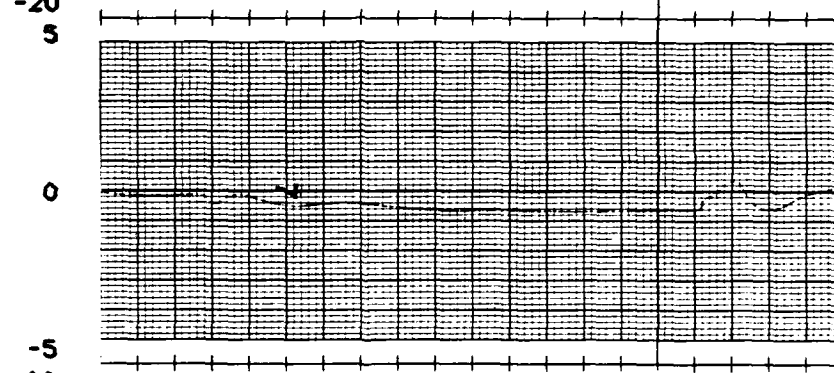
173
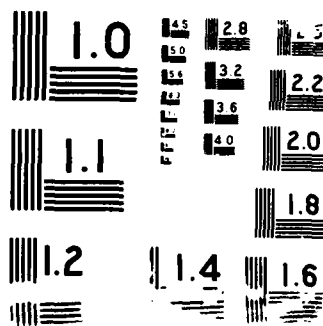
LATERAL
ACCELERATION
(FT/SEC²)
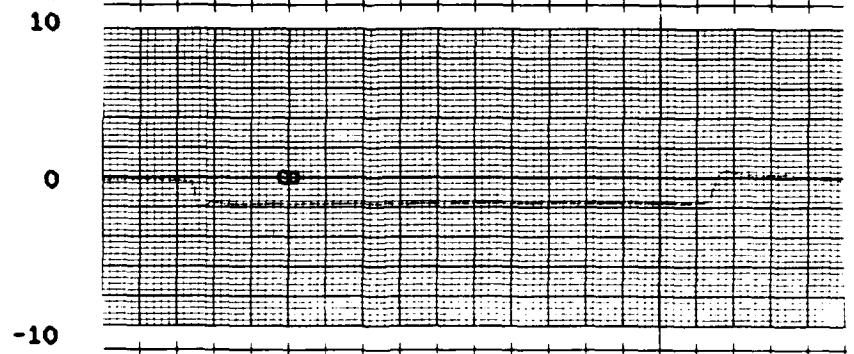
AILERON
DEFLECTION
(DEG)

RUDDER
DEFLECTION
(DEG)

LATERAL
STICK FORCE
(POUNDS)

TIME (SEC)

Figure D20 (CONTINUED). Forced Response $(\phi/\beta)_d = 0 - 0.6M$

174

APPENDIX E. Flight Test Data

Figures E1, E2, and E3 show inter and intra pilot repeatability for HUD Tracking task 1, HUD tracking task 2, and the air-to-air tracking task, respectively. The inter pilot comparisons are a plot of the pilot's highest rating versus lowest rating for each control law. The dashed line represents a difference of one Cooper-Harper rating. The intra pilot comparisons are a plot of one pilot's rating versus a second pilot's rating for each control law. The method used to determine a pilot's rating for each control law is discussed in Appendix F. The dashed line represents a difference of plus or minus one Cooper-Harper rating.
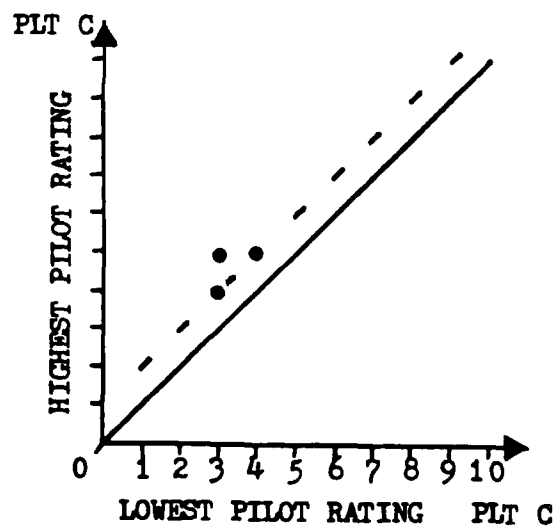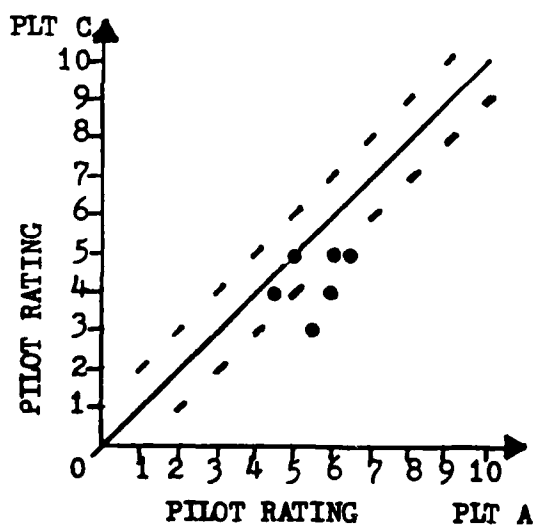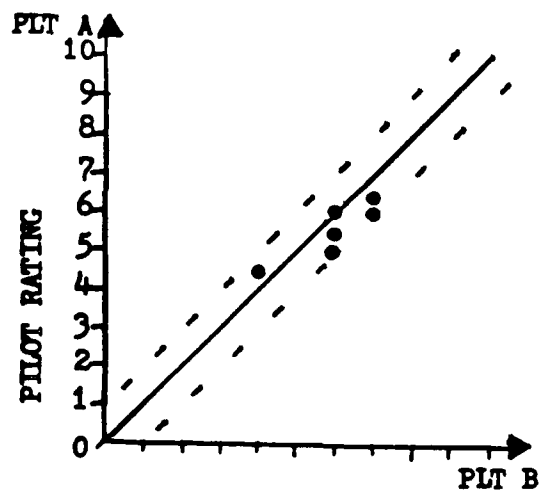
Figure E1. Inter and intra pilot Cooper-Harper Rating
Comparisons for HUD Tracking Task 1

Table E1

HUD Tracking Task 1 Cooper-Harper Ratings			
CONFIGURATION	PILOT A	PILOT B	PILOT C
Unaugmented YA-7D	5,5	N/A	5,5
Standard YA-7D	5,6	6,6,6	4,5,5,4

Phi/Beta Mag	Phi/Beta Phase	PILOT A	PILOT B	PILOT C
0	0	7,6	7,7,6	6,5,4
1.5	0	5,6	6,5,6	4,4,3
1.5	60	6,6	7,7,6	3,4,4
1.5	120	6,6	6,6,6	6,4,5
3.0	0	4,5	4,4,4	4,6,4
3.0	60	5,5	6,6,6	5,5,4
3.0	120	6,6	7,7,6	5,5,6
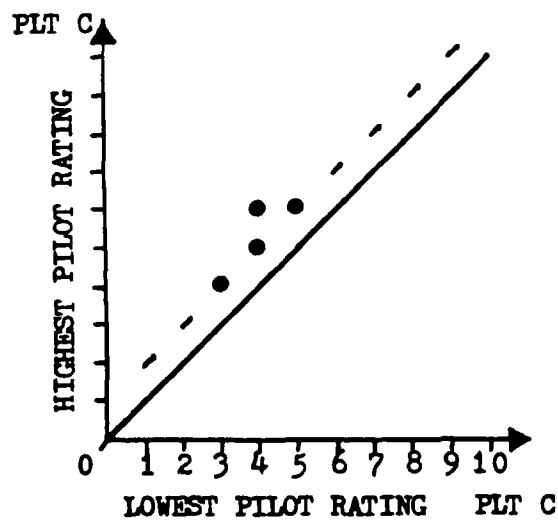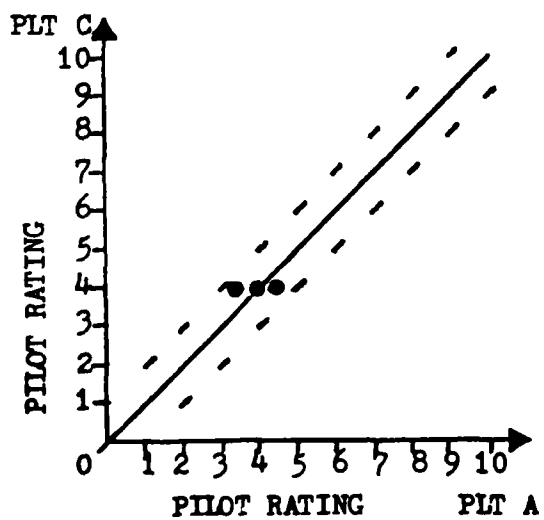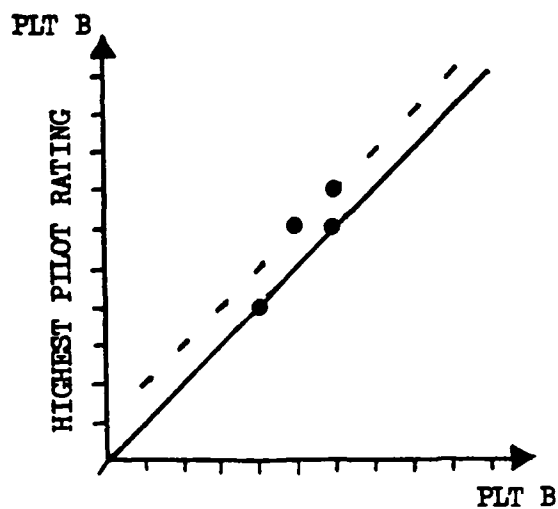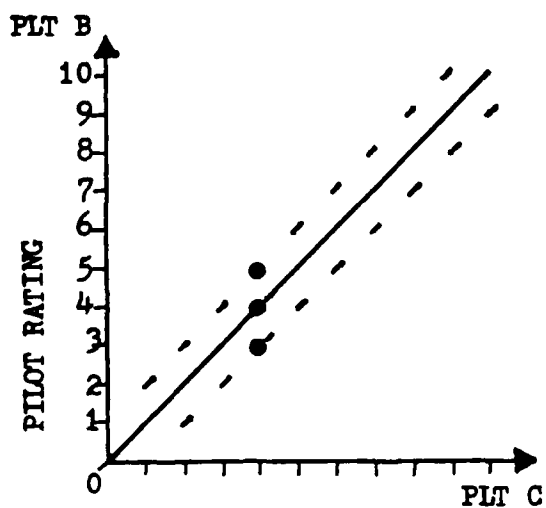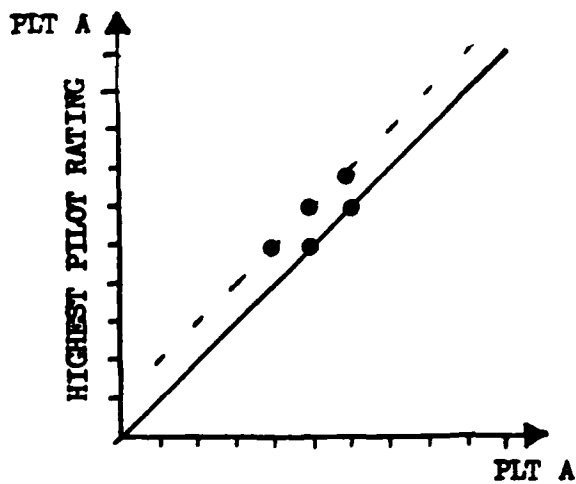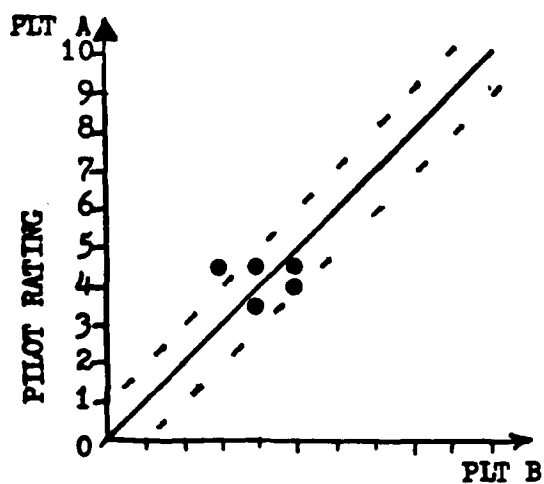
Figure E2.   Inter and intra pilot Cooper-Harper Rating
Comparisons for HUD Tracking Task 2

Table E2

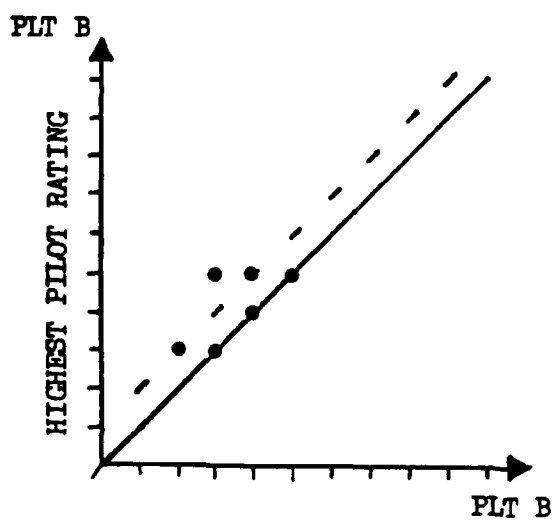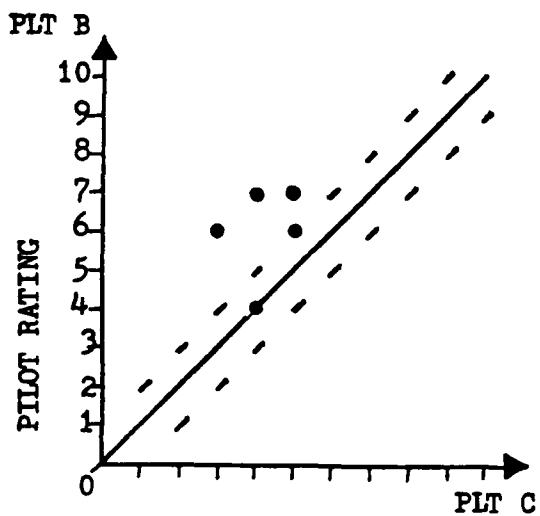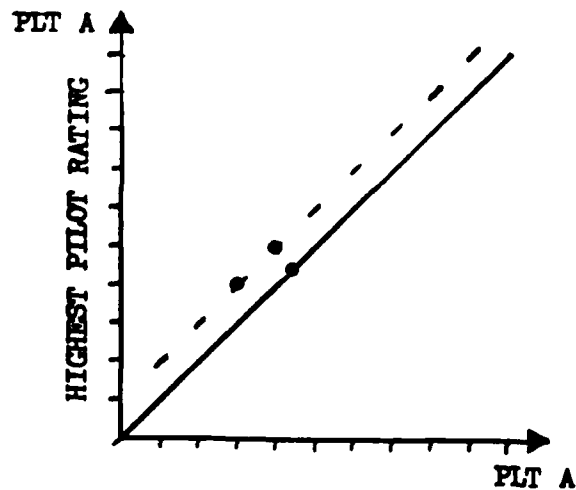| HUD Tracking Task 2 Cooper-Harper Ratings			
CONFIGURATION	PILOT A	PILOT B	PILOT C
Unaugmented YA-7D	4.5,4.5	6	4
Standard YA-7D	4,4	4,4,4	4,4,4,4

Phi/Beta Mag	Phi/Beta Phase	PILOT A	PILOT B	PILOT C
0	0	5,4.5	4,4	4,4,3,4,5,5,5
1.5	0	4,3	3,5,4,4	3,4,3,4,4,4,3
1.5	60	4,5,4.5	4,4	5,4,4,5,5,3,4
1.5	120	5,4	5,5,5	4,3,4,4,4,3
3.0	0	5,4.5	2,3,3	4,4,4,5,3,5,3
3.0	60	4.5	3,3,3	3,5,4,5,5,3,4
3.0	120	5,5,4	4,5,5	4,5,4,4,4,4,3
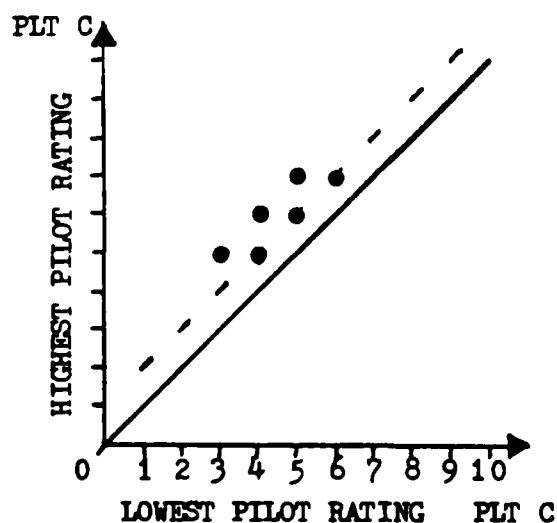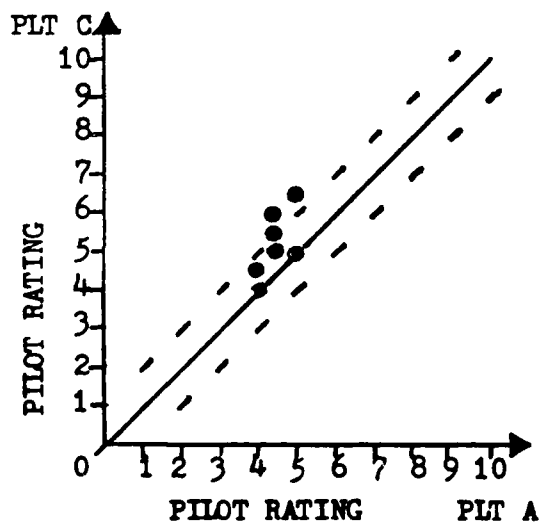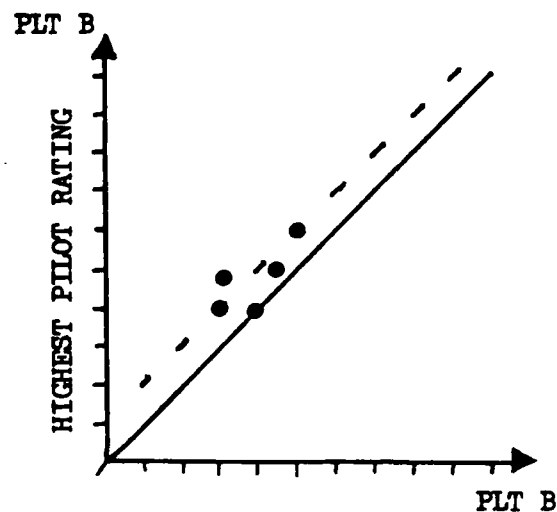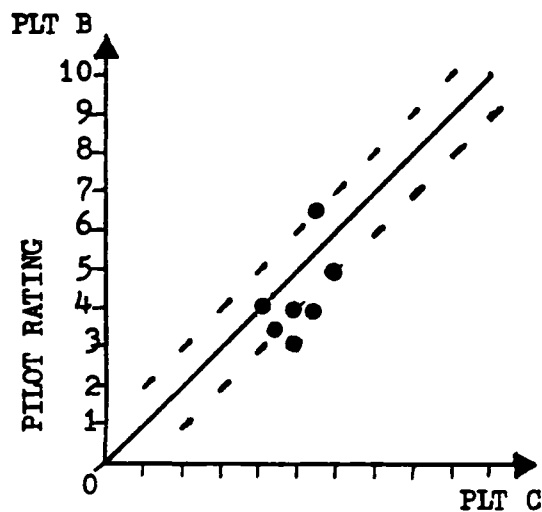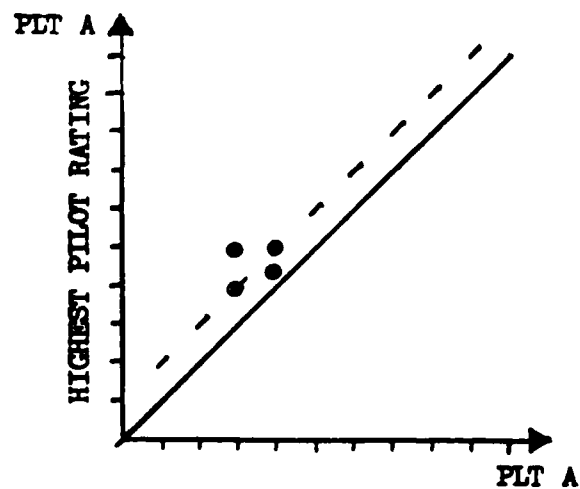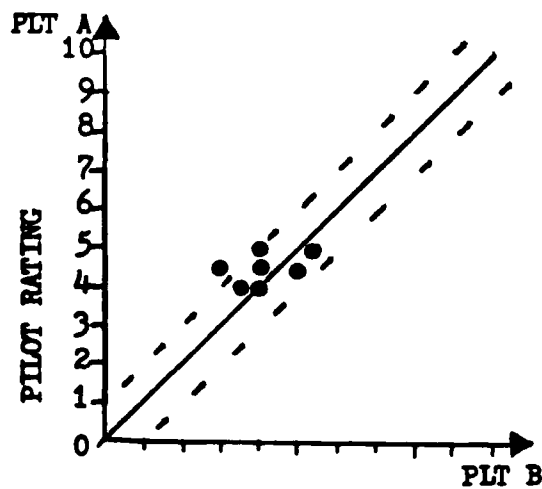
Figure E3. Inter and intra pilot Cooper-Harper Rating
Comparisons for air-to-air tracking task

Table E3

Air-to-air Tracking Task Cooper-Harper Ratings				
CONFIGURATION		PILOT A	PILOT B	PILOT C
Unaugmented YA-7D		4.5,5.5	7	N/A
Standard YA-7D		4,4,4,4.5	4,4,4,4	4,4,4,4
Phi/Beta Mag	Phi/Beta Phase			
0	0	5,4.5,4.5,4	4,4,4	5,6,6,5
1.5	0	4,5,5	4,4,4	6,5,5,4
1.5	60	3,3,5,5,4	3,3,4,4	5,5,4,4
1.5	120	4.5,4.5,4	5,4.5	7,6,6,5
3.0	0	3,4,5,4.5	3,3,4	4,5,4,3
3.0	60	4,5,4	5,3,4	4,4,5,3
3.0	120	4.5,5,4,5	5,6	7,6,6,6

APPENDIX F.   Flight Test Data Acquisition
and Analysis

Instrumentation and Data Reduction

The Ampex AR-700 magnetic tape recorder onboard the aircraft
recorded all 126 DIGITAC parameters for later playback and review. The
available parameters were listed in the Partial Flight Manual (15). The
primary parameters required were lateral stick force and position, roll
and yaw rate, lateral acceleration, and roll and sideslip angles. The
data were played back after a mission on two eight channel stripchart
recorders in the USAF Test Pilot School Telemetry station. The TM
station was also used for realtime reception and display instrumentation
data. The specific parameter / channel assignments were selected by the
test engineer for each mission based on data requirements.

Open loop testing was conducted to confirm the pole locations of
the lateral-directional axes. TM data were hand reduced from stripchart
output to determine roll mode time constant, dutch roll frequency and
damping, and phi/beta magnitude and phase angle. Figures F1 and F2 on
the following pages show how these system parameters were determined
from time history data.

Closed loop testing of each control law configuration was conducted
to assign Cooper-Harper ratings, as described in The Use of Pilot Rating
in the Evaluation of Aircraft Handling Qualties (13). The first test
point of each mission evaluated standard YA-7D lateral-directional
control laws. This procedure standardized mission-to-mission and
pilot-to-pilot performance. Camera film of the closed loop Head-up
Display was reviewed to standardize pilot aggressiveness and ensure

182
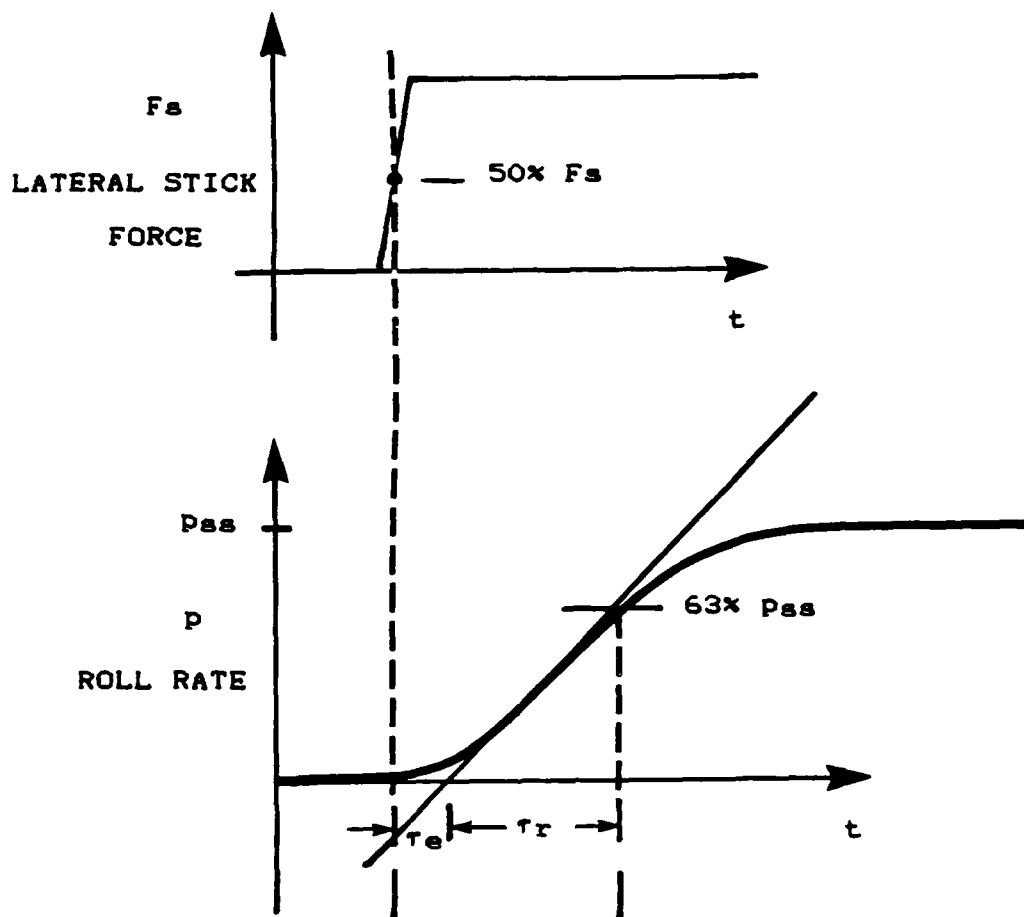
Figure F1. Determination of Open Loop Roll Parameters

$$|\phi/\beta|_d = \Delta\phi / \Delta\beta$$
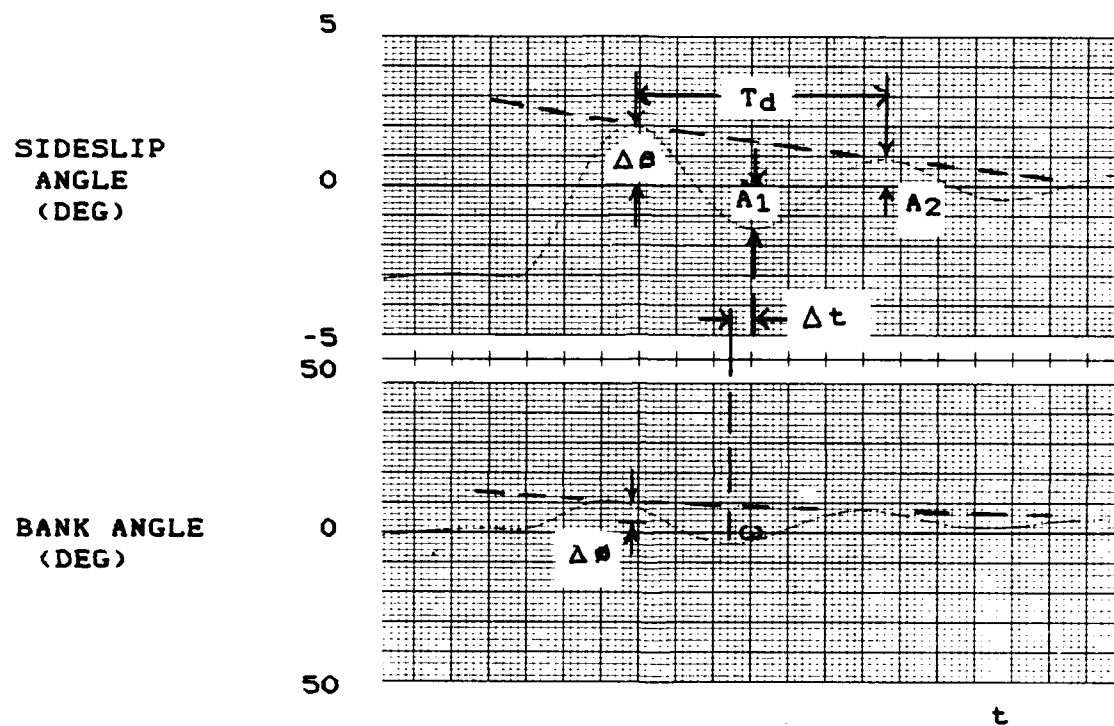
$$\arg(\phi/\beta)_d = \Delta t / T_d * 360$$

$$w_d = 2\pi / [T_d (1 - \zeta^2)^{1/2}]$$

$$\zeta_d = \mathrm{SIN} (\mathrm{TAN}^{-1}[\mathrm{LN} (A_2/A_1) / \pi)$$

Figure F2. Determination of Open Loop Dutch Roll Parameters

184

pilot performance supported the Cooper-Harper rating given in flight.
Qualitative data were collected using the pilot comment shown card in
Appendix G, and ratings influenced by external factors eliminated. The
raw data for all Cooper-Harper ratings assigned during testing are in
Tables E1, E2, and E3 for HUD tracking task 1, HUD tracking task 2, and
the air-to-air tracking task, respectively.

For each pilot/task/control law combination, a single Cooper-Harper
rating was determined by the test engineer. In most cases this rating
was the mode; however, in a few cases the number of ratings or
distribution warranted a rating based on pilot comments and engineer
judgment.

Cooper-Harper ratings were compared between pilots to ensure
consistent evaluations. Figures E1, E2, and E3 show inter and intra
pilot Cooper-Harper rating comparisons for HUD Tracking task 1, HUD
tracking task 2, and the air-to-air tracking task, respectively.
Cooper-Harper ratings were correlated by task for each pilot, as well as
a three rating pilot average, with the different control law
configurations. Although averaging Cooper-Harper ratings does not have
a strict mathematical basis, it was used here to show trends and make
presentation of data more meaningful. The averaged ratings only show
relative pilot preferences, and no longer correspond to the criteria on
the Cooper-Harper scale. Each control law represented various
combinations of design magnitude ratio and phase angle between roll
angle and sideslip angle. The design phi/beta ratios were used rather
than actual since the actual were generally within 15 percent of design
and this allowed more meaningful presentation of data.

Test Methods and Conditions

The phi/beta test matrix was completed at 15,000 feet Hc and 0.6 Mach with Automatic Maneuvering Flaps (AMF) off. Mach 0.6 corresponded to 305 Knots Calibrated Airspeed (KCAS) and 9.72 units (4.63 degrees) angle of attack at 27,000 pounds gross weight. Test points were accomplished within $\pm$ 5 Knots Indicated Airspeed (KIAS) and $\pm$ 1000 feet Hc of the specified conditions. The test matrix was not completed at 0.4 Mach due to the technical problems the software.

The Simulator for Aircraft Flight Test and Development verified the flight control gains produced the desired aircraft response. This also evaluated the effects of nonlinearities, such as the Digital Multimode Flight Control System and servo rate limits not modeled in the derivation of the control laws. Lateral stick step input deflections and release from wings level sideslips were performed for each control law configuration. In addition, each pilot practiced the open loop inputs and became familiar with the HUD tracking tasks prior to flight.

Open loop tests were conducted under the direction of the test engineer using realtime TM. For each control law configuraton, two inputs were made. The first was a lateral stick deflection roll from 45 degrees of bank through level flight to 45 degrees of bank in the opposite direction. The test engineer monitored the stick input and roll rate output to insure a near square step input and an output magnitude which allowed accurate roll mode time constant determination. The second input was a controls free release from a wings level, steady sideslip of approximately three degrees. A precise lateral trim shot was performed beforehand to minimize trim effects in the bank angle

186

response. The test engineer monitored the release to ensure bank angle and sideslip angle response magnitudes allowed accurate determination of dutch roll frequency and damping ratio, and phi/beta magnitude and phase angle. Both open loop tests were repeated as necessary to obtain quality inputs.

The test engineer assigned specific closed loop test points for each mission based on data requirements. The first testpoint of each mission evaluated standard YA-7D lateral-directional control laws. To prevent biased data, the pilots did not know which phi/beta ratio they were testing. Two HUD tracking tasks and air-to-air tracking task, described in the following section, were performed using stick inputs only. After each closed loop task, the pilot comment card in Appendix G was completed and Cooper-Harper ratings assigned using the scale in Figure G2. An A-7D safety chase aircraft was used as a target for the air-to-air tracking task. Each test team pilot evaluated each configuration at least twice.

HUD tracking Task 1. The closed loop tracking task consisted of an artificial target "+" driven to a lateral offset in a step function by a random number generator. A centered, fixed reticle consisting of five and ten milliradian (mil) diameter rings was also generated (Figure F3) The closed loop HUD tracking task was to acquire the mil center of the target "+" within the five mil reticle as expeditiously as possible. The target moved after the pilot tracked the target for one second. The task ran for 90 seconds.

187

Desired Performance: center of "+" within the five mil ring in less than 3 seconds, 90% of the time, and remained within the ring.

Adequate Performance: center of "+" within the five mil ring in less than 6 seconds, 90% of the time, and remained within the ring.
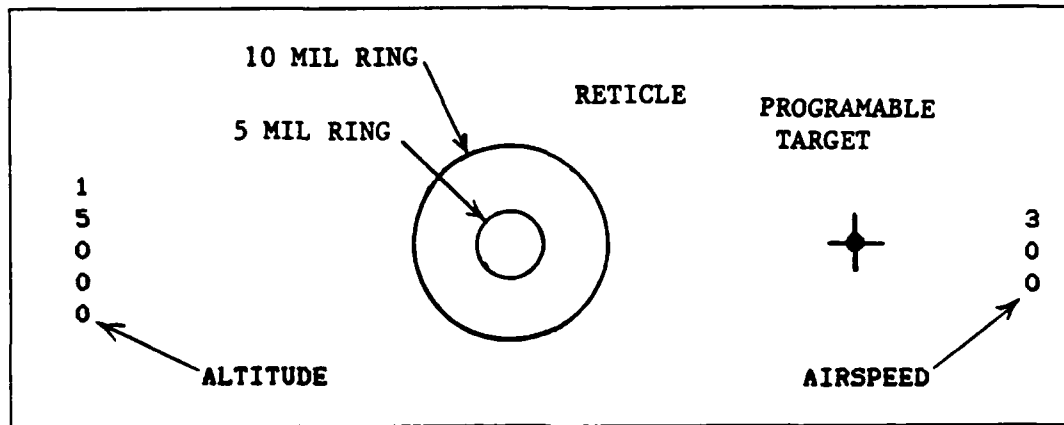
Figure F3. HUD Tracking Task 1 Symbology

HUD Tracking Task 2. This closed loop tracking task consisted of a roll command reference line with tic marks at ± 5 degree bank angles from level (Figure F4). The roll command line was driven by a random number to bank angles within ± 45 degrees of wing level such that the pilot generated rate was approximately 40 degrees/second. The pilot attempted to match the wing reference line (which was parallel to the test aircraft's wings) with the roll command reference line over a task period of 90 seconds.

Air-to-air tracking task. The target aircraft established level flight at 15,000 feet Hc and the design Mach number for the control system being evaluated and called, "Target Ready." When the TM engineer called, "TM ready," the test aircraft called, "Test ready, maneuver one." The target aircraft continued straight and level for maneuver one

Desired Performance: wings aligned within ± 5 degrees of the
artificial horizon 90% of the time.

Adequate Performance: wings aligned within ± 10 degrees of
the artificial horizon 90% of the time.

ROLL COMMAND
REFERENCE LINES
(±5°)

1
5   3
0   0
0   0
0   0

WINGLINE
REFERENCE BAR

ALTITUDE   AIRSPEED
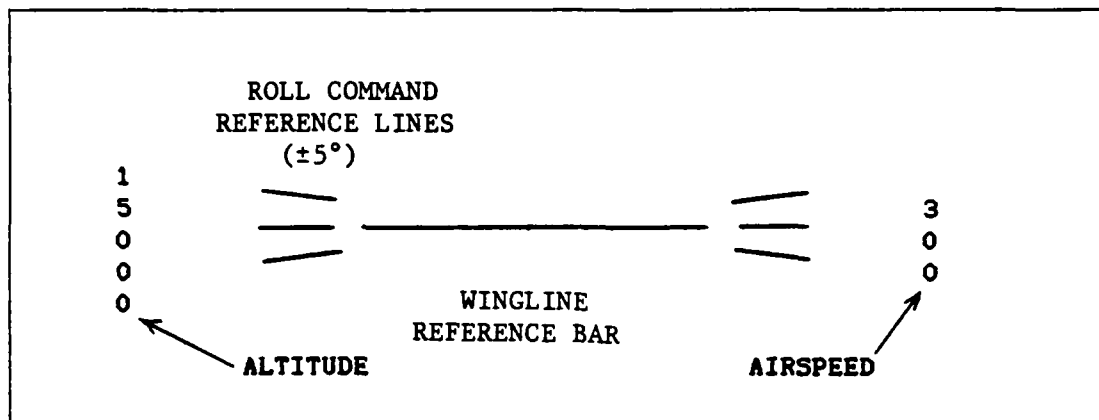
Figure F4. HUD Tracking Task 2 Symbology

and maneuver two. When the test aircraft called, "Test ready, maneuver

three," the target aircraft began a series of roll reversals at a random

interval between one and three seconds at a roll rate less then 20

degrees/second. The target did not bank greater than 40 degrees, nor

did it exceed 1.5 g's. Maneuvering continued until the test aircraft

called, "Maneuver complete," or any participant called, "Knock it off."

Maneuvering was conducted within the following data band:

Altitude: 15,000 ± 1000 feet Hc
Airspeed: Design Mach +20, -5 KIAS
Load factor: 1.0 - 1.5 g
Power: As required

A five and ten mil ring reference mark was drawn on the canopy bow

of the test aircraft approximately two inches aft of the canopy bow

along the centerline.

Three maneuvers were performed in a buildup approach. The first two maneuvers did not receive Cooper-Harper ratings, but were designed to expose poor handling qualities before moving to a high gain task close to the target aircraft. The test aircraft positioned co-speed, 200 feet behind, 20 feet below the jetwash, and offset 200 feet laterally behind the target aircraft. When the target aircraft was ready, the test aircraft called, "Maneuver one," and moved aggressively to the six o'clock position, 200 feet aft of the target while maintaining longitudinal and vertical spacing. After completing the maneuver, the test aircraft called, "Maneuver one complete." The test aircraft then adjusted position to one ship length the target, 20 feet below the jetwash, and offset 50 feet laterally. On the call, "Maneuver two," the test aircraft moved aggressively to position the canopy reference mark on the intersection of the target tailpipe and vertical stabilizer while maintaining longitudinal and vertical spacing. After attaining position, the test aircraft called, "Maneuver three," and maneuvered aggressively to keep the reference mark on the target tailpipe/vertical stabilizer intersection. After sufficient tracking time, the test aircraft called, "Maneuver complete." The test aircraft was limited to less than 2 g's and was cautious to avoid the target's jetwash. Rating criteria during maneuver three was:

Desired performance: within 5 mils of intersection of target tailpipe and vertical stabilizer, 90% of the time.

Adequate Performance: within 10 mils of intersection of target tailpipe and vertical stabilizer, 90% of the time.

APPENDIX G. Miscellaneous Information

Sortie Summary

A summary of the flight times and personnel are given in Table G1.

Table G1

Sortie Summary				
Date	Pilot	Duration	Chase	Chase Duration
8 Oct	Costigan	1.3	Pitotti	1.4
8 Oct	Gregory	2.0	Pitotti	2.1
9 Oct	Gregory	1.3	Pitotti	1.4
13 Oct	Mitchell	1.7	Pitotti	1.8
13 Oct	Gregory	1.8	Waggoner	1.9
14 Oct	Mitchell	1.7	Pitotti	1.8
14 Oct	Mitchell	1.7	Pitotti	1.8
15 Oct	Mitchell	1.5	Waggoner	1.6
15 Oct	Gregory	1.8	Pitotti	1.9
20 Oct	Costigan	1.5	Pitotti	1.5
21 Oct	Costigan	1.5	Waggoner	1.6
21 Oct	Costigan	1.3	Waggoner	1.4
27 Oct	Gregory	1.8	Pitotti	1.8
27 Oct	Mitchell	1.6	Waggoner	1.7
12 Nov	Costigan	2.0	Waggoner	2.1
13 Nov	Gregory	2.2	McCorry	2.2
17 Nov	Mitchell	1.6	Waggoner	1.7

Pilot Experience

Three pilots participated in this flying qualities investigation.

All three were students at the USAF Test Pilot SChool during the test

program. Their backgrounds were:

Pilot A - 2,000 total flight hours with 1,300 hours in the T-38 and 600
hours in operational F-4E's. Operational experience was
primarily air-to-air.

Pilot B - 1,200 total flying hours with 1,100 hours in the F-111.
Operational experience was primarily air-to-ground.

Pilot C - 3,200 total flying hours with 1,400 hours in F-4's and 1,100 in F/A-18''s. Operational experience included both air-to-air and air-to-ground.

Pilot Cards

The test team developed cards to be carried on each mission to standardize pilot comments and to facilitate correlating data. The pilot card is shown in Figure G1. Figure G2 shows the Cooper-Harper rating scale used by the pilots to evaluate the aircraft in each task.

PILOT COMMENT CARD

DATE_____   MISSION_____

PILOT_____   CHASE_____

Multimode Control Panel Settings:

  P2_____   P3_____   P4_____   Fuel Weight_____

Configuration (phi/beta)_____ (filled by engineer)

TASK   HUD TASK 1   HUD TASK 2   AIR-AIR TRACKING

Cooper-Harper Rating   1 2 3 4 5 6 7 8 9 10

Did external factors affect the test?   Yes   No

      Turbulence   Calm   Slight   Moderate

      Other _____

Did the longitudinal characteristics affect the test?   Yes   No

Response characteristics

      Roll Response   Sluggish   Satisfactory   Abrupt

      Roll Predictability   Imprecise   Satisfactory   Precise

      Roll Oscillations   Negligible   Noticeable   Objectionable

      Adverse/Proverse Yaw   Negligible   Noticeable   Objectionable

      Yaw Predictability   Imprecise   Satisfactory   Precise

Pilot Comments:

Tracking Task Score   _____

Engineer Comments:
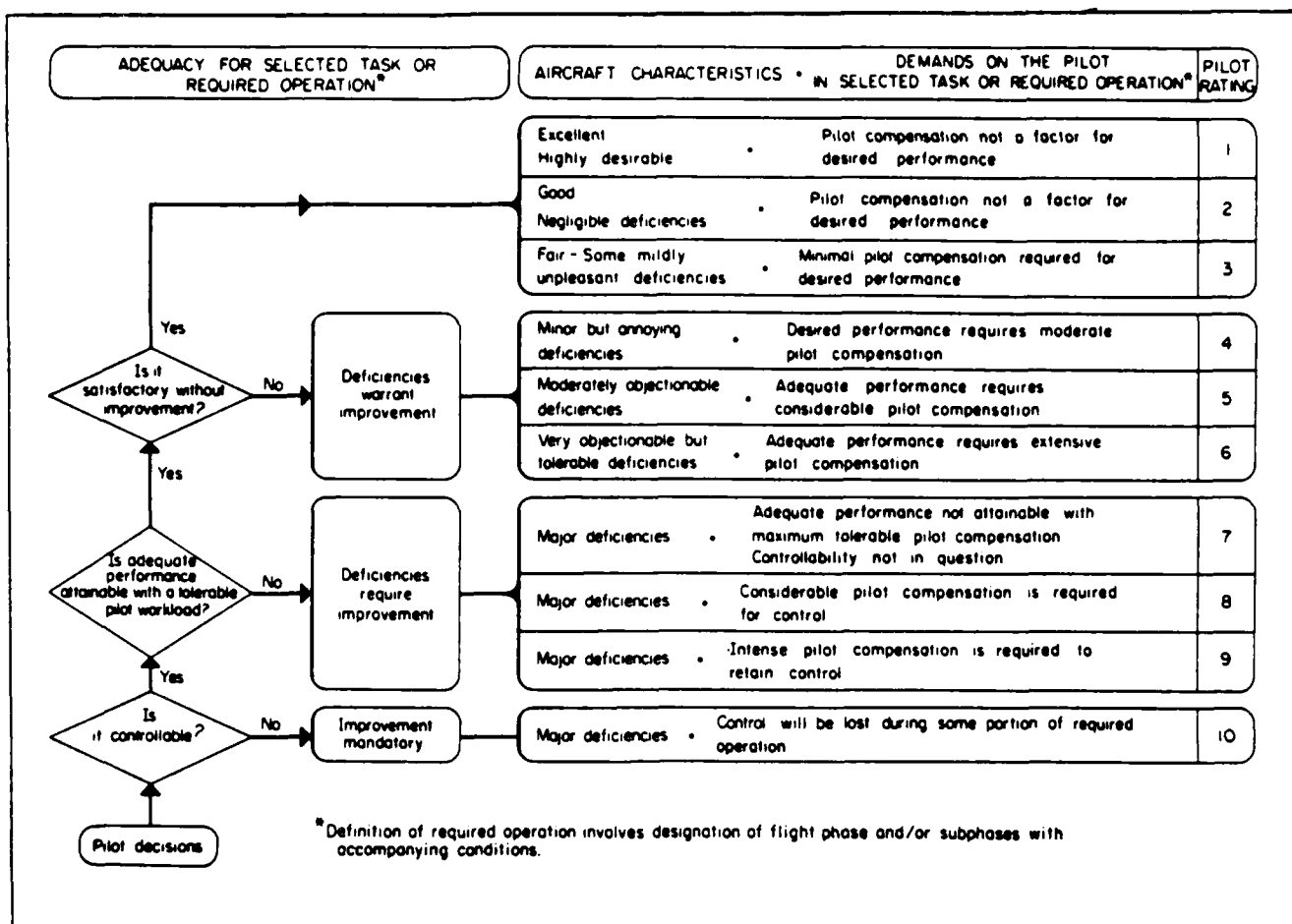
Figure G1.   Pilot Comment Card

Figure G2. Cooper-Harper Scale

Bibliography

1. Costigan, Michael J., Capt, et. al. <u>YA-7D DIGITAC Lateral-Directional Flying Qualities Evaluation Using Eigenstructure Analysis</u>. HAVE EIGEN Final Report. Edwards AFB, California: USAF Test Pilot School/TENR, 11 December 1987.

2. Cunningham, T.B. "Eigenspace Selection Procedures for Closed Loop Response Shaping with Modal Control" <u>Proceedings of IEEE Conference on Decision and Control</u> 1980.

3. Andry, Jr., A.N., et. al. "On Eigenstructure Assignment for Linear Systems," <u>IEEE Transactions on Aerospace and Electronic Systems</u>, AES-19: 711-729 (September 1983).

4. Klemma, V.C. and Laub, J. "The Singular Value Decomposition: Its Computation and Some Applications," <u>IEEE Transactions on Automatic Control</u>, AC-25: 164-176 (1980).

5. Harvey, C.H. and Stein, G. "Quadratic Weights for Asymptotic Regulator Properties," <u>IEEE Transactions on Automatic Control</u>, AC-23: 378-387 (June 1978).

6. McRuer, D., et al. <u>Aircraft Dynamics and Automatic Control</u>. Princeton: Princeton University Press, New Jersey, 1973.

7. Seth, W. A. <u>A-7D Estimated Flying Qualities</u>. Report No. 2-533300/8P-8089. Vought Aeronautics Division, LTV Aerospace Company, 19 February 1969 (AD 847912).

8. Bender, M. A. and Wolf, J. D. <u>Flight Test Evaluation of a Digital Flight Control System for the A-7D Aircraft</u>. Contract F33615-73-C-3098. Wright-Patterson AFB, Ohio: Aeronautical Systems Division, 15 February 1974.

9. Aeronautical Systems Division, Air Force Systems Command. <u>Military Specification, Flying Qualities of Piloted Vehicles</u>. MIL-F-8785C (USAF). Wright-Patterson AFB, Ohio: Aeronautical Systems Division/ENESS, 5 November 1980.

10. Aeronautical Systems Division, Air Force Systems Command. <u>Military Specification, Flying Qualities of Piloted Vehicles</u>. MIL-STD-1797 (USAF). Wright-Patterson AFB, Ohio: Aeronautical Systems Division/ENES, 31 March 1987.

11. Gilbert, E.G. "Conditions for Minimizing the Norm Sensitivity of Characteristic Roots," <u>Proceedings of the 22nd IEEE Conference on Decision and Control</u>, 1: 325-330 (1983).

Bibliography (Concluded)

12. Department of the Air Force. Flight Manual, USAF Series A-7D Aircraft. T.O. 1A-7D-1, Change 20, July 1987. Tinker AFB, Oklahoma: Oklahoma City ALC/MMED, 15 February 1979.

13. Cooper, G.E. and Harper, R.P., Jr. The Use of Pilot Rating in the Evaluation of Aircraft Handling Qualities. NASA TN-D-5153. Dryden Flight Test Center: National Aeronautics and Space Administration, April, 1969.

14. Hoh, Roger. "Highly Augmented Airplane Handling Qualities". Lecture notes distributed in handling qualities course, USAF Test Pilot School Course. Edwards AFB, California, July 1987.

15. Department of the Air Force. Partial Flight Manual, YA-7D Serial Number 67-14583. Edwards AFB, California: Air Force Flight Test Center (AFFTC), 7 April 1980.

16. Costigan, Michael J., Capt, et. al. YA-7D DIGITAC Lateral-Directional Flying Qualities Evaluation Using Eigenstructure Analysis. Unpublished HAVE EIGEN Test Plan. USAF Test Pilot School, Edwards AFB, California, September 1987.

17. USAF Test Pilot School, Air Force Systems Command. Instrumentation Handbook. Edwards AFB, California: USAF Test Pilot School/TENR, November 1985.

VITA

Major Michael J. Costigan was born in Cincinnati, Ohio on 25
February 1953. He received a Bachelor of Science Degree in Aerospace
Engineering from the University of Cincinnati in June 1976. While
attending the University of Cincinnati, he worked at the Johnson Space
Center in a cooperative work education program. Upon graduation, he was
commissioned a Second Lieutenant in the United States Air Force through
the Reserve Officer Training Corps program. He continued to work at the
Johnson Space Center as an engineer until called to active duty. After
graduating from Undergraduate Pilot Training in June 1978, Major
Costigan remained at Columbus Air Force Base as an instructor pilot in
the T-38. He subsequently upgraded to the F-4E Phantom and flew for
three years at Ramstein Air Base, Germany. While overseas, he earned a
Master of Science Degree in Aviation Science from Embry-Riddle
Aeronautical University. In 1985, Major Costigan was selected for the
Joint Air Force Institute of Technology - Test Pilot School Course. He
entered the School of Engineering, Air Force Institute of Technology, in
September 1985. After completing formal course work at Wright-Patterson
Air Force Base, he began the United States Air Force Test Pilot School
course in January 1987. He completed Test Pilot School as a
distinguished graduate and received the Liethan-Tittle Award as the top
pilot in the class. Major Costigan is now assigned as a test pilot to
the 6512th Test Squadron, Edwards Air Force Base, California.

Permanent Address: 9057 Esther Drive
                     Loveland, Oh 45140

197

REPORT DOCUMENTATION PAGE

Form Approved
OMB No. 0704-0188

1a. REPORT SECURITY CLASSIFICATION UNCLASSIFIED	1b. RESTRICTIVE MARKINGS
2a. SECURITY CLASSIFICATION AUTHORITY	3. DISTRIBUTION/AVAILABILITY OF REPORT
2b. DECLASSIFICATION/DOWNGRADING SCHEDULE	Approved for public release; distribution unlimited

4 PERFORMING ORGANIZATION REPORT NUMBER(S) AFIT/GAE/AA/88J-1	5. MONITORING ORGANIZATION REPORT NUMBER(S)

6a. NAME OF PERFORMING ORGANIZATION School of Engineering	6b. OFFICE SYMBOL (If applicable) AFIT/ENY	7a. NAME OF MONITORING ORGANIZATION

6c. ADDRESS (City, State, and ZIP Code) Air Force Institute of Technology Wright-Patterson AFB, Ohio 45433	7b. ADDRESS (City, State, and ZIP Code)

8a. NAME OF FUNDING/SPONSORING ORGANIZATION USAF Test Pilot School	8b. OFFICE SYMBOL (If applicable) USAFTPS/TENR	9. PROCUREMENT INSTRUMENT IDENTIFICATION NUMBER

8c. ADDRESS (City, State, and ZIP Code) Edwards AFB, CA 93523	10. SOURCE OF FUNDING NUMBERS			
	PROGRAM ELEMENT NO.	PROJECT NO.	TASK NO	WORK UNIT ACCESSION NO.

11 TITLE (Include Security Classification)

See Box 19

12 PERSONAL AUTHOR(S)
Michael J. Costigan, M.S., Major, USAF

13a. TYPE OF REPORT MS Thesis	13b. TIME COVERED FROM ____ TO ____	14. DATE OF REPORT (Year, Month, Day) 1988 June	15. PAGE COUNT 216

16 SUPPLEMENTARY NOTATION

17	COSATI CODES		18. SUBJECT TERMS (Continue on reverse if necessary and identify by block number)
FIELD	GROUP	SUB-GROUP	DIGITAC, Handling Qualities, Eigenstructure Assignment, Flight Controls
01	04		

19 ABSTRACT (Continue on reverse if necessary and identify by block number)

Title: An Analysis of LAteral-Directional Handling Qualities and
         Eigenstructure of High Performance Aircraft

Thesis Chairman: Dr. Robert Calico
                   Professor of Aerospace Engineering

Approved for public release IAW AFR 190.1.

LYNN E. WOLAVER   15 Jun 88
Dean for Research and Professional Development
Air Force Institute of Technology (AFIT)
Wright-Patterson AFB OH 45433

20 DISTRIBUTION/AVAILABILITY OF ABSTRACT ☑ UNCLASSIFIED/UNLIMITED ☐ SAME AS RPT. ☐ DTIC USERS	21. ABSTRACT SECURITY CLASSIFICATION UNCLASSIFIED	
22a. NAME OF RESPONSIBLE INDIVIDUAL Dr. Robert Calico	22b. TELEPHONE (Include Area Code) 513-255-2362	22c. OFFICE SYMBOL AFIT/ENY

DD Form 1473, JUN 86   Previous editions are obsolete.   SECURITY CLASSIFICATION OF THIS PAGE

This investigation examines the relationship between an aircraft's lateral-directional handling qualities and its corresponding eigenstructure. Historical data were used to identify eigenvalues expected to yield satisfactory handling qualities. Intuition and simple mathematical models were used to develop desirable eigenvectors. For conventional aircraft, the dutch roll eigenvector was shown to a function of the roll to sideslip (phi/beta) ratio.

Flight control laws to produce the desired eigenstructures were derived using eigenstructure assignment with output feedback. The control laws were based on a twelfth order linear model of the lateral-directional dynamics of the YA-7D DIGITAC, and varied the dutch roll phi/beta ratio.

The handling qualities of the YA-7D were examined analytically and during flight testing at Edwards Air Force Base. The flight testing consisted of both open loop tasks, and closed loop tasks in which Cooper-Harper ratings were assigned. The control laws produced the desired open loop response, although pilot ratings were degraded by the stick dynamics of the YA-7D. The phi/beta magnitude had a negligible effect on the pilot ratings, while the phase angle had only a slight effect.

END

DATE

FILMED

8-88

DTIC